Titre: Title:	Volume change modeling for partially saturated compacted soils
Auteur: Author:	Ghassem Habibagahi
Date:	1990
Type:	Mémoire ou thèse / Dissertation or Thesis
Référence: Citation:	Habibagahi, G. (1990). Volume change modeling for partially saturated compacted soils [Ph.D. thesis, Polytechnique Montréal]. PolyPublie. https://publications.polymtl.ca/57961/

UNIVERSITE DE MONTREAL

VOLUME CHANGE MODELING FOR PARTIALLY SATURATED COMPACTED SOILS

Par

Ghassem HABIBAGAHI

DEPARTEMENT DE GENIE CIVIL

ECOLE POLYTECHNIQUE

THESE PRESENTEE EN VUE DE L'OBTENTION
DU GRADE DE PHILOSOPHIAE DOCTOR (Ph.D.)
(GENIE CIVIL)

DECEMBRE 1990

ISBN 0-315-64329-3

UNIVERSITE DE MONTREAL

ECOLE POLYTECHNIQUE

Cette thèse intitulée :

VOLUME CHANGE MODELING FOR PARTIALLY SATURATED COMPACTED SOILS

présentée par : Ghassem Habibagahi

en vue de l'obtention du grade de Philosophiae Doctor

a été dûment acceptée par le jury d'examen constitué de :

M. Jean Lafleur ..... Ph.D., président

M. Michel Soulié ..... D.Sc.A., directeur

M. Vincenzo Silvestri ... Ph.D., codirecteur

M. Ghislain Lessard ..... Ph.D.

M. Michel Massiera ..... Ph.D.

To My Family

SOMMAIRE

Cette recherche consiste à étudier le comportement des sols compactés et partiellement saturés à l'aide d'un programme expérimental et théorique. La partie expérimentale porte sur l'amélioration du système d'essai triaxial GDS. Les travaux concernent les modifications de la cellule triaxiale ainsi que son programme d'informatique associé qui permet au système de tester les échantillons de sols non saturés.

Dans la partie théorique, une relation contraintes-déformations est presentée afin de modéliser le comportement du changement de volume des sols partiellement saturés. Le modèle doit tenir compte des déformations induites par un chargement ainsi que des compressions provoquées par un accroissement du degré de saturation ("effondrement"). Le phénomène d'effondrement est supposé être responsable des comportements étranges de plusieurs barrages en terre cités par différents auteurs.

Le modèle proposé est consideré comme généralement appliquable par les différentes relations constitutives telles que l'élasticité, l'élastoplasticité, etc. Dans cette étude, le modèle est formulé à l'aide d'une approche élastique non linéaire, plus précisément, le modèle hyperbolique

généralement utilisé dans la prédiction des variations de volume dans les remblais et barrages en terre. Un programme d'éléments finis incorporant le modèle est développé et les résultats sont qualitativement discutés en référence avec le comportement réel observé. En outre, les résultats prédits sont quantitativement comparés avec les données expérimentales disponibles dans la littérature. Une très bonne concordance donne plus de fiabilité au modèle proposé pour la prédiction de changement de volume dans les sols partiellement saturés.

La sensibilité du modèle à la variation des données est étudiée pour chaque paramètre varié en testant son influence sur les résultats. De plus, un schéma de couplage du modèle avec le programme PERCO (programme de l'écoulement de l'eau à travers les sols saturés et partiellement saturés developpé à l'Ecole Polytechnique de Montréal comme une partie du projet CASTOR) est proposé en vue de décrire le processus de la consolidation dans les sols partiellement saturés.

Finalement, il est supposé que le modèle est capable de décrire d'autres aspects mécaniques des sols non saturés, comme la résistance au cisaillement en ayant, auparavant, déterminé les paramètres correspondants.

ABSTRACT

This study consists of both experimental and theoretical investigations on partially saturated compacted soils. In the experimental part, works are undertaken to upgrade the GDS triaxial testing system. These works include modifications to the triaxial cell as well as its accompanying computer program which enables the system to deal with partially saturated soil specimens. Results from K_o compression on compacted glacial till specimens are analyzed.

In the theoretical part, this thesis presents a stress - strain relationship for modelling volume change behavior of partially saturated soils. The model is to account for deformations resulting from loading as well as compressions caused by an increase in degree of saturation ("collapse"). Collapse phenomena is believed to be responsible for unusual behavior of numerous earth dams reported by various authors.

The proposed model is quite general in that it may be formulated using different types of constitutive laws, i.e., elastic, elastoplastic, etc. In this research the model is formulated using a nonlinear elastic approach, more specifically, hyperbolic modeling which is commonly used for volume change prediction in embankments and earth dams. A finite element program incorporating the model is developed and the results are discussed qualitatively with reference to observed field behavior. Moreover, predicted results are compared quantitatively with actual experimental data available in

literature where close agreements with the latter further support suitability of the model for volume change prediction in partially saturated soils.

Finally, it is believed that the model is capable of describing other mechanical aspects of unsaturated soils, such as shear strength, provided pertinent parameters are properly determined.

ACKNOWLEDGEMENT

The author wishes to express his sincere gratitude to his research director Dr. M. Soulié, professor of civil engineering department, for his continuous guidance, advice, and constructive criticism which played an important role in rapid progress of this work.

In addition, the author is greatly in debt to his research co-director Dr. V. Silvestri, professor of civil engineering department, for his valuable suggestions during the course of this study.

Acknowledgement is also due to CASTOR and CASTOR PLUS projects for their financial supports through this research program.

Also, the author wishes to thank his colleagues in geotechnical engineering and Mr. B. Barakat in particular for their encouragement and helpful discussions.

Finally, the author acknowledges the assistance received from Mr. A. Ducharme in the performance of the experimental works.

Table of Contents

List of Figures

List of Tables

CHAPTER 1

INTRODUCTION

1.1 General :

Research works on the mechanical behavior of partially saturated soils date back to about forty years ago. Since then a lot of investigations have been performed to explain the volume change behavior of unsaturated soils both qualitatively and quantitatively. Bishop (1959) attempted to extend the principle of effective stress to partially saturated soils. He proposed the following relationship :

$$\sigma' = \sigma - u_a + \chi(u_a - u_w) \qquad (1.1)$$

where :

σ' : effective stress.

σ : total stress.

u_a : pore air pressure.

u_w : pore water pressure.

χ : parameter which depends on the degree of saturation, soil type and hysteresis effect.

Unsaturated soils may undergo excessive deformation at constant applied load (called "collapse") if free access to water is provided. The amount of this deformation depends on factors such as placement conditions, amount of change in degree of saturation and stress level at which free access to water is provided. Collapse involves a major rearrangement of the particles to a denser state of packing and is irre-

versible.

Applicability of the principle of effective stress to partially saturated soils has been seriously questioned by many investigators such as Jennings and Burland (1962) who have shown that the effective stress principle is incapable of describing the collapse phenomenon.

1.2 Practical Significance of the Problem :

Soil engineers in practice mostly must deal with soils in partial saturation condition both in natural soils as well as artificially compacted soils. This study is restricted to the compacted soils, examples of which are compacted road embankments and rolled earth dams. The importance of understanding volume change behavior of these structures both during construction and afterwards is undoubted. During construction as new lifts are added to the previously compacted fill layers, pore pressures continuously change till full height of embankment is reached. Thereafter, upon partial filling of the reservoir, earthfill may undergo some volume change depending on the amount of infiltration of water from the upstream face of the embankment which will change the degree of saturation and pore pressures and will eventually establish a steady state flownet.

Two case histories regarding volume change behavior of compacted fills are discussed below :

-Roussieres Earth Dam : This is a small earth dam located

in the territory of Saint-Quentin-en-Yvelines, France. It has a length of 238 m and is 17 m high. Its base and crest dimensions are 150 m and 65 m respectively. The behavior of this dam during construction and afterward during reservoir filling is reported by Jardin et al (1984). They reported additional settlement during reservoir filling. Fig. 1.1 shows a section of the dam with the observed deformations. This kind of deformation as a result of increase in saturation degree can not be explained by the principle of effective stress.

-The other case concerns the observations reported by Hight and Farrar (1978) for the vertical pressures in the cores of two earth dams. The total pressure was measured using pressure cells placed inside the core during construction. Vertical pressures of the order of 70% to 50% of the total overburden pressure were recorded. Arching action in the core which transfers some of its load to the shoulders was believed to be responsible for this reduction in total stress. The arching action was then argued to be as a result of differential settlement between the core and the shoulders. This differential settlement was thought to decrease by placing the core on the dry side of optimum water content. However, the field measurement showed the opposite, that is, the wetter core exhibited less reduction in vertical stress. At this point it is obvious that a proper model for the volume change behavior will enable us to determine the deformations in the core of the dam as the reservoir is filled. And for this case it is

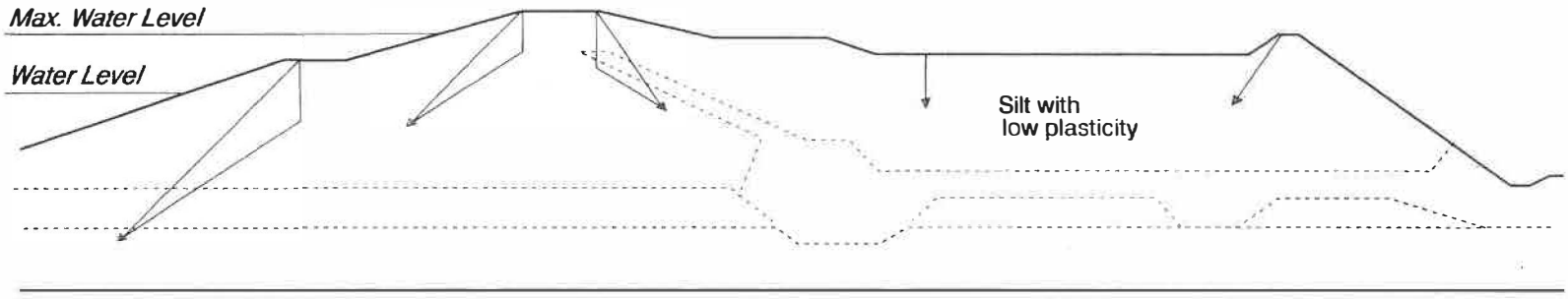

Fig. 1.1 - Measured Displacements During Reservoir Filling For Roussières Dam (after Jardin et al 1984)

highly probable that the lower part of the core experiences excessive deformations which can be responsible for arching action and reduction in total stress. This argument can be further supported by observations made by Cox (1978). He showed that an embankment wetted from the base will tend to collapse before swelling since this is the predominant behavior at the base.

Similar observations are reported by Penman (1970) who argued that arching followed by hydraulic fracture had occurred in clay cores of two earth dams in Norway and England. Leaking took place when the reservoirs were being filled for the first time. He stated that hydraulic cracking was most likely in clay soils with low swelling coefficient which was related to low plasticity index. Again it is worthwhile mentioning that these kinds of soils are also susceptible to collapse phenomena and this phenomenon is at least partly responsible for the observed behavior.

With the above descriptions the need for a thorough study of volume change behavior of partially saturated compacted soils is beyond doubt.

1.3 Definition of Partial Saturation :

Aitchison (1956) defined three main categories of partly saturated soils, namely, "quasi-saturated", "partially saturated", and "unsaturated".

-Quasi-saturated : This is attributed to a soil having all

the pores filled with water but the pressure in the pore water is less than atmospheric pressure. In sands the quasi-saturated state can only extend over a small range of pore pressure deficiency while in very compressible clays the range can be very large.

-Partially saturated : A soil having degree of saturation less than one but the pore water pressure greater or equal to atmospheric pressure. The air phase in partially saturated soil is essentially occluded.

-Unsaturated : Unsaturated soil is characterized by degree of saturation less than unity and pressure deficiency greater than zero. The air may be present in occluded bubbles or continuous free air connected to the atmosphere or both.

For the purpose of this study the terms "partly", "partially", and "unsaturated" are used interchangeably to represent a soil if it possesses at least one of the followings:

-A degree of saturation less than unity.

-A pressure deficiency greater than zero.

1.4 Objective and Outline of this Research :

The objective of this research is to study the volume change behavior of partly saturated compacted soils and to establish a proper stress strain relationship which takes into account the volume changes resulting from a change in boundary stresses as well as a change in degree of saturation. Such a relationship should be capable of predicting swell as

well as collapse phenomena if present.

This thesis is organized in seven chapters as follow :

- Chapter 1 : Introduction
- Chapter 2 : Literature review
- Chapter 3 : Proposed Model
- Chapter 4 : Experimentation
- Chapter 5 : Finite Element Formulation and Computer Program
- Chapter 6 : Results and Discussion
- Chapter 7 : Conclusion

CHAPTER 2

LITERATURE REVIEW

2.1 General :

Almost from the very beginning of the science of soil mechanics the subject of partial saturation in soils and its mechanical influence on soil behavior has received particular attention. For years this topic has been the subject of discussions among various authors. In this chapter a summary of the investigations in this area which were made by different researchers is presented and reviewed.

2.2 Effective stress equation :

Terzaghi (1943) is one of the first who tried the extension of the effective stress principle to partially saturated soils:

$$\sigma' = \sigma - u \qquad (2.1)$$

Where : σ': Effective stress

σ :total stress

u :pore water pressure

He stated that the effective stress will increase as the pore water pressure becomes negative and equal to the capillarity pressure i.e.,$u=-u_c$. Actually Terzaghi did not treat the problem for the case where the pores are desaturated, in other words , he assumed that the pores remain saturated and the air water menisci are formed just over the boundary of the soil sample under consideration. This applies to the particular

case of high saturation degree, that is, the so-called "quasi-saturated" as defined in Chapter 1.

Later, Aitchison & Donald (1956) proposed the following relationship for the equivalent pore pressure in unsaturated soils :

$$\sigma'' = \frac{1}{100}\left\{ S_r . P'' + \sum_{0}^{P} 0.3\overline{P}'' . \Delta S_r \right\} \qquad (2.2)$$

In which :

σ'' : Component of effective stress resulting from pore pressure deficiency.

P'' : Pressure deficiency ($u_a - u_w$)

S_r : Degree of saturation

$\overline{P}''$: Average Pressure deficiency

u_w : Pore water pressure

u_a : Pore air pressure

For cases where the degree of saturation is close to 1.0 the equation will give $\sigma''=P''$, that is, the whole pressure deficiency will contribute to the effective stress as stated by Terzaghi for quasi-saturated soils.

Jennings and Knight (1957) proposed a general form of the effective stress equation of the following form :

$$\sigma' = \sigma + \beta P'' \qquad (2.3)$$

Where : β is a parameter which must be estimated or measured experimentally.

Bishop (1959) discussed the use of effective stress equation

for unsaturated soils and proposed a relationship which includes a term for the air pressure as follow :

$$\sigma' = \sigma - u_a + \chi(u_a - u_w) \qquad (2.4)$$

Where σ, σ', u_a, and u_w are as defined before. χ is a parameter which is a function of the degree of saturation, soil type, and hysteresis effect.

For the case of fully saturated soil, there will be no air phase present and the value of χ is equal to 1.0 therefore, equation (2.4) reduces to the conventional effective stress. If the soil is completely dry, equation (2.4) becomes :

$$\sigma' = \sigma - u_a \qquad (2.5)$$

χ is equal to zero in this case since air is acting over the whole of any section through soil. For the case where air phase is continuous (it has atmospheric pressure, $u_a = 0$) the equation reduces to :

$$\sigma' = \sigma - \chi u_w \qquad (2.6)$$

If in Bishop's equation all pressures are measured with respect to the air pressure it will result :

$$\sigma' = \sigma + \chi P'' \qquad (2.7)$$

which is equivalent to Jennings's revised equation.

Aitchison (1960) by making use of capillary model confirmed his earlier assertion that pressure deficiency acts over a proportionate area of any plane through soil given by the

geometry of the system and the proposed equivalent pore pressure is given by :

$$\frac{\sigma''}{P''} = \psi \qquad (2.8)$$

where σ" and P" are equivalent pore pressure and pressure deficiency respectively. If $\psi = \beta$, then it is exactly the same as equation (2.3) given by Jennings.

Radhakrishna (1967) derived a relationship for intergranular stress by considering equilibrium of forces on a wavy plane passing through interparticular contact points. This expression has the following form :

$$\sigma_{ij} = \bar{\sigma}_{ij} + A_w u_w \delta_{ij} + A_a u_a \delta_{ij} - \delta_{ij} \int T\, dx \qquad (2.9)$$

Where :

σ_{ij} :Total stress tensor.

$\bar{\sigma}_{ij}$:Equivalent stress transmitted by the solid contacts.

u_a and u_w are pore air and pore water pressure respectively.

A_a and A_w are ratio of air and water area to the total area respectively.

δ_{ij} :Kronecker delta (=1 if i=j and =0 if i ≠j).

T :Surface tension force per unit of air water meniscus.

x :Perimeter of the air - water meniscus.

He did a thorough experimental work on partially saturated compacted samples and since later in this thesis reference will be made to his data, a brief description of his work is presented here. The soil used was a mixture of 20% kaolin and 80% flint powder with the basic properties described in Table 2.1. He performed a series of K_o triaxial consolidation tests and measured the amount of collapse deformation under different applied loads. Some of his results which will be used later in the present study are reproduced in Fig. 2.1.

Jennings and Burland (1962) considered the principle of effective stress for volume change behavior in partially saturated soils and they showed that it is not followed below a critical degree of saturation. They also suggested that this critical degree of saturation is the same as the one mentioned by Jennings and Knight below which collapse may occur. They further showed that collapse will occur even under condition of isotropic external stress. They concluded that collapse is not due to interparticular shear stress resulting from applied boundary stresses. This argument was later questioned by Leonards (1962) who stated that "the principal mechanism producing compression in clayey soils is sliding of particles with respect to each other regardless of whether or not external shear stresses are applied. Thus even an all-round compression test is in reality a microscopic shear test."

Aitchison (1973) stated that there is no evidence that

Table 2.1 - Basic Characteristics of The Soil Mixture Used By Radhakrishna (1967)

Liquid Limit	29
Plastic Limit	25
Plasticity Index	4
Specific Gravity	2.63
Passing No. 200	100%
Clay Size (<2 μm)	18%

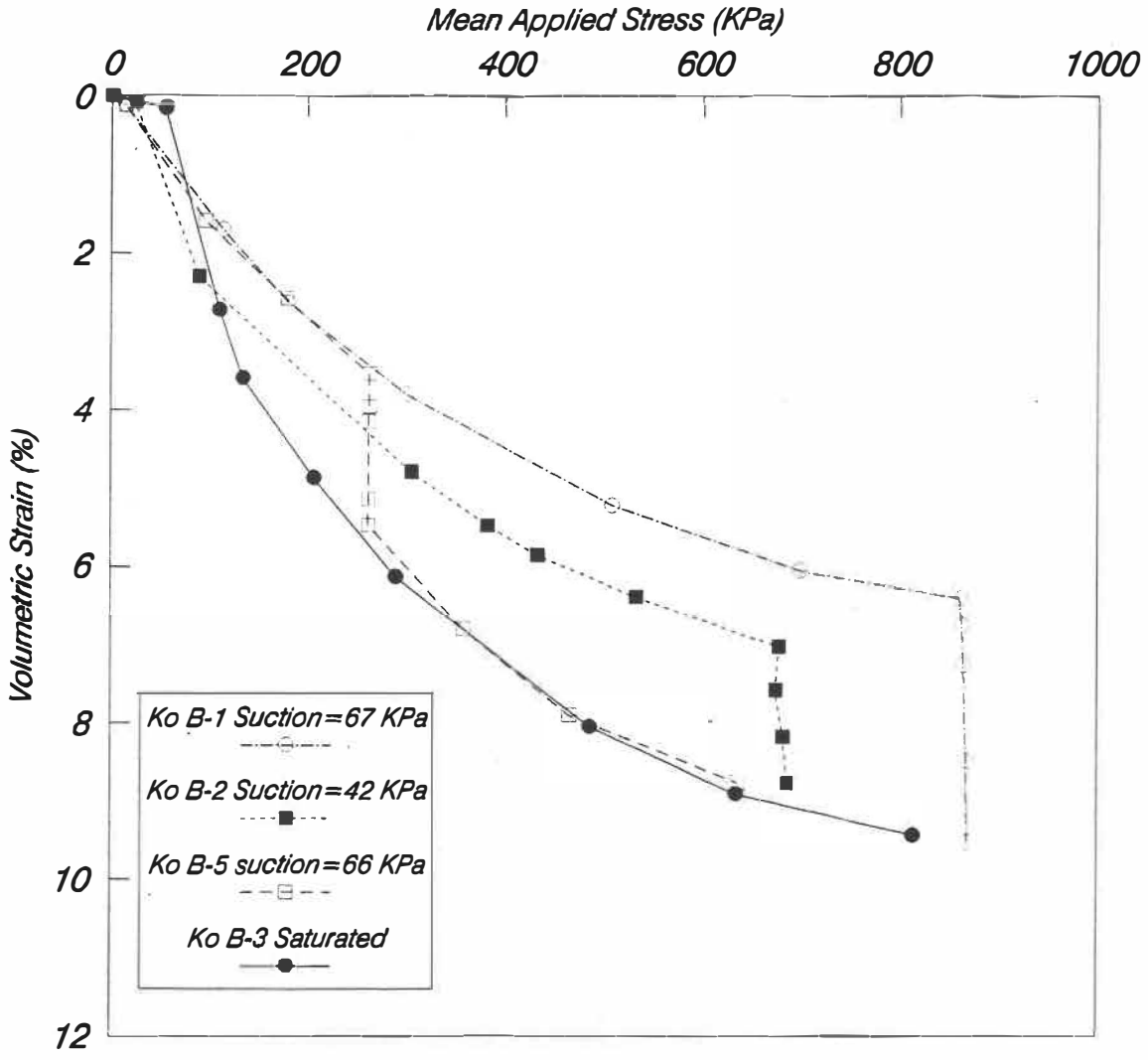

Fig. 2.1 - Compressibility Curves For Ko Consolidation Tests

the principle of effective stress is invalid if a model correctly representing the soil is derived and if the stresses are correctly defined. But so far, such a model has not been achieved. In fact the main goal of this study is to propose a proper model which satisfies the necessary requirements.

Aitchison (1965) put forward an effective stress equation that takes into account both matrix suction as well as solute suction. It is given in the following form :

$$\sigma' = \chi_m P''_m + \chi_s P''_s \qquad (2.10)$$

where :

P"$_m$: matrix suction (=u_a-u_w)

P"$_s$: solute suction (osmotic pressure)

χ_m and χ_s are factors in the range of zero to one and are stress path dependent.

Hence for using equation (2.10) it is necessary to have an adequate knowledge of the applied stress together with matrix suction and solute suction for each point followed on the stress path. For any prediction of volume change by this relationship, present value of matrix and solute suction at the point under consideration as well as its final values are needed a priori.

Bishop and Blight (1963) studied the validity of effective stress by performing some triaxial tests. They showed that for the case of volume change, the path of the two components of effective stress namely, $(\sigma - u_a)$ and $(u_a - u_w)$should be taken

into account. This is in contrast to saturated soils where the principle of effective stress can be applied and only effective stress path is accounted for. Their work was further questioned by Burland who showed that negative values of the χ parameter in Bishop's equation will be obtained for a wide range of compression curves.

Blight (1965) supports the validity of the effective stress equation over a considerable range of suction. He acknowledged the restriction of collapse phenomenon and postulated it will occur when resistance to the concentration of secondary shear stresses at interparticular contacts is reduced. Thereby, he suggested that the collapse phenomena although imposing a limitation on the prediction of principle of effective stress in partly saturated soils, actually occurs as a consequence of the principle.

Burland (1965) considered the equilibrium of normal and shear forces at grain contacts and suggested that in view of the large number of contact points, the displacement in the sense of translation and rotation can only take place as a result of slip at grain contact points. Then he discussed the nature of contact forces originated from boundary stresses compared with those generated by water menisci at grain contact points. He concluded that while boundary stresses produce both normal and shear forces at grain contacts, the high curvature menisci generate interparticle forces whose lines of action are essentially perpendicular to the plane of

contact. Therefore in the latter case the menisci tend to stabilize the soil structure while in the former the increase in shear force may cause more slip and rotation of grains within the soil matrix. Moreover, the phenomena of collapse may occur as that portion of the normal stress at grain contact which comes from menisci and tend to stabilize the soil structure suddenly disappears upon saturation. In other words a meniscus fulfils the function of a glue. He concluded that any model for predicting the behavior of partly saturated soils must embrace the extremes of collapse and swelling and any associated phenomena.

Blight (1967) proposed a method of determining the χ parameter in Bishop's equation for effective stress. For instance for volume change the following relationship for volumetric strain can be written :

$$\frac{\Delta V}{V} = C\Delta\{\sigma - u_a + \chi(u_a - u_w)\} \qquad (2.11)$$

In which, C is the compressibility of the soil skeleton measured over the interval ΔV. If conditions of the soil is considered in two close and similar states, then :

$$\frac{(\Delta V/V)_1}{(\Delta V/V)_2} = \frac{\Delta\{\sigma - u_a + \bar{\chi}(u_a - u_w)\}_1}{\Delta\{\sigma - u_a + \bar{\chi}(u_a - u_w)\}_2} \qquad (2.12)$$

Where $\bar{\chi}$ is the average value of χ for the loading increment considered. Blight applied this type of equation for a case of compression at constant water content and the value of χ thus obtained showed considerable deviation from the χ value

found from comparison of saturated and unsaturated samples at the same volume change. His work is based on the assumption that the principle of effective stress is valid and applicable to unsaturated soils in exactly the same way as in saturated soils. However, as mentioned before many investigators have seriously doubted this approach. Blight also formulated an expression for χ parameter based on an ideal unit cell of spheric particles and showed that the value of χ may exceed unity at low suctions.

Newland (1965) suggested that there are two parts to effective stress in a partially saturated soil. A part is due to forces arising at the point of contact and acting normal to the tangent at the point of contact. Another part is due to forces external to the points of contact and is associated with shear forces at the point of contact. He called these stresses "endogenic" and "exogenic" effective stresses respectively. He postulated that when endogenic forces are somehow reduced, the soil would increase or decrease in volume depending on whether the applied stress was respectively smaller or larger than the equilibrium applied stress which could be supported by the shear resistance at interparticular contact points.

Matyas and Radhakrishna (1968) supplied more evidence regarding deficiency of the effective stress principle in explaining volume change behavior. They stated that the use of effective stress equation for both change in stress and

degree of saturation gives anomalous results for the χ parameter. This indicates that χ is highly path dependent. They proposed an alternative approach which will be explained later in this chapter. They concluded that the behavior of a partially saturated soil subjected to different stress paths can not be explained or predicted in terms of any single equation without taking into account the changing state of the soil.

Coleman (1962) proposed the following relationship :

$$\begin{Bmatrix} -dV_w/V \\ -dV/V \\ -d(\epsilon_1-\epsilon_3) \end{Bmatrix} = \begin{pmatrix} C_{11} & C_{12} & C_{13} \\ C_{21} & C_{22} & C_{23} \\ C_{31} & C_{32} & C_{33} \end{pmatrix} \begin{Bmatrix} d(u_a-u_w) \\ d(\sigma_m-u_a) \\ d(\sigma_1-\sigma_3) \end{Bmatrix} \qquad (2.13)$$

Where :

C_{ij} are coefficients which depend on stress and stress path.

dV_w is change in volume of water.

$d(\epsilon_1-\epsilon_2)$: deviatoric strain.

dV :total volume change.

If the following equalities hold true then Bishop's equation can be regarded as a special form of Coleman's equation :

$$\frac{C_{11}}{C_{12}} = \frac{C_{21}}{C_{22}} = \frac{C_{31}}{C_{32}} = \chi \qquad (2.14)$$

This idea was studied by Karube et al (1978) by performing isotropic and axial compression tests to investigate whether or not the above equalities hold good. Equality (2.14) could not be satisfied from the experimental results thus obtained.

Barden et al (1969) by means of several tests on partially saturated soils assessed the complexity of Coleman's equation parameters. They assumed path independency provided there is no swell or desaturation. Consequently the coefficients C_{ij} are only stress level dependent and for the simple one-dimensional compression gives :

$$\frac{dV}{V} = C_1 d(\sigma - u_a) + C_2 d(u_a - u_w) \qquad (2.15)$$

All terms are as defined before.

Gili and Alonso (1988) treated the partially saturated soil as a particulate medium by modeling the interparticular forces for an array of spherical particles. They modeled the contact forces by a system of dashpots and springs. The main disadvantage of this approach is the difficulty in choosing the physical contact parameters, namely, spring stiffness, and damping coefficient. Hence, their analysis is purely theoretical in the sense that the model could not be calibrated for a specific soil type and thus selection of parameters is more or less arbitrary.

2.3 State Surface :

Matyas and Radhakrishna (1968) put forward the idea of representing the state of a soil element graphically by a point in the space enclosed by a system of coordinate axes signifying the "state parameters". The point called "state point" and the trace of this point with a change in the state

of the element called "state path". The state parameters selected were $\sigma - u_a$, $u_a - u_w$, and e (void ratio). If void ratio was a state function then all the points in this space and all the state paths would lie on a single surface. This type of surface was actually first suggested by Bishop and Blight (1963).

Matyas and Radhakrishna furthermore studied the uniqueness of this surface. They concluded that its uniqueness is complied with the following restrictions :

-The degree of saturation is a non-decreasing parameter.

-The soil is not permitted to swell.

Fredlund and Morgenstern (1976) and (1977) treated the air water interface as an independent phase and they showed that any two of the three possible normal stress variables can be used to define the stress state. Possible combinations are as follow :

(1) $\sigma - u_a$, $u_a - u_w$

(2) $\sigma - u_w$, $u_a - u_w$

(3) $\sigma - u_a$, $\sigma - u_w$

Furthermore, they suggested the following constitutive equations for the soil structure and water phase :

$$\frac{\Delta V}{V} = m_1^s d(\sigma - u_a) + m_2^s d(u_a - u_w) \qquad (2.17)$$

$$\frac{\Delta V_w}{V} = m_1^w d(\sigma - u_a) + m_2^w d(u_a - u_w) \qquad (2.18)$$

Where :

V : total volume.

V_w: volume of water.

m_1^s : compressibility of soil structure when $d(u_a-u_w)=0$.

m_2^s : compressibility of soil structure when $d(\sigma-u_a)=0$

m_1^w : slope of water volume versus $\sigma-u_a$ when $d(u_a-u_w)=0$.

m_2^w :slope of water volume versus u_a-u_w when $d(\sigma-u_a)=0$.

The constitutive relation for the air phase is found from the difference of equation (2.17) and (2.18).

Later, Fredlund (1979) emphasized the significance of this stress state for partially saturated soils. For a considerable portion of the state surface, Fredlund proposed the following empirical expression :

$$e = e_0 - C_t \log \frac{\sigma - P_a}{(\sigma - P_a)_0} - C_m \log \frac{P_a - P_w}{(P_a - P_w)_0} \qquad (2.16)$$

In which :

e :Void ratio.

e_o :Initial void ratio.

P_a and P_w are pore air and pore water pressures respectively.

The subscript o represents the initial stress state.

C_t and C_m are constants; C_t is approximately equal to C_m as the degree of saturation approaches 100% . At lower degree of saturation C_t will be greater than C_m.

Lloret and Alonso (1980) used spline functions for approximation of state surface in solving consolidation problem in unsaturated soils.

Also Lloret and Alonso (1985) tried several functions for approximating the state surface and based on their analysis the following relationships were proposed :

$$e = a + b(\sigma - P_a) + c\log(P_a - P_w) + d(\sigma - P_a)\log(P_a - P_w) \qquad (2.19)$$

and :

$$e = a + b\log(\sigma - P_a) + c\log(P_a - P_w) + d\log(\sigma - P_a)\log(P_a - P_w) \qquad (2.20)$$

In which a, b, c, and d are constants and the other parameters were defined before.

Equation (2.19) was found suitable for a limited range of total stress and if the range of significant stress variation is large use of equation (2.20) was recommended.

2.4 Collapse Phenomenon :

The word "collapse" is used in partially saturated soils to refer to an excessive or considerable reduction in void ratio at constant applied pressure when it is given access to water by wetting or inundation. Collapse involves a major rearrangement of soil particles to a denser state and is irreversible.

2.4.1 Mechanism of collapse :

Knight (1961) presented the hypothesis of existing clay bridges between unweathered grains in an open structure which

carry a large portion of interparticular forces. He expressed collapse as failure of these bonds that happens at a particular combination of shear stress and moisture content.

Booth (1975) from observations on microstructure of soil samples by electron microscopy indicated that clay bridges existing in undisturbed samples were absent when they were recompacted. However, although there were no clay bridges in recompacted samples, these samples showed higher collapse potential than the undisturbed samples for a wide range of degree of saturation.

Burland (1965), as stated earlier in this text, explained the phenomena of collapse in terms of the ratio of normal to shear forces at intergranular contact points.

Kane (1973) attempted to reproduce the correct value of negative pore water pressure by stress path technique and concluded that collapse in loess is a shear phenomena.

Holtz and Hilf (1961) explained the collapse phenomena to be a result of release in confining pressure (capillary stress) upon an increase in degree of saturation and thus the sample will fail in shear going through additional settlement. He showed also that it can occur in compacted soils with high densities when compacted dry of optimum.

Barden et al (1973) suggest that three conditions are required for appreciable collapse of partly saturated soils. These conditions are as follow :

1. An open potentially unstable structure, such as flocculated structure of soils compacted dry of optimum.
2. Strong bonding or cementing agents at inter-particular contact points.
3. High applied stress to develop a metastable structure.

2.4.2 Factors Influencing Collapse :

Many investigators such as Zur and Wiseman (1973) had shown that collapse is a stress level dependent phenomena. Also David et al (1973) and Matyas and Radhakrishna (1968) have shown that collapse will occur at high applied pressures while swelling can occur at low stress levels. For natural soils, cementing agents such as iron oxides, carbonates, and organic material will provide the temporary strength for many collapsible soils, being the main agents for loessial soils.

Aitchison and Donald (1956) indicated that for uniform spherical grains in an open or cubical packing the maximum capillarity effect occurs at a moisture content of about 32%. For the densest packing this value of moisture content is as low as 10%.

Numerous results show that a low dry density is one of the main factors in many collapsible soils. Booth (1975) investigated various parameters influencing collapse of compacted materials. Compacted samples were made using three

types of residual soils. He showed that the most significant factors were initial dry density and moisture content prior to collapse. It was also shown that collapse for soils compacted wet of optimum is not very significant. Moreover, for any set of initial conditions there was a pressure at which the amount of collapse is the largest. Both this pressure and the amount of collapse increased with reducing moisture content.

Barden (1972) showed that collapse can occur in almost pure clay and even in montmorillonite. It seems, however, that due to large amount of swell occurring simultaneously the collapse will be absent in the global observations.

2.4.3 Collapse Potential :

Bally et al (1973) defined the total collapsible potential of a soil as :

$$I_{M.C.} = \sum_{j=1}^{n} i_{M.C.,j} \cdot h_j \qquad (2.21)$$

In which :

h_j =Thickness of the component layers

$i_{M.C.,j}$ = Oedometric additional strain resulting from moistening the sample of the "j" th layer under its corresponding overburden pressure.

This is a parameter which quantifies the collapse potential and could be used to serve for the purpose of comparison among different collapsible soils. A value of $I_{M.C.}$ up to 150 centimeters is recorded.

Abelev (1948) was the first to define a collapse potential for collapsible soils expressed by :

$$CP = \frac{\Delta e_c}{1 + e_1} \qquad (2.22)$$

In which :

CP : Collapse potential

Δe :Change in void ratio upon saturation at a particular applied stress.

e_1 : void ratio at the beginning of saturation.

Equation (2.22) can also be expressed in the following form:

$$CP = \frac{\Delta H_c}{H_1} \qquad (2.23)$$

Where ΔH_c is the change in height of sample as a result of increase in saturation degree and H_1 is height of the sample before saturation.

Jennings and Knight (1975) have suggested the following categories of collapse potentials :

CP (%)	Severity of Problem
0 - 1	No Problem
1 - 5	Moderate trouble
5 - 10	Trouble
10 - 20	Severe Trouble
> 20	Very Severe Trouble

There are over ten different criteria defining collapse potential and its severity suggested by different authors which are all summarized in a paper by Lutenegger and Saber (1988).

2.5 Empirical and Experimental Approaches For Determination of Amount of Volume Change in Partly Saturated Soils :

Some of such relationships were stated earlier in this chapter as those proposed by Lloret and Alonso (equations (2.19), (2.20)). One of the first empirical relationships for assessing volume change behavior of partially saturated soils comes from the research program at M.I.T. (1963). They found that the ordinary effective stress equation will yield in negative value of χ and they proposed the following empirical equation for the volumetric strain :

$$\frac{\Delta V}{V} = \frac{K_1}{\bar{\sigma}}\{\Delta\sigma_a + \Delta(a_i u_c)\} + \frac{K_2}{\bar{\sigma}^2}\{(a_i u_c)\Delta\sigma_a + \sigma_a \Delta(a_i u_c)\} \qquad (2.24)$$

For which :

$\sigma_a = \sigma - u_a$:Applied pressure.

$u_c = u_a - u_w$: Suction pressure.

$\bar{\sigma} = \sigma - u_a + a_i(u_a - u_w)$

a_i is the area ratio of the air water curved meniscus.

K_1 and K_2 : constants for small volume changes.

This equation is not derived rigorously but was intuitively believed to be correct.

Dolezalova and Leitner (1981) used the following relationship based on experimental observations to predict performance of Dalesica Dam :

$$\epsilon_s = [a(w) + b(w)e + c(w)e^2]j^n \qquad (2.25)$$

Where :

ϵ_s : Strain caused by submergence (collapse).

a(w), b(w), and c(w) are coefficients depending on the moisture content before submergence.

n is a constant and j is defined as :

$$j = \frac{\sigma_y}{\sigma_{exp}}$$

σ_y : Current vertical stress on the soil element, and, σ_{exp} is the vertical stress used in laboratory to calculate the coefficients.

Similar relationships were used by Hayashi (1975) to predict settlements in a rockfill dam.

Nwabuokei and Lovell (1986) proposed a method using statistical regression on data obtained from laboratory experimentation on compacted soils. For one dimensional consolidation they obtained the following relationship :

$$\frac{\Delta V}{V}(\%) = -3.0284903 - 0.39039732e_0^2\sqrt{\sigma_0} + 0.63841268e_0\sqrt{\sigma_0}$$

$$-0.32104883\times 10^{-3}w^2\sigma_0 + 0.369098\times 10^{-2}w^2 \qquad (2.26)$$

In which :

e_o :is the as-compacted void ratio.

w : compaction water content.

σ_0 : is the equivalent fill pressure.

Another semi-empirical approach was offered by Nagaraj and Murthy (1985) who used the concept of double layer theory to find the parameters governing the equilibrium condition in partly saturated soils. They indicated that in the equilibrium condition, stress level is a function of void ratio and degree of saturation as follows :

$$\sigma = f\left\{ \frac{e}{e_L} \ , \ \sqrt{S_r} \right\} \qquad (2.26)$$

In this equation e and e_1 are void ratio and void ratio at liquid limit ($e_1=w_1G$), respectively. S_r stands for degree of saturation.

Then by analyzing test results obtained from consolidation tests on partly saturated soils they proposed the following possible form of interaction between various parameters :

$$\frac{e}{e_L}\sqrt{S_r} = a - b\log P \qquad (2.27)$$

Where P is the total stress, a, and b are constants.

Jennings and Knight (1975) put forward the idea of double oedometer test for predicting the amount of collapse in the field. Two undisturbed similar samples are trimmed into consolidometer rings and placed in consolidometer under 1 kPa seating load for 24 hours. At the end of this period one sample is flooded with water while the other is kept at its

natural moisture content. Both samples are left for another 24 hours. If the soaked sample swells, the soil may be of the heaving type and generally for the collapsible soils, the amount of this swell is very small and negligible. Then the test on both samples is carried on as in conventional tests. The consolidation curves thus obtained are adjusted for their initial conditions as shown in Fig. 2.2. Then the change in void ratio, Δe_s, under any load, ΔP and its subsequent collapse Δe_c upon saturation can be determined as shown on Fig. 2.2.

Gibbs and Bara (1962) suggested the use of natural dry density and liquid limit as the criteria for distinguishing collapsible soils. Their method is based on the fact that a soil which has a void ratio greater than the void ratio at liquid limit is susceptible to collapse on wetting. Graphical representation of this idea is shown on Fig. 2.3.

Houston et al (1988) modified the laboratory method proposed by Jennings and Knight by running only a single test for a given soil. The consolidation test is run on the sample at its in situ water content until the stress on the sample is equal to or greater than the stress the soil is expected to experience in the field. At this time the sample is flooded with water and the collapse is monitored. The inundated sample is subjected to additional stress increments to complete the test. Fig. 2.4 shows a typical such curve obtained from the test. Line DA is constructed and used to approximate the soil behavior if the sample was flooded at the beginning of the

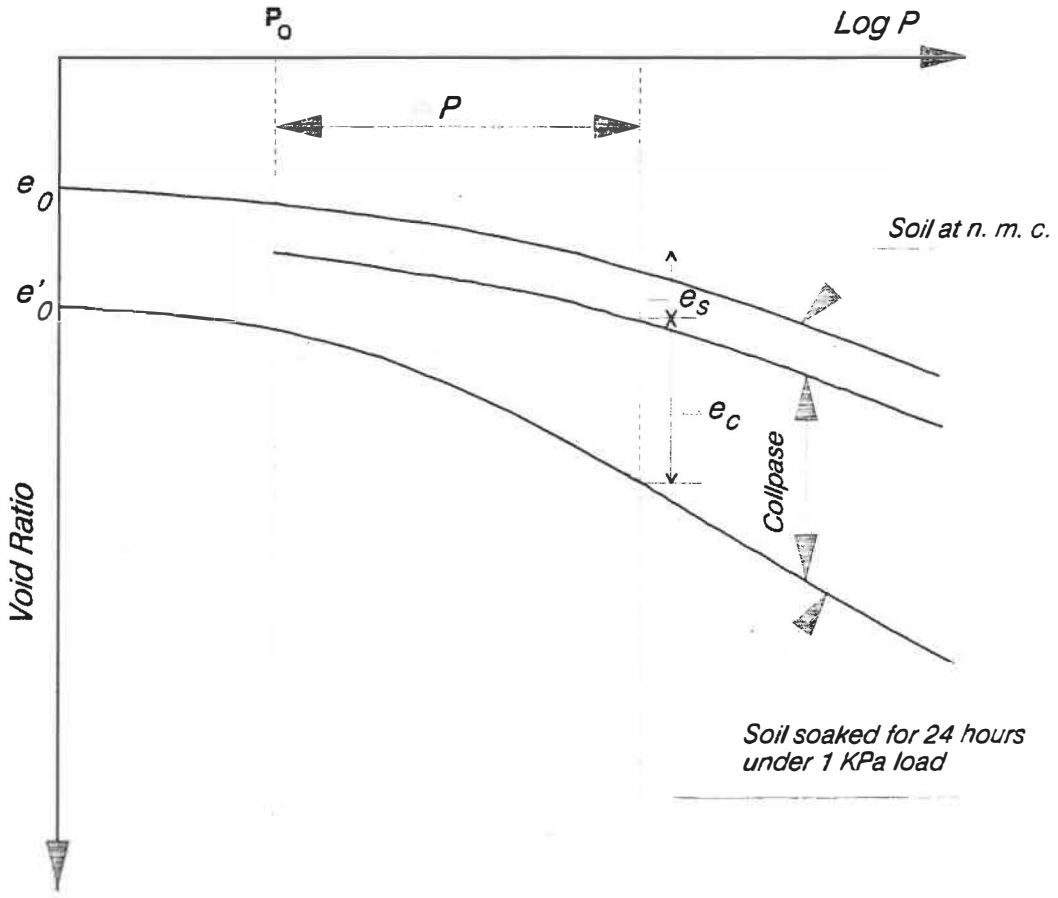

Fig. 2.2 Double Oedometer Test For Normally Consolidated Soils

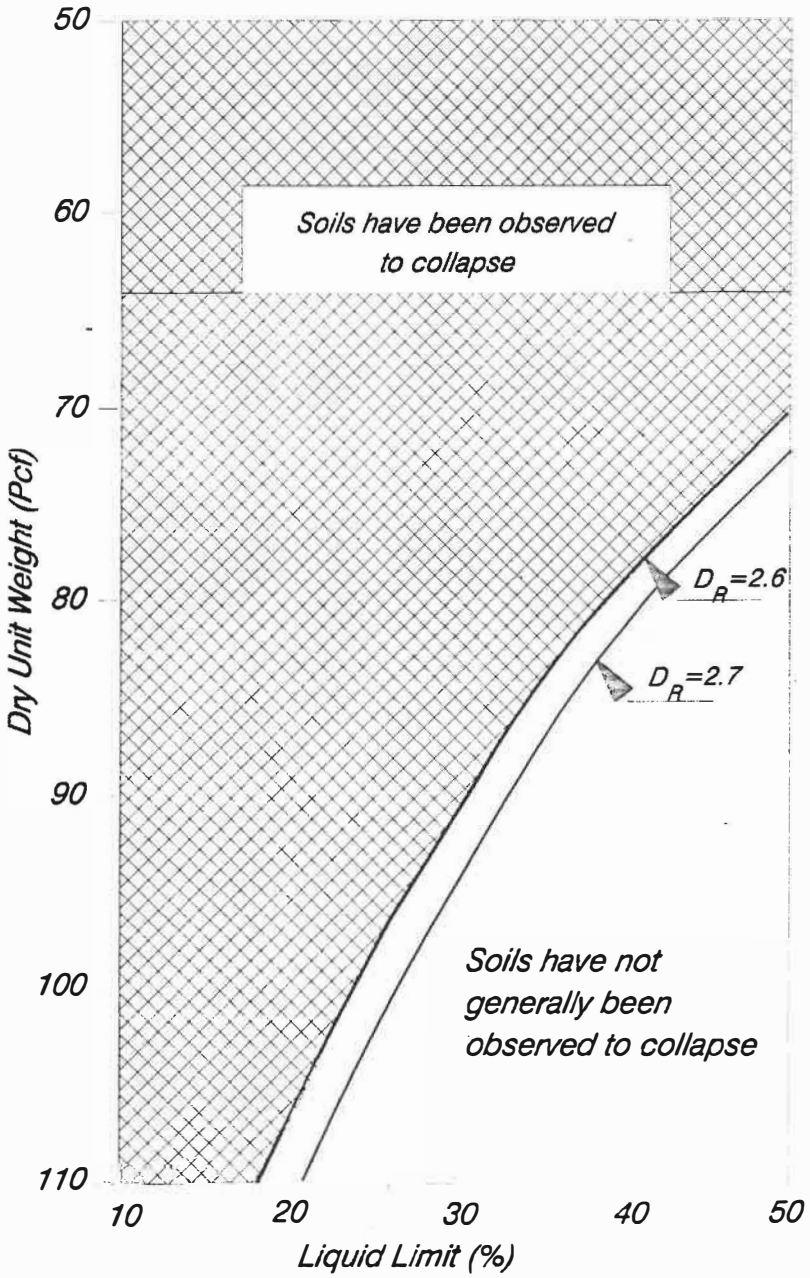

Fig. 2.3 - Collapsible and Non-Collapsible Loess

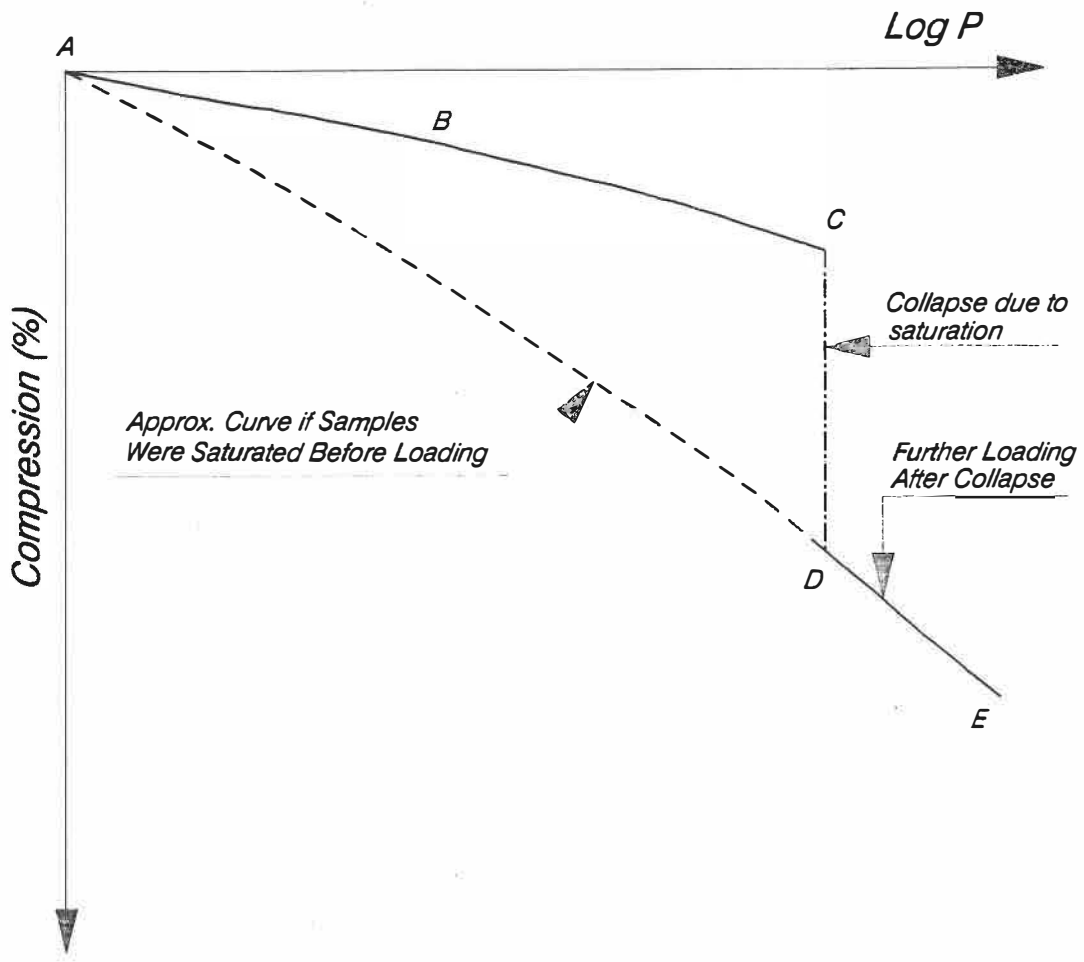

Fig. 2.4 - Typical Curve For Modified Double Oedometer Test

test. By doing a series of such tests for different zones under a foundation, collapse can be predicted. There are two main shortcomings for the above mentioned method and the original method proposed by Jennings and Knight. First, in the latter method suggested by Houston et al, the line DA is roughly constructed which makes it inaccurate for estimating collapse at stress levels other than the one actually tested; secondly, both the latter method and the original method suggested by Jennings and Knight are incapable of predicting the amount of collapse upon partial increase in degree of saturation. For partial increase in saturation degree, the amount of collapse will be somewhere between point C and D in Fig. 2.4 . In fact, this is very common in practical situations where infiltration of water into soil produces zones of different degrees of saturation and partial collapse occurs in each zone responding to the associated increase in degree of saturation.

Josa et al (1987) performed a series of tests with samples prepared from kaolin. They observed different amounts of collapse following different stress paths. The difference in their results should mainly be due to a hysteresis effect resulted from saturation - desaturation since the saturation degree was not monotonically increasing in some of the tests.

CHAPTER 3

PROPOSED MODEL

3.1 General :

In this chapter, first a brief look at the principle of effective stress is presented for both saturated and partly saturated soils. Then the proposed model describing volume change behavior of partly saturated soil is developed. It is noteworthy to emphasize the basic assumption of "compacted soil" as the material dealt with through out this chapter. Therefore, the terms : partly saturated, unsaturated or partially saturated soil refer to a soil artificially compacted such as road embankments, earth dams, ...etc.

Next, the model is discussed and the physical significance of each of its parameters is explained. The method is also verified numerically using a set of available data on a partially saturated soil. Finally, the calibrated model and its prediction for both collapse and swell phenomena is further discussed.

3.2 Effective stress :

3.2.1 Effective stress in saturated soils :

Terzaghi (1936) stated the principle of effective stress as follows :

"...The stresses in any point of a section through a mass of soil can be computed from the total principal stresses $\sigma_1, \sigma_2, \sigma_3$

which act in this point. If the voids of soil are filled with water under a stress u, the total principal stress consists of two parts. One part, u, acts in the water and in the solid in every direction with equal intensity. It is called neutral stress (or pore water pressure). The balance $\sigma_1' = \sigma_1 - u, \sigma_2' = \sigma_2 - u, \sigma_3' = \sigma_3 - u$ represents an excess over the neutral stress u and it has its seat exclusively in the solid phase of the soil...". He added "..this fraction of the total stress will be called effective stresses .... A change in neutral stress produces practically no volume change and has practically no influence on the stress conditions for failure....All measurable effects of a change in stress such as compression, distortion and a change of shear resistance are exclusively due to change in effective stresses $\sigma_1', \sigma_2' \sigma_3'$.

A more general and precise definition of the effective stress principle was stated by Bishop and Blight (1963) as follow :

" The effective stress is by definition that function of total stress and pore pressures which controls the mechanical effects of a change in stress, such as volume change and change in shear strength. The principle of effective stress is the assertion that such a function exists, with determinate parameters, under a given set of conditions".

Based on this definition of effective stress for volume change behavior of a saturated soil we can write :

$$de = C_1 d\sigma' \tag{3.1}$$

or :

$$d\epsilon = C_2 d\sigma' \tag{3.2}$$

Where :

de and $d\epsilon$ are the change in void ratio and volumetric strain respectively.

$\sigma' = \sigma - u$

C_1 and C_2 are compressibility coefficients.

3.2.2 Effective Stress in Partly Saturated Soils :

Bishop (1959) extended the concept of effective stress to partially saturated soils. According to the concept of the effective stress principle, the effective stress must be a function of total stress and pore pressures, i.e. :

$$\sigma' = f(\sigma, u_a, u_w) \tag{3.3}$$

In which σ is total stress, u_a and u_w are pore air pressure and pore water pressure respectively.

Bishop presented the following expression for effective stress in partly saturated soils :

$$\sigma' = \sigma - u_a + \chi(u_a - u_w) \tag{3.4}$$

All terms are as defined before, χ is a parameter which depends on degree of saturation, soil type and hysteresis effects.

If all mechanical effects are attributed to a change in effective stress, for volume change we may write :

$$de = C\,d\sigma' \tag{3.5}$$

or :

$$de = C\,d\{\sigma - u_a + \chi(u_a - u_w)\} \tag{3.6}$$

Applicability of this kind of relationship and validation of effective stress principle in unsaturated soils has been seriously argued by many investigators as discussed in chapter 2. In the following section a mathematical model controlling volume change behavior in partially saturated soils is presented.

3.3 Derivation of Proposed model :

3.3.1 Structure of Compacted soils :

In derivation of the relationship for volume change behavior of unsaturated soils it is assumed that the soil is free from clay bridges and cementation which are usually present in natural soils. This assumption is in agreement with the observations made by authors such as Booth (1975). Hence, the only important mechanism contributing to glue grain particles together is the capillary forces arising by the menisci. This force will contribute to the rigidity of the soil structure. This portion of rigidity produced by capillarity phenomena is further discussed in the following section.

3.3.2 Additional Rigidity Produced by Partial Saturation :

As stated before capillarity acts as cohesion between soil particles and gives rise to another component for the soil rigidity, say K_2. Consider two ideal soil particles, spherical in shape, and bound together by capillary force as shown below:

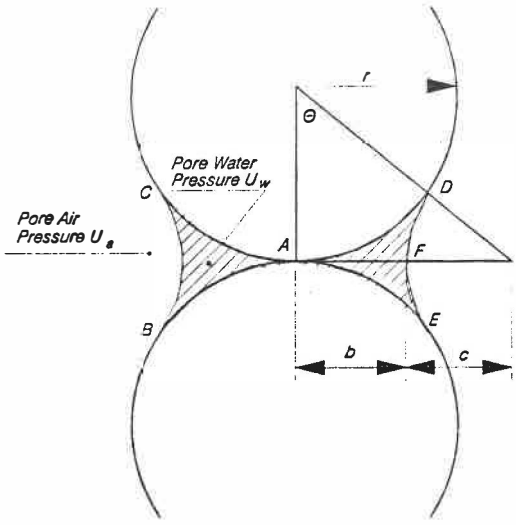

The negative pore pressure and surface tension force will result in a normal force P acting at the contact point between the two particles. The suction pressure (u_a-u_w) may be found from the following relationship :

$$u_a - u_w = T\left(\frac{1}{c} - \frac{1}{b}\right) \qquad (3.7)$$

Where T is the surface tension of soil water (0.0735 N/m, at 20 °C); b and c are radii defining the curved surface of water edge and are related to the sphere radius r, and the subtended angle Θ .

Considering equation (3.7) and equilibrium of the two

spherical particles, the intergranular force P may be expressed as :

$$P = \frac{\pi T r \tan\theta(\mathrm{Sin}\,\theta + \cos\theta - 1)}{(1 - \cos\theta)} \qquad (3.8)$$

This equation indicates the direct dependence of the intergranular force P on the subtended angle θ or, in other words, the degree of saturation.

If we assume simple friction law at contact points, the maximum value of the resistance force will be $F=\mu P$; where μ is a friction coefficient. Note that the force F is directly a function of negative pore water pressure and thus degree of saturation. Consequently this stiffness increases with a decrease in degree of saturation which is accompanied by an increase in negative pore water pressure. At any stage during loading, only a portion of this resistive force is mobilized and as the strain level increases, more of this frictional resistance is mobilized and also more particles become active in contributing to this resistance. Therefore, rigidity produced because of partial saturation is not only a function of degree of saturation but also strain level as well, i.e. $K_2(S,\epsilon)$. This conclusion is well in agreement with experimental observations as will be explained in section 3.4 of this chapter.

3.3.3 Development of the Model :

Before proceeding forward it is necessary to state the assumptions made explicitly or implicitly in deriving the proposed model. It is assumed that the soil is homogeneous and artificially compacted without any cementation (due to organic matter or carbonates). Since hysteresis causes certain non-unique characteristics in soils, it is assumed that saturation degree has increasing value, in other words, hysteresis phenomena is prevented.

Let $K_2(S,\epsilon)$ represent the additional stiffness of soil structure as a result of partial saturation. According to the principle of effective stress we can write :

$$d\sigma' = (K_1(\epsilon) + K_2(S,\epsilon))de \qquad (3.9)$$

or :

$$d\sigma' = (K_1(\epsilon) + K_2(S,\epsilon))d\epsilon \qquad (3.10)$$

In which :

$d\sigma'$: the change in effective stress (effective stress refers to equation (3.4) proposed by Bishop).

$K_1(\epsilon)$: Rigidity of soil as a result of applied load.

$K_2(S,\epsilon)$: rigidity resulted from partial saturation.

de and $d\epsilon$: Change in void ratio and volumetric strain respectively.

But equations of this form can not deal with the cases where rigidity of soil may change upon saturation ("collapse phenomena"). In other words, this type of expression is only

suitable for dealing with deformation resulting from a change in effective stress and is incapable of predicting deformation produced by a change in the rigidity of soil skeleton. A more general relationship may be written in the following form :

$$d\sigma' = (K_1(\epsilon) + K_2(S,\epsilon))d\epsilon + \beta dK_2(S,\epsilon) \qquad (3.11)$$

In which the second term takes into account the change in modulus with a change in degree of saturation. The reason why this type of equation is valid for partially saturated soils and the exact form of the second term are discussed next.

For each increment of strain the amount of force taken by the rigidity coming from partial saturation is equal to $K_2(S,\epsilon)d\epsilon$. The total force taken by this rigidity at any strain level is equal to :

$$\int_0^{\epsilon} K_2(S,\epsilon)d\epsilon$$

Upon an increase in the degree of saturation, the stiffness $K_2(S,\epsilon)$ will drop in magnitude and the soil skeleton loses some of its rigidity depending on the amount of increase in saturation degree. If the degree of saturation at any stage during loading is S_1 and the increase in degree of saturation is ΔS_1 then the force taken by the soil structure due to degree of saturation S_1 is equal to :

$$\int_0^{\epsilon} K_2(S_1,\epsilon)d\epsilon$$

And the force taken by the soil structure, if it had the degree of saturation $S_i+\Delta S_i$ for the same strain level, is given

by :

$$\int_0^{\epsilon} K_2(S_i+\Delta S_i,\epsilon)d\epsilon$$

Therefore the change in load carrying capacity of the soil structure due to partial increase in degree of saturation ΔS_i is equal to :

$$\int_0^{\epsilon} K_2(S_i+\Delta S_i,\epsilon)d\epsilon-\int_0^{\epsilon} K_2(S_i,\epsilon)d\epsilon=\int_0^{\epsilon}\frac{\partial K_2(S,\epsilon)}{\partial S}dSd\epsilon \quad (3.12)$$

This means that an equivalent of the same amount of force is redistributed on the present rigidity available, that is, $K_1(\epsilon)$ and the remaining $K_2(S, \epsilon)$ resulting in more deformation at constant applied load, that is, the so-called collapse.

Therefore the equation (3.11) can be written in the general form of :

$$d\sigma'-\int_0^{\epsilon}\frac{\partial K_2(S,\epsilon)}{\partial S}dSd\epsilon=(K_1(\epsilon)+K_2(S,\epsilon))d\epsilon \quad (3.13)$$

In this expression the term :

$$-\int\frac{\partial K_2(S,\epsilon)}{\partial S}dSd\epsilon$$

is the force released upon an increase in degree of saturation. The negative sign is introduced to counter balance the sign for a change in $K_2(S,\epsilon)$ which is negative for an increase in

degree of saturation. Rewriting equation (3.11) in the following final form yields :

$$d\sigma' = \{K_1(\epsilon) + K_2(S,\epsilon)\}d\epsilon + \int_0^{\epsilon} \frac{\partial K_2(S,\epsilon)}{\partial S} ds d\epsilon \qquad (3.14)$$

In this equation σ' is the effective stress relationship defined by Bishop (eq. (3.4)). $K_1(\epsilon)$ is the soil rigidity in the fully saturated state and $K_2(S,\epsilon)$ is the soil rigidity due to partial saturation.

In the proposed model (eq. (3.14)), value of σ' is substituted by the equation (3.4) proposed by Bishop for the effective stress. The mathematical form of the proposed model is evidently in disagreement with the principle of effective stress which states that any change of mechanical properties is solely related to a change in effective stress. On the other hand, in partially saturated soils an increase in the degree of saturation would result in a change in total rigidity of the soil. Therefore, the soil structures before and after saturation are not similar. Effective stress principle is not applicable for a transition between the soil structures. Consequently applicability or inapplicability of the effective stress principle may be argued from different points of view. At this stage, the author suggests that the value of σ' given by equation (3.4) be regarded as an intergranular stress to avoid confusion for its use in the model. Henceforth, the term "effective stress" implies this intergranular stress.

3.4 Significance of the model parameters :

3.4.1 Rigidity K2(S,ϵ) :

In the previous section the nature of rigidity arising from partial saturation was discussed. It was shown that it is a function of degree of saturation as well as strain level. This fact can be further verified by experimental results available for partially saturated soils. The Fig. 3.1 shows a schematic representation of strain-stress behavior of such results for Ko-compression condition of a partially saturated soil (curve A). Curve B is compression behavior of the same soil in fully saturated condition.

In this figure σ is the applied total stress which is also equal to effective stress for the saturated soil since $u_w=0$ in this case.

The necessary load to reach to a certain strain level ϵ_1 for the case of saturated soil is equal to σ_{1s} as shown on the figure. But for the partially saturated soil to reach to the same strain level the required load is equal to σ_1. The stress σ_{1s} represents the amount of load carried by the soil skeleton in absence of capillary forces. Hence, the difference $\sigma_1 - \sigma_{1s}$ gives an idea of the excess load carried as a result of partial saturation to reach to the same strain level. This extra force corresponds to the additional rigidity of soil structure due to partial saturation, i.e., $K_2(S,\epsilon)$. Curve C in the previous figure represents the difference of curve A and B subtracted

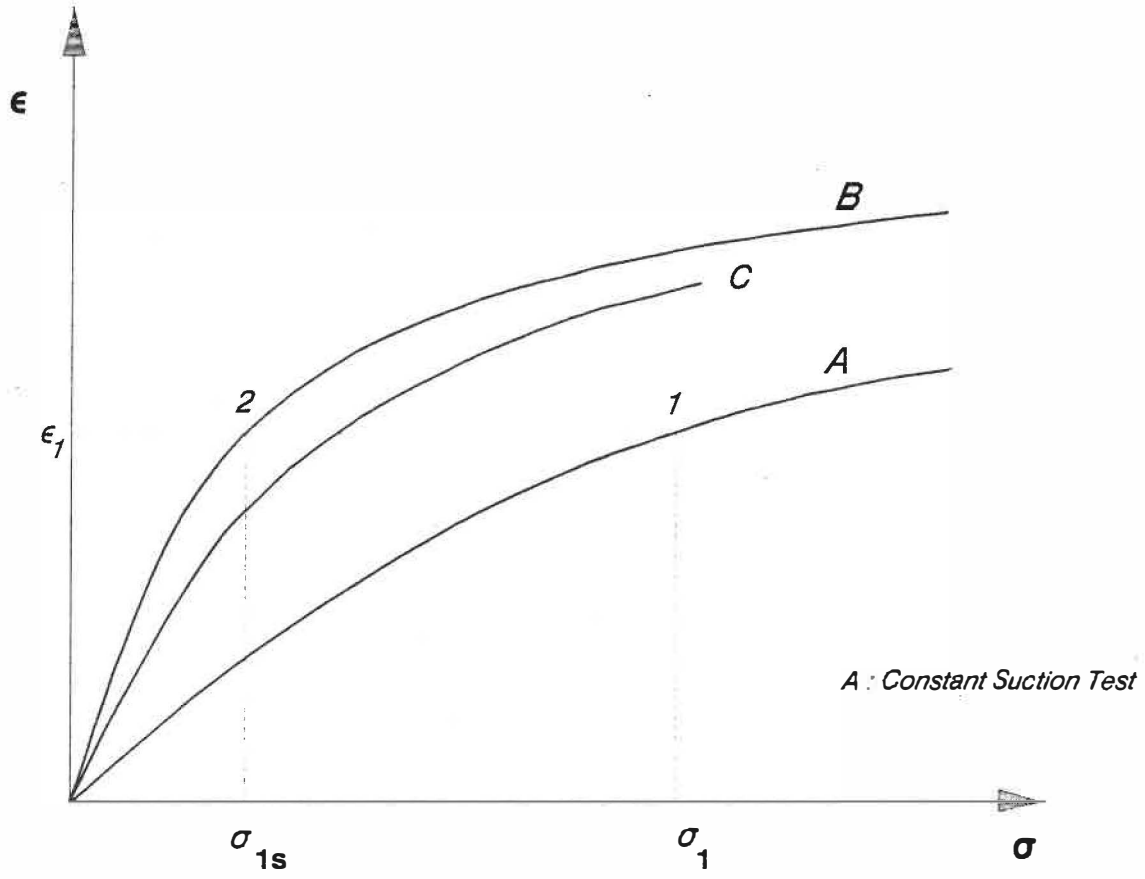

Fig. 3.1 - Schematic Representation of Ko Compression Test on Partially Saturated Soil

at same strain levels. As shown on the figure this difference is not a straight line supporting the previous discussion that this stiffness is not only a function of degree of saturation but strain level as well. It is worth stating that the curve for partly saturated soil is obtained under constant suction which means that the degree of saturation is essentially constant throughout the test (in reality there is a little change in degree of saturation with change in stress level at constant suction test but the change is not considered to be significant).

The dependence of the additional rigidity due to partial saturation on strain level is well in agreement with investigations documented by many researchers who have shown that the collapse phenomenon is stress-level dependent. Since stress and strain are inter-related by the constitutive equation, $K_2(S,\epsilon)$ indirectly depends on stress level.

3.4.2 Significance of χ Parameter :

In order to investigate the significance of the χ parameter in the Bishop's relationship for effective stress (equation (3.4)), consider the schematic representation of oedometric test results, Fig. 3.2, on two identical samples but one saturated at the beginning of the test (curve A). Curve B is the compression of the sample with natural moisture condition. At a given applied stress the unsaturated sample will have a strain ϵ_1 if at this strain the sample is inundated and the

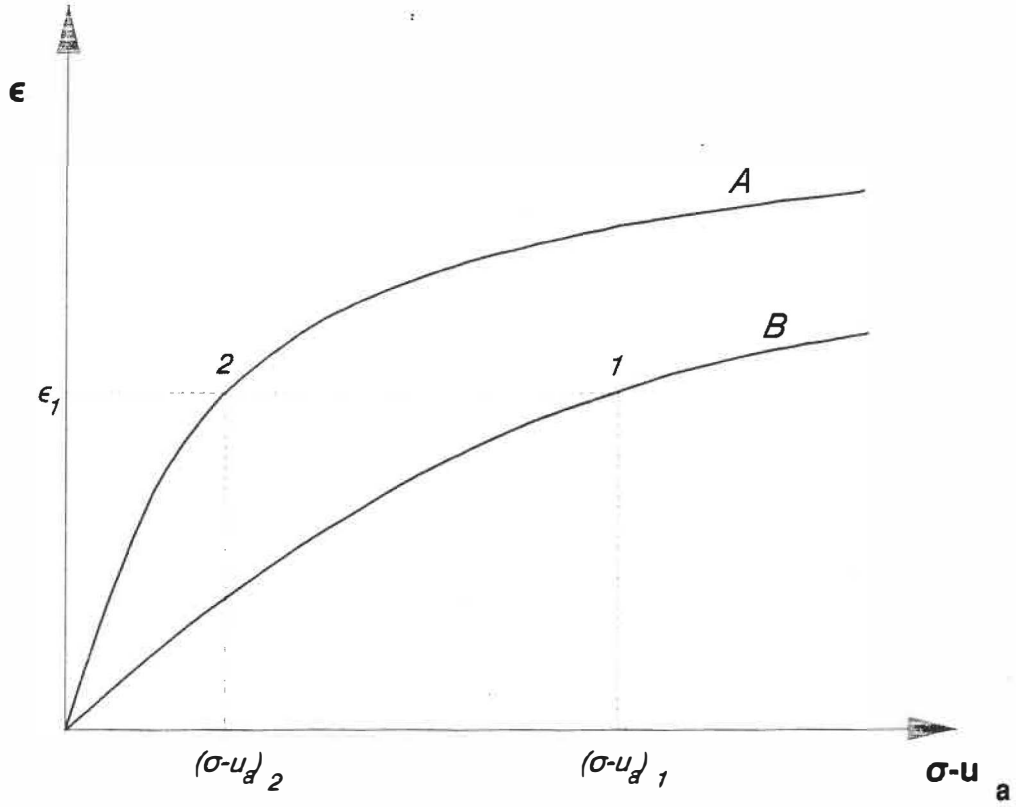

Fig. 3.2 - Typical Oedometric Behavior of Partially Saturated Soils

strain is held constant, it will follow the path 1-2 shown on the figure.

If we assume the applicability of principle of effective stress we have :

$$d\sigma' = K\,d\epsilon \qquad (3.15)$$

and :

$$\sigma' = (\sigma - u_a) + \chi(u_a - u_w)$$

Therefore :

$$d(\sigma - u_a) + d(\chi(u_a - u_w)) = K\,d\epsilon$$

In which :

σ : Applied total stress.

u_a : Pore air pressure.

u_w : Pore water pressure.

K : Stiffness of the soil.

χ : Parameter which is function of degree of saturation, soil type, and hysteresis effects.

In the absence of hysteresis and for a particular soil χ is only a function of saturation degree. For the test explained, since $d\epsilon=0$, we have :

$$d(\sigma - u_a) + d(\chi(u_a - u_w)) = 0 \qquad (3.16)$$

or, in terms of points 1 and 2 for the path shown on Fig. 3.2:

$$(\sigma - u_a)_2 - (\sigma - u_a)_1 + \chi_2(u_a - u_w)_2 - \chi_1(u_a - u_w)_1 = 0 \qquad (3.17)$$

Because at point 2 we have full saturation, consequently $(u_a-u_w)_2=0$, which gives :

$$\chi_1 = \frac{(\sigma - u_a)_2 - (\sigma - u_a)_1}{(u_a - u_w)_1} \tag{3.18}$$

The denominator of equation (3.16) is always positive but the numerator is negative since $(\sigma-u_a)_2$ is always less than $(\sigma-u_a)_1$. This will yield negative values for the χ parameter and since the χ parameter can only have positive values between zero and one, it imposes a limitation to the use of the effective stress principle in unsaturated soils.

Now, we apply the proposed model to investigate the χ parameter for the same conditions considered. According to the model we have :

$$d\sigma' = \{K_1(\epsilon) + K_2(S,\epsilon)\}d\epsilon + \int_0^{\epsilon} \frac{\partial K_2(S,\epsilon)}{\partial S} ds d\epsilon \tag{3.19}$$

Since $d\epsilon=0$ and substituting for σ' will give :

$$d(\sigma - u_a) + d(\chi(u_a - u_w)) = \int_0^{\epsilon} \frac{\partial K_2(S,\epsilon)}{\partial S} ds d\epsilon \tag{3.20}$$

Rewriting equation (3.20) for the path 1-2 on Fig. 3.2 and putting $(u_a-u_w)_2=0$ will yield :

$$\chi = \frac{d(\sigma - u_a) - \int_0^{\epsilon} [\partial K_2(S,\epsilon)/\partial S] ds d\epsilon}{(u_a - u_w)_1} \tag{3.21}$$

Here the denominator is positive, $\Delta(\sigma - u_a)$ is negative but the second term in the numerator is positive since an increase

in the degree of saturation will be always accompanied with a reduction in stiffness $K_2(S,\epsilon)$ i.e. :

$$-\int_0^{\epsilon}\frac{\partial K_2(S,\epsilon)}{\partial S}dsd\epsilon > 0$$

Therefore the χ parameter will be positive with the following condition :

$$\left|\int_0^{\epsilon}\frac{\partial K_2(S,\epsilon)}{\partial S}dsd\epsilon\right| \geq |\Delta(\sigma - u_a)| \qquad (3.22)$$

It will be shown later in this chapter that this condition is numerically satisfied when actual test results are used.

3.4.3 Critical Applied Stress :

Critical applied stress is defined as the load at which a compacted fill changes over from swelling to decrease in volume on saturation. The magnitude of this load depends on the soil type, compactive effort, and placement water content. It may be found from the proposed model by applying the necessary conditions, that is, $d\epsilon=0$ and since the applied load is held constant $d\sigma$ is equal to zero too. Substituting these values in equation (3.14) yields :

$$d(-u_a) + d(\chi(u_a - u_w)) = \int_0^{\epsilon}\frac{\partial K_2(S,\epsilon)}{\partial S}dsd\epsilon \qquad (3.23)$$

If the air pores are considered continuous with atmospheric pressure, $u_a=0$, then :

$$d(-\chi u_w) = \int_0^{\epsilon}\frac{\partial K_2(S,\epsilon)}{\partial S}dsd\epsilon \qquad (3.24)$$

Knowing the appropriate function for $K_2(S,\epsilon)$ the above equation would give the proper strain level associated with the critical applied stress. This strain level may be called critical strain level. A numerical procedure to determine the critical applied stress is demonstrated in section 3.6.

3.5 Further Development of The Model :

Substituting for σ' in the model (eq. (3.14)) will give:

$$d(\sigma - u_a) + d(\chi(u_a - u_w)) = \{K_1(\epsilon) + K_2(S,\epsilon)\}d\epsilon + \int_0^{\epsilon} \frac{\partial K_2(S,\epsilon)}{\partial S} ds d\epsilon \qquad (3.25)$$

In order to solve any volume change problem with this equation it is necessary to define three functions, namely, $K_1(\epsilon)$, $K_2(S,\epsilon)$, and χ. The stiffness $K_1(\epsilon)$ according to its definition is independent of capillarity and degree of saturation and therefore can be found by means of test results carried out on same soil samples but flooded at the beginning of the test.

Because of the complexities in the nature of $K_2(S,\epsilon)$, it is postulated that a suitable form may be expressed as multiplication of two separate functions :

$$K_2(S,\epsilon) = f_1(S).f_2(\epsilon) \qquad (3.26)$$

These two functions were then interrelated only by imposing physical boundary through conditions such as :

$$K_2(S,\epsilon)|_{s=1.0} = 0 \qquad (3.27)$$

For the first function since the rigidity decreases rapidly with increase in degree of saturation the following expression was used :

$$f_1(S) = B_1 e^{-\alpha S^D} \tag{3.28}$$

where : α, B_1, and D are dimensionless constants.

S is the degree of saturation.

Fig. 3.3 shows the shape of this function depending on the value of the constant D. It is clear that this function has good flexibility for describing the variation of rigidity with degree of saturation.

The function $f_2(\epsilon)$ represents the effect of strain level on magnitude of the stiffness produced. Since the mobilization of this part is similar to the increase in rigidity of a saturated sand under isotropic confining pressure and since in this case the stress strain relationship is best described by a hyperbolic relationship, then this part of rigidity may be expressed as follow :

$$f_2(\epsilon) = \frac{B_2 P_a}{(1 - C\epsilon)^2} \tag{3.29}$$

In which B_2 and C are dimensionless constants and P_a is the atmospheric pressure. Other parameters are as defined before. Substituting equations (3.28) and (3.29) in (3.26) yields :

$$K_2(S, \epsilon) = \frac{B P_a}{(1 - C\epsilon)^2} e^{-\alpha S^D} \tag{3.30}$$

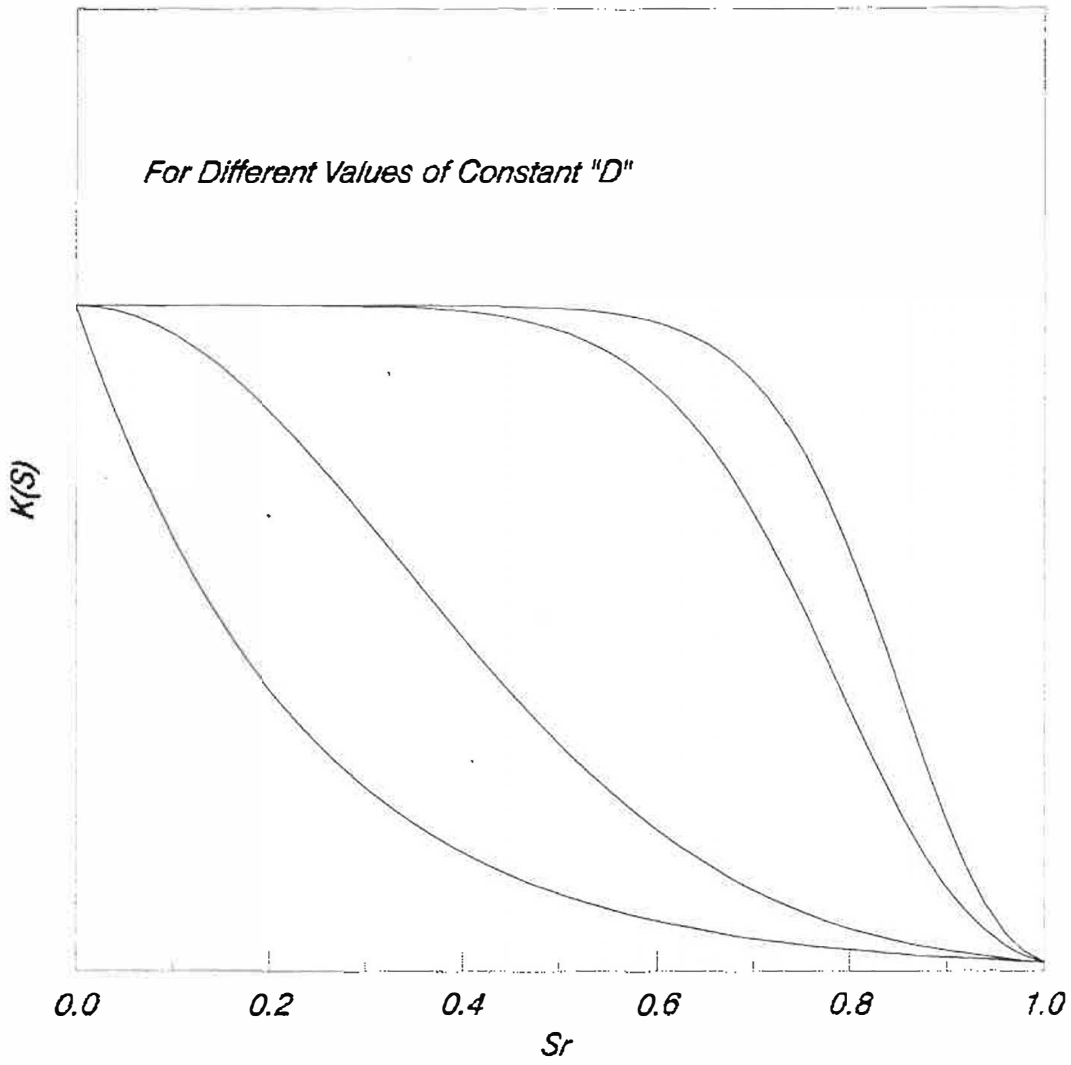

Fig. 3.3 - Variation of K(S) With Degree of Saturation

where $B=B_1B_2$. By imposing the condition of equation (3.27) ($K_2(S,\epsilon)|_{s=1.0}=0.5P_a$ is assumed) one of the constants can be determined and after some mathematical manipulations equation (3.30) can finally be written as follows :

$$K_2(S,\epsilon)=0.5P_a\left\{\frac{2B}{(1-C\epsilon)^2}\right\}^{1-S^D} \qquad (3.31)$$

In this equation B and D are two dimensionless constants, ϵ, S, and P_a are strain, degree of saturation, and the atmospheric pressure respectively.

Another function in the model is the χ parameter. This parameter is only a function of degree of saturation for a particular soil if hysteresis is prevented, i.e. $\chi=f(S)$. Based on physical and theoretical evidences, since f(s) represents the fraction of pressure deficiency contributing to the effective stress, it has a value between zero and one. Hence the following function was considered to have necessary requirements :

$$f(s)=1.1(1-e^{-2.4s^A}) \qquad (3.32)$$

In which : S: degree of saturation.

A: constant.

This function satisfies the necessary limiting conditions of f(S)=0 for S=0 and f(S)=1 for S=1. Moreover, it can assume different behaviors between these limits based on the value of the constant A as shown in the Fig. 3.4.

Finally, if equations (3.31) and (3.32) are substituted

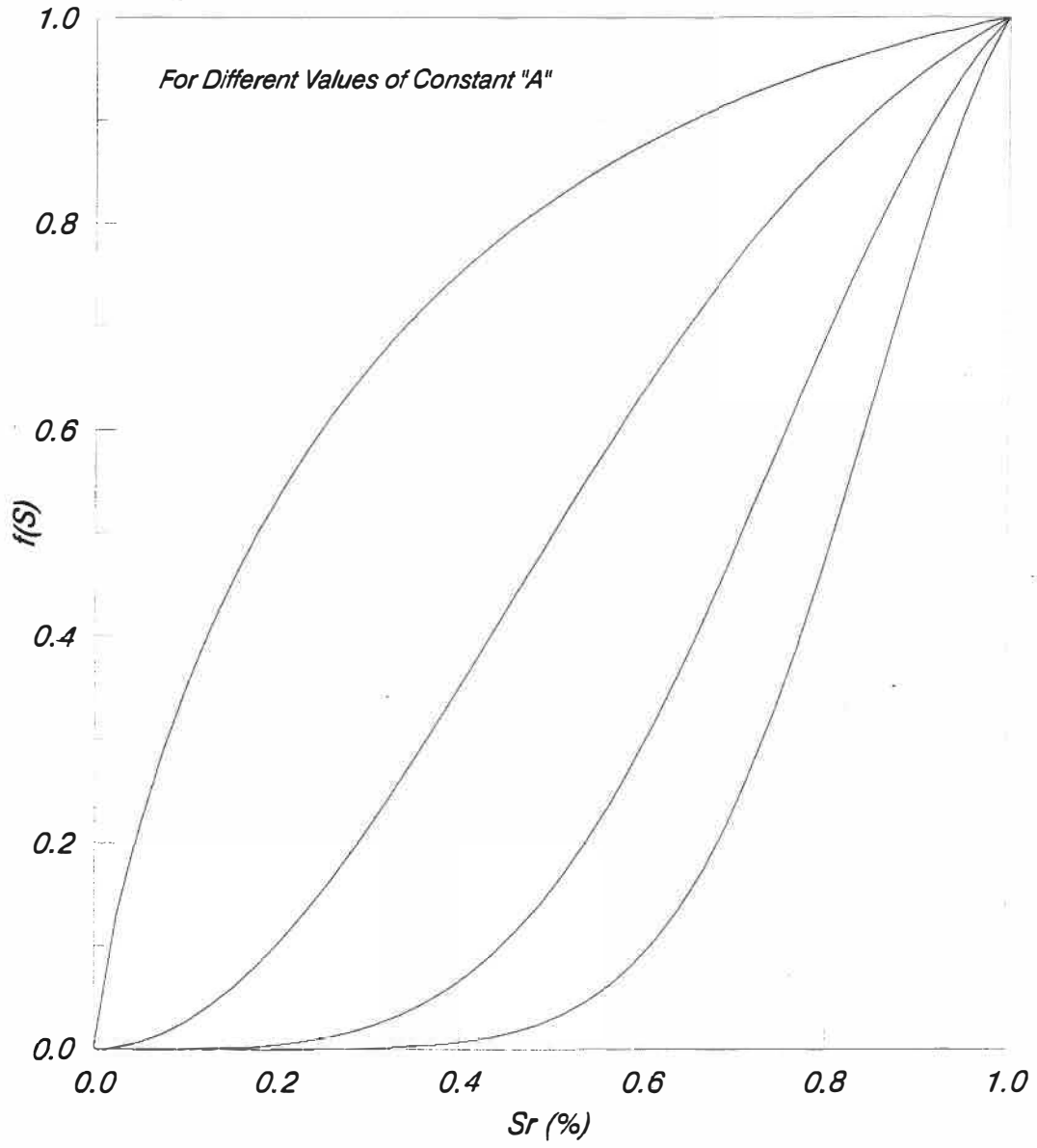

Fig. 3.4 - Variation of f(S) With Degree of Saturation

into the model (eq. (3.25)) it will give rise to four constants A, B, C, and D. These constants must be determined using experimental data obtained from tests performed on the particular soil under consideration. For this purpose a mathematical method using a non-linear optimization scheme with constraints was used to find the constants. Further explanation is provided in the following section.

3.6 Numerical Verification of the Model :

A computer program was prepared to calibrate the model by a difference method using a non-linear optimization scheme with constraints (Box 1966). A set of data obtained from experimental results published by Matyas and Radhakrishna (1968) were used to calibrate the model. The calibrated model together with experimental data is shown in Fig. 3.5, 3.6, and 3.7.

Graphical representation of the two functions f(S) and $K_2(S,\epsilon)$ for this particular soil is also shown in Fig. 3.8 and 3.9, respectively. Furthermore, the capability of the model to predict collapse phenomena was tested by keeping the load constant and increasing the degree of saturation. The amount of collapse predicted at three different stress levels versus the experimentally measured values are given below :

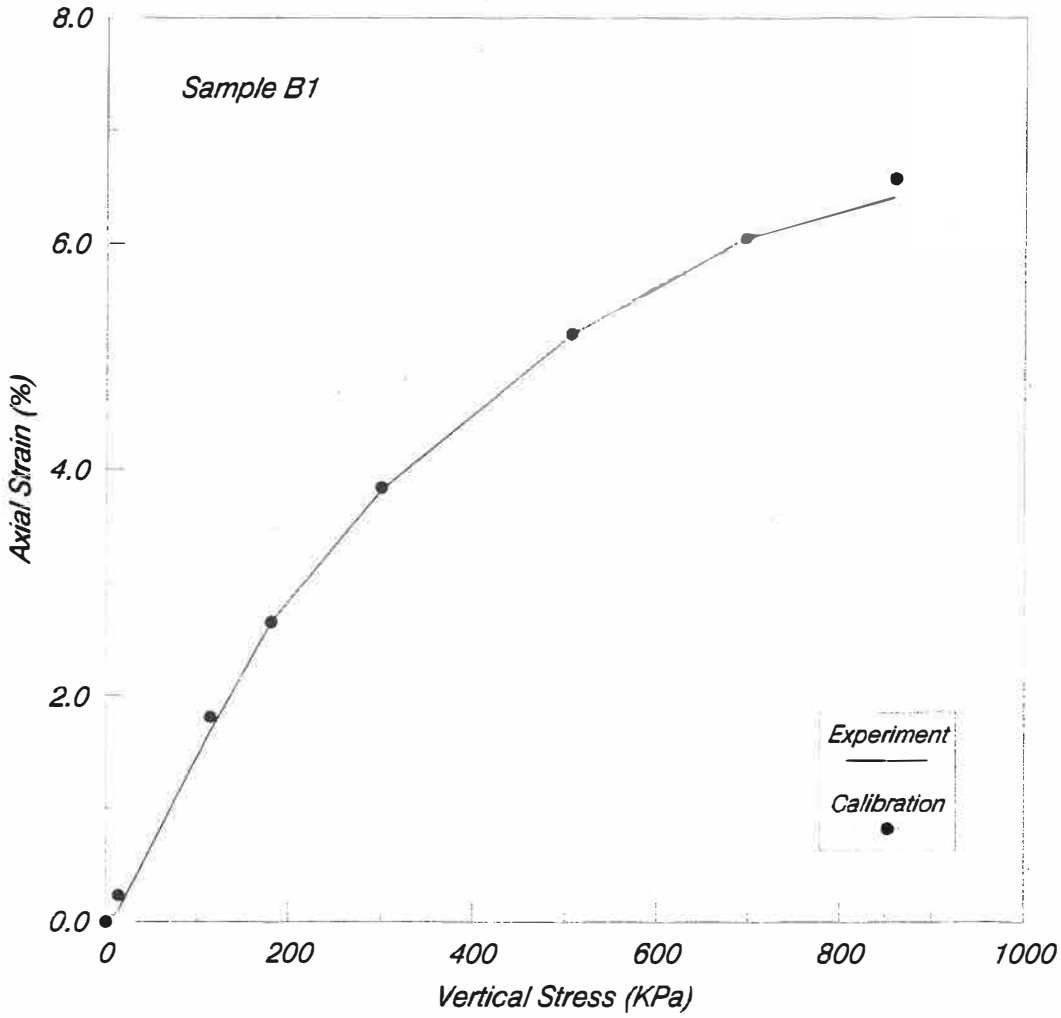

Fig. 3.5 - Stress Strain Relationship For Ko - Compression

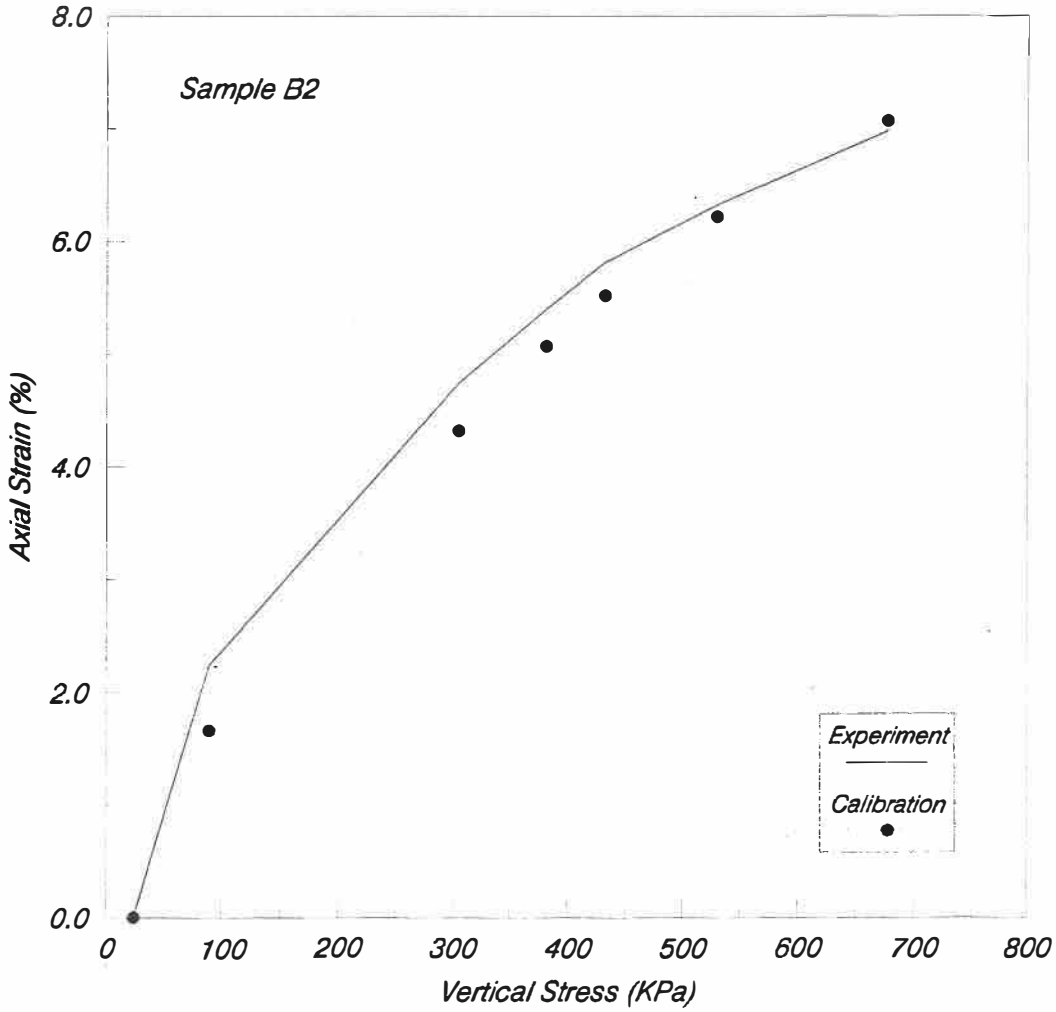

Fig. 3.6 - Stress Strain Relationship For Ko - Compression

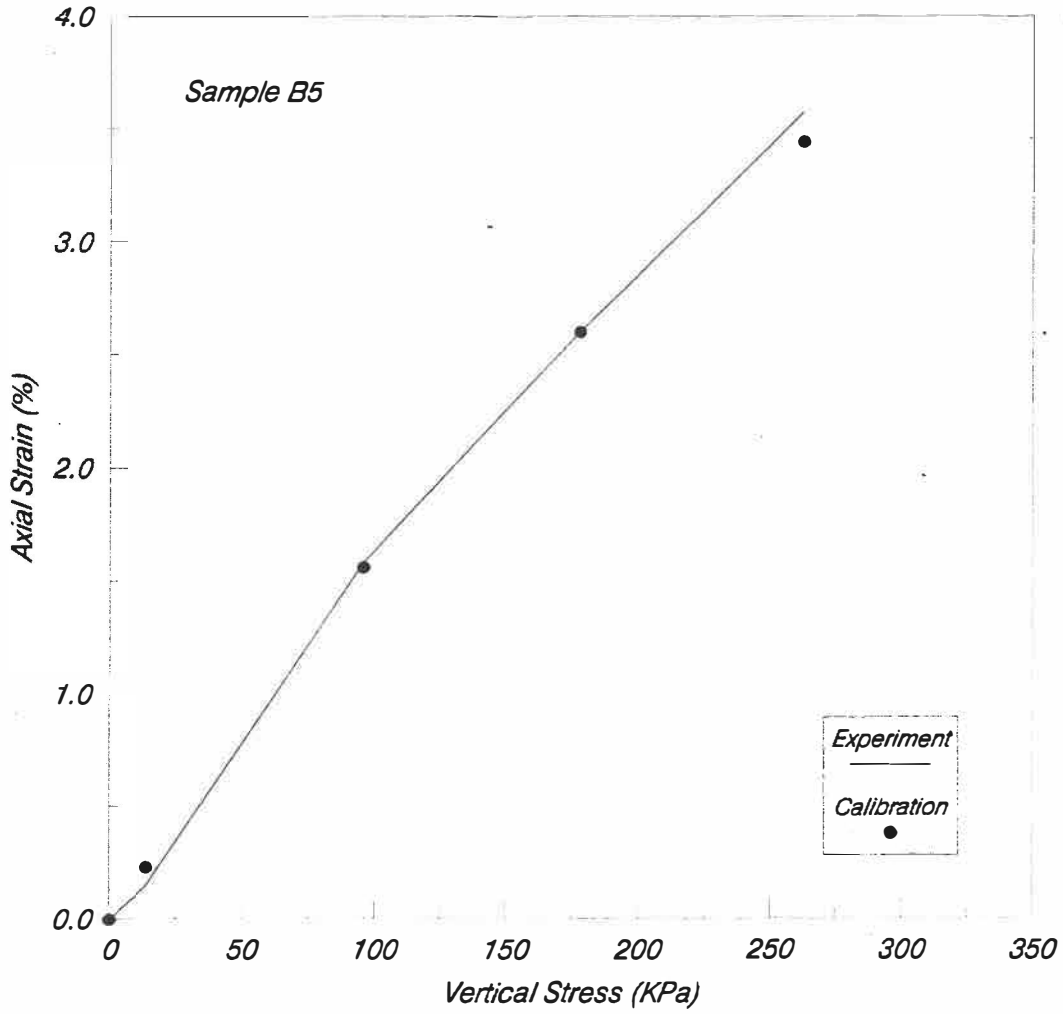

Fig. 3.7 - Stress Strain Relationship For Ko - Compression

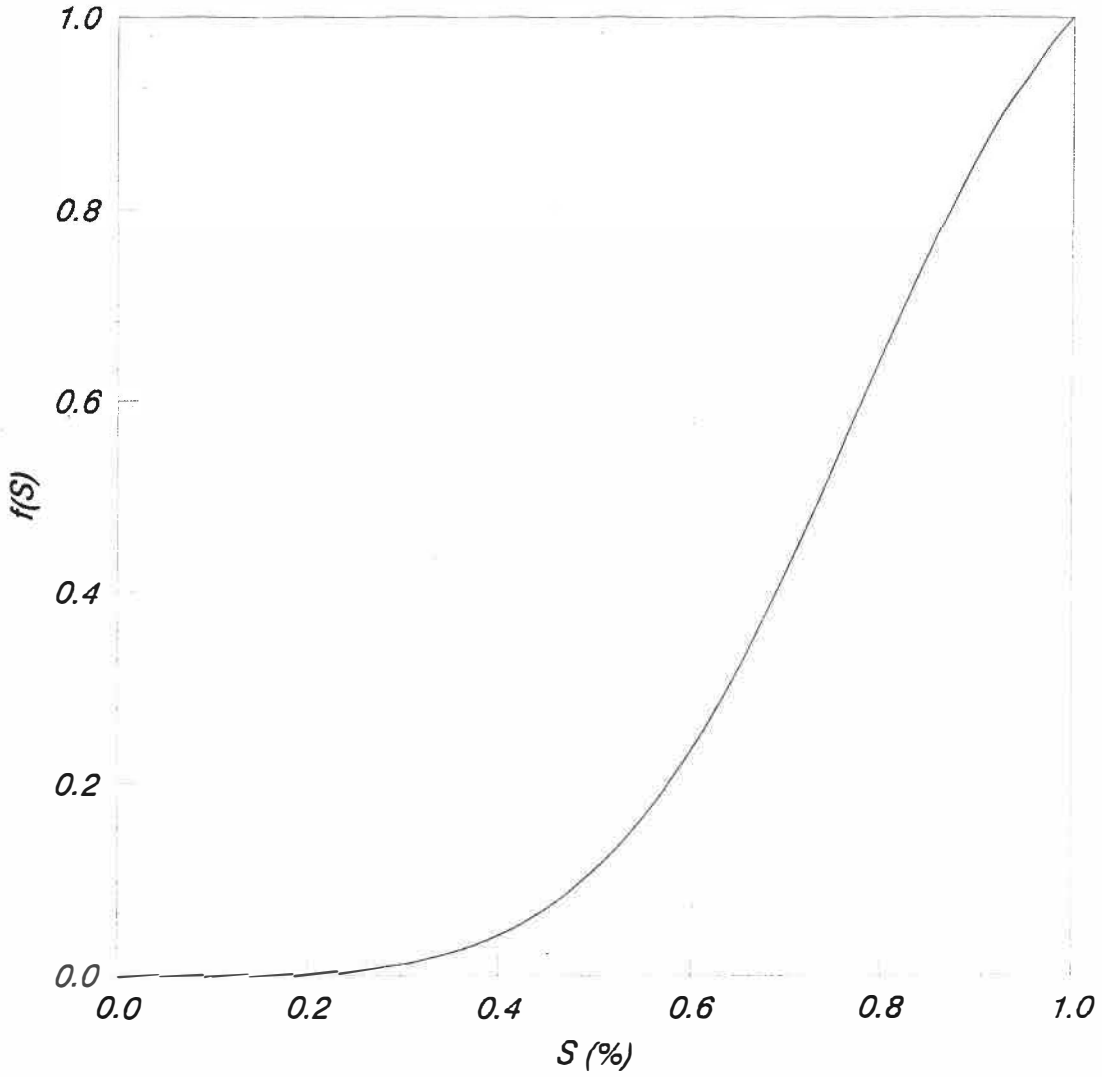

Fig. 3.8 - f(S) Function

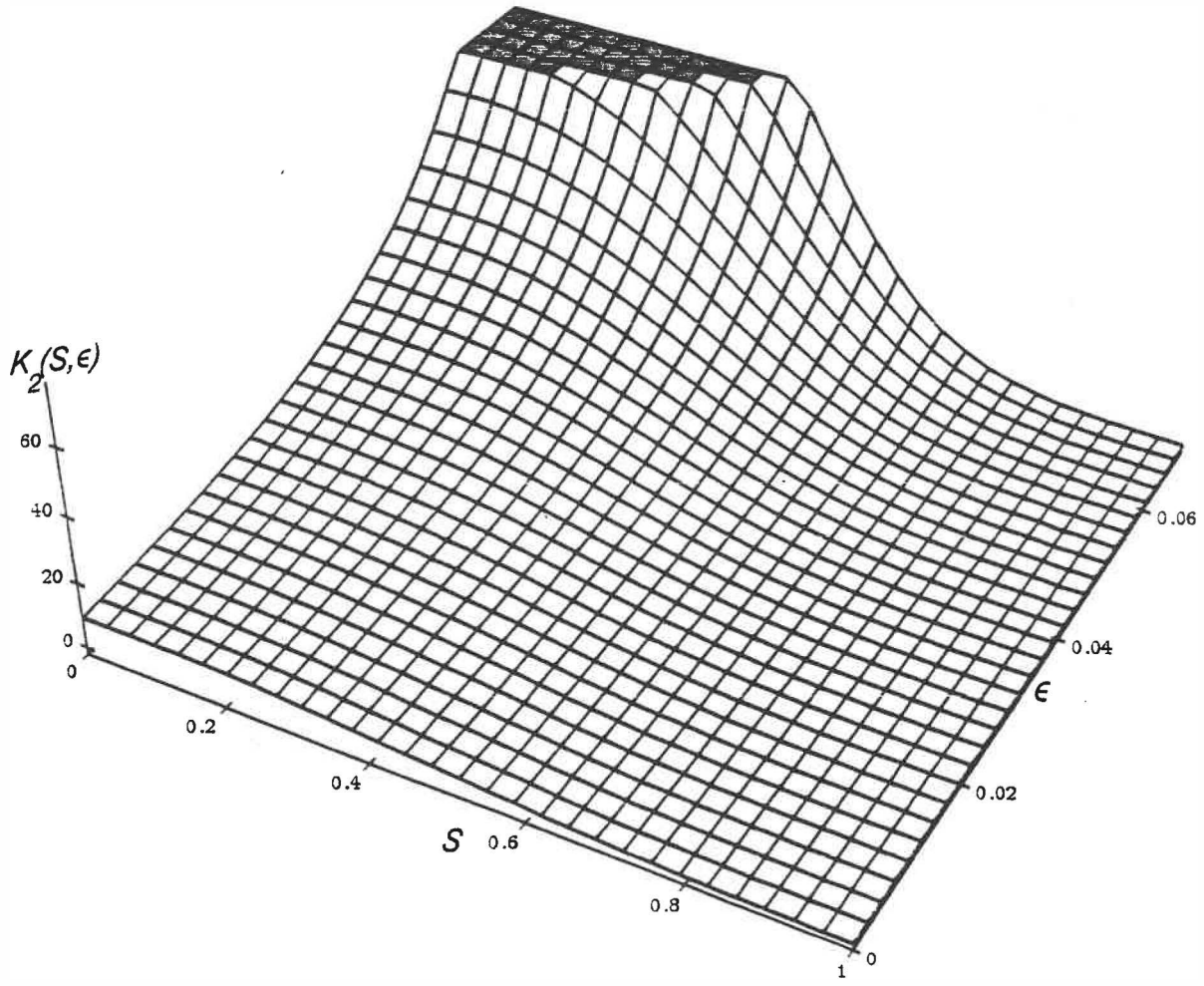

Fig. 3.9 - Function $K_2(S,\epsilon)$

Sample	Stress-Level (kPa)	Collapse (exp. %)	Collapse (pred. %)
B1	860	3.1	2.9
B2	678	1.7	1.8
B5	263	2.1	2.5

As shown, the model is fairly accurate in predicting the collapse phenomenon. The model is also capable of predicting swell if present. For instance, for this set of data the authors had observed swelling potential at low applied stresses. They stated that the critical applied stress for which no swelling or collapse occurred on wetting was between 70 and 84 kPa. The model was tested for the two stresses of 70 and 113 kPa and it gave $d\epsilon=-3.69\times10^{-3}$ and $d\epsilon=+7.76\times10^{-3}$ respectively. With a linear interpolation, the critical stress is estimated to have the value of 84 kPa which is fairly close to the experimental range given by the authors.

3.7 Extension of The Model For Two Dimensional Conditions :

In order to apply the developed model to two dimensional problems certain hypotheses should be made. Hayashi (1975) assumed that the collapse phenomena occurred mainly in the direction of gravity in order to assess the amount of settlements in a rockfill dam upon impoundment of the reservoir. This assumption is not in agreement with experimental observations which, for instance, indicate that an almost isotropic collapse deformation would happen under isotropic

loading. It may be justified, however, for certain areas in an embankment where the state of stress is close to K_o condition and the major principal stress has the same direction as gravity. Consequently, this assumption does not serve as a suitable tool for interpreting two dimensional collapse behavior.

A more reasonable hypothesis which is in accord with the experimental evidence would be to assume that the principal directions of collapse strain coincide with those of the total stress. Therefore, the term accounting for collapse deformation in the proposed model can be evaluated in the principal stress directions to obtain the principal collapse forces (stresses) and thereby the collapse stresses in the coordinate of the problem. Details for a non - linear formulation of the model for two dimensional applications are described in chapter 5.

CHAPTER 4

EXPERIMENTATION

4.1 General :

The purpose of this experimental work is to investigate the presence of collapse phenomenon in a glacial till soil that has been used as core material for embankment dams in North-East Canada. It is also intended to develop suitable equipments and to lay out an experimental procedure for testing partially saturated soils. The equipment and experimental procedure described in this chapter can provide necessary data in order to calibrate the proposed model described in the previous chapter.

4.2 Soil Description and basic properties :

The term till is frequently used to describe a heterogeneous mixture of clay, silt, sand, and gravel. From a geological point of view glacial tills are the result of glacial abrasion and mechanical disintegration of parent rocks. The soil used in this study was air dried bulk samples of till brought from North-East Quebec in James Bay area, about 1000 Km from Montreal. This type of material is very abundant in this area and is widely used as core material in construction of earth dams (La Grande Complex of the James Bay Hydro-electric project). The main reason behind its use in these projects is its good mechanical properties such as high friction angle (in the range of 34 to 45 degrees), and low coefficient of

permeability of the order 10^{-8} to 10^{-10} m/s for a range of compaction degrees of .96 to 1.06 (Loiselle and Hurtubise 1975).

4.2.1 Atterberg Limits and Specific Gravity :

Atterberg limit tests were performed on the soil sample passing sieve No. 40 according to ASTM D423 and the soil was found to be non-plastic. A specific gravity test was also conducted for the till samples according to ASTM D854 and a value of D_R =2.65 was obtained.

4.2.2 Grain Size Distribution :

Sieve and hydrometer analysis were carried out on till sample. The resulting grain size distribution is shown in Fig. 4.1.

As seen from the grain size distribution, the soil has 28% fines (silt & clay size) and more than 60% passing sieve no.4 . The soil can be classified as a sand silt mixture (SM) according to the Unified Classification System (ASTM D2487).

4.2.3 Compaction :

A standard Proctor test (ASTM D698) was performed on the till soil samples passing sieve No.4 and the results are shown in Fig. 4.2. The soil's compaction curve shows a smooth peak with a maximum dry density of 21.1 KN/m^3 and an optimum water

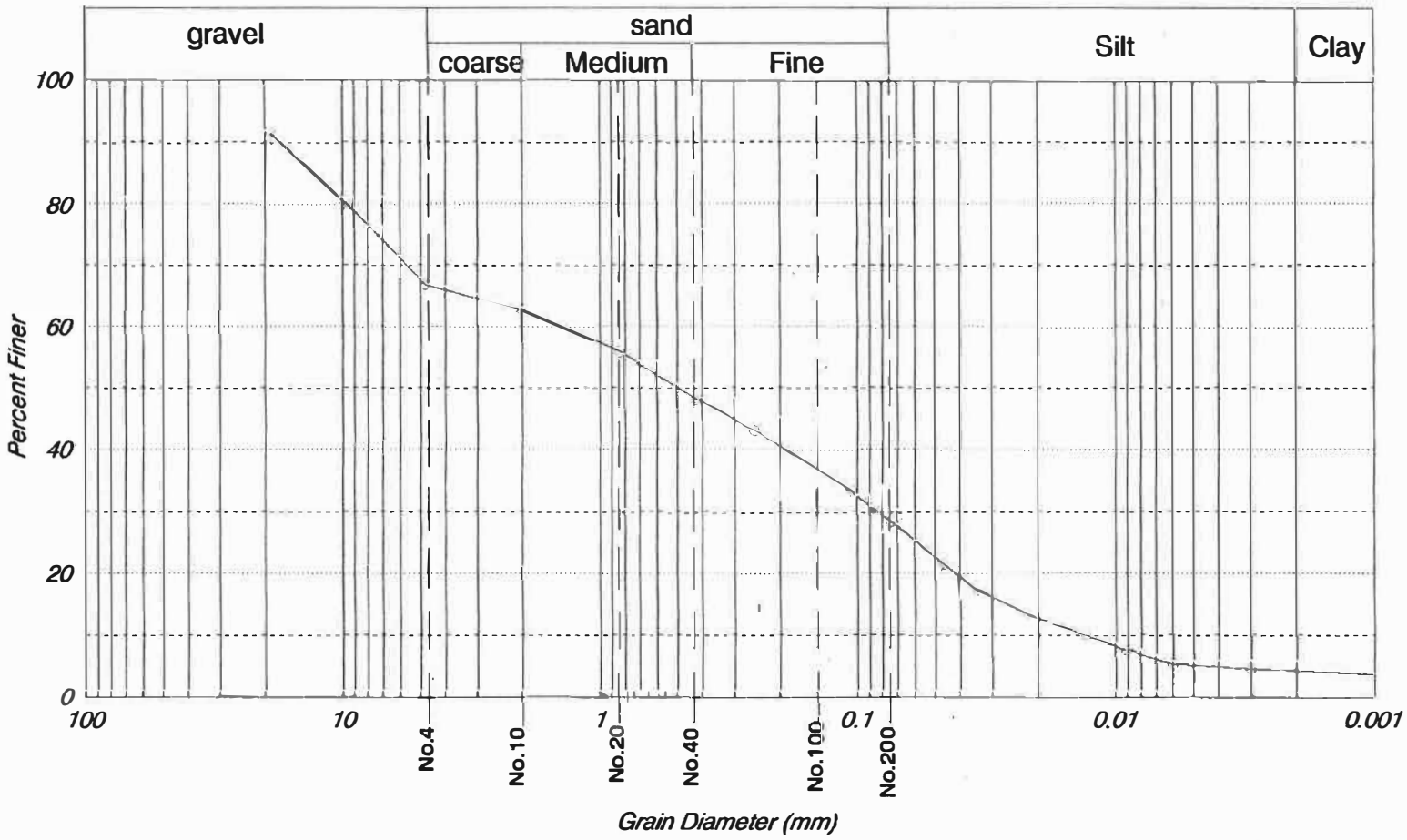

Fig. 4.1 - Grain Size Distribution Curve For Till

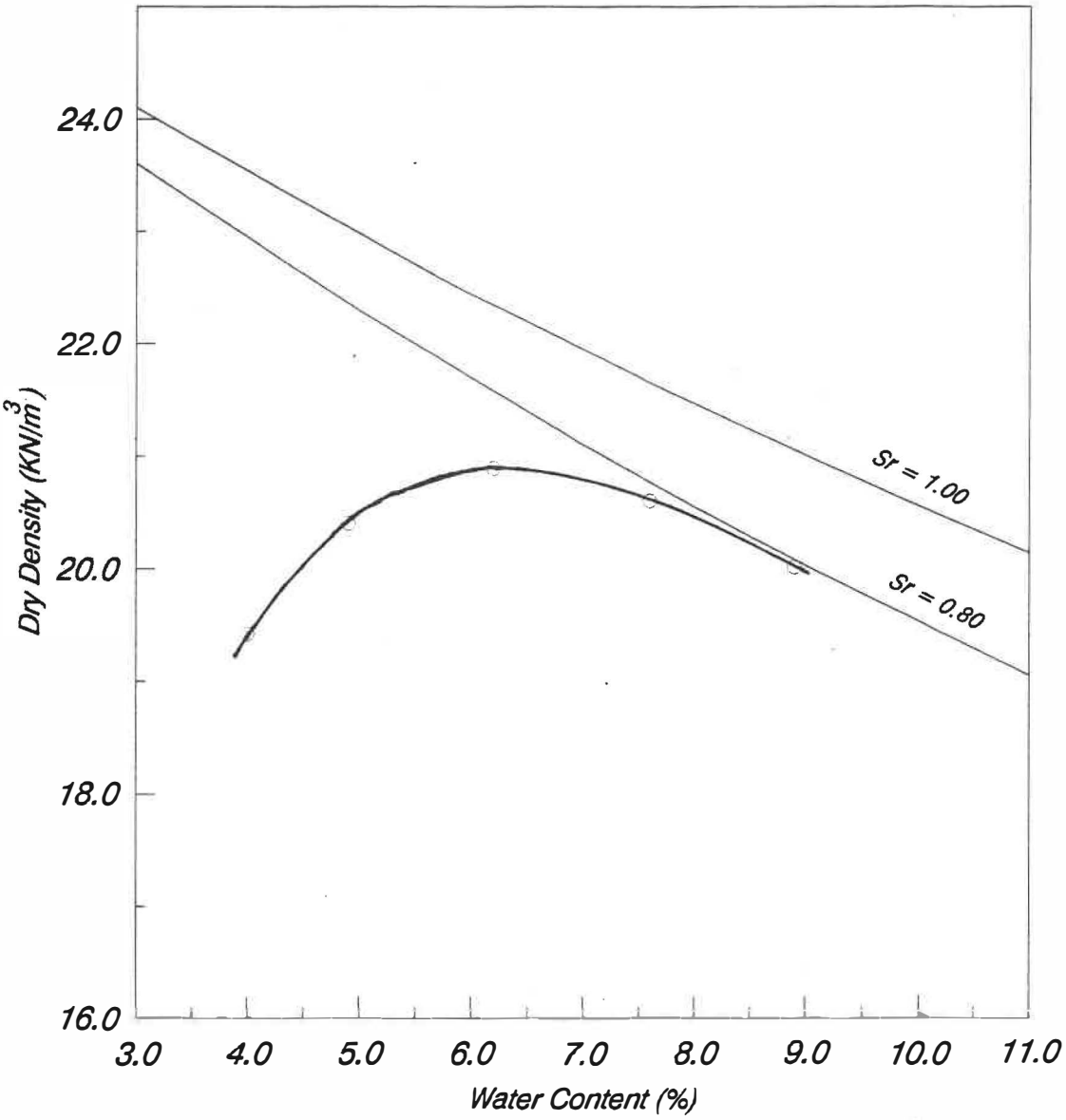

Fig. 4.2 - Standard Compaction Curve

content of 6.5% . The degree of saturation at optimum moisture content is about 70%. At water contents above 10% the soil became too wet and the compaction test could not be carried out.

4.3 Preliminary tests :

In order to examine the existence of collapse phenomenon in compacted till samples, a set of preliminary oedometric tests were performed on 100 mm diameter compacted samples. The equipment and test procedure are described in the following sections.

4.3.1 Test Equipment :

a. Loading Apparatus -Servo-hydraulic INSTRON machine (model 1350) was employed as the loading device. A schematic diagram of this machine is shown in Fig. 4.3. The machine is capable of maintaining the specimen under constant pressure during different load increments and thereby simulating the conventional oedometric test procedure. The machine was connected to a plotter to plot the deformation versus time for each load increment.

b. Compaction Mold -A compaction mold 100mm in diameter and 80mm high together with a 30mm spacer were used. This combination would provide cylindrical samples with a height to diameter ratio of 0.5 (50mm X 100mm). A Marshal test hammer was used to compact the soil samples since it was believed that it can better simulate the field compaction and

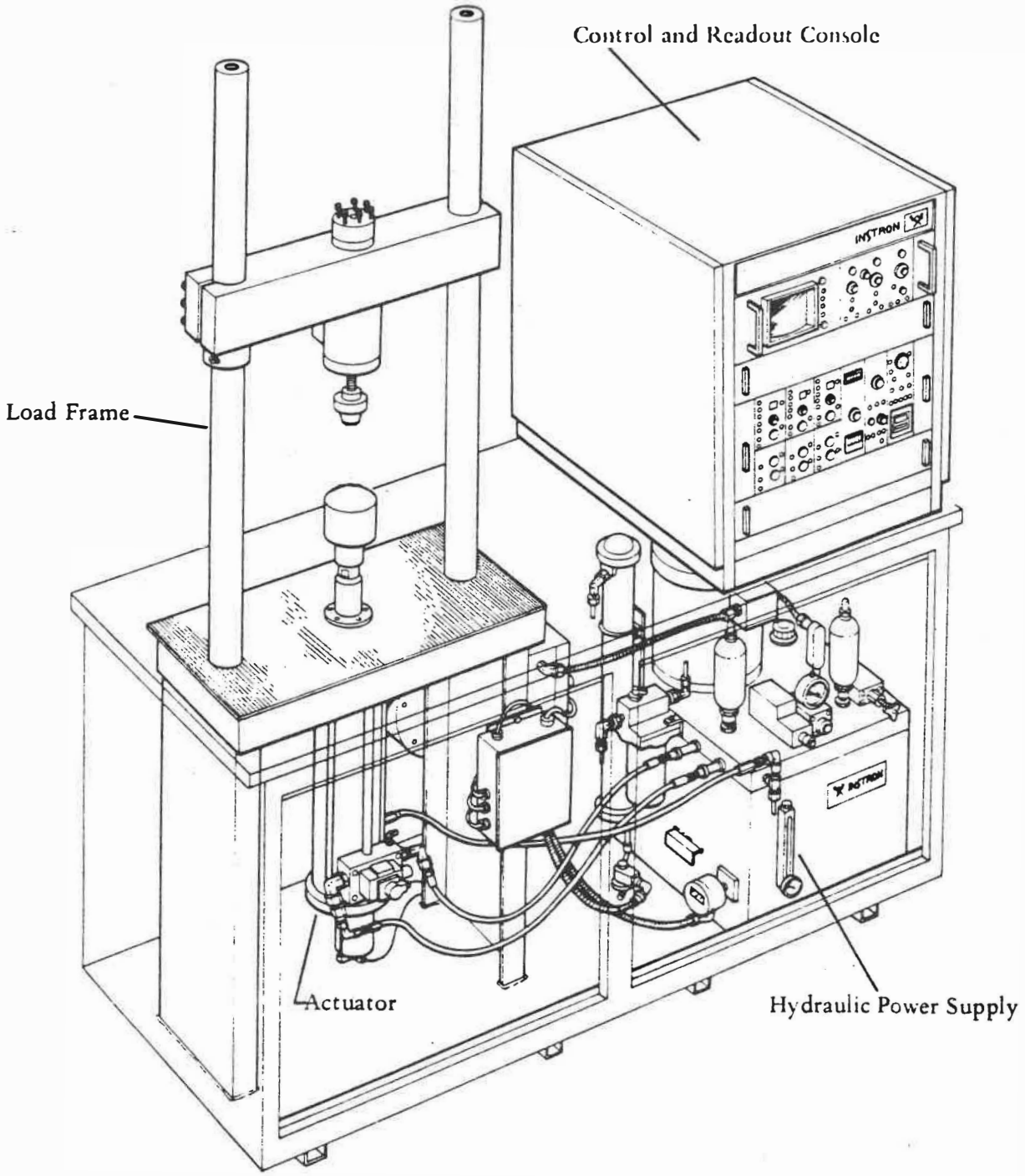

Fig. 4.3 - INSTRON Servohydraulic Testing System

give a more uniform compaction over the sample cross section. The Marshal hammer used was the same as the conventional hammer except that its head surface was partially trimmed to obtain a plane surface perpendicular to its vertical axis.

4.3.2 Specimen Preparation :

A series of five samples were prepared for this part of testing program. First, the soil was sieved on no.4 and the fraction above this sieve was discarded. The resulting grain size distribution of the soil is shown in Fig. 4.4. The soil was then thoroughly mixed with a predetermined amount of water and left in the humid room to cure for more than 24 hours. The amount of water used to make the mixture was estimated such as to obtain compacted samples with the degree of saturation around 40% . After the 24 hours of curing a water content determination was done to check the water content and additional water was added before compaction to adjust the initial water content.

The inner surface of the mold was lubricated with a very thin film of vaseline and spacer was placed at the bottom of the mold. The soil was compacted in the mold in three layers and each layer received seven blows of the Marshal hammer. Each layer surface was carefully scratched to obtain good bonding between the layers. Soil samples obtained in this way had the dry density ,water content, and the degree of saturation as shown in Table 4.1. The position of these samples on the

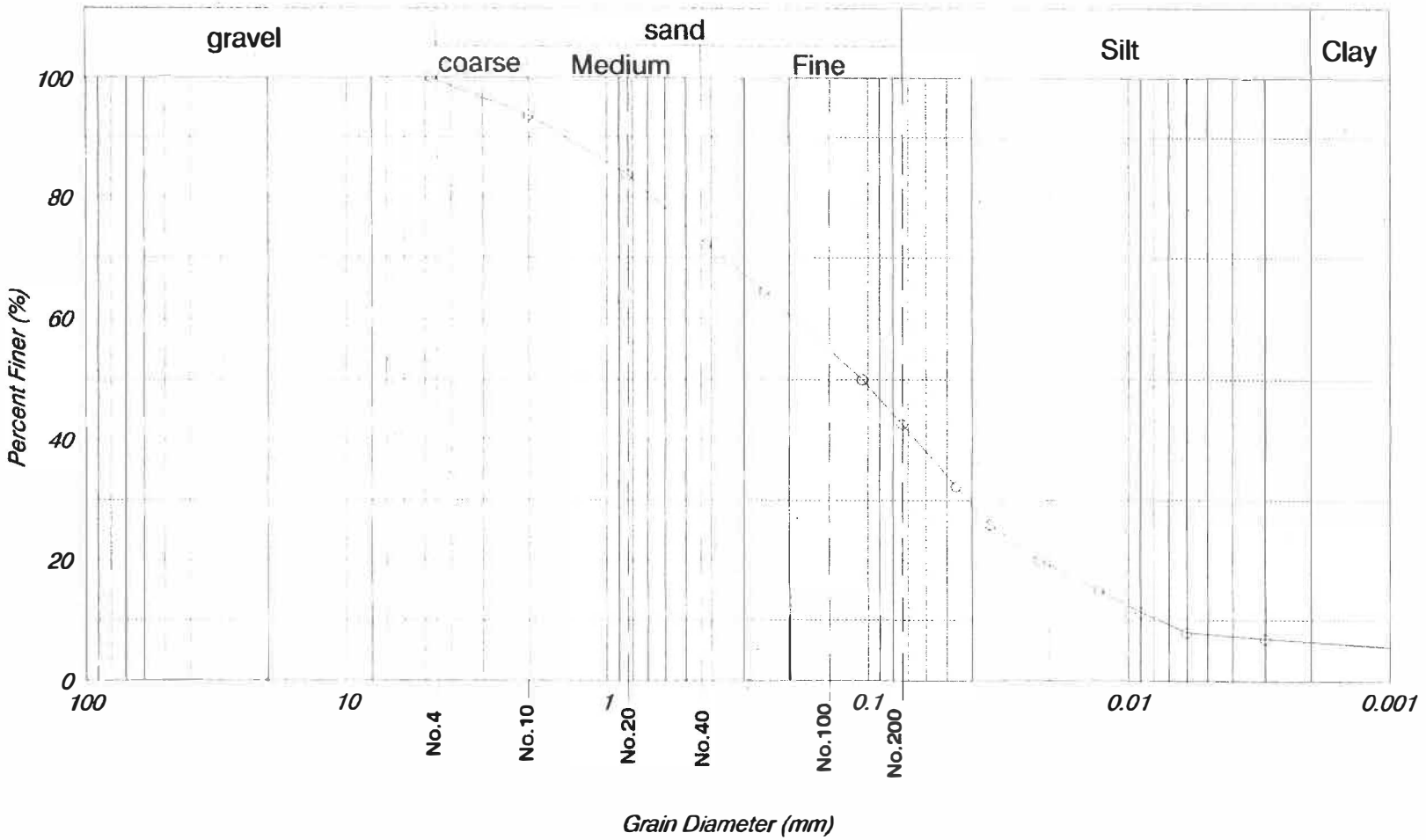

Fig. 4.4 - Grain Size Distribution Curve For The Till Samples Used in This Study

Table 4.1 - Initial Condition of The Preliminary Test Specimens

Sample	Water Content (%)	Saturation Degree (%)	Dry density (KN/m^3)
A1	3.80	27.9	19.13
A3	4.35	33.9	19.42
A4	3.40	23.7	18.84
A5	4.40	33.3	19.22

dry density chart is shown in Fig. 4.5. After trimming the top surface the base and spacer were removed and the mold with the soil inside was mounted on another base with a porous stone inside the base. The soil in the mold was then cautiously pushed with the spacer down the mold, the spacer was removed, and finally a cap was mounted on top of the mold. This final combination ready for loading is presented in Fig. 4.6.

4.3.3 Test Procedure :

This combination was then put in the loading apparatus described previously in section 4.3.1 and an initial seat load of 30 kPa was applied. The bottom valve at the base was connected to a water burette to saturate the sample when needed. The top valve was left open during the test to let the air pressure remain atmospheric. The sample was then loaded with an axial stress increment of Δ p/p=1 . For each load increment the sample was left under the applied pressure until the variation of axial deformation versus time traced by the plotter suggested the stabilization under the applied load increment.

Sample A1 was consolidated to a stress level of 1750 kPa and then the bottom valve was opened and the sample was saturated from the bottom by applying a small back pressure. Magnitude of the back pressure was limited to a value of 10 kPa in order to minimize disturbance of the soil structure during saturation. As soon as the saturation process started

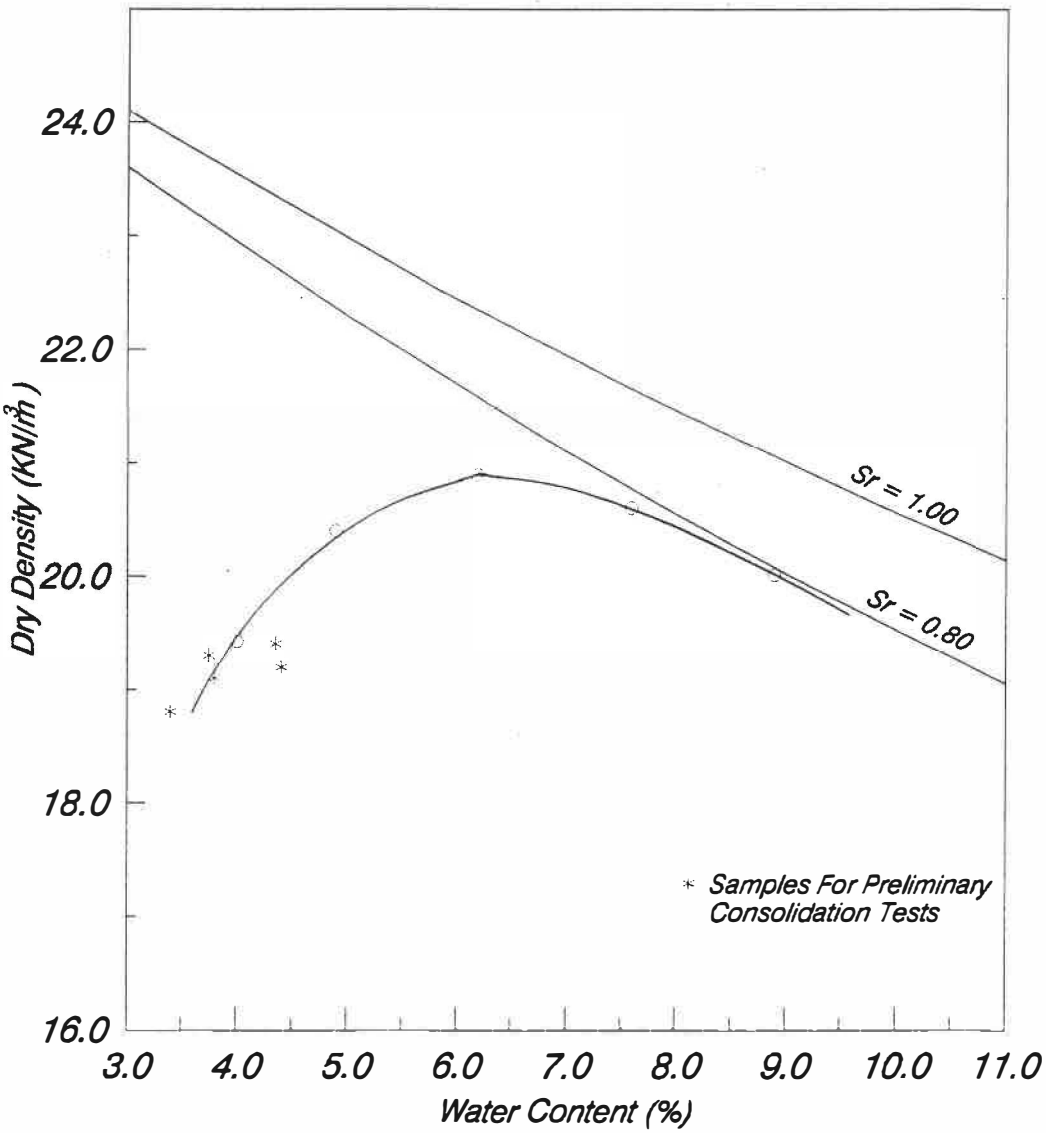

Fig. 4.5 - Position of Specimens on Standard Compaction Curve

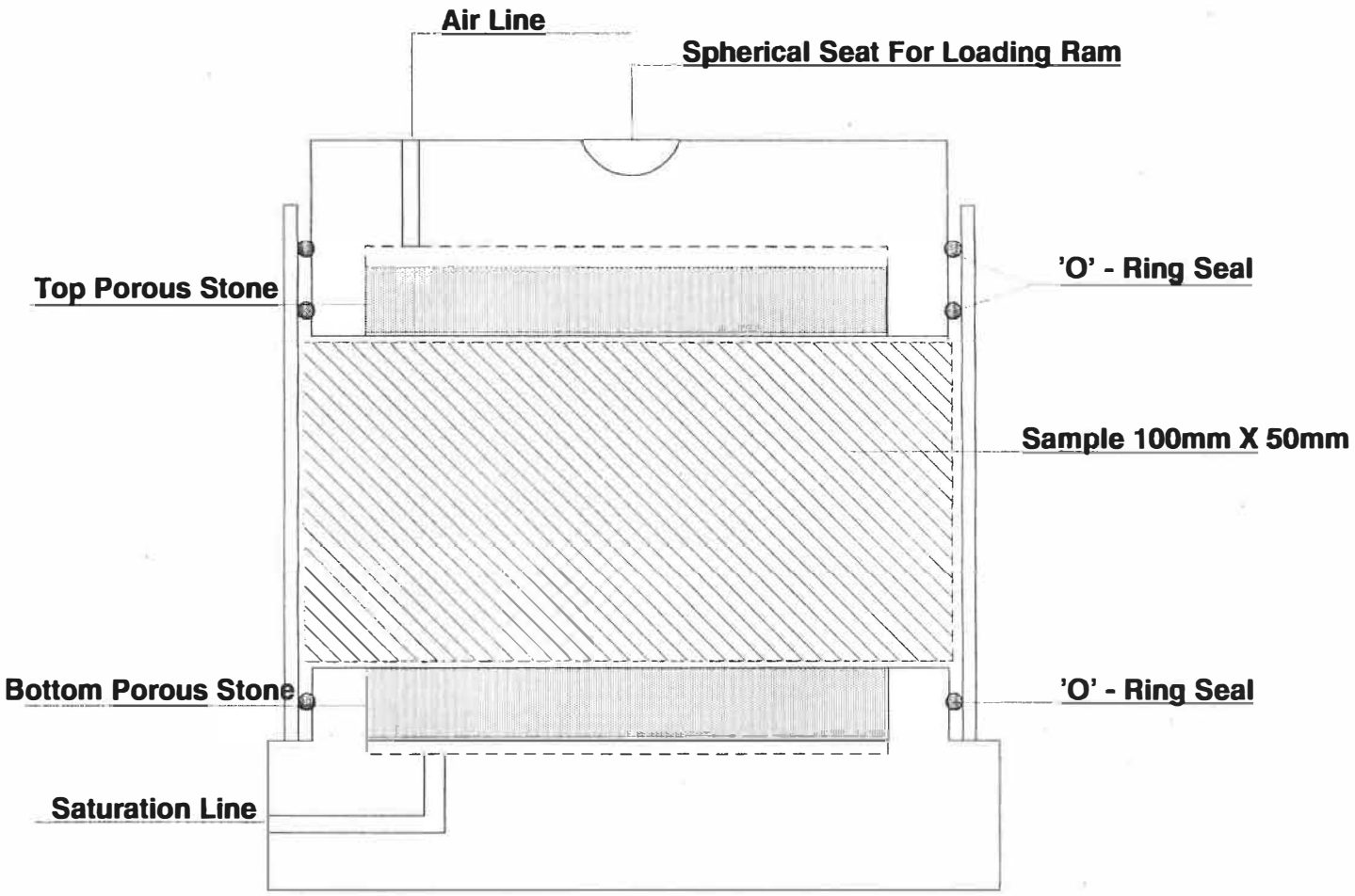

Fig. 4.6 - Apparatus Assembly For One Dimensional Consolidation

the collapse deformation also started to occur. The additional deformation due to saturation versus time is shown in Fig. 4.7. After the excess deformation had ceased the back pressure was removed. The total collapse deformation is the sum of deformation during saturation and after removing the back pressure. When the collapse deformation stopped, the loading in increments was resumed and the sample was stressed to 7000 kPa. Similar procedures were undertaken for the other samples and the results are summarized in Fig. 4.8. Sample A2 showed anomalous results and its data were discarded. The reason was found to be due to improper alignment of the top cap with respect to the loading ram which, in turn, resulted in a partial load transfer through the specimen. Samples A1, A3, A4, and A5 were subjected to the same process except that the stress level at which saturation was permitted was different. In all samples tested stabilization under each load increment was achieved within a maximum time of 20 minutes.

4.3.4 Results of Preliminary Tests :

The test results showed that the collapse phenomenon exists in partially saturated compacted till samples and its magnitude varied from 0.4% to 1.15% depending on the stress level and degree of saturation before inundation. Table 4.2 shows a summary of test results. Samples A3 and A4 were saturated at about the same stress level but sample A4 showed much higher collapse deformation than sample A3. The reason

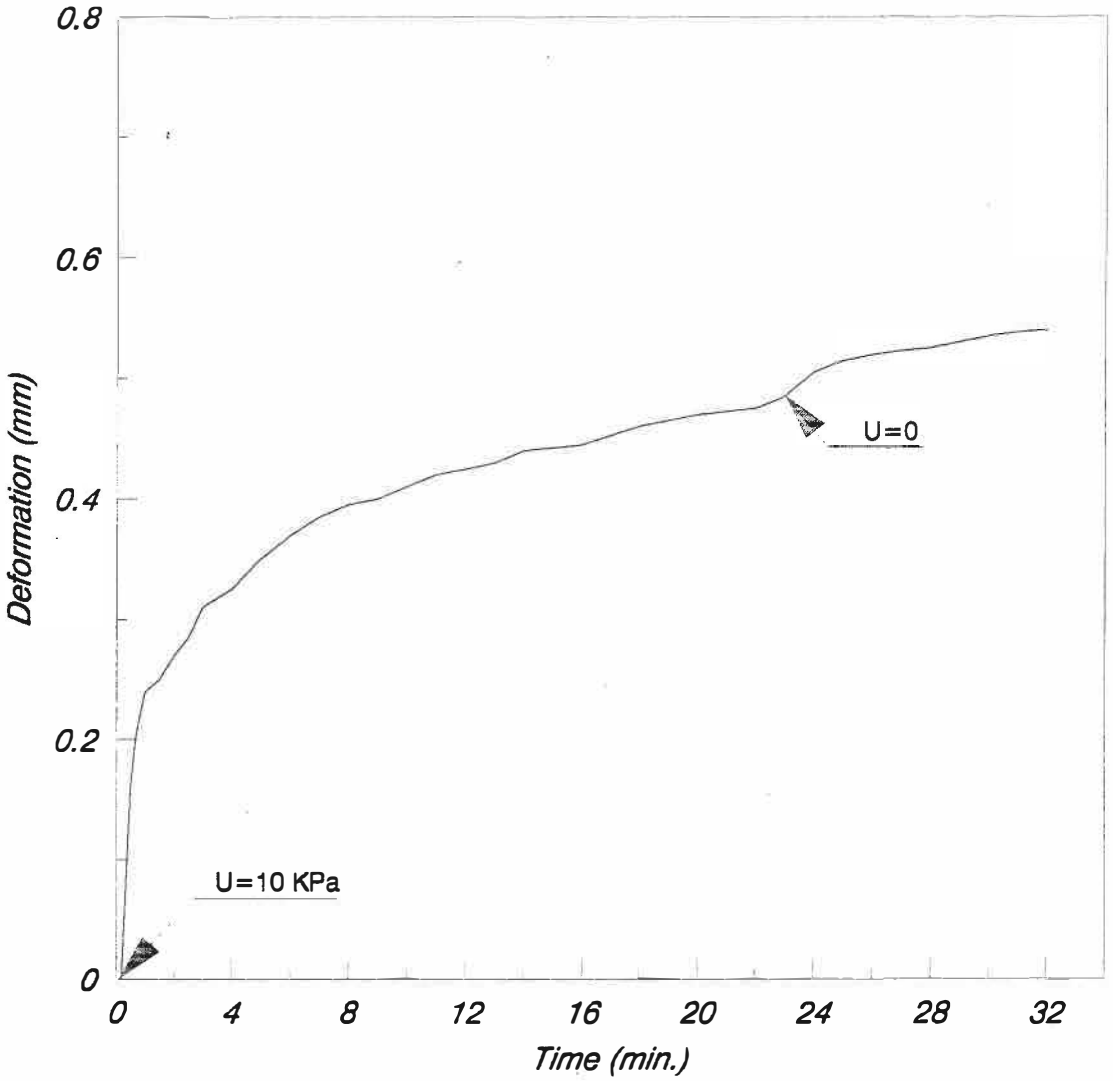

Fig. 4.7 - Collapse Deformation Versus Time For Sample A-1

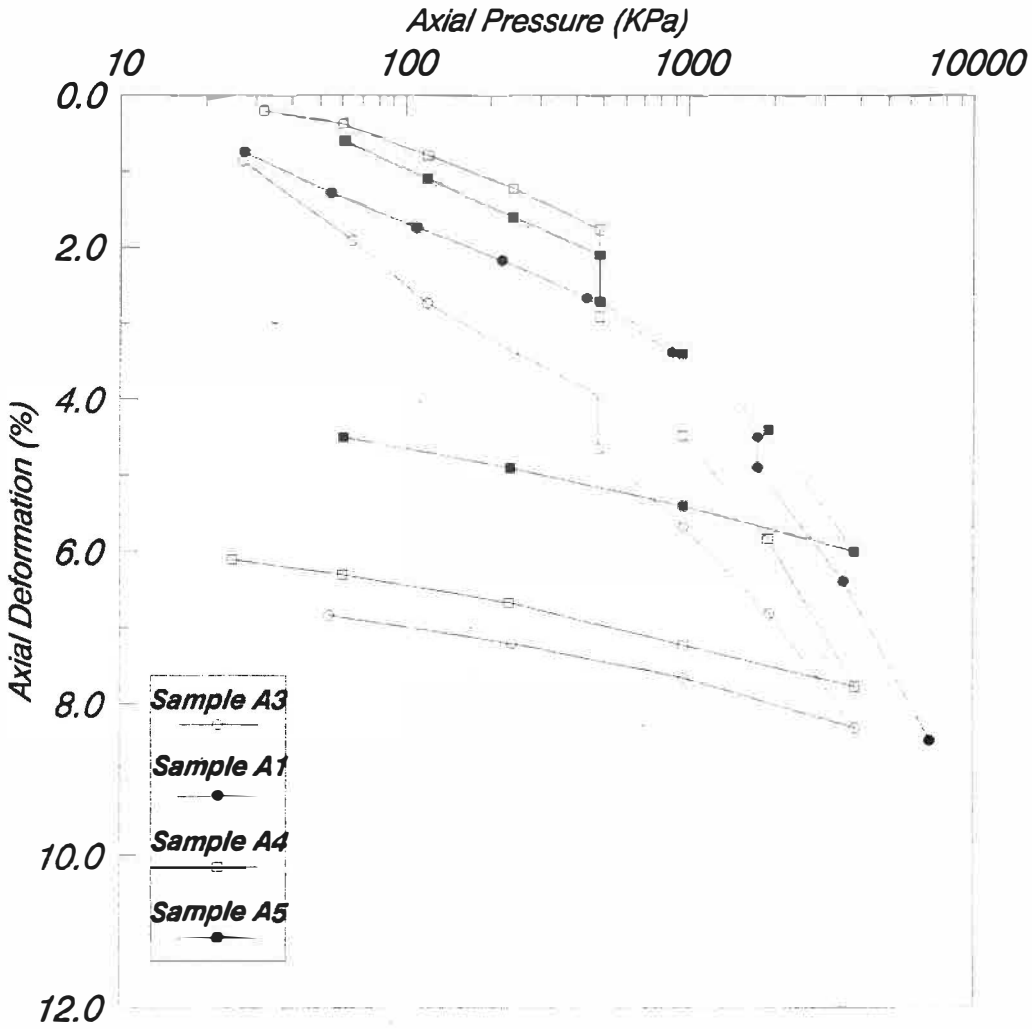

Fig. 4.8 - One Dimensional Consolidation Behavior For Till Samples

Table 4.2 - Summary of Preliminary Test Results

Sample	Before Submergence		Applied Stress (KPa)	Collapse Deformation (%)
	Void ratio	Sat. Deg. (%)		
A1	0.30	34	1750	0.4
A3	0.29	40	482	0.7
A4	0.35	25	485	1.1
A5	0.32	36	487	0.6

is the higher initial void ratio and lower degree of saturation of the sample A4. Samples A3 and A5 showed almost the same amount of collapse deformation since their initial conditions and the applied load at saturation were very close to each other.

Sample A1 underwent the least collapse deformation despite its high applied stress during saturation. The effect of side friction between the mold and the sample could have played a significant role in reducing the amount of collapse deformation. Generally, the percentage of load taken by side friction is a direct function of D/H, diameter to height ratio of the sample, and it increases with a decrease in this ratio. In this set of tests, the diameter height ratio was about 2 as compared to a minimum of 2.5 in conventional oedometric tests (ASTM D2435). Therefore a higher percentage of the applied load is expected to be resisted by the wall friction. Nevertheless, the collapse phenomena was detected clearly in all samples at various loads.

4.4 Triaxial Tests :

A series of triaxial tests was performed on compacted samples of glacial till to study the volume change behavior of this type of soil during loading and also during saturation under constant applied stress. For doing so, a triaxial cell was required with the capabilities of measuring or controlling

pore air and pore water pressures during the test. The system should also be capable of measuring the overall volume change as well as the axial deformation.

4.4.1 GDS Triaxial System :

The GDS triaxial system (fabricated by Geotechnical Digital System Ltd. in Great Britain) was employed as a basis for the triaxial configuration and some necessary modifications were made in order to make it capable of dealing with partially saturated soils.

GDS triaxial equipment is a computer controlled hydraulic system. A desktop computer is linked to a hydraulic triaxial cell via three microprocessor controlled hydraulic actuators and two subsystems as shown in Fig. 4.9a. The controllers are used to measure or control pore water pressure, cell pressure, axial load, and axial deformation. The digital controllers are connected to the IEEE 488 standard parallel interface of the computer.

Diagrammatic layout of a digital controller is shown in Fig. 4.9b. The controllers have the following characteristics:

- Volumetric capacity of 1000 Cm^3
- Pressure range : up to 2000 kPa
- Pressure measurement : resolved to 0.2 kPa
- Volume change : measured and controlled to 1 mm^3

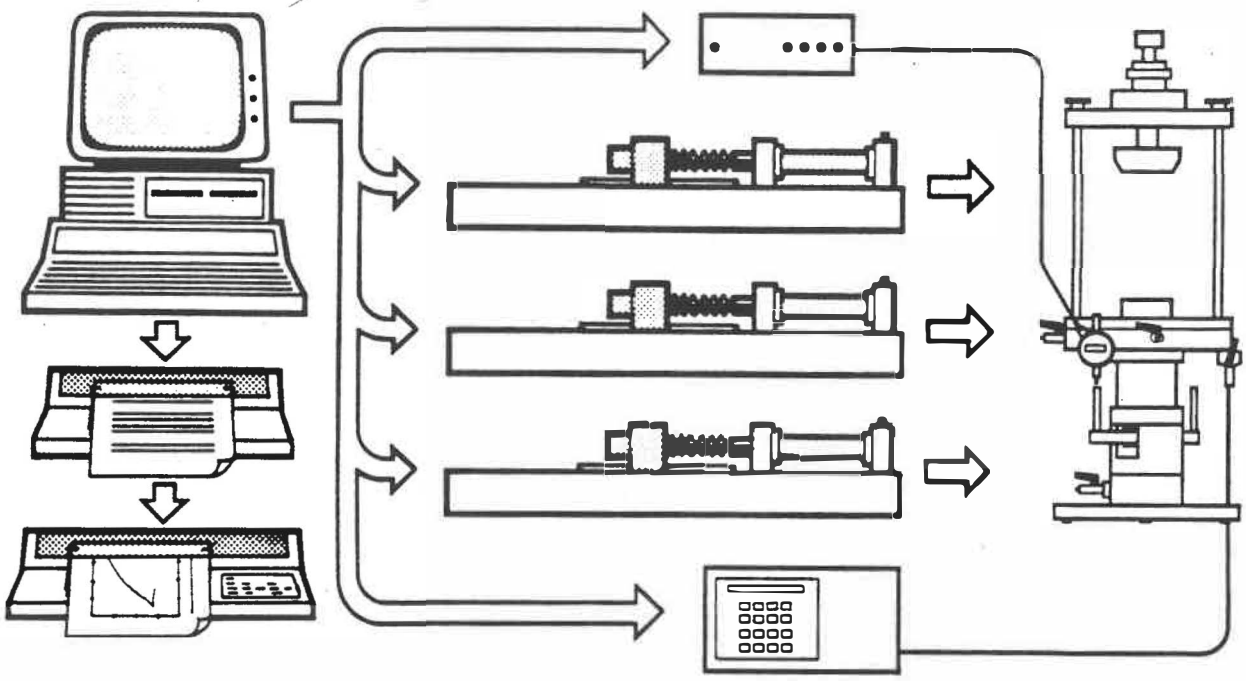

(a) *Diagrammatic layout of the system*

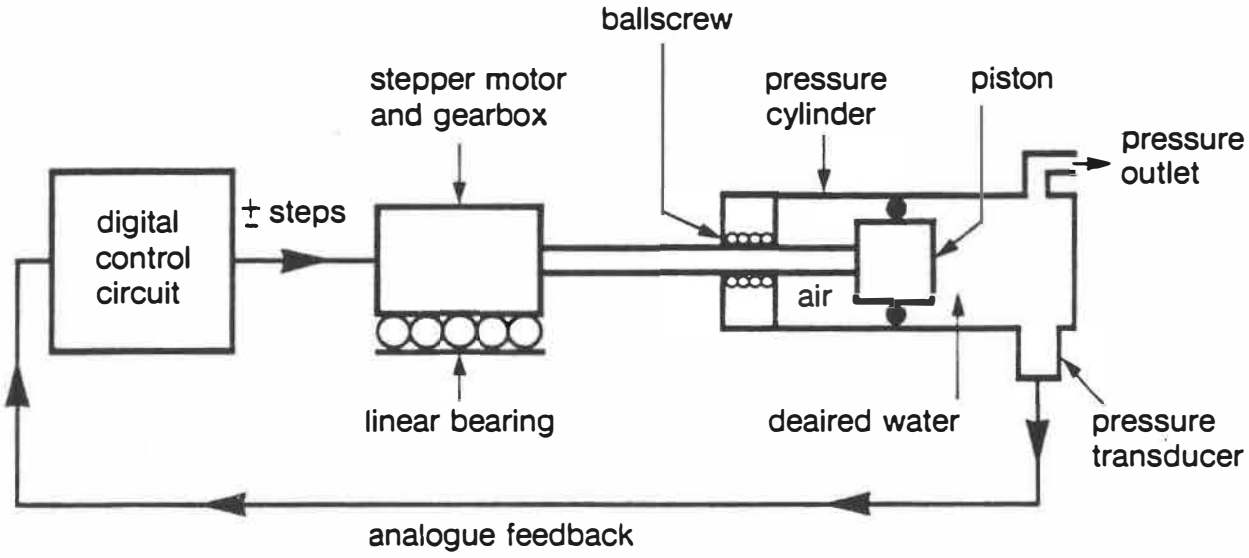

(b) *Diagrammatic layout of digital controller*

Fig. 4.9 - GDS Triaxial Testing System

The triaxial cell is based on the design of Bishop and Wesley's (1975) hydraulic triaxial apparatus for controlled stress path. A diagram of this type of cell is shown in Fig. 4.10. In this kind of cell the relation between the applied axial pressure and radial stress is obtained from the statics of the cell and is given below :

$$\sigma_a = P\left(\frac{a}{A}\right) + \sigma_r\left(1 - \frac{a}{A}\right) - \frac{W}{A} \qquad (4.1)$$

Where :

σ_a : Average axial total stress

σ_r : Radial stress

P : Pressure in the lower chamber

A : Current average cross sectional area of the specimen

a : Effective area of the Bellofram rolling diaphragm

W : Weight of the loading ram.

4.4.2 Modifications to GDS Triaxial System :

In order to perform triaxial tests on partially saturated soil specimens, certain modifications to the cell configuration and also in the GDS computer programs were required. A new pedestal was fabricated and a high air entry (300 kPa) ceramic disc was buried inside the pedestal as shown in Fig. 4.11. Epoxy resin type of glue was employed to attach the ceramic disc to the pedestal and to seal it completely. The high air entry disc was required to allow the passage of

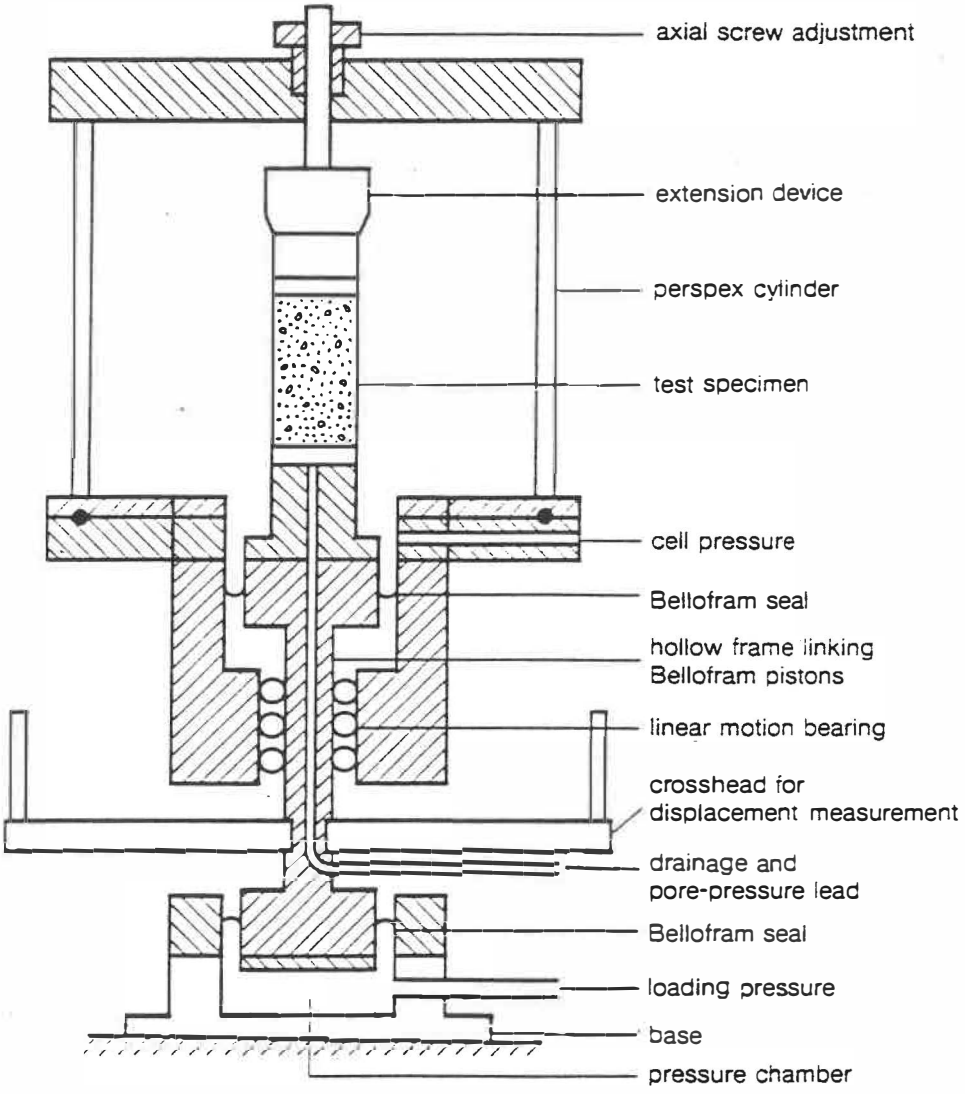

Fig. 4.10 - Layout of The Hydraulic Triaxial Apparatus, After Bishop & Wesley

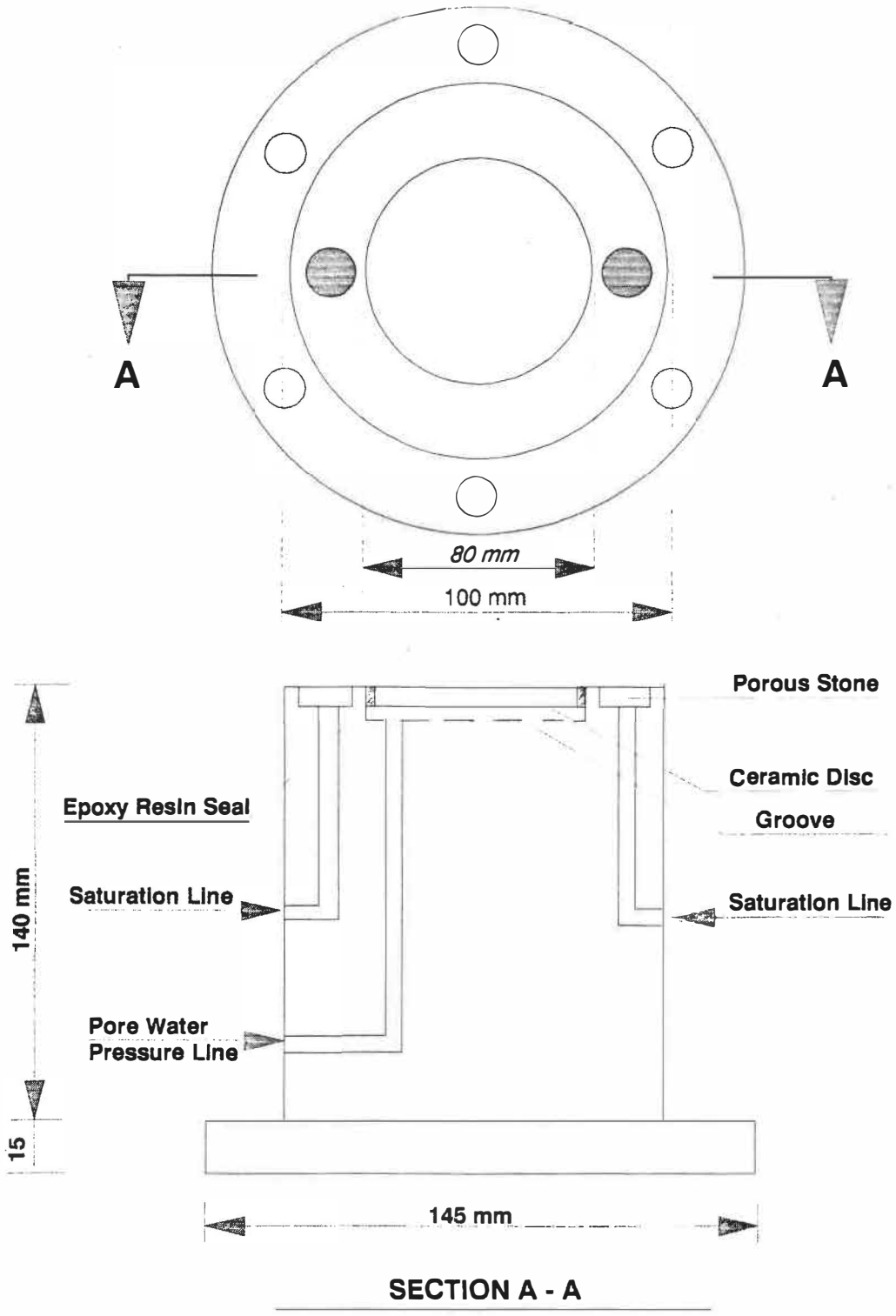

Fig. 4.11 - Details of Pedestal Fabricated For Unsaturated Soils

water but to prevent flow of free air. The air entry value of three bars for ceramic disc was considered to be sufficient for the range of suction values expected in the tests. Two small coarse porous stones were installed at the sides of the pedestal across a diameter as indicated in Fig. 4.11. These two small porous stones would serve for the saturation process since the high air entry stone had a very low permeability (1.0×10^{-9} m/s) and it would take a lot of time to saturate the specimen through the ceramic disc. The saturation line connected to the small porous stones was moved out of the cell through a line which was already available in the top piston. The line in the top piston was originally meant to serve for extension tests in order to applying a small suction to the top cap of the specimen. This modification required another piece to be fabricated and placed between the top piston ram and piston head. Next, an additional (fourth) controller was connected to the saturation line for operating the saturation process when needed. Fig. 4.12 shows a diagrammatic assembly of the system. The back pressure line connected to the top cap was separated from pore water pressure line and was used for controlling air pressure of the sample and may be connected to an air pressure system to control the air pressure. Finally, a 3 mm thick coarse porous stone was placed on top of the specimens to facilitate air pressure control in the samples.

The computer program also needed some modifications for

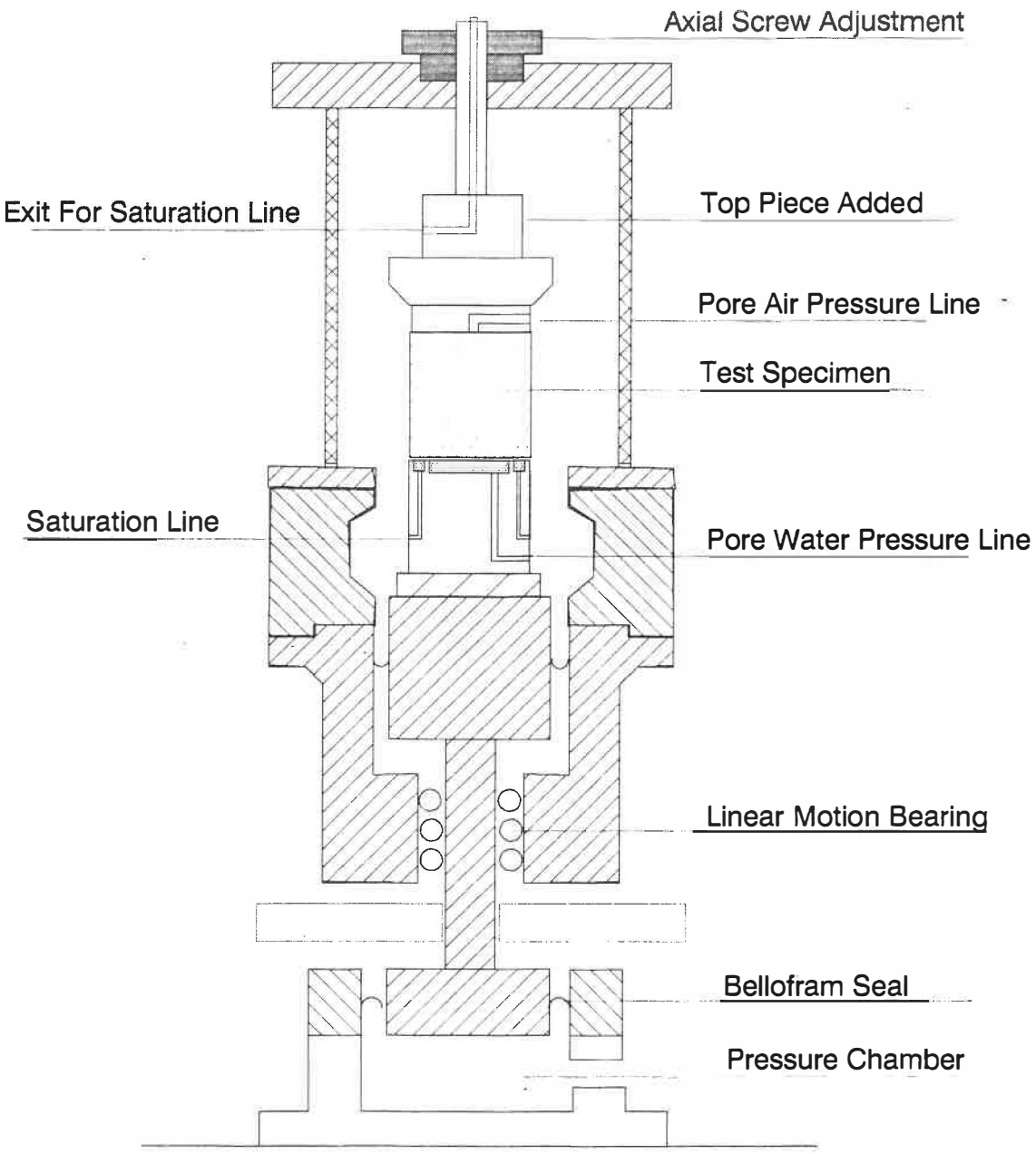

Fig. 4.12 - Diagrammatic Layout of The Modified GDS Apparatus

dealing with partially saturated specimens. In fully saturated samples the volume change was determined from the amount of water leaving the specimen. Since this method is not applicable to partially saturated soil samples, the volume change of a specimen was calculated from the change in volume of cell water obtained from the net amount of water leaving or entering the cell taking into account the upward movement of the piston into the cell. Other factors influencing this volume measurement include change of room temperature, change of temperature in the controller, the expandibility of the triaxial system, and stiffness of the membrane. Volume change of the cell itself was considered by calibrating the cell for a range of internal pressures. The cell calibration curve is shown in Fig. 4.13. Room temperature variation was not significant during the course of any tests and the controllers were warmed up about two hours before each test in order to minimize the temperature effect.

The change in diameter of the specimens is then calculated from the following equations :

$$A = A_o\left(1 + \frac{\Delta V_s}{V_o}\right)/(1 - \epsilon_1)$$

$$\epsilon_2 = 0.5(A/A_o - 1)$$

$$D_2 = \epsilon_2 . D_o$$

Where :

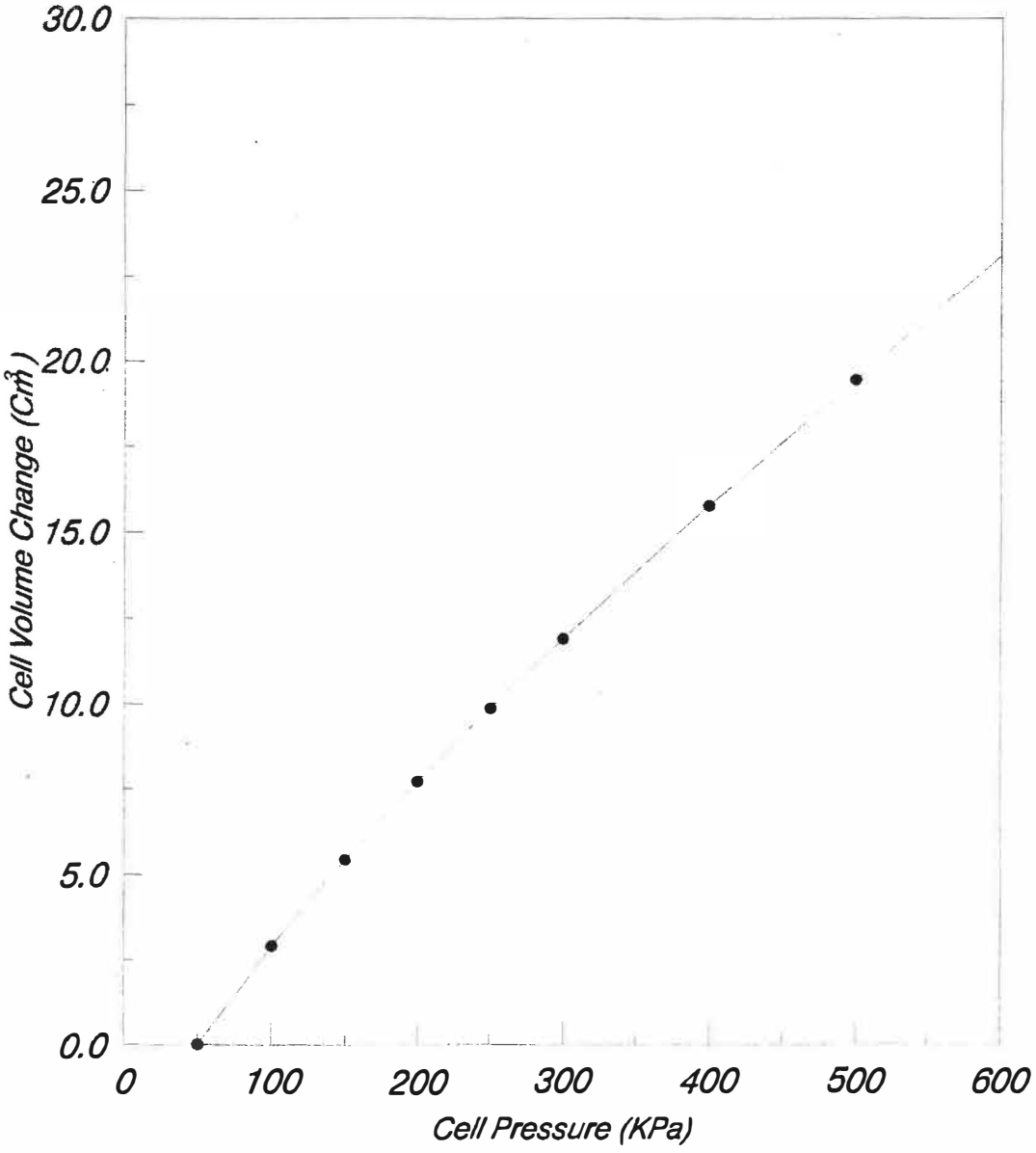

Fig. 4.13 - Cell Calibration Curve

A_o & A : Initial and current area of the specimen respectively

ΔV_s : Change in the volume of the specimen

V_o : Initial volume of the specimen

ϵ_1 & ϵ_2 : Axial and radial strains respectively

D_o & D_2 : Initial and current diameter of the specimen respectively

4.4.3 Specimen Preparation :

Passing sieve No.4 fraction of till as shown in Fig. 4.4 was used again in this part of experimental program. Again the soil was mixed with a predetermined amount of water and left in the humid room for a period of at least 24 hours. The soil was then compacted in three layers in a conventional compaction mold with five blows of the modified Marshal hammer per layer. This will yield in samples of 100 mm in diameter and 100 mm high. Visual inspections of the first few samples thus obtained showed weak bonding between the compacted layers although surface of each layer was carefully scratched before next layer was compacted into the mold. This fact could be clearly detected when breaking the samples by knocking the samples on the sides which caused splitting of the samples along their interlayer surfaces. Consequently, it was decided to use a standard Proctor hammer and the soil was compacted in three layers with 15 blows per layer. The surface of each layer was again carefully scratched before pouring the next

layer. Some of the specimens were again tested for interlayer bonding and it was found to be very satisfactory. Fig. 4.14 shows the position of the samples obtained in this way with respect to the standard compaction curve. The samples had a dry density of 94% maximum Proctor test and an initial degree of saturation around 40 % . Specimens prepared with this procedure were carefully wrapped and sealed in plastic bags and left in the humid room for at least 24 hours before testing.

4.4.4 Equipment Set-up :

In order to saturate the high air entry ceramic disc the triaxial cell was filled with deaired water and the cell pressure was raised to 800 kPa and left for few hours. Then the pore water pressure valve was opened to flush the deaired water through the ceramic disc for eight minutes under the constant cell pressure of 800 kPa. This procedure was repeated five times to ensure full saturation of the ceramic disc. The permeability of the ceramic disc was also measured after full saturation was achieved under a constant cell pressure of 800 kPa. Fig. 4.15 shows the permeability of the three bar air entry ceramic disc. Finally the pore water pressure response of the ceramic disk was measured and the result is shown in Fig. 4.16. The response was tested for different increments of pressure over a range of up to 100 kPa. From Fig. 4.16 the time required for the complete response to a change in pressure in all cases was less than one minute.

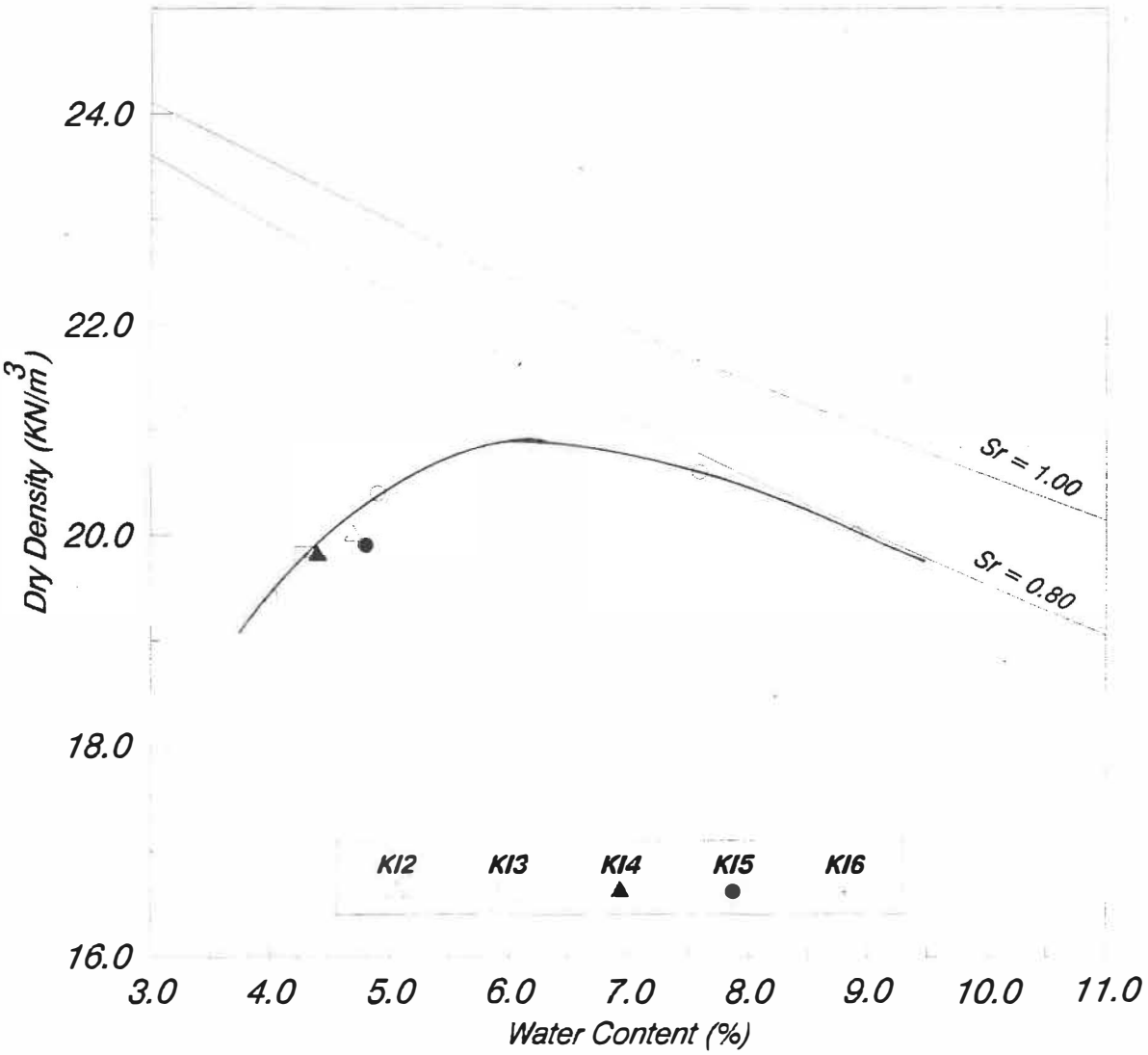

Fig. 4.14 - Initial Condition of Specimens Relative To Standard Compaction Curve

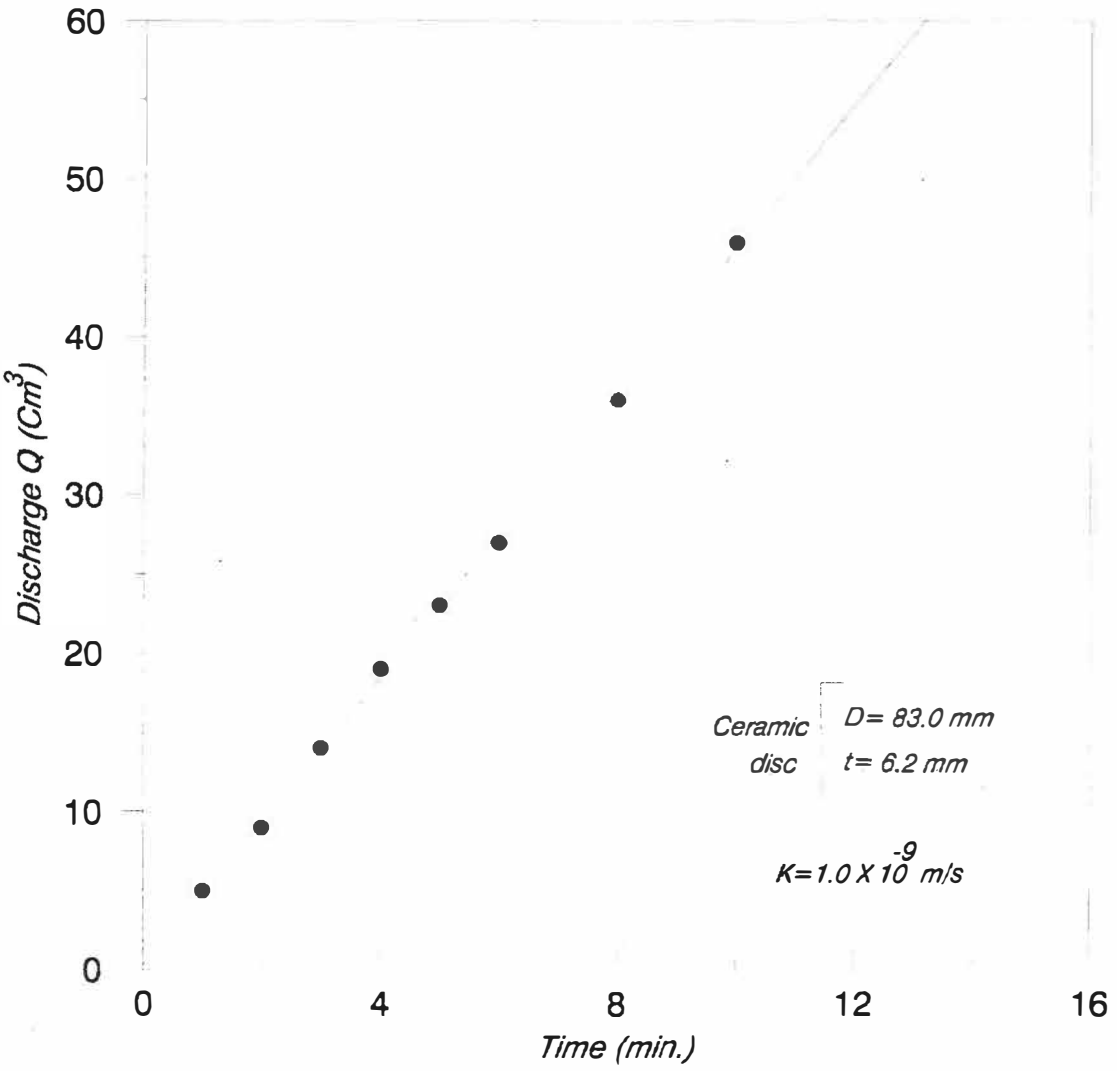

Fig. 4.15 - Permeability Test For The High Air Entry Ceramic Disc

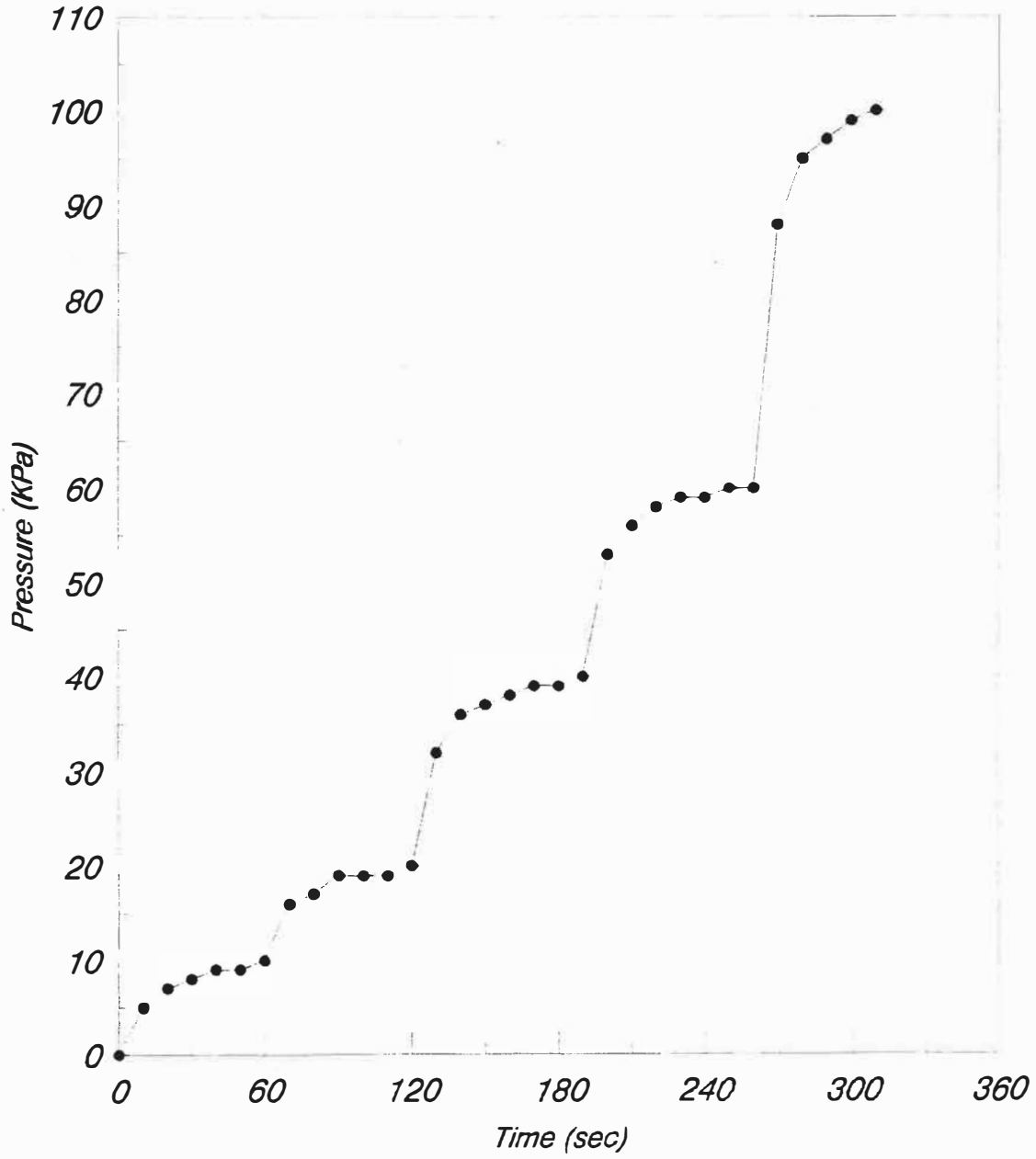

Fig. 4.16 - Pore Pressure Response of High Air Entry Ceramic Disc

4.4.5 Test Type :

Controlled stress path consolidation tests were carried out on all specimens with the total principal stress ratio of $K = d\sigma_3/d\sigma_1 = 0.42$. Previous works by other investigators such as Loiselle & Hurtubise (1976) revealed that this type of deposit has a friction angle in the range of 35^o to 45^o depending on the degree of compaction. Therefore the value of K=0.42 was deliberately chosen to approach the Ko condition based on the so called Jaky 's relationship given as :

$$K_o = 1 - \sin\phi'$$

Where:

ϕ' : the internal angle of friction.

K_o : coefficient of lateral pressure at rest

Based on preliminary tests results, an axial loading rate of 90 kPa/hour was chosen. This rate was considered to be slow enough to allow for pore pressure equalization and consolidation of the soil sample.

The modifications to the cell allows us to translate all pressures to positive values using the axis - translational technique proposed by Hilf (1956). This technique consists of increasing the air pressure to a value high enough that the pore water pressure reading becomes positive and the suction value is calculated as the difference between pore air and water pressures. This technique was not employed in these series of tests since the range of suction pressures

encountered were less than 30 kPa and could well be recorded using the available controllers and no attempt was made to desaturate the samples either. Moreover, by keeping the air pressure at atmospheric level, the amount of diffused air through the ceramic disc or rubber membrane was minimized.

4.4.6 Test Procedure :

A specimen fetched from the humid room was unwrapped and placed on the pedestal with direct contact with the high air entry porous stone. An annular shape paper filter was prepared and placed between the pedestal and the specimen. The filter covered only the outer metallic surface of the pedestal and over the small porous stones to facilitate the process of saturation when required. A paper filter, the 3mm coarse porous stone, and the top cap were placed on top of the specimen successively. The rubber membrane was then carefully rolled up on the specimen and two 'O' rings were installed at each end. After sealing the sample, the cell was filled with deaired water at a slow rate (about 1.5 hour to fill up) in order to avoid any turbulences that would dissolve some air into the cell water. Also care was exercised to prevent air bubbles from trapping in the cell by wetting the membrane surface and the 'O' rings with deaired water before filling the cell.

An initial cell pressure of 50 kPa was applied and the specimen was left overnight for the pore pressures to equilibrate and consolidate under this pressure. The air pressure

line was left open to atmospheric pressure at all times during the test. On the following day the initial suction pressure of the specimen was recorded from the pore water pressure controller, the pore air pressure being atmospheric. All the samples at this step showed a suction pressure in the range of 24 to 28 kPa. The negative pore water pressure on the controller was offset to zero, that is, the current negative pressure was then set as the new datum line for pressure measurement by the controller. This allows us to perform drained tests under constant initial suction. The next step was to load the modified GDS computer program and to run it for controlled constant stress ratio of K=0.42 .

The initial degree of saturation of samples KI3, KI5, and KI6 was increased to 0.5, 0.7, and full saturation respectively. The suction pressure of samples KI3, and KI5 decreases to 15 and 13 kPa respectively. The saturation process was performed using the fourth controller attached to the saturation line. A small water pressure of 15 kPa was applied and the water volume reading was recorded till a predetermined amount of water had entered the sample. This process took about 3 and 7 hours for samples KI3, and KI5 respectively and more than 48 hours for sample KI6 (full saturation). After the change in degree of saturation was achieved the samples were left overnight for pressures to reach equilibrium condition. All samples were saturated from the bottom and the top air line was kept open to exit excess air from the sample.

Sample KI6 was almost saturated after 24 hours when the water started to leave the sample. It was then left for another 24 hours at the end of which the sample was supposed to be saturated. All samples were then loaded up to an axial total stress of 600 kPa and radial pressure of 281 kPa from their initial state of all round pressure of 50 kPa . Sample KI4 was loaded while keeping its initial suction pressure of 26 kPa through out the test. At the end of loading, all partially saturated samples were saturated under constant applied axial and radial stresses and the collapse deformation measured. This was achieved by setting the axial and radial controllers to the final load and recording the corresponding volume changes while the samples were being saturated. From the cell and the lower chamber volume change readings, the sample volumetric and axial strains could be calculated.

4.5 Results and Discussion :

The test results illustrated in Fig. 4.17 show axial strain versus axial stress behavior for the four samples tested with the major principal stress ratio of K=0.42 . As expected and clear from this figure the partially saturated samples showed less compressibilities compared to the initially saturated sample KI6. However, the difference in compressibilities of the three partly saturated samples was not significant. The reason is due to the fact that although these three specimens had different degrees of saturation but the

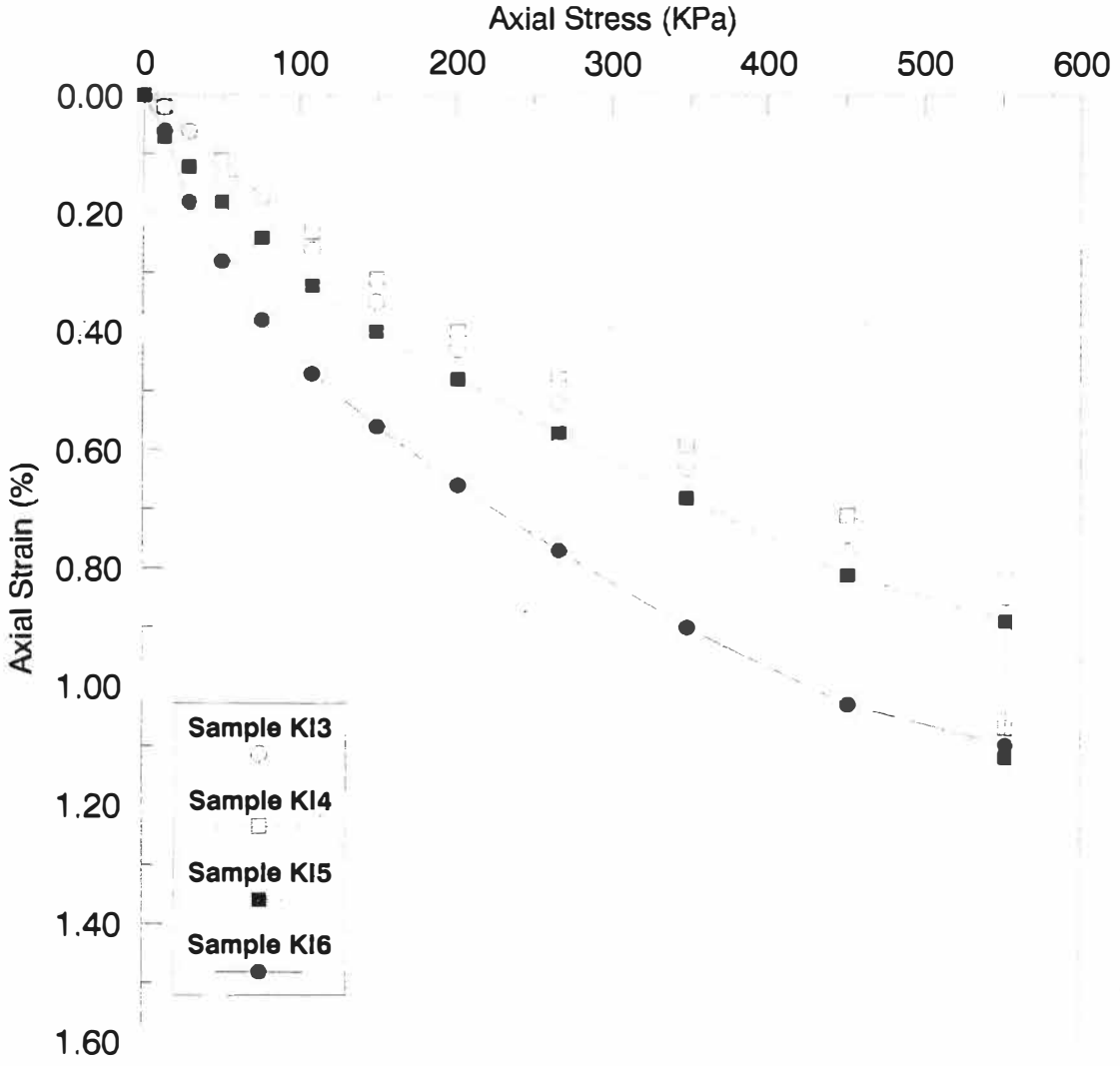

Fig. 4.17 - Axial Stress Strain Behavior of The Samples

difference in their initial suction pressure was not very broad, the largest difference being 13 kPa between samples KI4 and KI5.

Fig. 4.18 shows the radial deformation of the four samples tested. As expected, since the principal stress ratio was kept constant with an assigned value close to at rest pressure coefficient Ko, little lateral deformation occurred. Samples KI5 and KI6 showed a little lateral expansion at the beginning followed by some compression but, since the total lateral deformation was negligible, this behavior did not seem to be very important.

Fig. 4.19 shows the volume change behavior of the samples tested. Sample KI5 is less compressible than sample KI4 and KI3 which was not the case in Fig. 4.17. The reason is due to the small radial expansion of this sample at the beginning which reduced the total volume change, yet all partially saturated samples showed less compressibilities compared to the fully saturated sample.

Finally, all samples showed radial and axial collapse deformation. The amount of axial collapse deformation and its variation with saturation time is shown in Fig. 4.20. This figure indicates that as soon as the saturation process began the collapse phenomena also started to occur and about 40% of the collapse occurred in the first minute and about 70% in the first four minutes. A similar type of behavior was reported by Booth (1975) who studied collapse deformation

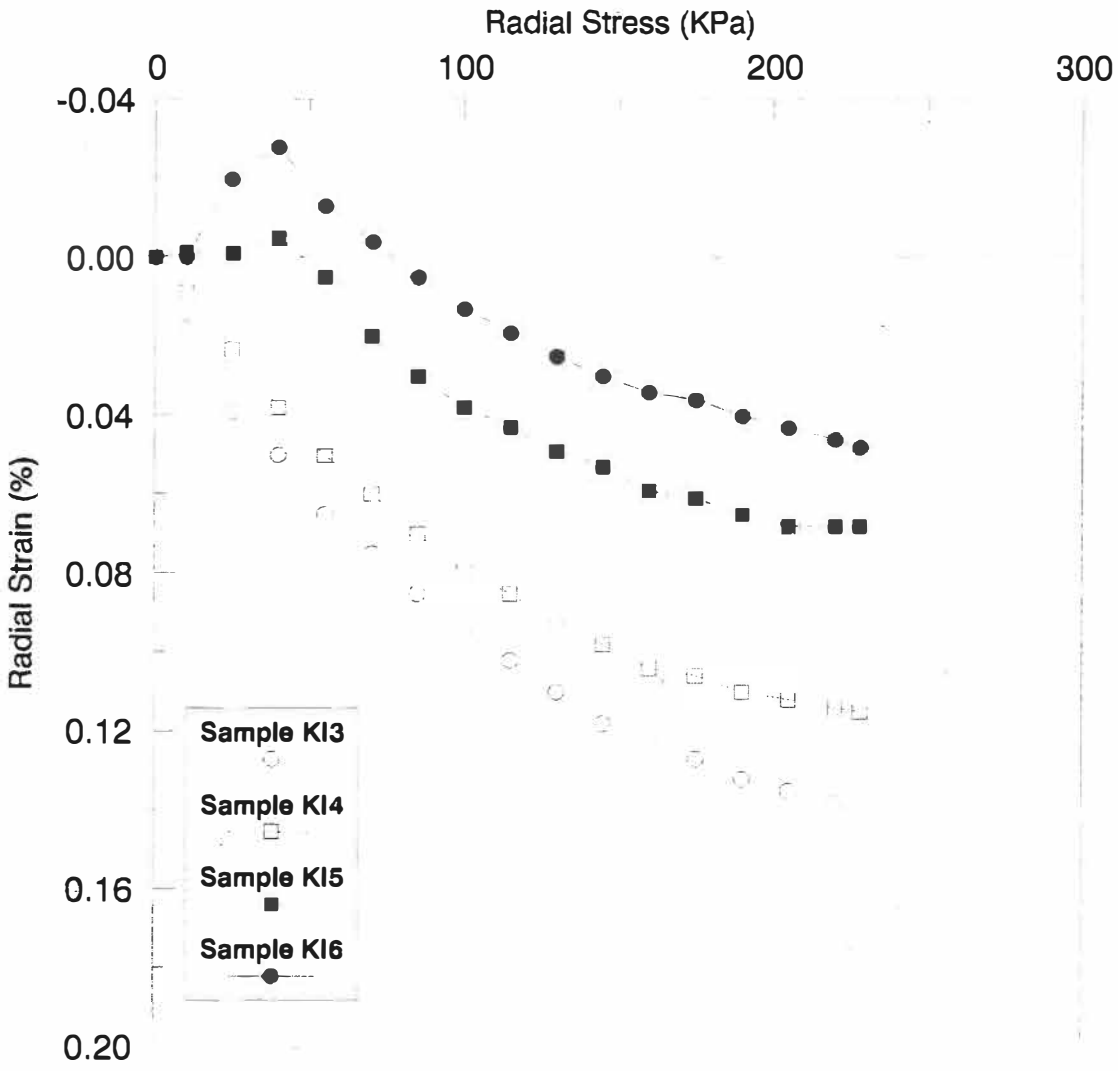

Fig. 4.18 - Radial Stress Strain Behavior For The Samples Tested

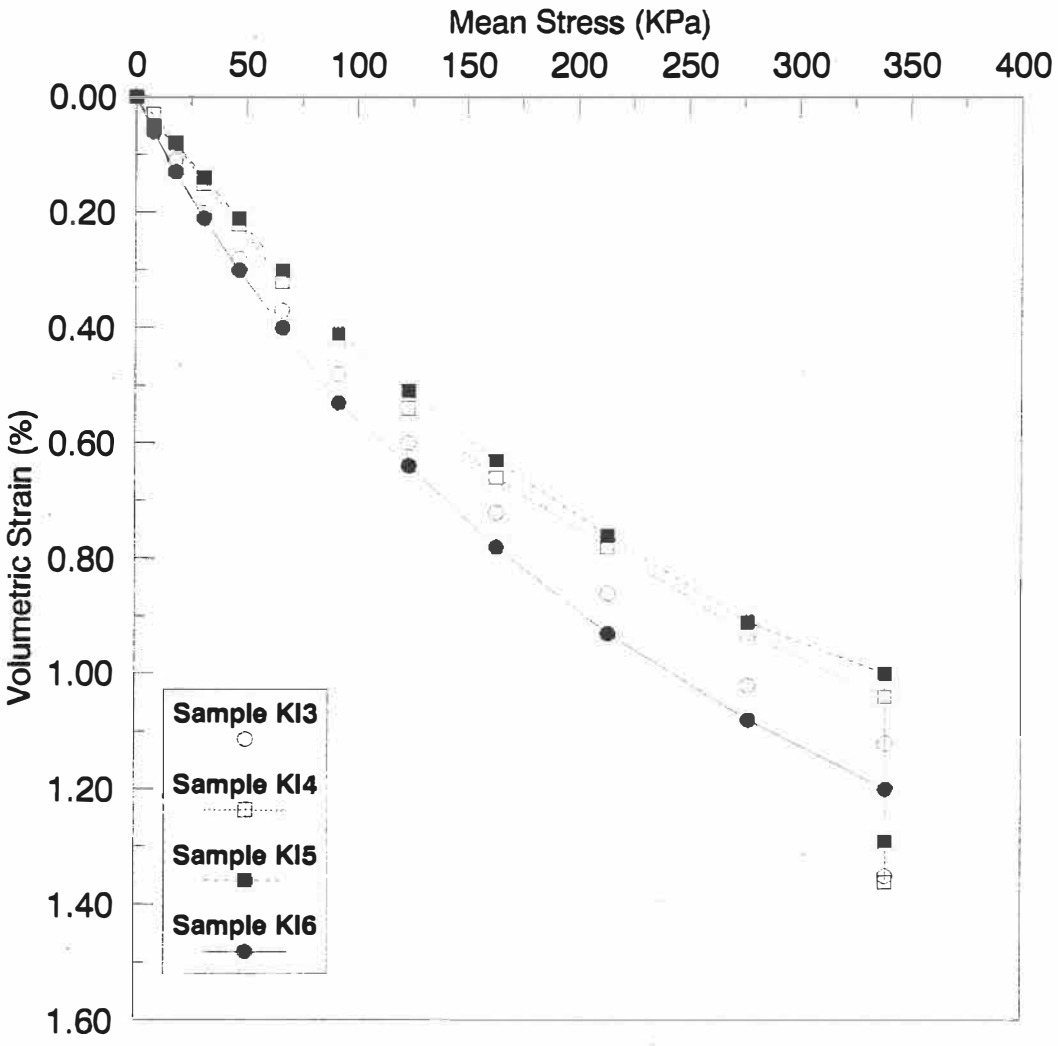

Fig. 4.19 - Volume Change Behavior of the Samples Tested

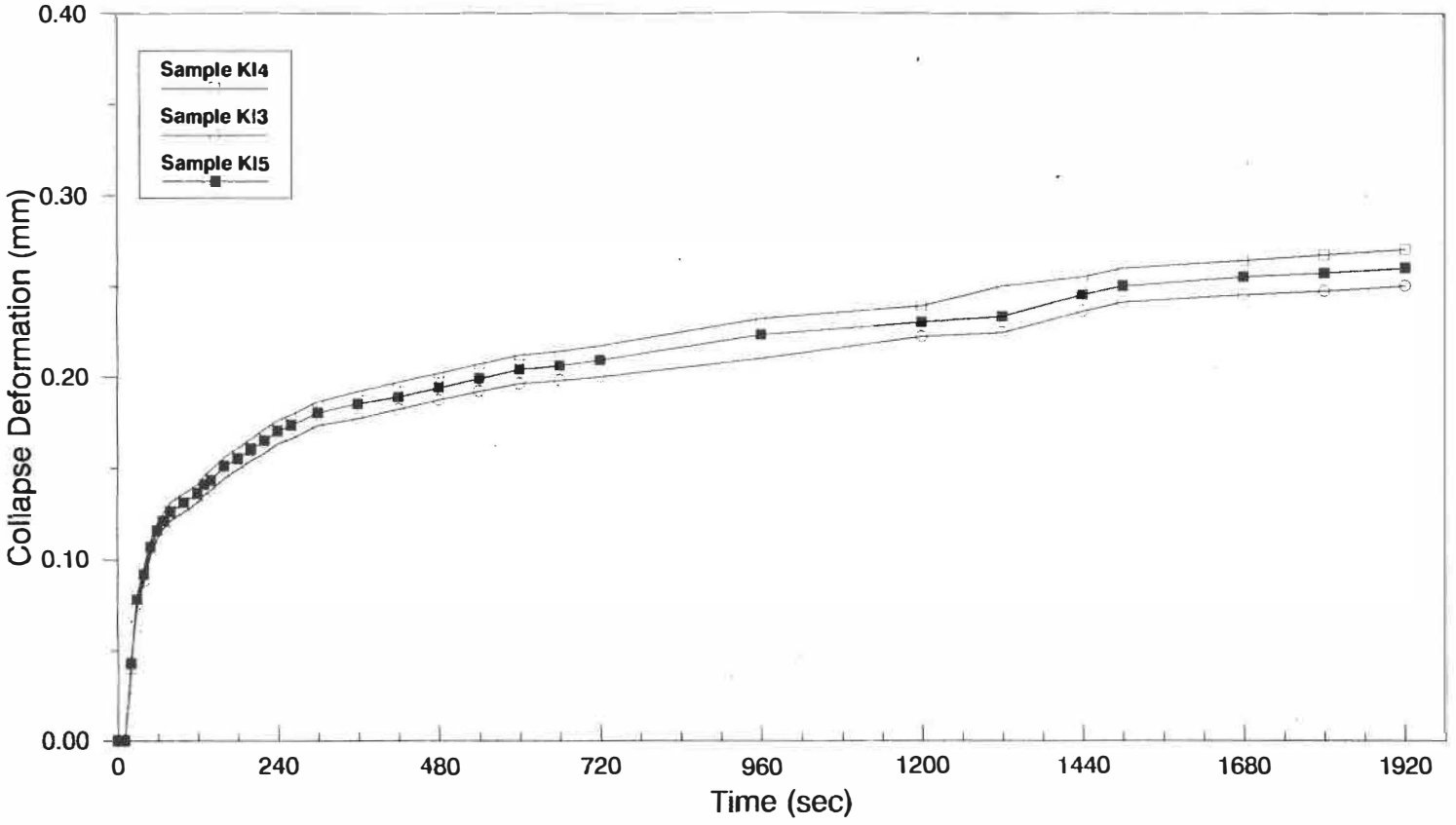

Fig. 4.20 - Axial Collapse Deformation Versus Time

in some compacted soil samples and found that about 90% of collapse deformation was complete after five to ten minutes. It can be therefore concluded that the collapse phenomenon happens fast during submergence of partially saturated compacted soils due to a sudden reduction in suction pressure.

The last sample KI2 was consolidated under constant initial suction of 24 kPa. The soil was consolidated from the initial stress state of 55 kPa axial pressure and 50 kPa radial stress to the final axial and radial stress of 605 and 600 kPa respectively. This stress path corresponds to an isotropic consolidation (K=1). Initially the axial pressure was more than the radial pressure by 5 kPa to serve as a contact pressure between the top piston and the sample through out the test and thereby being capable of measuring the axial deformation via the lower chamber volume change. The total volume change was measured as in the other tests and the radial deformation could be calculated. The test result is shown in Fig. 4.21. Test result indicated that the soil sample behaved isotropically and the radial and axial deformations were almost the same at any stress level. Although compacted samples will have some degree of anisotropy but the extent of this anisotropy is largely dependent on the extent of shear strains produced in the soil during compaction which, in turn, depends for a given method of compaction on the placement conditions. The induced anisotropy in the specimen tested under isotropic loading was not significant and could have

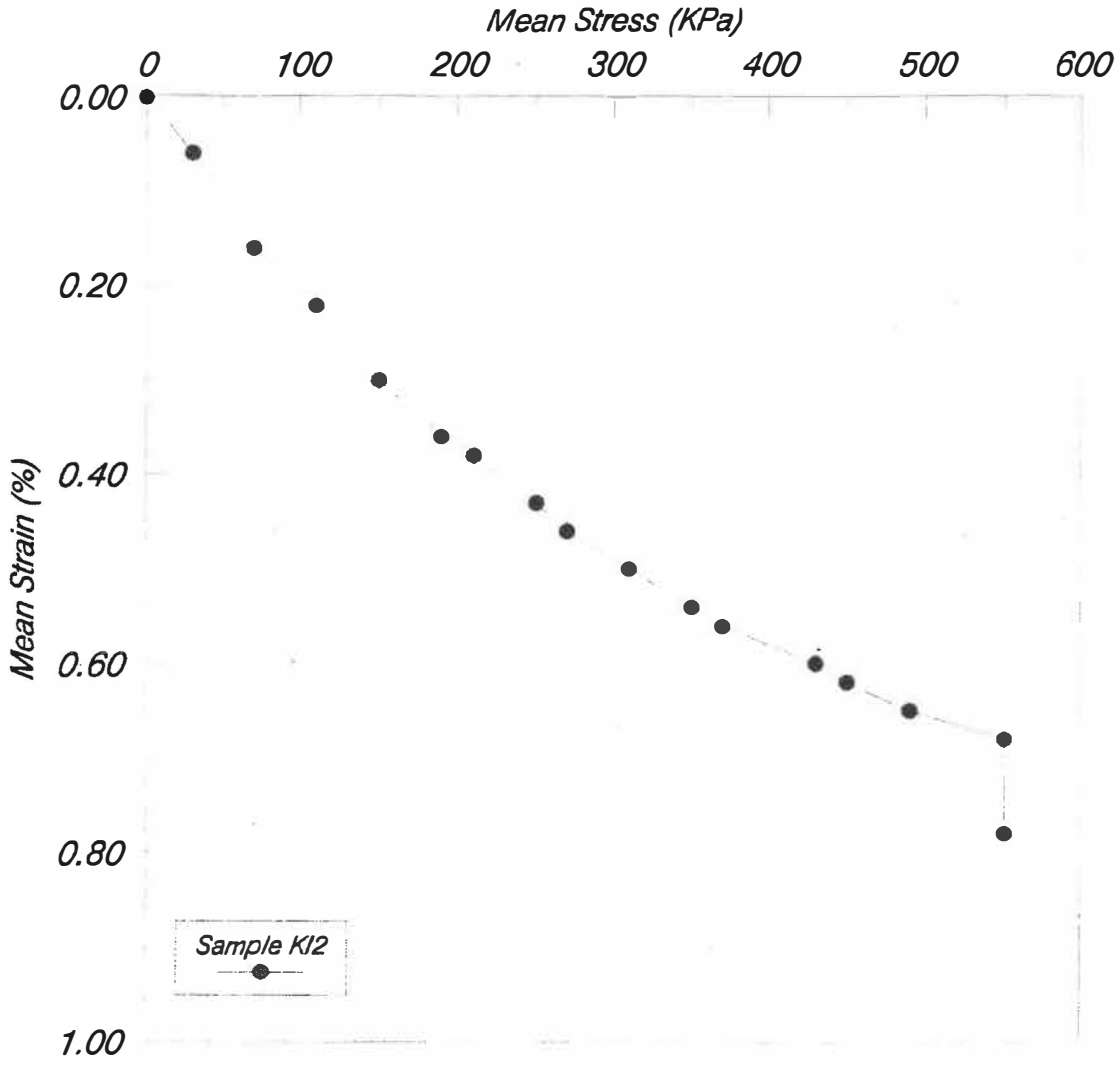

Fig. 4.21 - Compression Under Isotropic State of Stress

been erased by the application of the initial all round pressure of 50 kPa. The collapse deformation was then measured by saturating the sample. Collapse deformation occurred rapidly but it did not amount to a significant magnitude (about 0.1%) and its behavior in axial and radial directions were alike.

Regarding the results of this experimental program the following conclusions can be drawn :

- The compacted soil sample showed almost isotropic behavior under isotropic load.
- The collapse deformation is also isotropic under isotropic load.
- As the loading condition approaches the Ko condition the radial collapse deformation also becomes negligible.
- Finally, although the collapse phenomenon was detected in the compacted till samples, it did not have a considerable magnitude under the conditions of the test. Belfadhel (1986) obtained collapse deformations of the order of 5% for the same type of soil but prepared under different procedure and his test specimens had a much lower initial dry density and water content compared to the ones tested in this study.

In general, one important point to bear in mind is that the magnitude of collapse may vary significantly for the same samples (same initial conditions) depending on the type of water (water chemistry) used. This is clearly due to the

different type of interaction between the soil and the pore fluid. Consequently, to simulate closely the field condition, it is essential to prepare laboratory specimens with the same type of water and the saturation process must be carried out with the same type of water as well.

CHAPTER 5

FINITE ELEMENT FORMULATION AND PROGRAMING

5.1 General :

In this chapter, the proposed model is expressed by an elastic nonlinear formulation and its pertinent parameters are defined. A finite element formulation of the model presented previously is discussed. Moreover, incorporation of the collapse phenomena in the finite element formulation is further discussed. The structure of the finite element computer program and its specific features are also described.

5.2 Elastic Nonlinear Formulation :

5.2.1 Basic Concepts :

In the present study, an elastic nonlinear formulation was employed in order to incorporate the model into a finite element program. It makes use of the generalized Hooke's law in an incremental form in which the elastic parameters are functions of current stress (strain) state. This type of formulation is sometimes classified among quasilinear, hypoelastic, or variable elastic models. The generalized incremental Hooke's law in two dimensional form for plane strain condition is given by :

$$\begin{Bmatrix} d\sigma'_x \\ d\sigma'_y \\ d\sigma'_{xy} \end{Bmatrix} = \begin{pmatrix} B+\frac{4}{3}G & B-\frac{2}{3}G & 0 \\ B-\frac{2}{3}G & B+\frac{4}{3}G & 0 \\ 0 & 0 & 2G \end{pmatrix} \begin{Bmatrix} d\epsilon_x \\ d\epsilon_y \\ d\epsilon_{xy} \end{Bmatrix} \qquad (5.1)$$

where B and G are the tangent bulk modulus and the tangent shear modulus respectively. There are various types of quasilinear models such as K-G model, EC-Ko model, and hyperbolic model and the reader may refer to Naylor et al (1986), or Desai and Siriwardane (1984) for detailed description. All the above mentioned models approximate the nonlinear behavior in essentially a pair of elastic parameters, i.e. (B,G), (E,ν), or (B,E) which are functions of the state of stress and therefore are revised for each load increment.

Clough and Woodward (1967) suggested the following form of equation (1), in which, he defined the plain strain bulk and shear moduli :

$$\begin{Bmatrix} d\sigma'_x \\ d\sigma'_y \\ d\sigma'_{xy} \end{Bmatrix} = \begin{pmatrix} M_B+M_D & M_B-M_D & 0 \\ M_B-M_D & M_B+M_D & 0 \\ 0 & 0 & 2M_D \end{pmatrix} \begin{Bmatrix} d\epsilon_x \\ d\epsilon_y \\ d\epsilon_{xy} \end{Bmatrix} \qquad (5.2a)$$

Where :

$$M_B = \frac{d\sigma'_b}{d(\epsilon_1+\epsilon_3)} \qquad M_D = \frac{d\sigma'_d}{d(\epsilon_1-\epsilon_3)} \qquad (5.2b)$$

$$d\sigma'_b = \frac{d(\sigma'_1+\sigma'_3)}{2} \qquad d\sigma'_d = \frac{d(\sigma'_1-\sigma'_3)}{2}$$

Note that in the above equations the plane strain bulk modulus M_B is equal to B+G/3 and the plane strain shear modulus is

the same, i.e., M_D=G. These two moduli can also be expressed in terms of the Young modulus and the bulk modulus as given below :

$$M_B = \frac{9B^2}{B-E} \qquad M_D = \frac{3BE}{9B-E} \tag{5.2c}$$

Next, a hyperbolic formulation was employed to find these tangent elastic parameters, namely, the bulk and Young moduli. The choice of hyperbolic modeling was based upon several considerations such as its suitability for volume change prediction and its widespread use for prediction of movements in different types of soil structures particularly earth embankments and earth dams (Seed et al 1975). Values of the hyperbolic parameters for more than 150 different types of soils are presently available in literature (Duncan et al 1980).

Two dimensional plane strain condition was assumed in order to pursue the necessary formulation. This choice was based on the fact that in many geotechnical problems such as embankments, slopes, tunnels, and retaining walls the soil condition is reasonably represented by plane strain condition. Eisenstein and Simmon (1975) compared 3D and 2D analyses for the behavior of Mica Dam. Their studies showed that a 2D plane strain modeling is capable of producing the results which are in very good agreement with the 3D case. Also keeping in mind that the computer cost for a 3D analysis is likely to be more than five times that of a 2D problem, the use of a 2D analysis

is further justified. However, in any particular case the designer must consider whether errors introduced by such assumptions are acceptable and on the safe side.

5.2.2 Hyperbolic Formulation :

The hyperbolic model is originally attributed to Kondner (1963) who suggested that deviatoric stress - axial strain behavior of many soils can be modeled up to failure by hyperbolas with the equation of the following form (also see Fig. 5.1.a) :

$$\sigma_1 - \sigma_3 = \frac{\epsilon}{a + b\epsilon} \qquad (5.3)$$

By plotting the data in the form shown in Fig. 5.1.b and fitting a straight line to data, the values of the parameters a and b are determined. It is commonly found that the value of compressive strength is less than the asymptotic value of $(\sigma_1 - \sigma_3)$ by a small amount, therefore we may write :

$$(\sigma_1 - \sigma_3)_f = R_f (\sigma_1 - \sigma_3)_{ult} \qquad (5.4)$$

Where R_f is failure ratio, a dimensionless parameter whose value is less than unity.

Except in the case of unconsolidated undrained tests on saturated soils, both tangent modulus and compressive strength have been found to increase with increase in confining pressure. Janbu (1963) suggested the following relationship for initial tangent modulus :

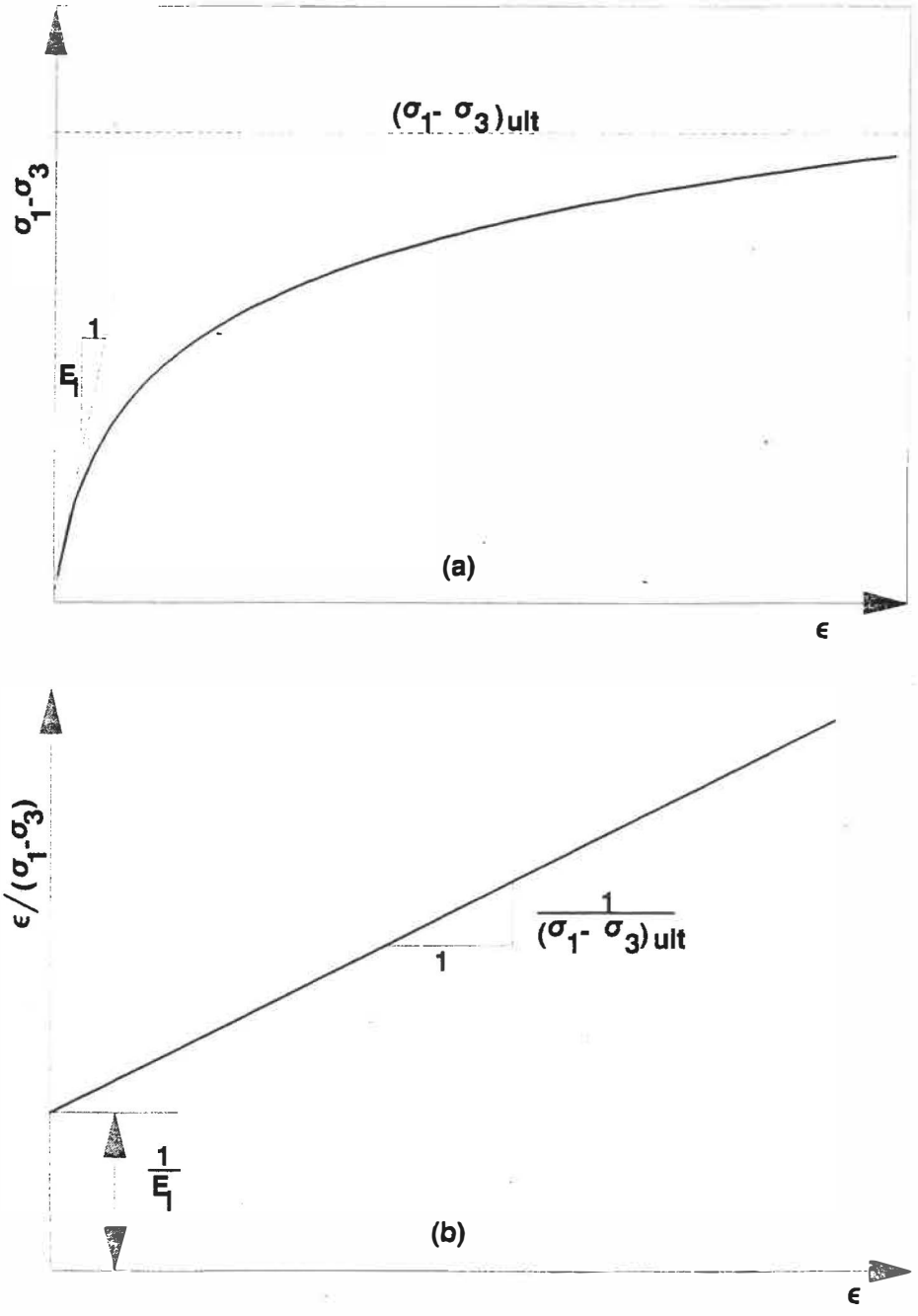

Fig. 5.1 - Hyperbolic Representation For Young Modulus

$$E_t = K P_a \left(\frac{\sigma_3}{P_a} \right)^n \tag{5.5}$$

where : σ_3 : Minor Principal stress.

Pa : Atmospheric pressure (same unit as σ_3).

K : Modulus number.

n : Modulus exponent.

Both modulus number and modulus exponent are dimensionless numbers. Furthermore, stress dependency of $(\sigma_1 - \sigma_3)_f$ can be accounted for using the Mohr Coulomb failure criterion as:

$$(\sigma_1 - \sigma_3)_f = \frac{2C\cos\phi + 2\sigma_3 \sin\phi}{1 - \sin\phi} \tag{5.6}$$

The tangent Young modulus corresponding to any point on the stress strain curve is expressed as:

$$E_t = \frac{\partial(\sigma_1 - \sigma_3)}{\partial \epsilon} \tag{5.7}$$

Performing the above differentiation on equation (5.3) and substituting equation (5.4), (5.5), and (5.6) the expression for tangent Young modulus E_t is found to be :

$$E_t = \left(1 - \frac{R_f (1 - \sin\phi)(\sigma_1 - \sigma_3)}{2C\cos\phi + 2\sigma_3 \sin\phi} \right)^2 K P_a \left(\frac{\sigma_3}{P_a} \right)^n \tag{5.8}$$

The second elastic parameter chosen for input into the generalized Hooke's law was the bulk modulus. Selig (1988) derived the values of tangent bulk modulus from isotropic compression tests with yet fitting another hyperbola of the form (Fig. 5.2a) :

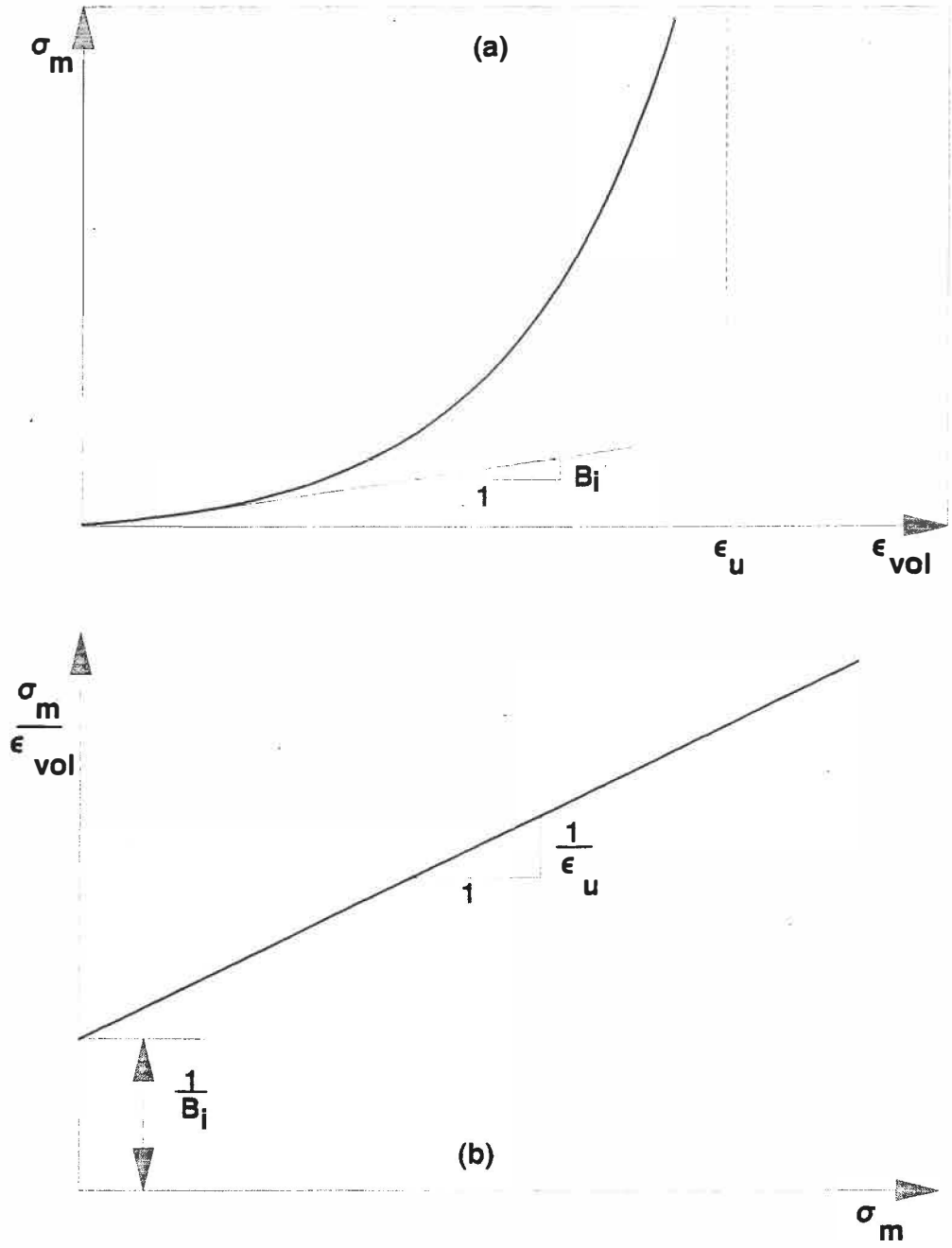

Fig. 5.2 - Hyperbolic Representation For Bulk Modulus

$$\sigma_m = \frac{B_i \epsilon_v}{1 - \epsilon_v / \epsilon_u} \qquad (5.9)$$

Where : ϵ_v : Volumetric strain.

B_i : Initial tangent bulk modulus.

ϵ_u : Asymptotic value of vol. strain.

σ_m : Mean confining pressure.

This approach has the advantage of measuring the volume change directly since the conventional triaxial tests typically generate volumetric strain data only for saturated samples. Taking the derivative of equation (5.9) with respect to volumetric strain the tangent bulk modulus B_t is obtained as :

$$B_t = \frac{B_i}{(1 - \epsilon_v / \epsilon_u)^2} \qquad (5.10)$$

Where values of B_i and ϵ_u are the intercept and the inverse of slope, respectively, of a plot σ_m/ϵ_v versus σ_m as shown in Fig. 5.2.b.

Having defined the tangent Young and bulk moduli, they may now be introduced into the generalized Hooke's law in order to describe the incremental stress strain relationship.

5.2.3 Hyperbolic Parameters for Unsaturated Soils :

In the previous section the hyperbolic modeling in terms of two tangent moduli, namely, the bulk modulus and the Young modulus was described. In order to incorporate the theoretical developments presented previously in chapter 4 for partially

saturated soils contribution of partial saturation to each of these two moduli should be separated as:

$$B_t = B_t(\epsilon_v) + B_t(S, \epsilon_v) \qquad (5.11a)$$

$$E_t = E_t(\sigma'_1, \sigma'_3) + E_t(S, \sigma'_1, \sigma'_3) \qquad (5.11b)$$

Where $B_t(\epsilon_v)$ and $E_t(\sigma'_1, \sigma'_3)$ are bulk modulus and Young modulus for saturated condition and $B_t(S, \epsilon_v)$ and $E_t(S, \sigma'_1, \sigma'_3)$ are the contribution to the same moduli, respectively, due to partial saturation. The functions $B_t(\epsilon_v)$ and $E_t(\sigma'_1, \sigma'_3)$ are obtained from isotropic and standard triaxial tests, respectively, on fully saturated samples using the hyperbolic formulation explained before (equations 5.80 and 5.10). It is assumed that the hyperbolic formulation is applicable to the fully saturated condition and therefore, effective values must be used for the stresses and the soil parameters appearing in the preceding equations. Performing another isotropic test on the same soil with the same initial condition but at its natural moisture content (unsaturated) will provide another set of data that together with the fully saturated data will enable us to determine the contribution to the bulk modulus due to partial saturation. A numerical procedure using non-linear optimization was suggested in chapter 4 to obtain the function $B_t(S, \epsilon_v)$. A similar procedure can be followed to determine the contribution of partial saturation to the Young modulus, $E_t(S, \sigma'_1, \sigma'_3)$. However, in the absence of proper triaxial shear test data on unsaturated samples their behavior

may be approximated using the same hyperbolic equation for tangent Young modulus used for saturated case but modified to take into account the effect of partial saturation. The Mohr Coulomb failure criteria for partially saturated soils, using Bishop's equation for effective stress (equation (3.4)), is of the following form:

$$\tau = C' + \{(\sigma - u_a) + \chi(u_a - u_w)\}\tan\phi' \qquad (5.12a)$$

or :

$$\tau = C' + (\sigma - u_a)\tan\phi' + (u_a - u_w)\chi\tan\phi' \qquad (5.12b)$$

Where :

C' : Cohesion.

ϕ' : soil friction angle.

u_a, u_w : pore air and water pressure respectively.

χ : parameter which is a function of degree of saturation as defined in chapter 3.

This equation is equivalent to the shear strength surface proposed by Fredlund (1985) for partially saturated soils provided that the term $\chi\tan\phi'$ is replaced with $\tan\phi_b$, where $\tan\phi_b$ is the rate of increase in shear strength with suction pressure.

If $(u_a - u_w)\tan\phi'$ is considered as a cohesion component due to partial saturation then we can write :

$$\tau = C^* + (\sigma - u_a)\tan\phi' \qquad (5.13)$$

Where :

$$C^* = C' + (u_a - u_w)\tan\phi'$$

Therefore equation (5.8) for partially saturated condition is modified as :

$$E_t = \left(1 - \frac{R_f(1-\sin\phi')(\sigma_1 - \sigma_3)}{2C^*\cos\phi' + 2(\sigma_3 - u_a)\sin\phi'}\right)^2 KP_a\left(\frac{\sigma'_3}{P_a}\right)^n \qquad (5.14)$$

Hence, the contribution to the Young's modulus due to partial saturation is determined as :

$$E_t(S, \sigma'_1, \sigma'_3) = E_t - E_t(\sigma'_1, \sigma'_3) \qquad (5.15)$$

In general, in order to determine a complete set of parameters for the proposed model two steps need to be followed. First, depending on the constitutive relationship chosen i.e., elastic, elastoplastic, etc, a set of parameters for saturated behavior of the soil is obtained. This set of parameters are obtained from appropriate test results on fully saturated soil samples which corresponds to the saturated rigidity K_1 of the proposed model (equation 3.14). Secondly, from similar test results on the same soil but at its natural (or compacted) moisture content together with the previous results from the fully saturated soil samples another set of parameters which accounts for the contribution of partial saturation is deduced. This set of parameters represents the rigidity K_2 of the proposed model.

5.2.4 Collapse Consideration :

The collapse load $\{d\sigma_c\}$ as presented previously in chapter 4 can be expressed in the following form :

$$\{d\sigma_c\} = \left[\frac{\partial}{\partial S}\int_0^{\epsilon} K_2 d\epsilon\right] dS \tag{5.16}$$

In difference form, equation (5.16) is written as :

$$\{d\sigma_c\} = \frac{\int_0^{\epsilon} K_2 d\epsilon|_{s=s_2} - \int_0^{\epsilon} K_2 d\epsilon|_{s=s_1}}{\Delta S}\Delta S$$

$$= \int_0^{\epsilon} K_2 d\epsilon|_{s=s_2} - \int_0^{\epsilon} K_2 d\epsilon|_{s=s_1} \tag{5.17}$$

Dividing the collapse load into deviatoric and volumetric part and assuming uncoupled behavior will give :

$$d\sigma_{vc} = \int_0^{\epsilon_v} M_B^s d\epsilon_v|_{S=S_2} - \int_0^{\epsilon_v} M_B^s d\epsilon_v|_{S=S_1}$$

$$d\sigma_{dc} = \int_0^{\epsilon_d} M_D^s d\epsilon_d|_{S=S_2} - \int_0^{\epsilon_d} M_D^s d\epsilon_d|_{S=S_1}$$

Where $d\sigma_{vc}$ and $d\sigma_{dc}$ are the volumetric and deviatoric components of collapse force. M_B^s and M_D^s are the contribution of partial saturation to the plane strain bulk modulus and the plain strain shear modulus, respectively, determined from equations (5.2c) using $B_t(S, \epsilon_v)$ and $E_t(S, \sigma'_1, \sigma'_3)$. Knowing these two components of the collapse force, the principal collapse stresses at any state of stress (or strain) can be calculated and implemented in the computer program that is described later in this chapter.

5.3 Finite Element Formulation :

The problems involved in the analysis of continuum media are generally defined by differential equations or integral statements for which no closed form solution exists and resort has to be made to numerical analysis. The finite element method has proved to be one of the most general, useful, and popular numerical method to deal with such problems. It allows us to include nonlinearity of the medium in each element and is capable of dealing with complex geometry.

In the following sections the variational formulation for the proposed model is explained and wherever needed, basic finite element concepts are stated without going into much details. Therefore, the reader is referred to finite element textbooks such as Zienkiewicz (1989) for detailed explanations.

5.3.1 Variational Formulation :

Considering an elasticity problem with the domain Ω bounded by a closed boundary Γ, two dimensional plane strain condition can be assumed provided that both boundary loading and body forces do not have any component in the Z direction and are uniformly distributed along the thickness (see Fig. 5.3).

The equilibrium equations for this case are given by :

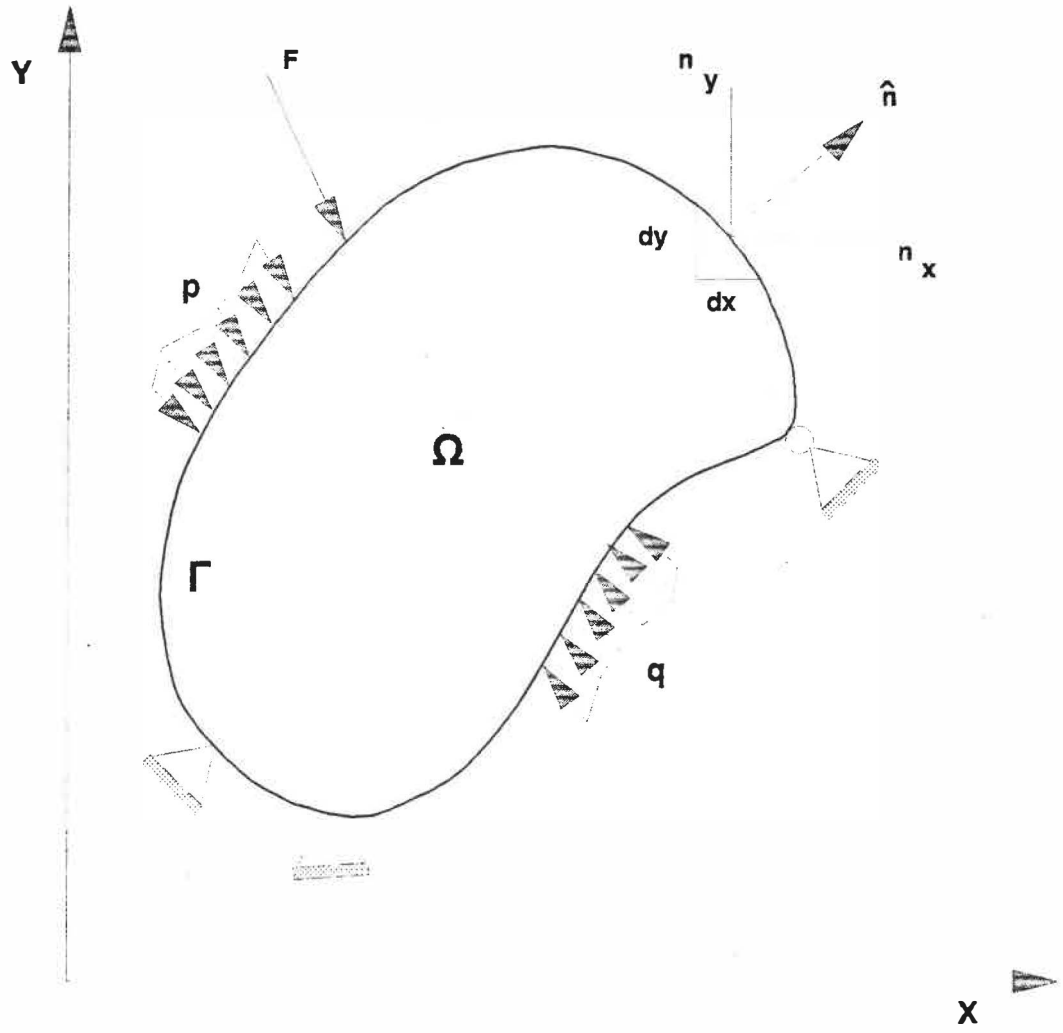

Fig. 5.3 - Two Dimensional Elasticity Problem

$$\frac{\partial \sigma_x}{\partial x} + \frac{\partial \tau_{xy}}{\partial y} + f_x = 0 \qquad (5.19a)$$

$$\frac{\partial \tau_{xy}}{\partial x} + \frac{\partial \sigma_y}{\partial y} + f_y = 0 \qquad (5.19b)$$

Where f_x and f_y denote the body forces in the x and y directions respectively.

Strain - displacement relationships are written as :

$$\epsilon_x = \frac{\partial u}{\partial x} \quad , \qquad \epsilon_y = \frac{\partial v}{\partial y} \quad , \qquad \gamma_{xy} = \frac{\partial u}{\partial y} + \frac{\partial v}{\partial x} \qquad (5.20)$$

Another set of equations needed for the variational formulation is the constitutive relationship which for the model proposed was given by equation (5.2). This equation can be written in the general form of :

$$\begin{Bmatrix} d\sigma'_x \\ d\sigma'_y \\ d\sigma'_{xy} \end{Bmatrix} = \begin{pmatrix} C_{11} & C_{12} & C_{13} \\ C_{21} & C_{22} & C_{23} \\ C_{31} & C_{32} & C_{33} \end{pmatrix} \begin{Bmatrix} d\epsilon_x \\ d\epsilon_y \\ d\epsilon_{xy} \end{Bmatrix} \qquad (5.21)$$

The coefficients C_{ij} are related to variable elastic bulk and shear moduli as presented previously (Equations 5.2a, and 5.2c). Finally, to relate the effective stresses in constitutive relationship with the total stresses in equilibrium equations, effective stress relationship must be used, given by :

$$\begin{Bmatrix} d\sigma_x \\ d\sigma_y \\ d\sigma_{xy} \end{Bmatrix} = \begin{Bmatrix} d\sigma'_x \\ d\sigma'_y \\ d\sigma'_{xy} \end{Bmatrix} + \begin{Bmatrix} 1 \\ 1 \\ 0 \end{Bmatrix} dP \qquad (5.22)$$

Where P is the equivalent pore pressure for partially saturated soil, which is :

$$P = u_a - \chi(u_a - u_w)$$

The natural and essential boundary conditions are :

Natural :

$$\sigma_x n_x + \tau_{xy} n_y = \hat{t}_x$$

$$\tau_{xy} n_x + \sigma_y n_y = \hat{t}_y \qquad (5.23)$$

Essential :

$$u = \hat{u}$$

$$v = \hat{v} \qquad (5.24)$$

Where $\hat{n} = (n_x, n_y)$ is the unit vector normal to the boundary. By substituting equation (5.20) in (5.21) and the results in (5.19) through the effective stress relationship, the following set of equations will be obtained :

$$\frac{\partial}{\partial x}\left(C_{11}\frac{\partial u}{\partial x} + C_{12}\frac{\partial v}{\partial y}\right) + C_{33}\frac{\partial}{\partial y}\left(\frac{\partial u}{\partial y} + \frac{\partial v}{\partial x}\right) + \frac{\partial p}{\partial x} + f_x = 0 \qquad (5.25a)$$

$$C_{33}\frac{\partial}{\partial x}\left(\frac{\partial u}{\partial y} + \frac{\partial v}{\partial x}\right) + \frac{\partial}{\partial y}\left(C_{12}\frac{\partial u}{\partial x} + C_{22}\frac{\partial v}{\partial y}\right) + \frac{\partial p}{\partial y} + f_y = 0 \qquad (5.25b)$$

and carrying out the same process for the natural boundary conditions will give :

$$\left(C_{11}\frac{\partial u}{\partial x} + C_{12}\frac{\partial v}{\partial y}\right) n_x + C_{33}\left(\frac{\partial u}{\partial y} + \frac{\partial v}{\partial x}\right) n_y = \hat{t}_x \qquad (5.26a)$$

$$C_{33}\left(\frac{\partial u}{\partial y} + \frac{\partial v}{\partial x}\right) n_x + \left(C_{12}\frac{\partial u}{\partial x} + C_{22}\frac{\partial v}{\partial y}\right) n_y = \hat{t}_y \qquad (5.26b)$$

The variational (weak) form of equations (5.25a), and (5.25b)

over an element domain Ω_e is derived by multiplying the two equations by two test functions w_1 and w_2, respectively, and using the Green theorem to reduce the order of differentiation which will finally yield :

$$\int_{\Omega e}\left[\frac{\partial w_1}{\partial x}\left(C_{11}\frac{\partial u}{\partial x}+C_{12}\frac{\partial v}{\partial y}\right)+C_{33}\frac{\partial w_1}{\partial y}\left(\frac{\partial u}{\partial y}+\frac{\partial v}{\partial x}\right)+\frac{\partial w_1}{\partial x}p-w_1 f_x\right]d\Omega-$$

$$\int_{\Gamma}(\bar{t}_x+pn_x)d\Gamma=0 \qquad (5.27a)$$

$$\int_{\Omega_e}\left[C_{33}\frac{\partial w_2}{\partial x}\left(\frac{\partial u}{\partial y}+\frac{\partial v}{\partial x}\right)+\frac{\partial w_2}{\partial y}\left(C_{12}\frac{\partial u}{\partial x}+C_{22}\frac{\partial v}{\partial y}\right)+\frac{\partial w_2}{\partial y}p-w_2 f_y\right]d\Omega-$$

$$\int_{\Gamma}(\bar{t}_y+pn_y)d\Gamma=0 \qquad (5.27b)$$

Substituting the test function W_1, W_2 by the interpolation function N_1 and writing in the matrix form will give :

$$\begin{pmatrix}K_{11} & K_{12}\\ K_{21} & K_{22}\end{pmatrix}\begin{Bmatrix}u\\ v\end{Bmatrix}=\begin{Bmatrix}F_1\\ F_2\end{Bmatrix} \qquad (5.28)$$

Where :

$$K_{11}=\int_{\Omega e}\left[C_{11}\frac{\partial N_i}{\partial x}\frac{\partial N_j}{\partial x}+C_{33}\frac{\partial N_i}{\partial y}\frac{\partial N_j}{\partial y}\right]d\Omega$$

$$K_{12}=\int_{\Omega e}\left[C_{12}\frac{\partial N_i}{\partial x}\frac{\partial N_j}{\partial y}+C_{33}\frac{\partial N_i}{\partial y}\frac{\partial N_j}{\partial x}\right]d\Omega$$

$$K_{22}=\int_{\Omega e}\left[C_{33}\frac{\partial N_i}{\partial x}\frac{\partial N_j}{\partial x}+C_{22}\frac{\partial N_i}{\partial y}\frac{\partial N_j}{\partial y}\right]d\Omega$$

$$K_{21}=K_{12}$$

$$F_1=\int_{\Omega e}N_i f_x d\Omega+\int_{\Gamma e}N_i t_x d\Gamma-\int_{\Omega e}\frac{\partial N_i}{\partial x}N_j\bar{p}\,d\Omega$$

$$F_2 = \int_{\Omega e} N_i f_y d\Omega + \int_{\Gamma e} N_i t_y d\Gamma - \int_{\Omega e} \frac{\partial N_i}{\partial y} N'_j \bar{p} d\Omega$$

Note that in the above developments we have assumed that there is no flow through the soil and the pore pressures are known at any instant during loading or may be determined solely from the volume change and the change in degree of saturation. Moreover, a different shape function N'_i was used for the pressure term. The reason is that since the value of P and not its derivatives appears in the above equations, for the sake of consistency of approximation, the interpolation function for the pressure term P should have one degree less than that of displacements.

5.3.2 Scheme to Include Collapse in the Finite Element Formulation :

In the previous section finite element formulation for a plane strain elasticity was presented. The constitutive relationship for this case (equation 5.21) did not include the term which takes into account the collapse force i.e., $d\sigma_c$. A procedure to express the principal collapse stresses in terms of bulk and shear moduli was explained in section 5.2.4. For implementation in a finite element program the equivalent nodal collapse forces for each element were found using the principle of virtual work expressed by :

$$\{F_{ci}\} = \int_{\Omega e} [B]^T \{d\sigma_c\} d\Omega$$

Where $\{dF_{ci}\}$ is the nodal collapse forces, and [B] is the strain matrix relating the strain inside the element to the nodal displacements ($\{\epsilon\}=[B]\{\delta\}$).

These nodal collapse forces are then considered as external forces applied to each element and since these forces are function of pore pressure and degree of saturation their values are not known a priori and hence an iterative procedure is called upon to deal with this type of problem. The steps required to resolve the problem are summarized as follow :

- Apply a load increment.
- Find the corresponding nodal displacements $\{d\delta\}$.
- Calculate the strain increment $\{d\epsilon\}=[B]\{d\delta\}$.
- Calculate the corresponding principal stress and strain increments.
- Find the change in the degree of saturation and suction pressure.
- calculate the principal collapse stresses due to the change in degree of saturation and transfer them to the problem coordinate system to obtain $\{d\sigma_c\}$.
- Find equivalent element nodal force $\{dF_{ci}\}$ (equation 5.29).
- Find additional displacements $\{d\delta_c\}$ due to $\{dF_{ci}\}$.
- Calculate the total displacement for the present load increment $=\{d\delta\}+\{d\delta_c\}$.
- Apply the next load increment.

It should be noted that since the problem is nonlinear for each load increment (both external and collapse load) an iterative scheme is followed to achieve convergence. This procedure is explained in the next section.

5.4 Computer Program :

5.4.1 Program Structure :

A flow chart of computer program showing the sequential processing of the finite element program is shown in Fig. 5.4. The computer program is structured to consist of the following main blocks :

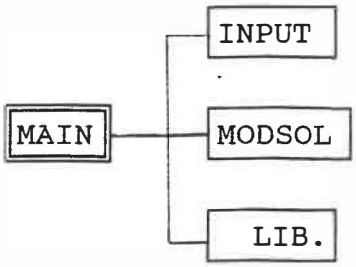

INPUT block consists of subroutines to read in necessary input data and to allocate them into appropriate matrices and vectors.

MODSOL block provides necessary subroutines to find the element stiffness, assembly, global stiffness, collapse load, global load vector, solution, and result output.

LIB block contains the subroutines for dynamic memory allocation in order to optimize memory allocation (provided by Dr. Pelletier).

The flow chart of these blocks together with other informations

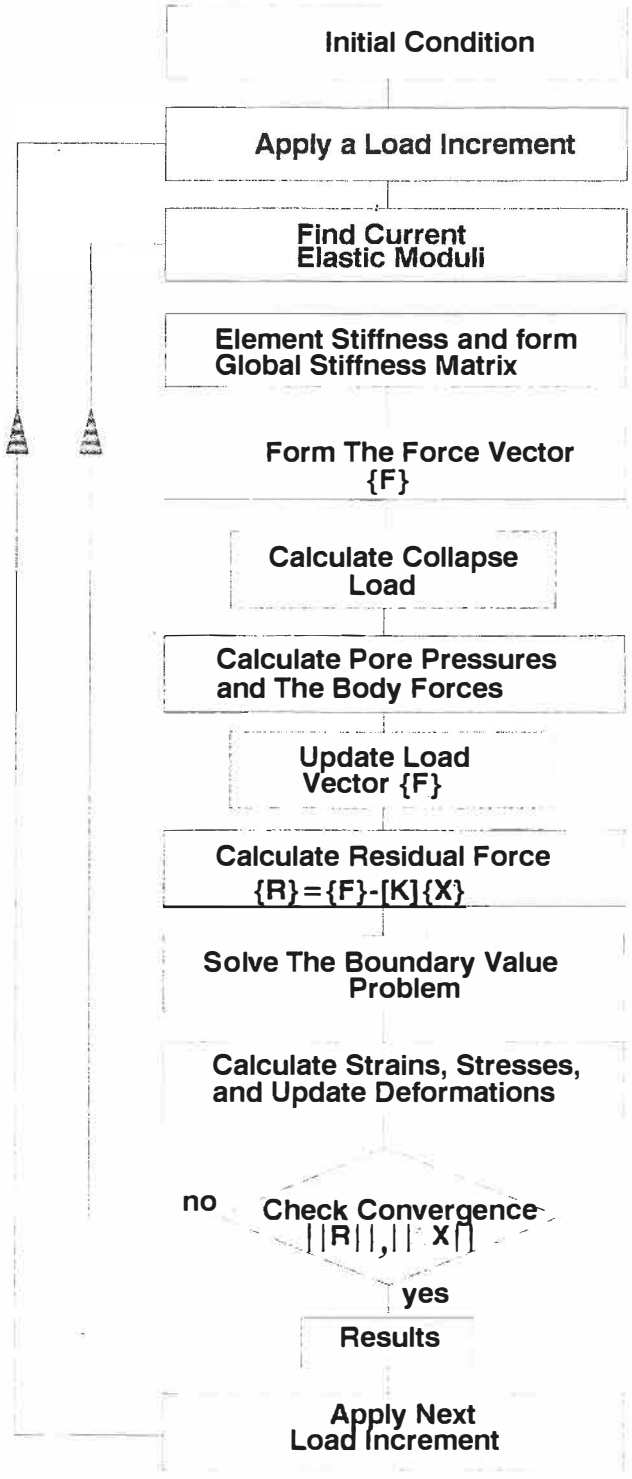

Fig. 5.4 - Flow Chart of Solution Procedure In The Computer Program

are given in the appendix.

5.4.2 Element Type :

Isoparametric quadrilateral element was formulated in the computer program. Two types of quadrilateral elements one linear with four nodes and another quadratic with nine nodes, as shown in Fig. 5.5, were employed. The user has the choice of any of them by inputting the corresponding flag parameter ITYPE (see appendix).

5.4.3 Solution Algorithm and Convergence Criteria:

The final set of equation to be solved for each load increment is a system of nonlinear equations of the following form :

$$[A(x)]\{x\} = \{B\}$$

An iterative procedure is needed to resolve this system of equations. This system was resolved using the following iterative scheme :

$$[A(x^n)]\{\Delta x\} = \{R(x^n)\}$$

$$x^{n+1} = x^n + \Delta x$$

Where $\{x^n\}$ is the x values at the nth iteration and $R(x^n)$ is the residual force vector given by :

$$R(x^n) = \{B\} - [A(x^n)]\{x^n\}$$

At each iteration the residual force is calculated and the value of the Δx is found and thus the value of x is updated for the next iteration until convergence is achieved.

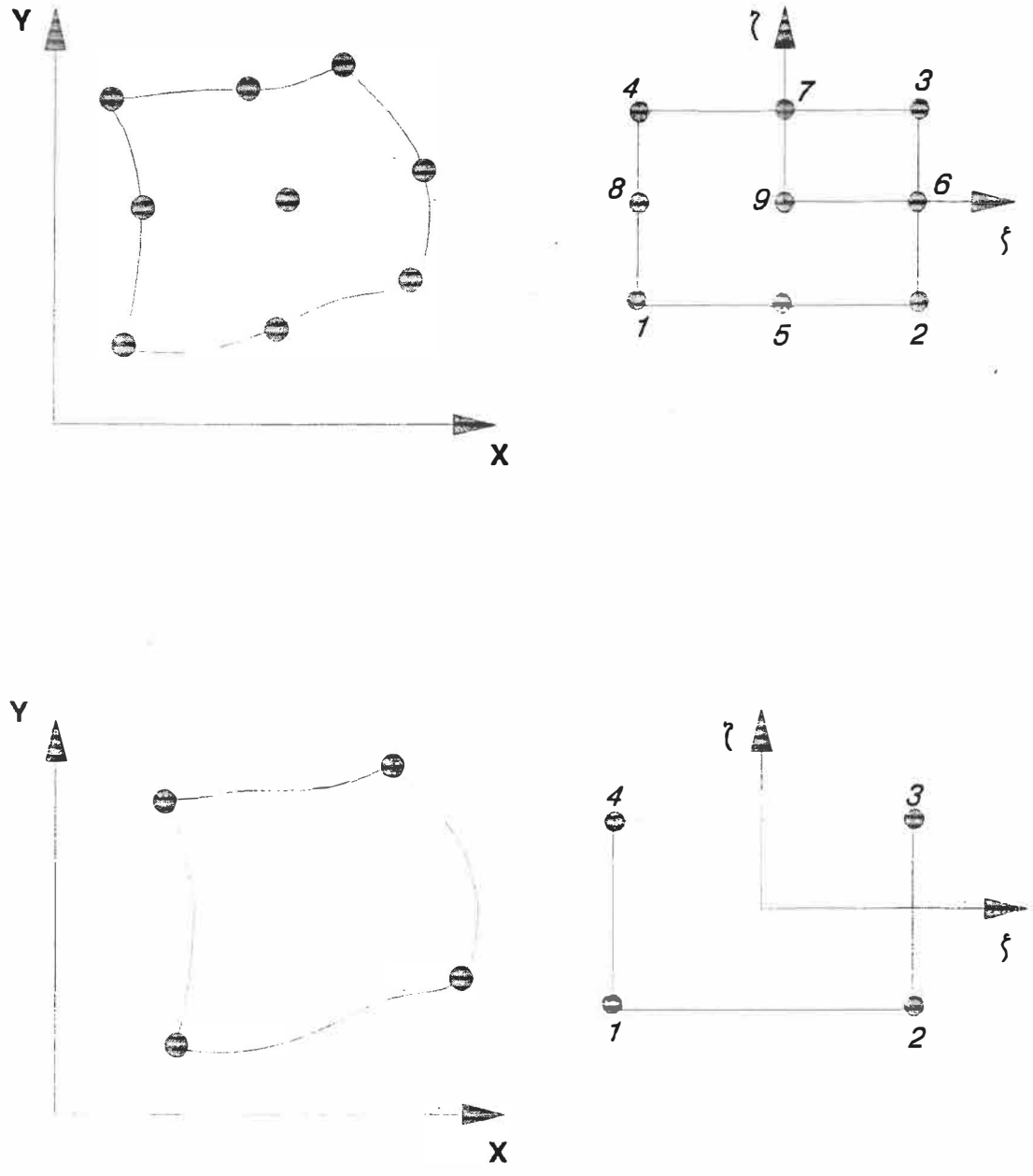

Fig. 5.5 - Four and Nine Node Isoprametric Elements Used In The Computer Program

Convergence of the results was achieved when the Euclidean and maximum norm of both the residual force and $\triangle x$ were less than specified tolerances.

CHAPTER 6

RESULTS AND DISCUSSION

6.1 General :

In this chapter, numerical results obtained from the computer program are presented and are discussed qualitatively with regard to the actual behavior of partially saturated soils observed in the field. Wherever experimental results are available, the results are also compared quantitatively and suitability of the model for numerical prediction is further investigated. Sensitivity of the results to input parameters is also investigated. Finally, for predicting deformations as a function of time when seepage through an earth dam or embankment occurs the model should be coupled with the continuity and flow equations, a procedure to couple the developed finite element program with PERCO (a computer program that simulates the flow of water through both saturated and unsaturated soils) is also presented.

6.2 Selection of Model Parameters :

In order to study numerically the collapse predictivity of the model, experimental data were needed to calibrate the model and find its relevant parameters. The test results on glacial till samples presented in chapter 4 did not show appreciable amount of collapse deformation for the specific test conditions considered. Hence, Ko triaxial test results on silty clay soil samples obtained by Radhakrishna (1967)

were used to calibrate the model. The basic soil properties and experimental results for this soil were described in chapter 2 (see Table 2.1 and Fig. 2.1). The set of parameters needed as input for the model is given in given in Table 6.1. The available experimental data were used to find the six volume change parameters, namely, parameters A, B, C, D, B_i, and ϵ_u. Since there were no shear strength data available for this soil, the other parameters, friction angle, cohesion, failure ratio, modulus number, and modulus exponent were estimated. The friction angle was estimated using Jaky relationship for normally consolidated soils given by :

$$K_o = 1 - \sin\phi' \qquad (6.1)$$

The other four parameters were selected based on the comparison of the basic soil properties (such as soil type, plasticity index, liquid limit, dry density, and initial water content) with those for which the hyperbolic parameters were available in the literature. As mentioned previously, the hyperbolic parameters for more than 150 different types of soils determined by various authors are available in literature (Duncan et al 1980). With the above consideration together with the fact that the final set of parameters should be able to satisfy Ko condition under the specified incremental stress ratio, the remaining parameters were selected. The complete set of parameters is presented in Table 6.2.

Table 6.1 - List of Parameters Used In Modeling

No.	Parameter	Function	Equation
1	A	Parameter In Function f(s)	3.32
2	B	Additional Rigidity $B(s,\epsilon)$	3.31
3	C	"	"
4	D	"	"
5	B_i	Bulk Modulus Parameter	5.10
6	ϵ_u	"	"
7	K	Modulus Number	5.14
8	n	Modulus Exponent	"
9	R_f	Failure Ratio	"
10	Co	Cohesion	"
11	Φ'	Friction Angle	"

Table 6.2 - Values of Parameters For Input To The Computer Program

No.	Parameter	Value
1	A	4.51
2	B	95.1
3	C	10.9
4	D	2.86
5	B_i	17.0
6	ϵ_u	0.12
7	K	130.0
8	n	0.95
9	R_f	0.82
10	Co (KPa)	25.0
11	Φ'	27.0

6.3 Numerical Results :

6.3.1 K_o Loading :

K_o test condition was simulated by the computer program using a single nine node isoparametric element with the boundary conditions shown in Fig. 6.1. The soil element was loaded successively with an applied load increment ratio of $d\sigma_3/d\sigma_1 = 0.55$ (shown in Fig. 6.1). The soil was then loaded under successive axial and radial stress increments to their final experimental values. The saturation process at the end of loading was also simulated and its corresponding collapse deformation calculated. The results for this type of test condition with the collapse calculated at different final applied loads are shown in Fig. 6.2. Comparison with the actual test results is presented later in this chapter.

6.3.2 Isotropic Loading :

Isotropic compression was simulated using the same type of element with a total incremental stress ratio $d\sigma_3/d\sigma_1 = 1$. Several load increments were applied and the radial and axial collapse deformation under the final applied load was calculated. The calculated collapse deformation for different final applied loads are shown in Fig. 6.3.

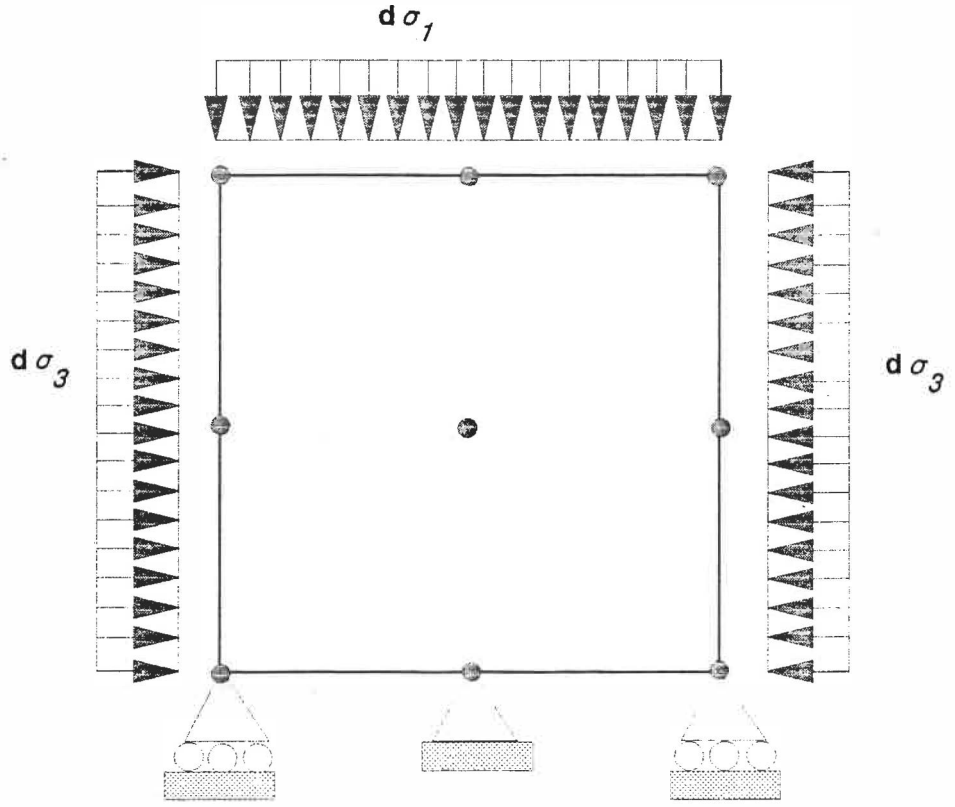

d σ_1 = 90 KPa
d σ_3 = 49.5 KPa

Fig. 6.1 - Boundary Conditions and The Applied Load Increment

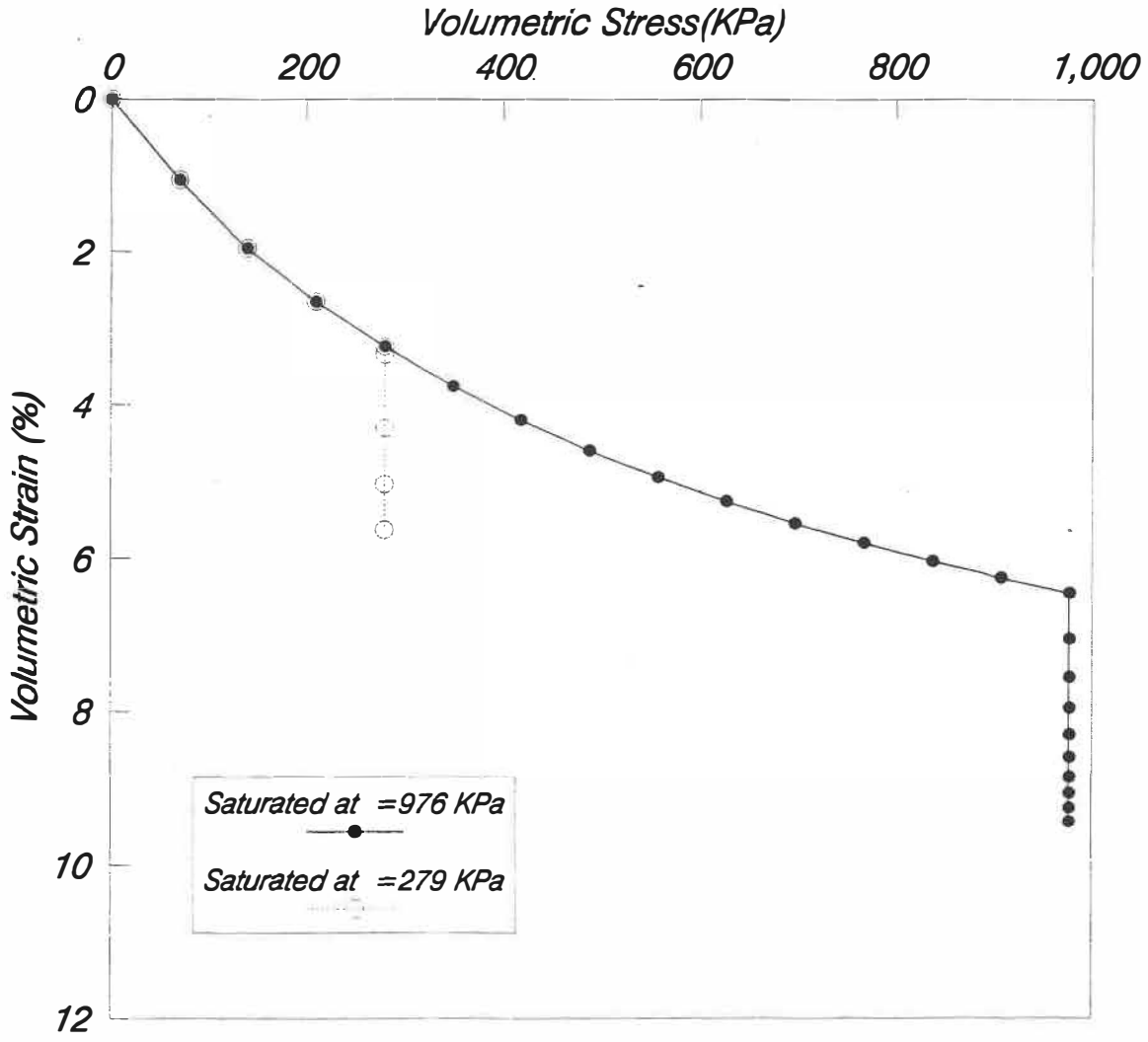

Fig. 6.2-Collapse Calculated For Two Different Final Applied loads (under Ko - condition)

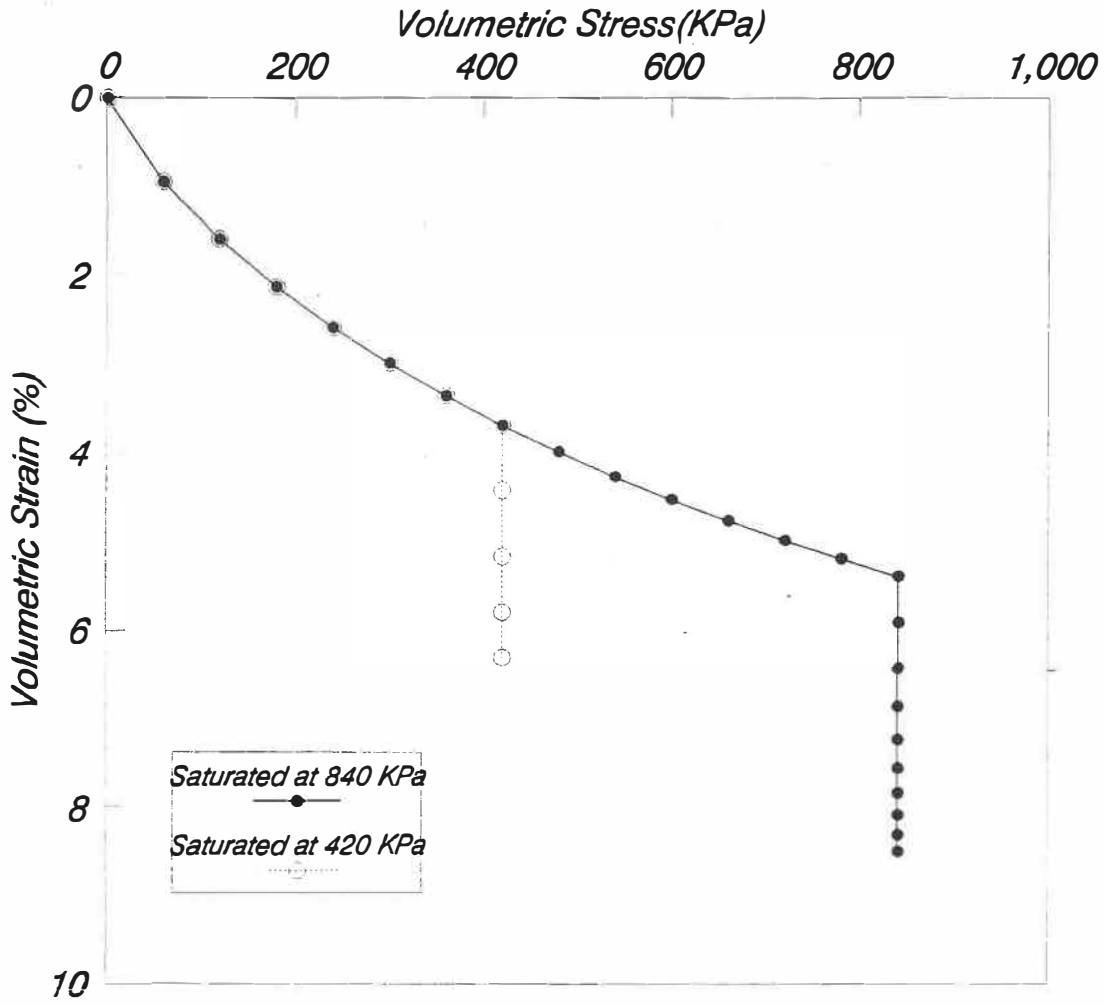

Fig. 6.3 - Collapse Calculated For Two Different Final Applied loads (Under Isotropic Stress Condition)

6.3.3 K < K_o Loading :

For this case a total incremental stress ratio of $d\sigma_3/d\sigma_1 = 0.40$ was applied and as before the radial and axial collapse deformations were calculated for different final applied loads. The corresponding results are shown in Fig. 6.4.

6.3.4 General State of Stress :

In this case the soil element was tested under a general condition of plane loading. The applied load increment is shown in Fig. 6.5a. This state of stress as shown in the 6.5b is essentially the same as the k_o condition but the applied stresses are oriented at an angle of 45° with respect to the principal stress directions (on Mohr circle). Distortion of the soil element at the end of loading and after saturation is shown in Fig. 6.5c. The complete set of results for this case is shown in Fig. 6.6.

6.4 Results Discussion :

For K_o condition the experimental results measuring the amount of collapse upon saturation were available and therefore, they were used to verify the predictivity of the model. The volume change results obtained in Fig. 6.2 for the sample K_o-B1 is redrawn in Fig. 6.7 as a function of mean confining stress ($=(\sigma_1 + \sigma_2 + \sigma_3)/3$) and comparison is made with the corresponding experimental results. Besides, predictivity of the model for the behavior of sample K_o-B5 which had the

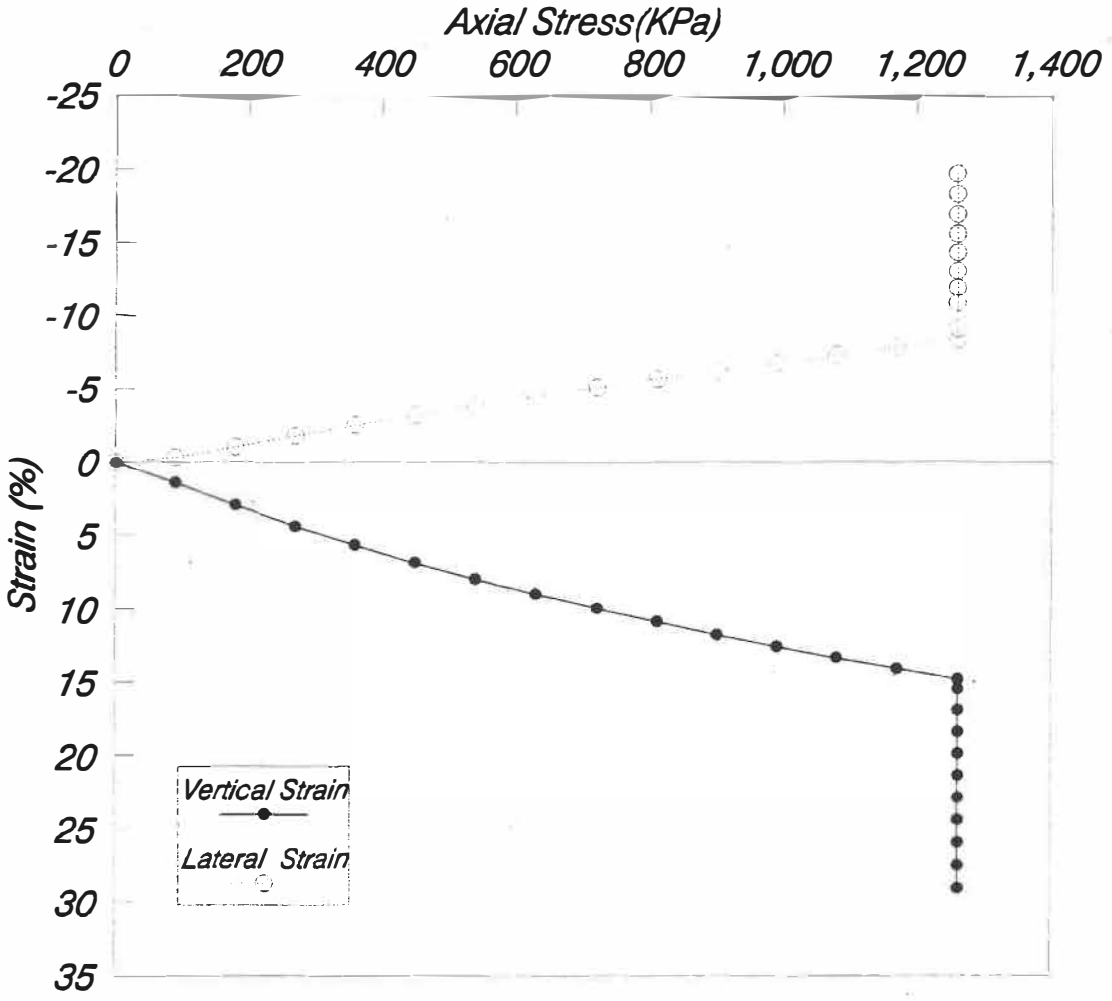

Fig. 6.4 - Axial and Lateral Deformation Upon Saturation For K=0.4

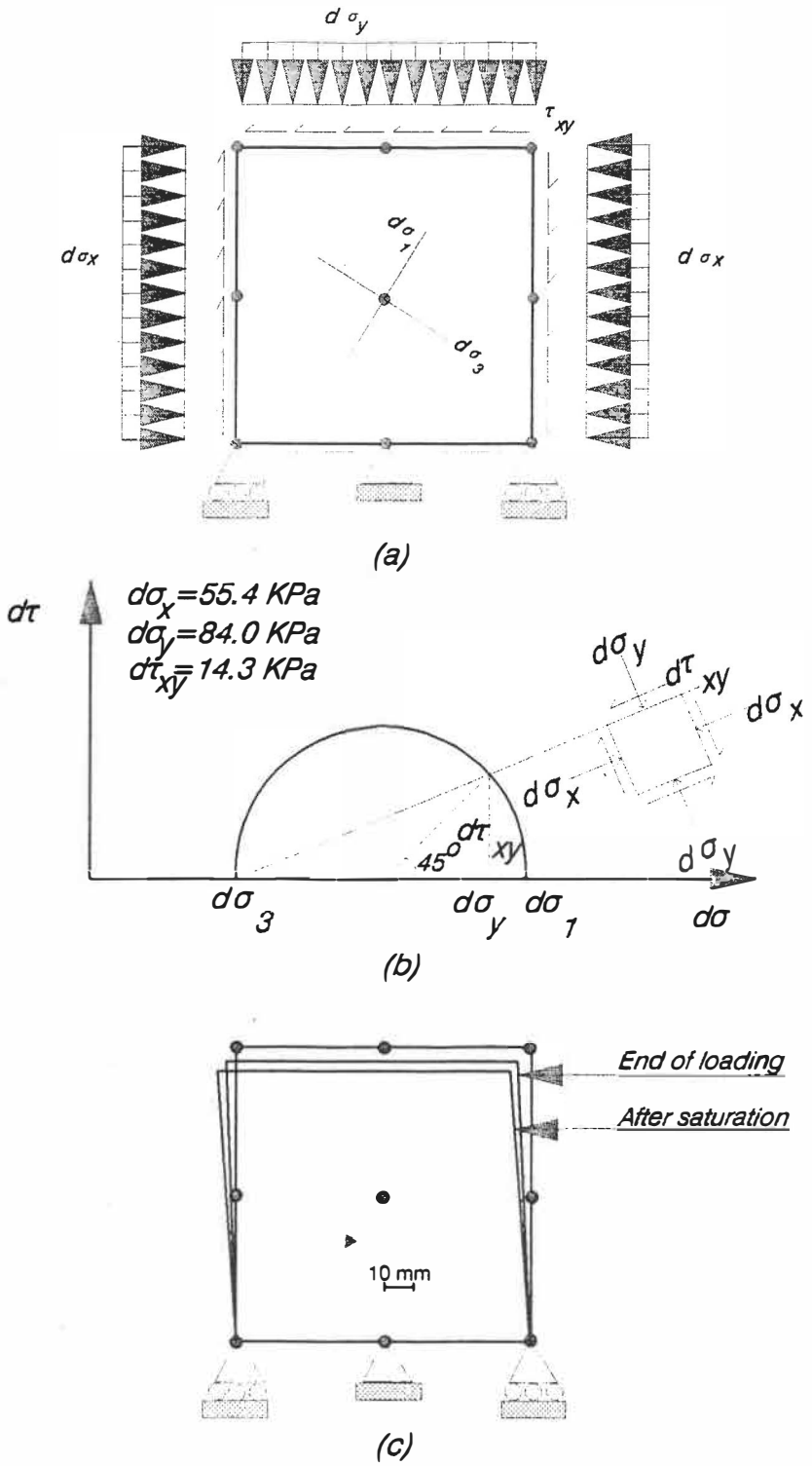

Fig. 6.5 - Load Increments, Mohr Circle, and Distortion of The Element For The General Loading Condition

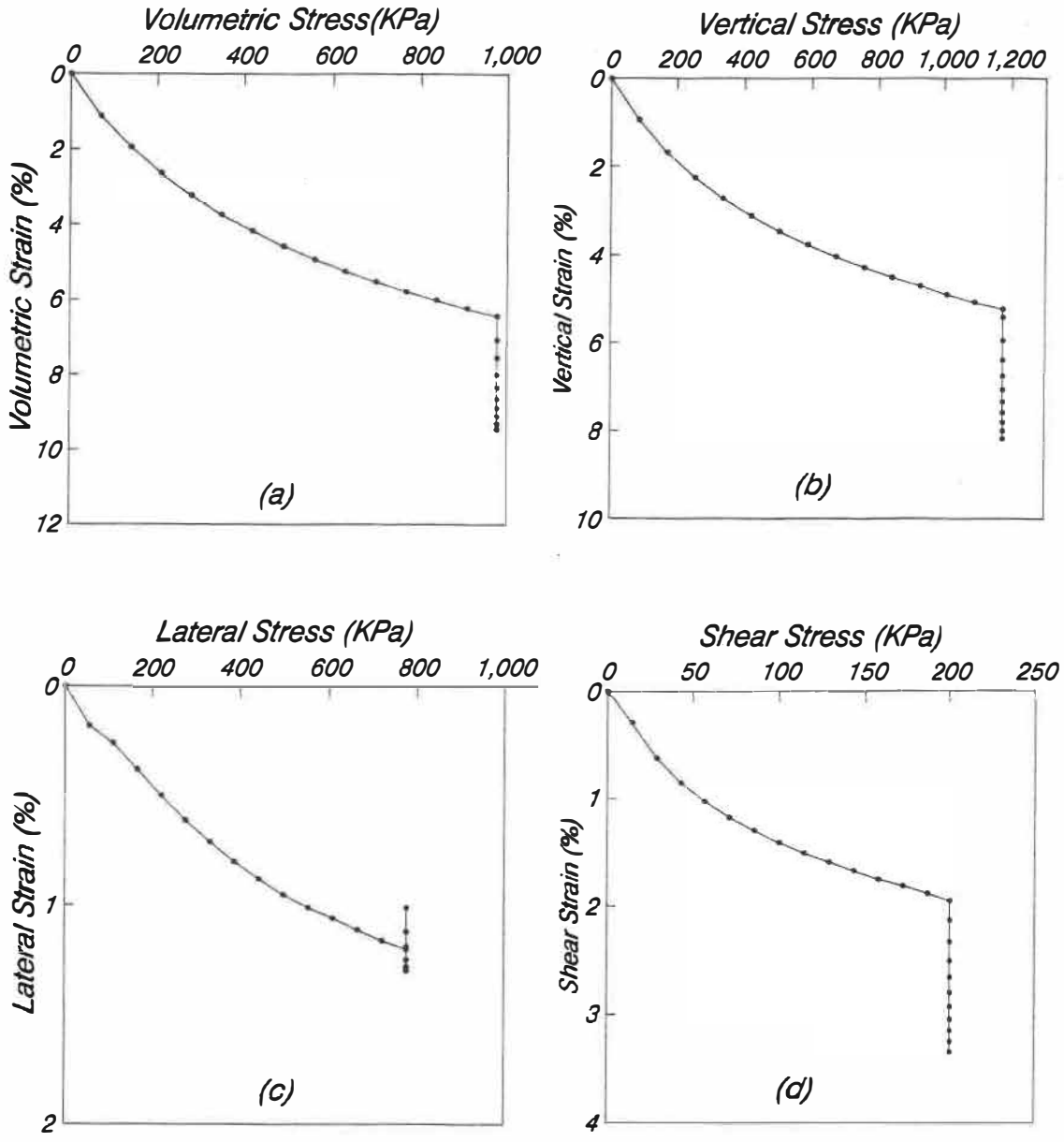

Fig. 6.6 - Collapse Deformations For The General Loading Condition

same initial condition but saturated under a different applied load was tested. The predicted behavior during loading, saturation, and reloading is compared with the experimental results in Fig. 6.7. Furthermore, collapse prediction for sample K_o-B2 which had the same initial condition as the previous samples except that its initial degree of saturation was partially increased before loading was also simulated with the model and the results are illustrated in Fig. 6.7. The results from all cases considered displayed the suitability of the model for the collapse behavior prediction and its accuracy for the quantitative prediction of collapse deformation.

Since in practice full saturation is rarely encountered upon soil submergence, expected behavior for partial increase in degree of saturation was also examined. Fig. 6.8 shows the collapse deformation and reloading for the sample K_o-B5 compared with the same case except that a partial increase in the degree of saturation to S=70% was allowed under constant applied load (S=52% before the saturation process). As expected the soil showed a smaller amount of collapse deformation and a lower compressibility upon reloading.

For the other cases presented previously in this chapter, that is, isotropic and $K<K_o$ loading no experimental data was available and therefore a qualitative comparison with the observed field behavior is discussed. A soil element in an embankment or earth dam before impoundment of reservoir can

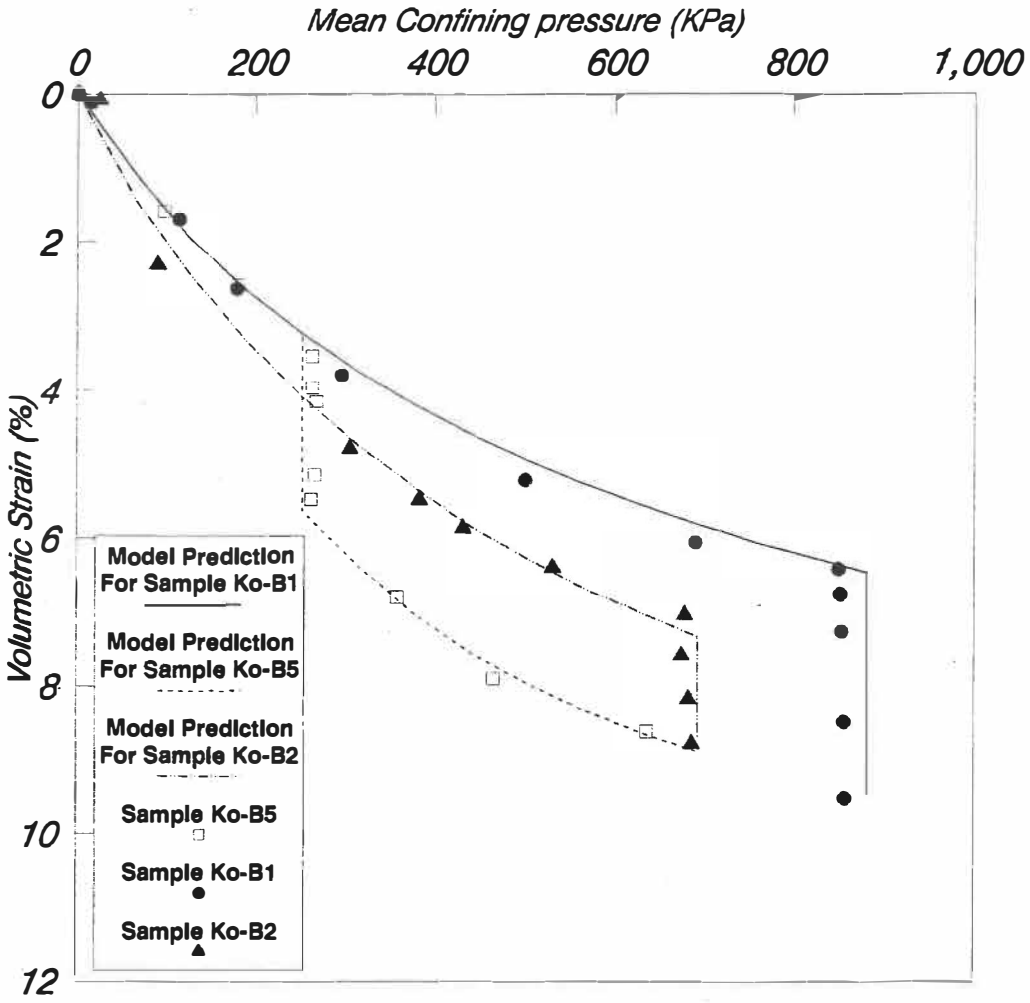

Fig. 6.7 - Volume Change Prediction of The Model Versus Experimental Results For Ko - Condition

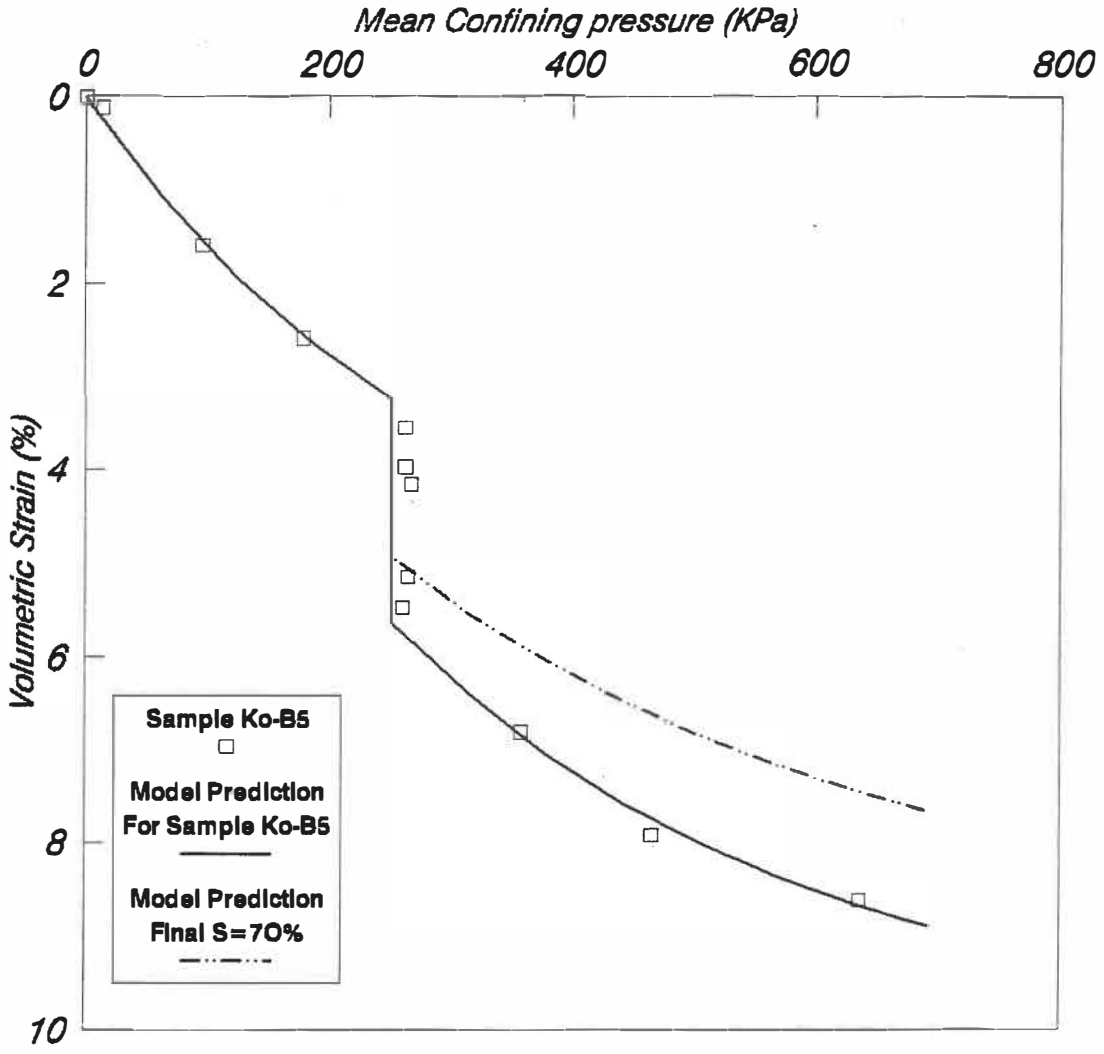

Fig. 6.8 - Effect of Partial Increase In Degree of Saturation On The Amount of Collapse Deformation

have different states of stress depending on its location in the body of the embankment. A typical stress distribution for LG4 dam cross section (the second largest structure on the La Grand Complex of the James Bay hydroelectric development) given by Paré et al (1984) is shown in Fig. 6.9a and Fig. 6.9b. As shown in this figure the principal stress ratios at various points have different values ranging from isotropic condition to very low values. Typical locations for different stress ratios are shown in Fig. 6.9c. The results from computer program presented before suggests no lateral deformation for K_o condition, isotropic collapse deformation for isotropic loading, and lateral expansion with axial compression for $K<K_o$. Field observations from different case histories suggest similar type of behavior. An example is the case of Gepatsch dam (Fig. 6.10) which indicated collapse displacements in the upstream part pointing outward and to the upstream direction while displacements at center (near K_o condition) are practically vertical. This type of behavior is consistent with the behavior predicted by the model.

Since in a finite element program, in general, the principal stress directions do not coincide with the local element coordinate system, there is always shear stresses acting on the element as well as normal stresses. Hence the general case of loading with normal stresses as well as shear stresses acting on the same soil element was studied. Since the applied stresses were chosen to have the same principal stresses as

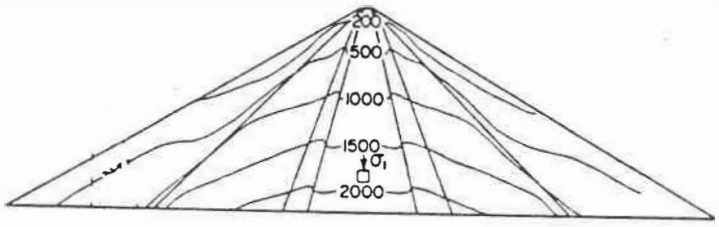

(a) Major Principal Stresses (after Paré et al 1984)

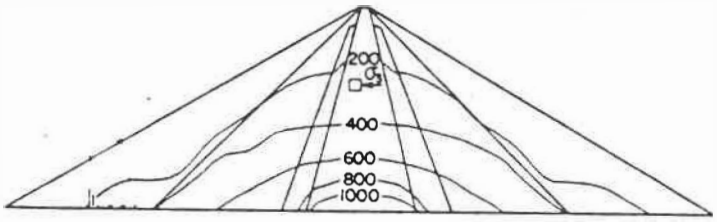

(b) Minor Principal Stresses (after Paré et al 1984)

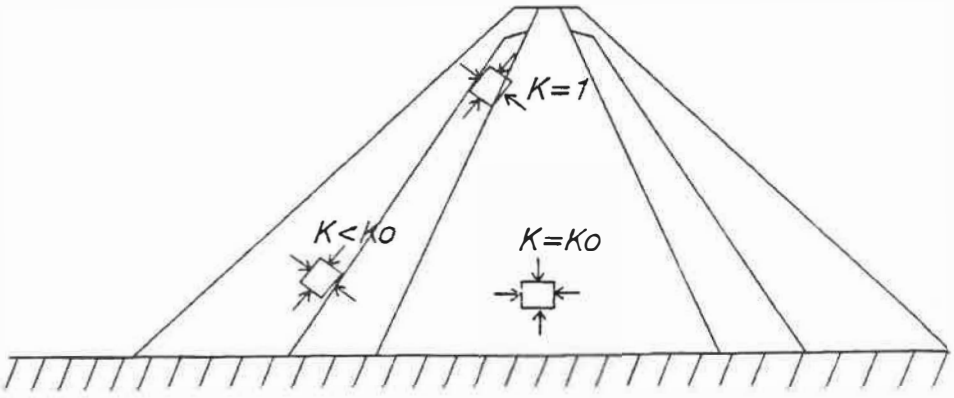

(c) Typical Locations For Different States of Stress

Fig. 6.9 - Stress State at The End of Construction In LG4 Earth Dam

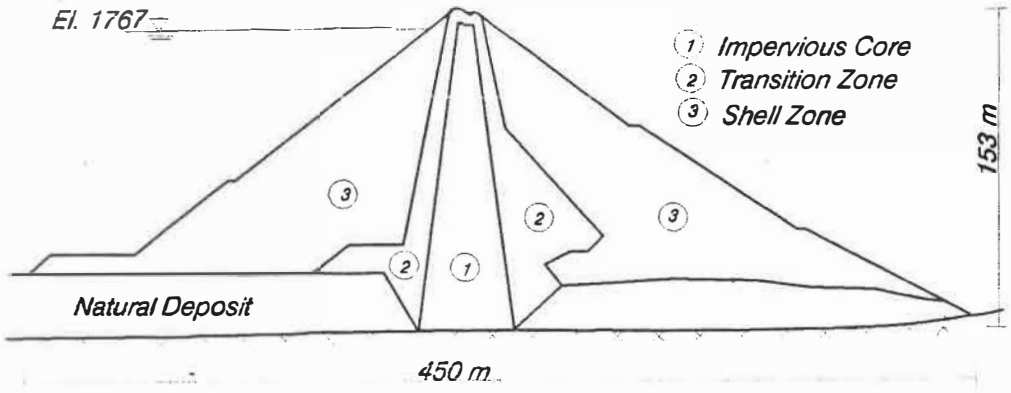

Typical Cross - Section

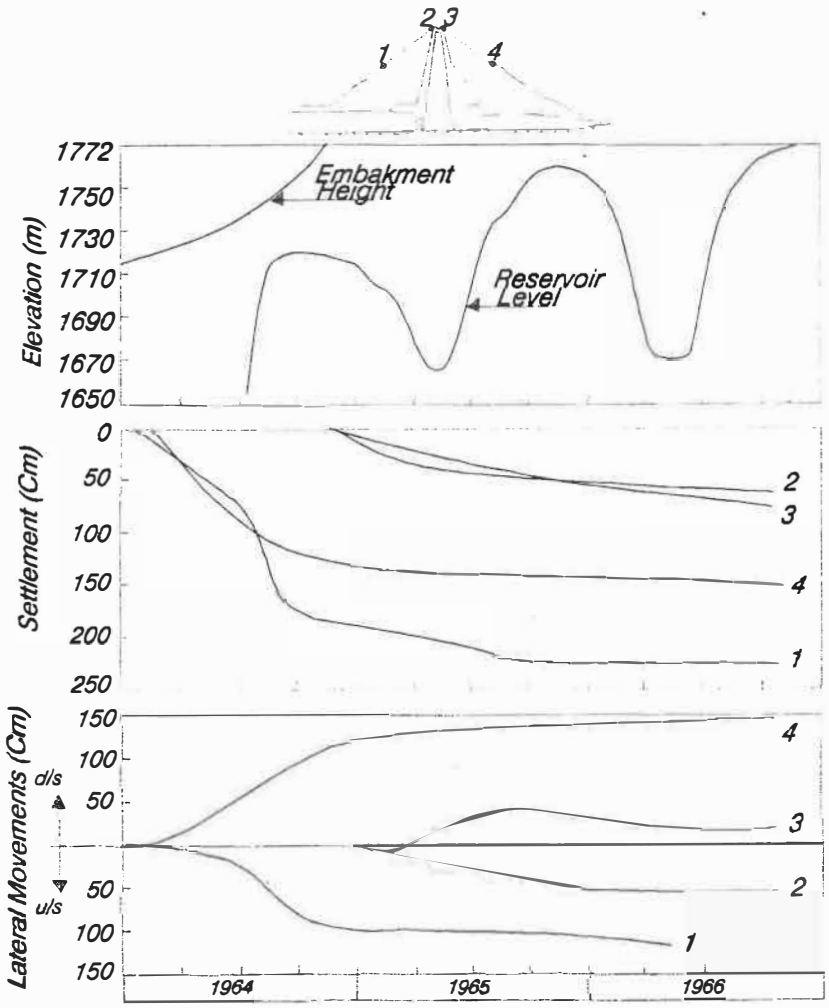

Fig. 6.10 - Movements of Surface Points In Gepatsch Dam (after Schober 1967)

the K_o condition the two cases were essentially the same. The results from the two cases showed the same amount of volume change and if the principal strains from the general case is calculated they would be identical to the strains from K_o condition.

6.5 Results Sensitivity to The Input Parameters :

In order to study the sensitivity of the results to the input parameters, each parameter was varied about 10% while keeping all the other parameters unchanged. The effect of parameter variation on the results was studied for the general case. The influence of any single parameter on the results is shown in figures 6.11 through 6.21. Results from this sensitivity analysis can be summarized as follow :

- Since the two elastic moduli, i.e., bulk modulus and Young modulus were determined independently, a change in parameters incorporated in Young modulus had no effect on volume change behavior (see figures 6.11 through 6.14, Fig. 6.20, and Fig. 6.21.
- All parameters may have some influence on shear distortion since the shear modulus was not input independently and was calculated from Young modulus and Bulk modulus according to the relationship :

$$M_D = \frac{3BE}{9B - E} \qquad (6.2)$$

However, some parameters did not show any appreciable influence on shear strain results (Fig. 6.14, Fig. 6.15, Fig. 6.17, Fig. 6.18, Fig. 6.19).

- For this analysis it was found that the parameter with the highest influence on volume change behavior was the parameter "C" used in the function $K(S,\epsilon)$ for additional rigidity due to partial saturation. Nevertheless, its effect on the results was not significant since for a 10% change in this parameter the results varied about ±5%.
- The parameters with most influence on shear distortion were found to be modulus number "K", failure ratio Rf, and friction angle ϕ. The maximum effect was about ±16% for ±10% change in friction angle.

In general, the model did not show significant sensitivity to a change in any single parameter for volume change prediction. For shear strain, again, the model did not show considerable sensitivity to a change in most parameters. The maximum variation as mentioned before was from a change in friction angle. However, this small sensitivity to friction angle did not have any influence on the results presented previously for testing predictivity of the model since in those cases volumetric behavior (equal to axial strain for K_o condition) was being studied.

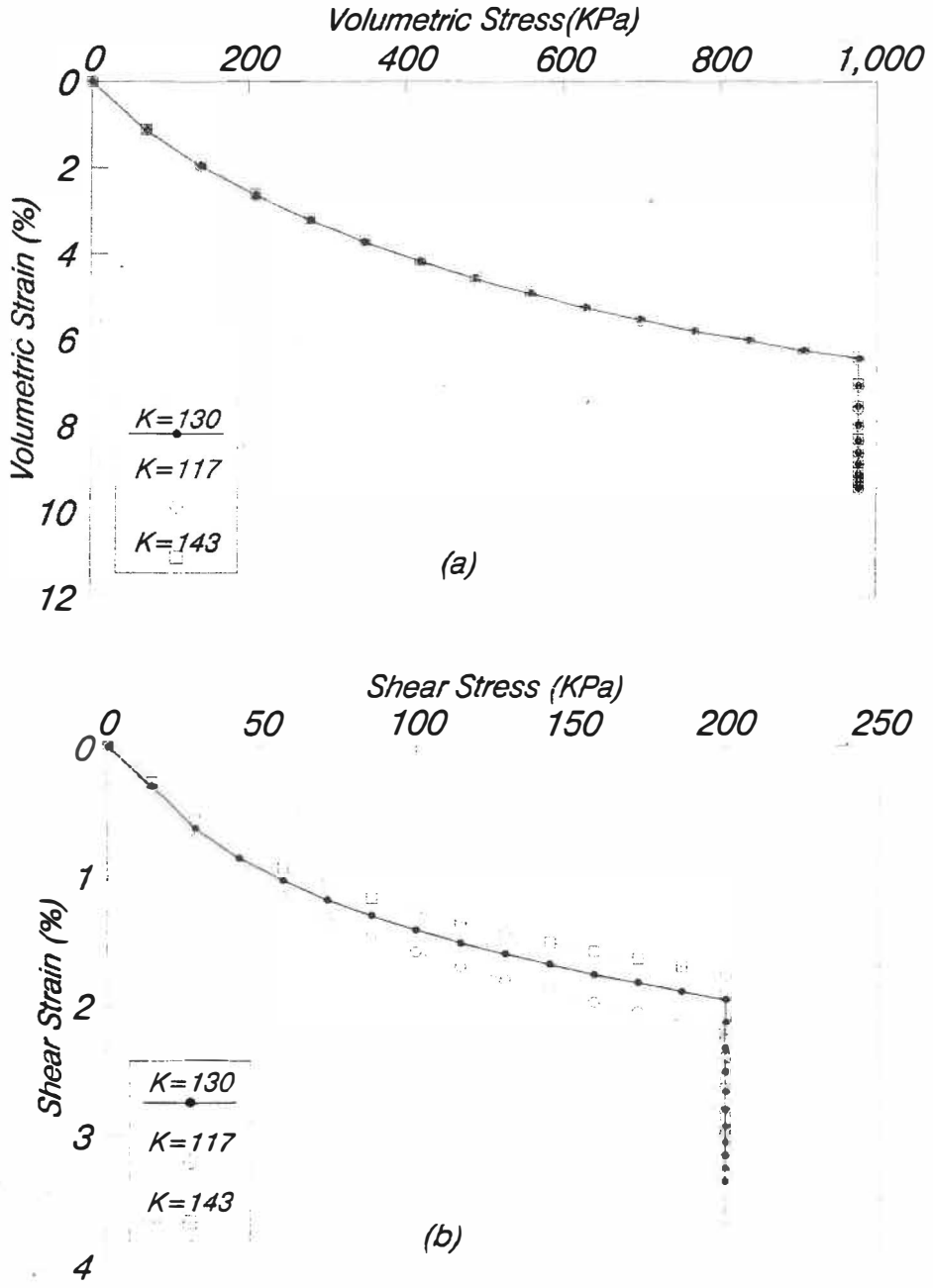

Fig. 6.11 - Sensitivity of The Results to a Change in Modulus No. "K"

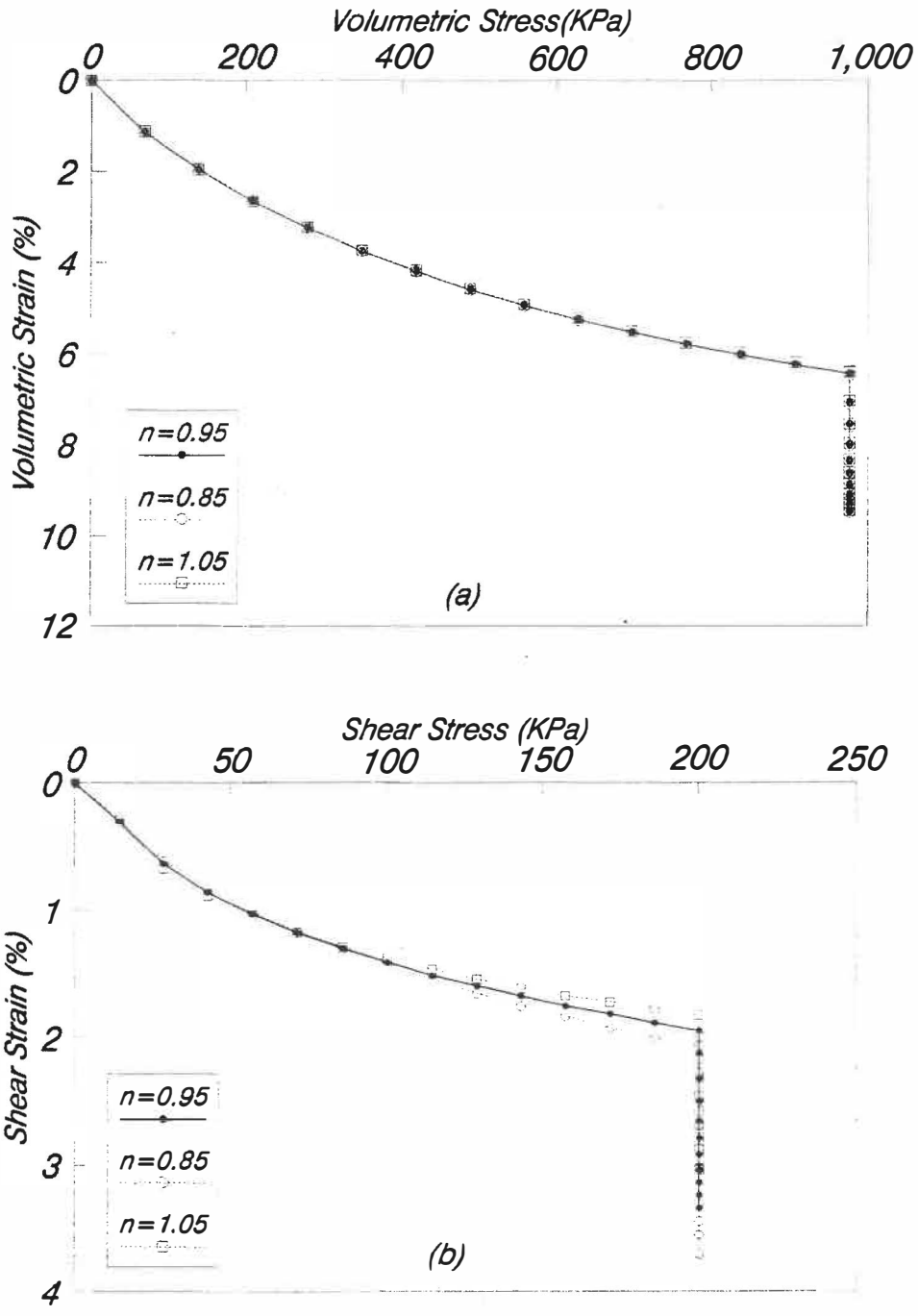

Fig. 6.12 - Sensitivity of The Results to a Change in Modulus Exp."n"

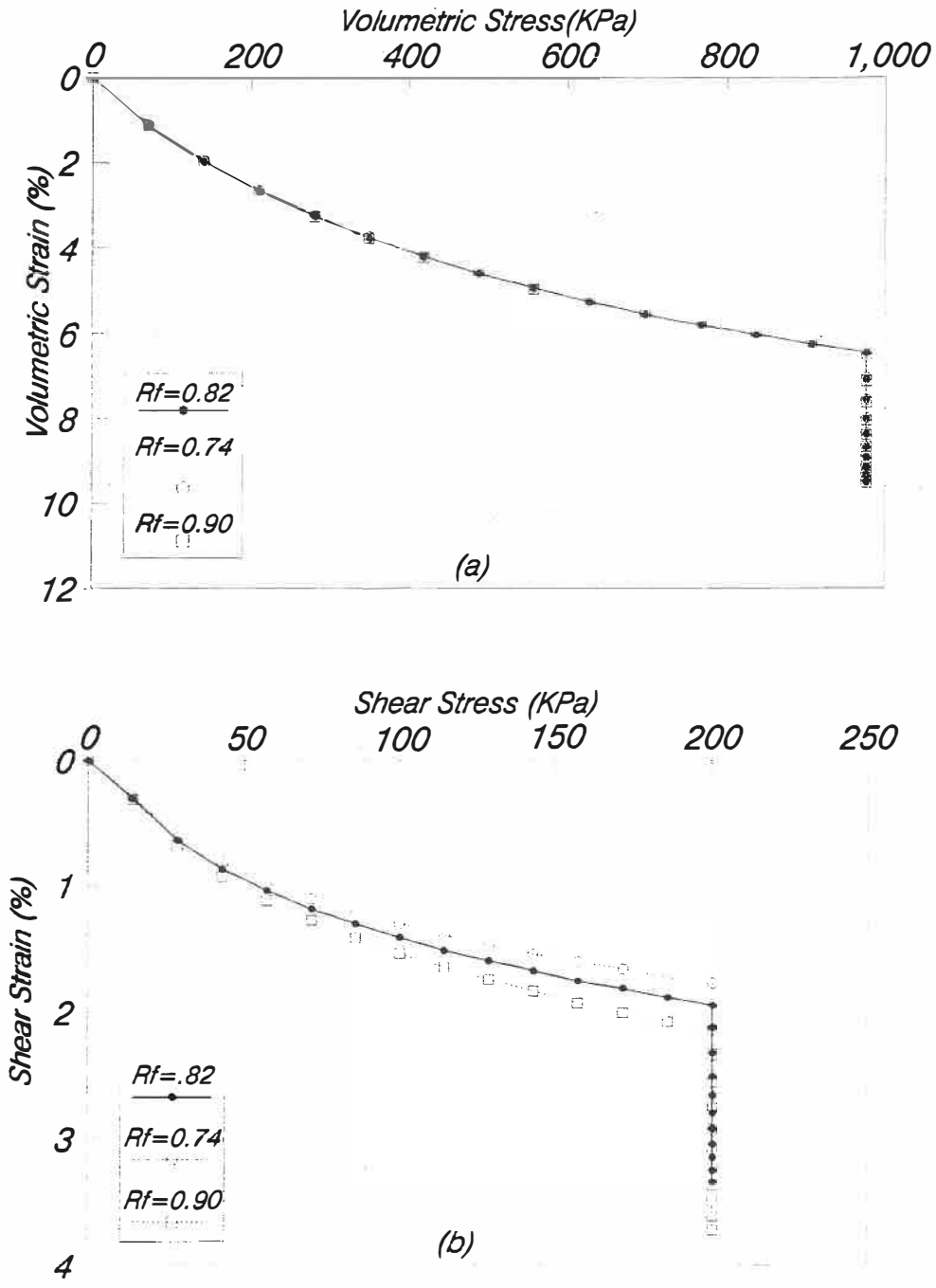

Fig. 6.13 - Sensitivity of The Results to a Change in Parameter "Rf"

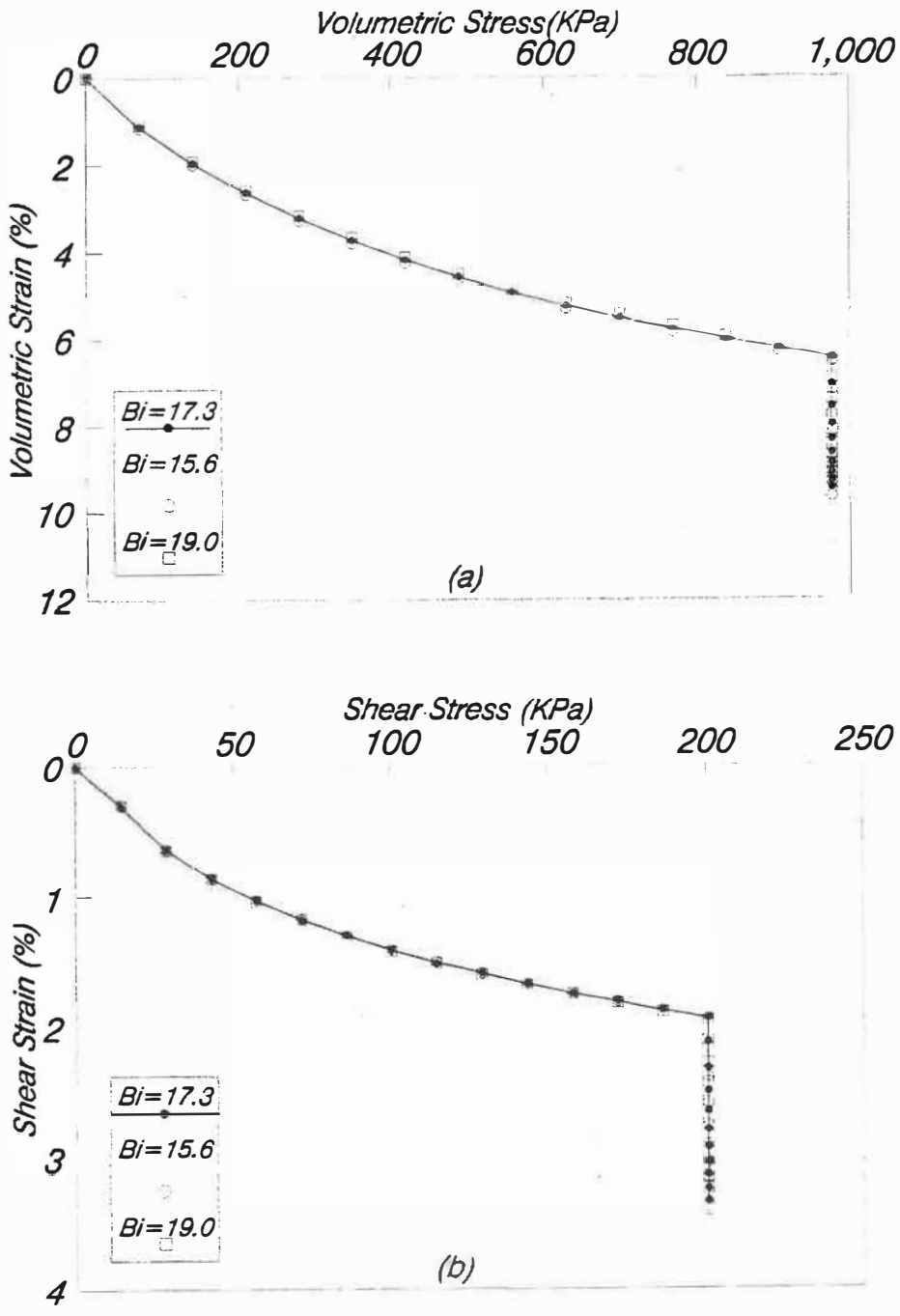

Fig. 6.14 - Sensitivity of The Results to a Change in Parameter "Bi"

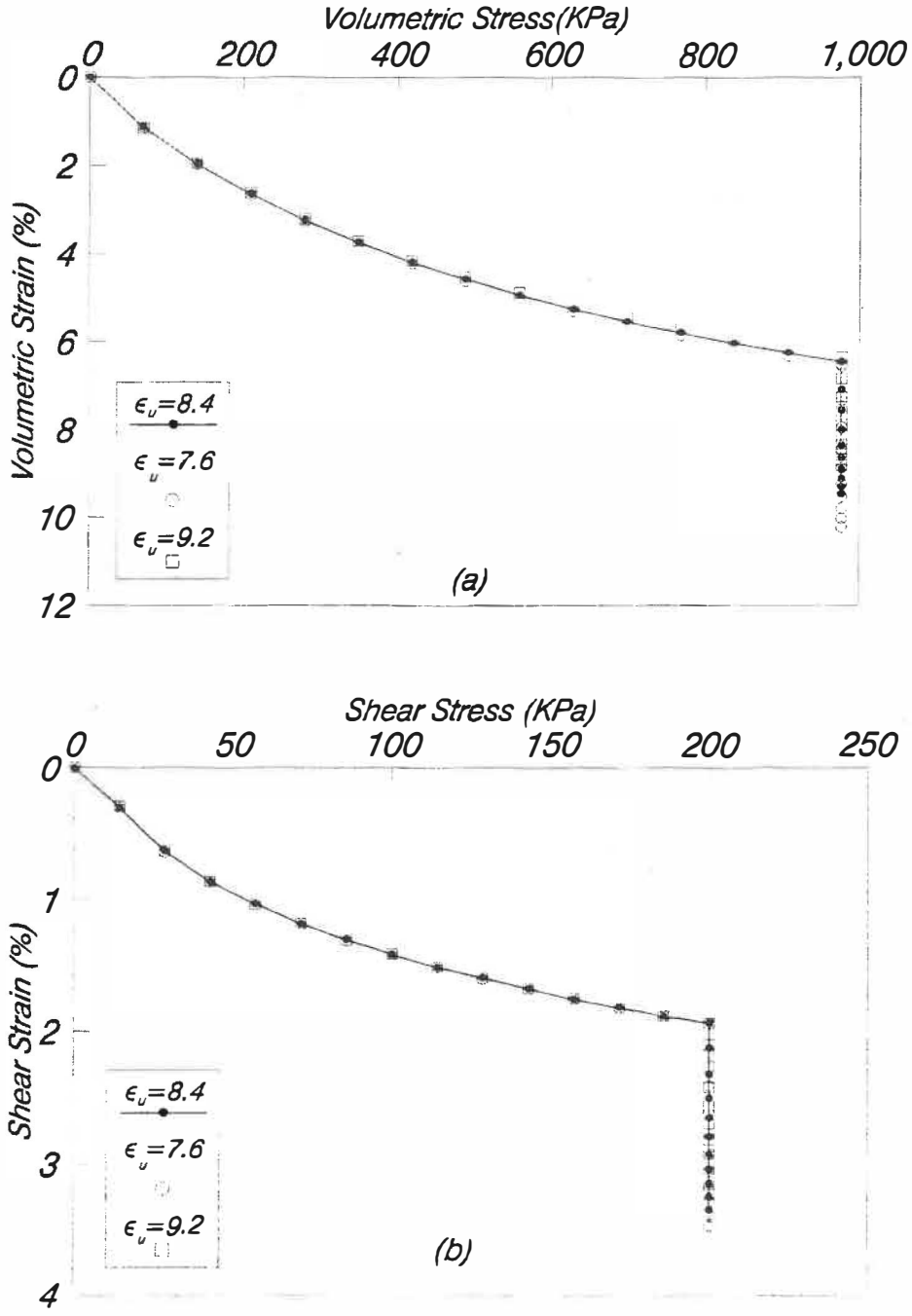

Fig. 6.15 - Sensitivity of The Results to a Change in Parameter "ϵ_u"

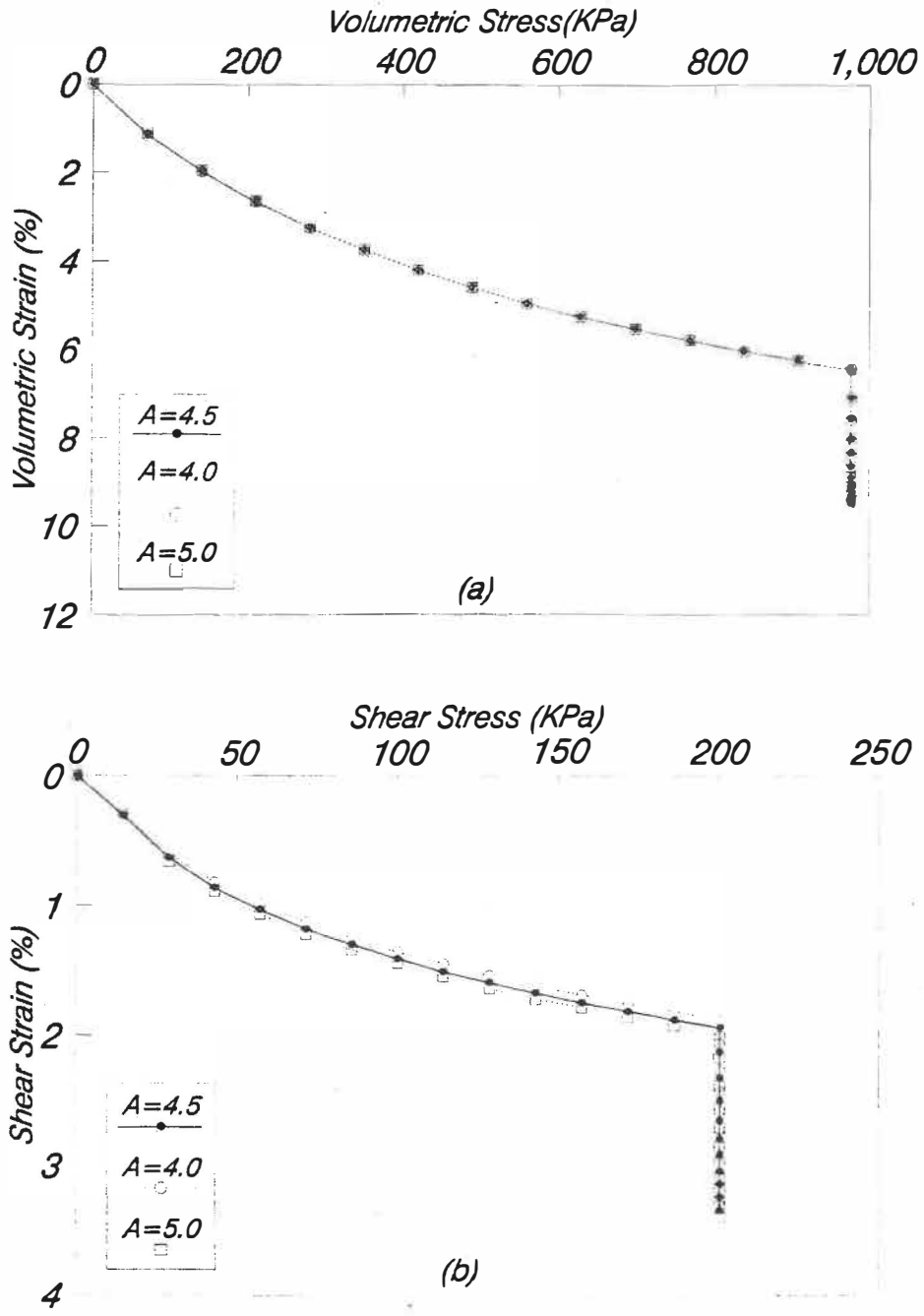

Fig. 6.16 - Sensitivity of The Results to a Change in Parameter "A"

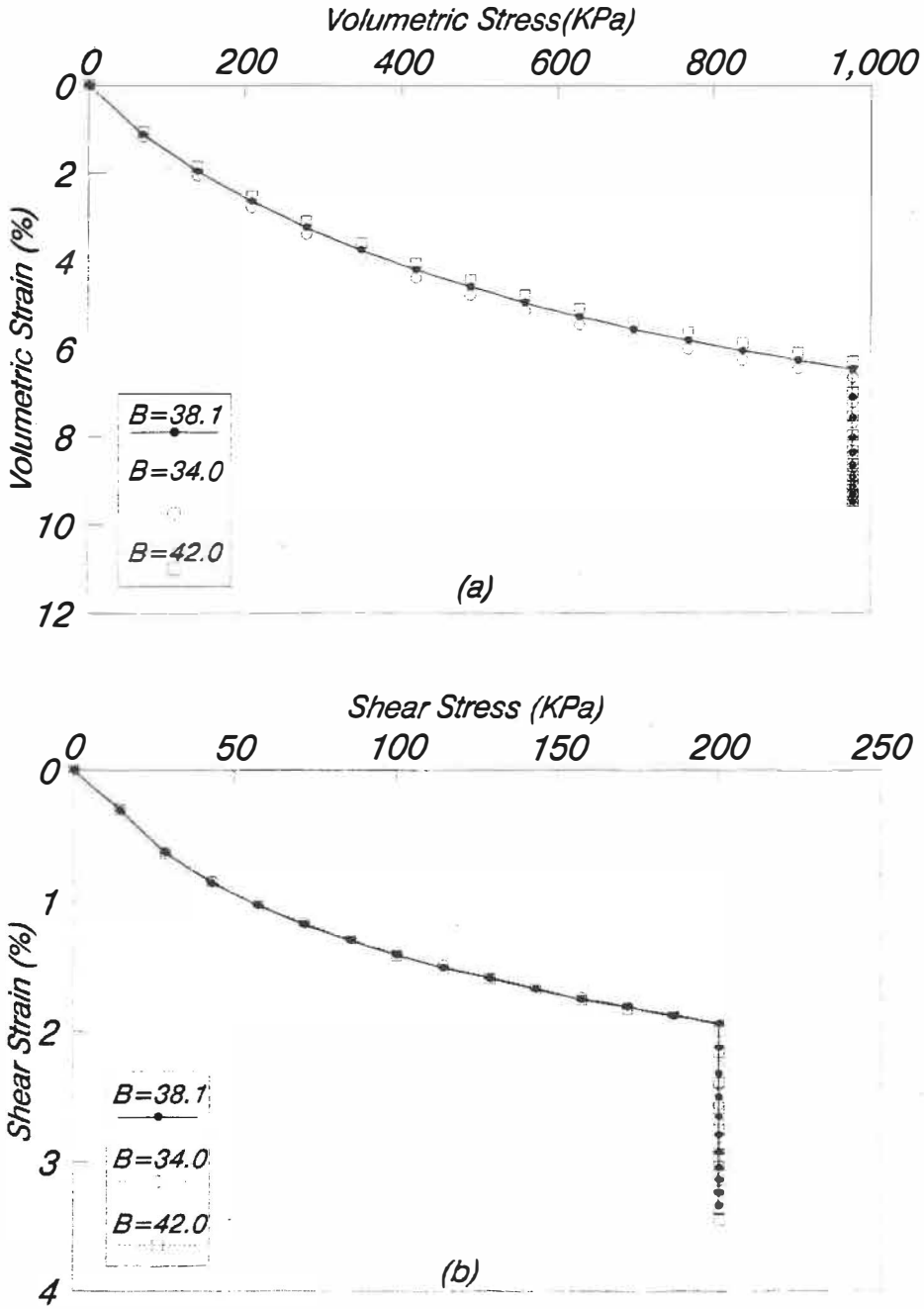

Fig. 6.17 - Sensitivity of The Results to a Change in Parameter "B"

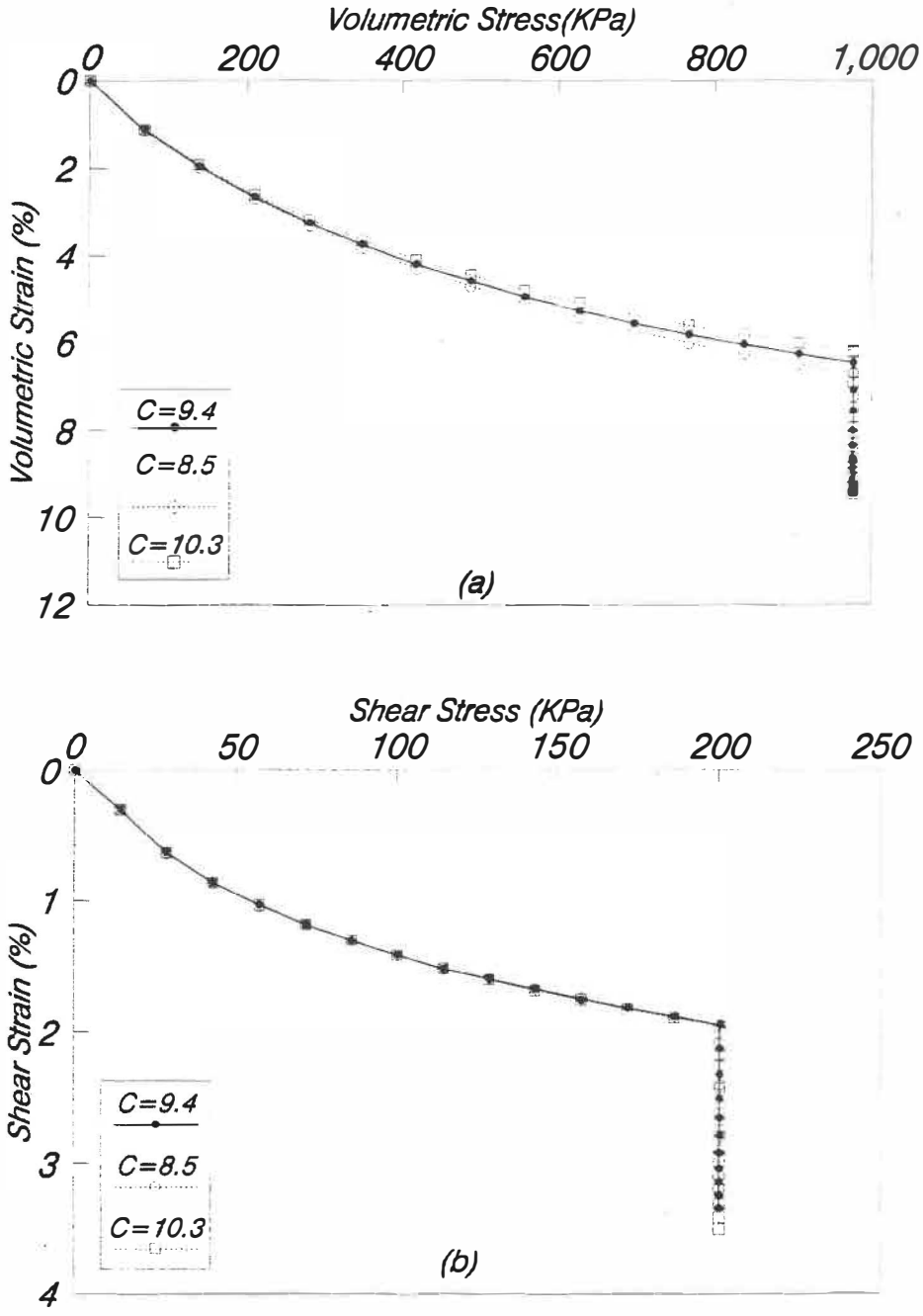

Fig. 6.18 - Sensitivity of The Results to a Change in Parameter "C"

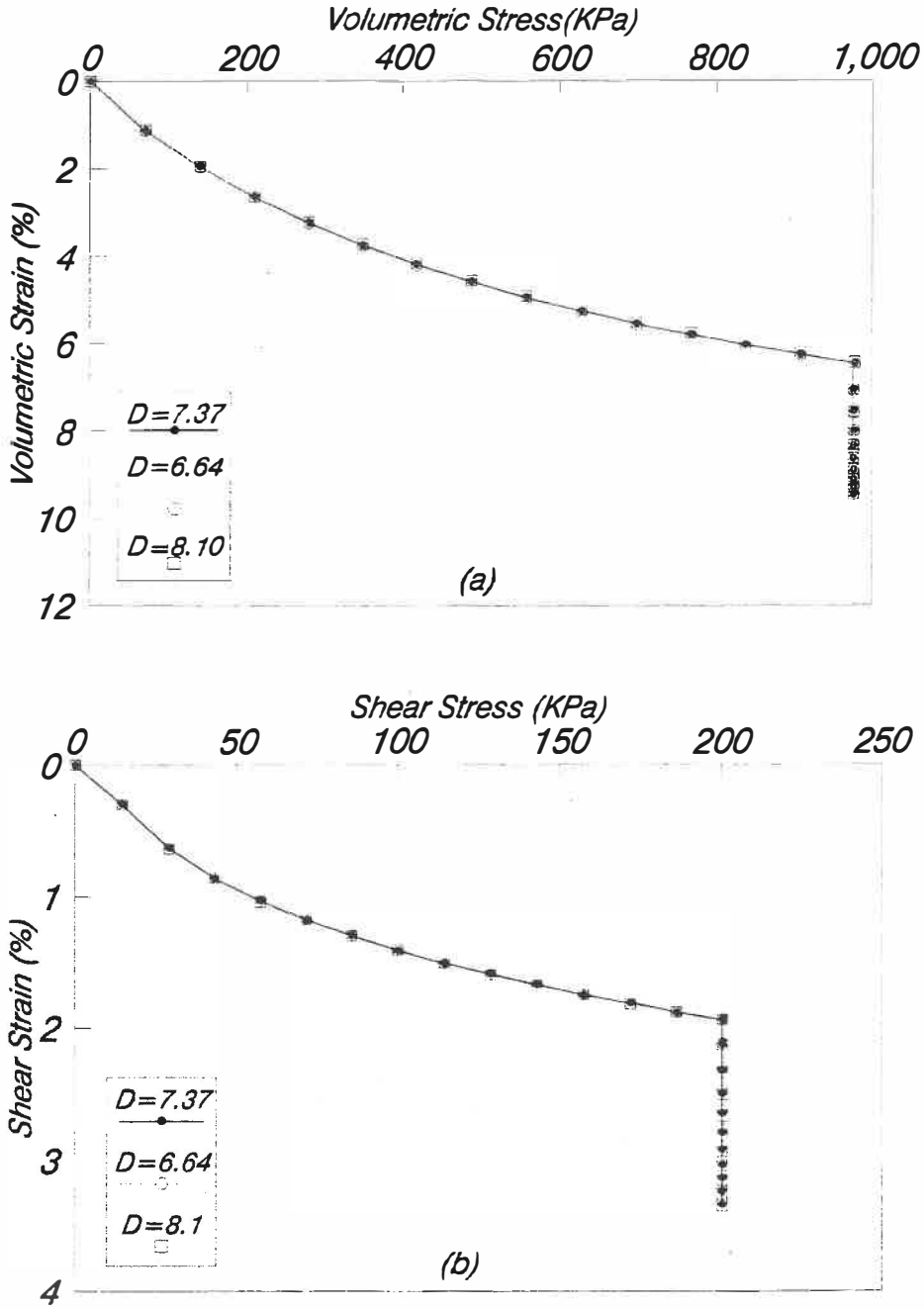

Fig. 6.19 - Sensitivity of The Results to a Change in Parameter "D"

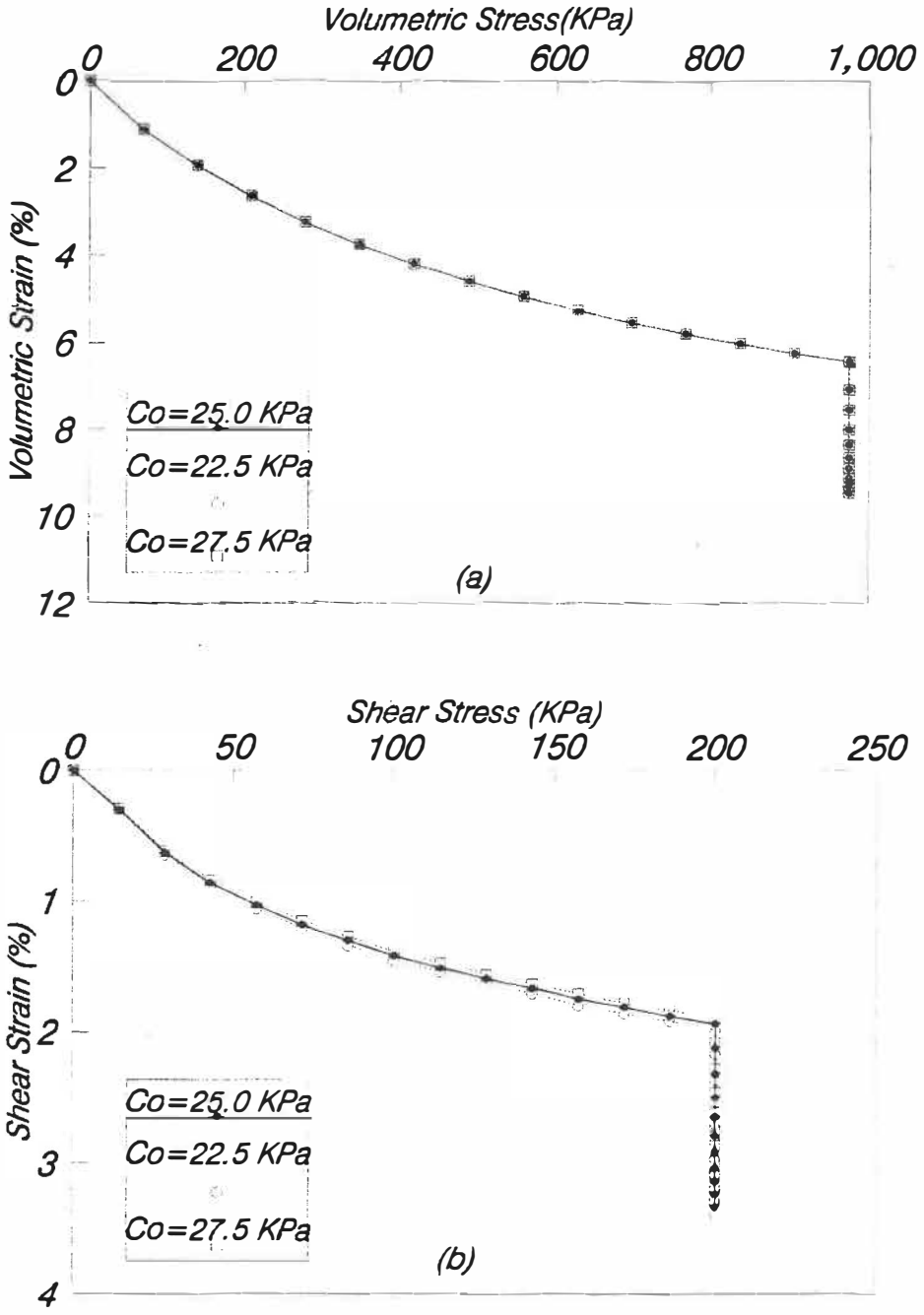

Fig. 6.20 - Sensitivity of The Results to a Change in Cohesion

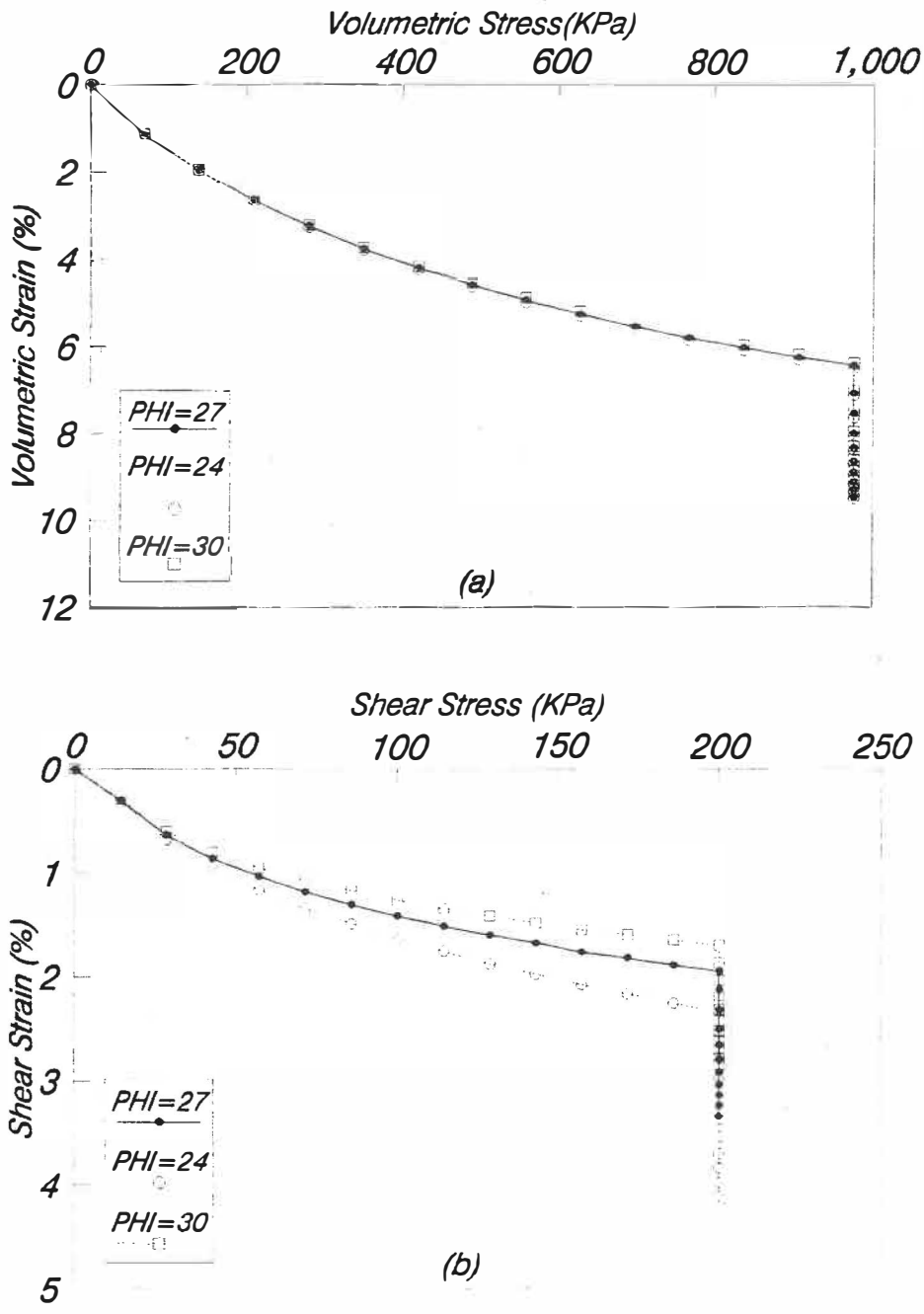

Fig. 6.21 - Sensitivity of The Results to a Change in Friction Angle

6.6 Coupling of The Proposed Model With Flow Equations :

In many geotechnical problems often encountered in practical situations such as slopes, foundations, and embankments, deformations resulting from a pore pressure variation (dissipation) must be studied together with the effect of a change in the applied load. In these cases a coupling of the proposed model with the appropriate flow equations for unsaturated soil is required. Here a procedure to couple the proposed model with the PERCO program is presented (PERCO is a program for the flow of water through saturated or unsaturated soils developed at Ecole Polytechnique de Montreal as a part of CASTOR project, Innocent et al (1988)). Using the generalized Darcy's law for the flow in unsaturated soils as well as the continuity equation for unsaturated porous media, the governing equation for flow through unsaturated soils was expressed in the following form (Innocent et al (1988)) :

$$div(K^{*}\nabla\phi) = C\frac{d\phi}{dt} + q \qquad (6.3)$$

Where :

$K^{*} = K_r(\psi).K$

$K_r(\psi)$: relative permeability

K : $\overline{K}/\mu$

$\overline{K}$: intrinsic permeability

μ : dynamic viscosity of the fluid

$C = C_s(\theta/n) + \partial\theta/\partial\psi$

C_s : specific storage coefficient

Θ : volumetric water content

n : porosity

$\Phi = \psi + Z$

ψ : pressure head (suction)

Z : elevation head

q : volumetric discharge

t : time

Using variational approach to find the weak form of the equation (6.3) and applying Galerkin method the resulting matrix equation was given by (Innocent et al (1988)) :

$$K\phi + C\frac{d\phi}{dt} = F \qquad (6.4)$$

Where :

$$K = \sum K_{nm} \quad ; \quad K^e_{nm} = \int_\Omega [N_{n,i} K N_{m,i}] d\Omega$$

$$C = \sum C_{nm} \quad ; \quad C^e_{nm} = \int_\Omega [N_n C N_m] d\Omega$$

$$F = \sum F_n \quad ; \quad F^e_n = \int_\Gamma N_n \bar{q} d\Gamma - \int_\Omega N_n q d\Omega$$

In general, coupled stress - flow equation can be written in the following form (Akai et al 1979) :

$$\begin{pmatrix} A & B \\ 0 & K \end{pmatrix} \begin{Bmatrix} U \\ \psi \end{Bmatrix} + \begin{pmatrix} 0 & 0 \\ B & C \end{pmatrix} \frac{d}{dt} \begin{Bmatrix} U \\ \psi \end{Bmatrix} = \begin{Bmatrix} E \\ F \end{Bmatrix} \qquad (6.5)$$

Where K, C, and F are as defined before and :

$$A = \sum A^{ik}_{nm} \quad ; \quad A^{ik}_{nm} = \int_\Omega N_{n,j} C_{ijkl} N_{m,l} d\Omega$$

$$D = \sum D^{i}_{nm} \quad ; \quad A^{i}_{nm} = \int_\Omega N_{n,j} \chi \delta_{ij} \gamma_w N_m d\Omega$$

$$B = \sum B^{i}_{nm} \quad ; \quad B^{i}_{nm} = \int_\Omega N_n S_w N_{m,i} d\Omega$$

$$E = \sum E^{i}_{n} \quad ; \quad E^{i}_{n} = \int_\Omega N_n f_i d\Omega - \int_\Gamma N_n T_i d\Gamma$$

Therefore, the proposed model can be easily incorporated into this type of formulation by pursuing an incremental procedure and replacing the matrix C_{ijkl} with the appropriate nonlinear matrix described before. Another important point is the addition of collapse load to the right hand term E, that is $E^* = E + F_c$. Again, since the collapse load is not known a priori an iterative procedure similar to the one described in section 5.3.2 must be followed.

CHAPTER 7

CONCLUSION

7.1 General :

In this thesis, previous investigations on partially saturated compacted soils were thoroughly reviewed. A model for stress-strain behavior in unsaturated compacted soils was proposed. The model being expressed in an incremental form, with an integral term taking into account the loading history of the soil, provides a unique relationship for describing various mechanical aspects in partially satutared soils such as the so-called collapse phenomenon. The model was then extended for two dimensional problems. Suitability of the model for quantitative prediction of the collapse deformation was verified numerically for both 1-D and 2-D cases by comparing the numerical results with the corresponding experimental data.

For two dimensional conditions a nonlinear elastic formulation (hyperbolic model) was used. It makes the model most suitable for volume change prediction in earth dams and embankments. A finite element program was developed to incorporate the model with a special procedure to take into account the collapse load in the formulation. Furthermore, a scheme for coupling the model with PERCO (program for the water flow through saturated and partially saturated soils developed at Ecole Polytechnique de Montreal as a part of

CASTOR project, innocent et al (1988)) was put forward which will be capable of describing the consolidation process in partially saturated soils. Finally, in this research some modifications to the GDS triaxial system were performed to enable the system to deal with unsaturated soils.

7.2 Practical Applications :

A change in degree of saturation in partially saturated soils is accompanied by a change in soil compressibility. The change in compressibility, in turn, is often an important factor influencing performance of earth embankments. Moreover, an additional collapse deformation due to increase in saturation degree may also severely influence the dam performance which can result even in piping and failure (Mesri 1988). Furthermore, subsidence problems are often encountered in heavy structures resting on compacted fills and embankments following wetting of the foundation. All these cases clearly indicate the need for a suitable stress strain relationship for partially saturated soil capable of describing its behavior properly.

7.3 Suggestions For Future Research :

Further future works are needed in the following areas :

- Studying the consolidation process in unsaturated soil by coupling the model developed in this research with flow and continuity equations for partially saturated soils.
- Extension of the model for three dimensional problems.

- To study the hysteresis effect on the volume change behavior of unsaturated soils which is encountered frequently in practice, for instance, drawdown of reservoir water behind earth dams.
- Finally, to study shear strength of partially saturated soils in view of the concepts and formulations presented herein in order to describe the change in shear strength due to an increase in the degree of saturation.

REFERENCES

Abelev, Y.M. (1948) "The essentials of Designing and Building on Microporous Soils", Stroital Naya Promyshlemast, No.10.

Aitchison, G.D. And Donald, IB. (1956) "Effective Stress in Unsaturated Soils", Proc. 2nd Aust.-New Zeal. Soil Mech. Conf. pp. 192-199.

Aitchison, G.D. (1956) "The Circumstances of Unsaturation in Soils, With Particular Reference to Australian Environment", Proc. 2nd Aust.-New Zeal. Soil Mech. Conf.

Aitchison, G.D. (1960) "Effective Stresses in Multiphase Systems" Proc. 3rd Aust.-New Zeal. Conf. on Soil Mech. and Found. Eng. pp. 209-212.

Aitchison, G.D. (1965) "Soil Properties, Shear Strength and Consolidation", Proc. 6 Int. Conf. Soil Mech. and Found. Eng., Montreal, vol. 3, pp. 318-321.

Aitchison, G.D. (1973) "Problems of Soil Mechanics and Construction on Structurally Unstable Soils (collapsible, expansive and others)", Proc. 8 Int. Conf. Soil Mech. and Found. Eng., Moscow, vol. 3, pp. 161-190.

Akai, K., Ohnishi, Y., Murakami, T. And Horita. M. (1979) "Coupled Stress Flow Analysis in Saturated Unsaturated Medium by Finite Element Method", 3rd Int. Conf. on Numerical Methods in Geomech., pp. 241-249.

Bally, R.J., Antonescu, I.I., Andrei, S.V., Iron, A., And Popescu, D., (1973) "Hydrotechnical Structures on Loessial Collapsible Soils", Paper submitted to specialty session No. 4, 8Int. Conf. Soil Mech. and Found. Eng., Moscow.

Barden, L., Madedor, A.O. And Sides, G.R. (1969) "Volume Change Characteristics of Unsaturated Clay", ASCE, 95, J. Of Soil Mech. & Found. Div. SM1, pp. 33-51.

Barden, L. (1972) "The Relation of Soil Structure to the Engineering Geology of Clay Soils", Q.J. Eng. Geology, vol. 5, pp. 85-102.

Barden, L., McGown, A., And Collins, K. (1973) "The Collapse Mechanism in Partly Saturated Soil", Eng. Geology, Elsevier Scientific Pub. Company, Amsterdam, pp. 49-60.

Ben Belfadhel, M. (1986) "Etude en Laboratoire de l'affaissement d'un Till à la Submergence", Memoire de Maîtrise en Science Appliquée, Faculté des Sciences Appliquées, Université de Sherbrooke, Qué. Canada.

Bishop, A.W. (1959) "The principle of Effective stress", Teknik Ukeblad, 39, pp. 859-863.

Bishop, A.W., And Blight, G.E. (1963) "Some Aspects of Effective Stress in Saturated and Unsaturated Soils", Geotechnique 13, No. 3, pp. 177-197.

Bishop, A.W. And Wesley, L.D. (1975) "A Hydraulic Triaxial Apparatus for Controlled Stress Path Testing", Geotechnique, vol. 25, pp. 657-670.

Blight, G.E. (1965) "A Study of Effective Stress for Volume Change", Proc. Of a Symp. On Moisture Equilibria and Moisture Changes Beneath Covered Areas, Sydney pp. 259-269.

Blight, G.E. (1967) "Effective Stress Evaluation for Unsaturated Soils", J. Soil Mech. and Found. Eng., ASCE, vol. 93, SM2, pp. 125-148.

Booth, A.R. (1975) "The Factors Influencing Collapse Settlement in Compacted Soils", 6 Reg. Conf. for Africa on Soil Mech. & Found. Eng., Durban, South Africa, pp. 57-63.

Box, M.J. (1966) "A Comparison of Several Current Optimization Methods, and the Use Transformation in Constrained Problems", Computer Journal, vol. 9, pp. 67-77.

Burland, J.B. (1965) "Some Aspects of the Behavior of Partly Saturated Soils", Proc. Of a Symp. On Moisture Equilibria and Moisture Changes Beneath Covered Areas, Sydney pp. 270-278.

Clough, R.W. And Woodward, R.J. (1967) "Analysis of Embankment Stresses and Deformations", J. of Soil Mech. and Found. Eng., ASCE, vol. 93, SM4, pp. 529-549.

Coleman, J.D. (1962) "Stress-Strain Relationship for Partly Saturated soil", Correspondence, Geotechnique 12, No.4, pp. 348-350.

Cox, D.W. (1978) "Volume Change of Compacted Clay Fill", Proc. Of the Conf. held at the Inst. of Civil Eng., London, pp. 79-86.

David, D., Komornik, A., And Goldberg, M. (1973) "Swelling and Bearing Characteristics in Clayey Sands and Loess", Paper submitted to specialty session No. 4, 8Int. Conf. Soil Mech. and Found. Eng., Moscow.

Desai, C.S. And Siriwardane, H.J. (1984) " Constitutive Laws For Engineering Materials With Emphasis on Geologic Material", Prentice Hall Inc., New Jersy, NJ07632, U.S.A.

Dolezalova, M., And Leitner, F. (1981) "Prediction of Dalesice Dam Performance", Proc. 10th Int. Conf. on Soil Mech. and Found. Eng., vol. 1, pp. 111-114.

Duncan, J.M., Byrne, P., Wong, K.S., And Mabry, P. (1980) "Strength, Stress-Strain and Bulk Modulus Parameters For Finite Element Analysis of Stresses and Movements In Soil Masses", Report No. UCB/GT/80-01 College of Eng., Univ. of California, Berekely, Ca.

Eisenstein, Z. And Simmon, J.V. (1975) "Three Dimensional Analysis of Mica Dam", Proc. of Int. Symp. at Univ. of Wales, Swansea, pp. 1052-1069.

Fredlund, D.G. And Morgenstern, N.R. (1976) "Constitutive Relations for Volume Change in Unsaturated Soils", Can. Geot. J., vol. 13, pp. 261-276.

Fredlund, D.G. (1977) "Stress-State Variables for Unsaturated Soils", ASCE J. Of Geot. Eng. Div. 103, GT5, pp. 447-466.

Fredlund, D.G. (1979) "Appropriate Concepts and Technology for Unsaturated Soils", Can Geot. J., vol. 16, No.1, pp. 121-139.

Fredlund, D.G. (1985) "Soil Mechanics Principles That Embrace Unsaturated Soils", Proc. of 11th Int. Conf. on Soil Mech. and Found. Eng., San Francisco, vol. 1, pp. 465-472.

Gibbs, H.J. And Bara, J.P. (1962) "Predicting Surface Subsidence from Basic Soil Tests", Soils Eng. Report No. EM658, U.S. Dept. of Int., Bureau of Recl. Denver, pp. 37.

Gili, J.A. And Alonso, E.E. (1988) "Discontinuous Numerical Model For Partially Saturated Soils at Low Saturation", Numerical Methods In Geomech., Rotterdam, pp. 366-372.

Hayashi, M. (1975) "Progressive Submerging Settlement During Water Loading to Rockfill Dam", Proc. Of Int. Symp. on Criteria and Assumptions For Numerical Analysis of Dams, Swansea, pp. 868-880.

Hight, D.W., And Farrar, D.M. (1978) "Discussion :Engineering Properties and Performance of Clay Fills", Proc. Of the Conf. held at the Inst. of Civil Eng., London pp. 219-241.

Hilf, J.W. (1956) "An Investigation of Pore Water Pressure in Compacted Cohesive Soils", Tech. Memorandum no. 654, U.S. Dept. of Interior, Bureau of Recl. Denver, Colorado.

Holtz, W.G. And Hilf, J.W. (1961) "Settlement of Soil Foundations due to Saturation", Proc. 5 Int. Conf. Soil Mech. and Found. Eng., vol. 3, pp. 673-679.

Houston, S.L., Houston, W.N., And Spadola, D.J. (1988) "Prediction of Field Collapsible Soils Due to Wetting", ASCE ,J. Geot. Eng. vol. 114, No.1, pp. 40-58.

Innocent, G., Langlois, P. And Soulié, M. (1988) "Manuel de l'usager PERCO", Projet CASTOR, Rapport no. CG-RE-03/03, Ecole Polytechnique de Montreal, Montreal, Canada.

Janbu (1963) "Soil Compressibility as Determined by Oedometer and Triaxial Tests", Proc. European Conf. on Soil Mech. and Found. Eng., Wiesbaden, Germany, No. 1, pp. 19-25.

Jardin, J., Baldit, R. And Delfaut, A. (1984) "Constatations Sur La Digue des Roussieres", Bult. Liaison labo P. Et Ch., 131, pp. 29-44.

Jennings, J.E.B. And Knight, K. (1957) "Properties and Behavior of Silty Soils Originated from Loess Formation". Proc. 4 Int. Conf. Soil Mech. and Found. Eng., vol. 1, pp. 9-12.

Jennings, J.E.B. And Burland, J.B. (1962) "Limitations to the use of Effective Stress In Partly Saturated Soils", Geotechnique 12,No. 2, pp. 125-144.

Jennings, J.E.B. And Knight, K. (1975) "A Guide to Construction on or with Materials Exhibiting Additional Settlement

Due to Collapse of Grain Structure", 6 Reg. Conf. for Africa on Soil Mech. & Found. Eng., Durban, South Africa, pp. 99-105.

Josa, A., Alonso, E.E., LLoret, A., And Gens, A. (1987) "Stress-Strain Behavior of Partially Saturated Soils", Proc. 9th European Conf. on Soil Mech. and Found. Eng. vol. 2, pp. 561-564.

Kane, H. (1973) "Confined Compression of Loess ", Paper submitted to specialty session No. 4, 8Int. Conf. Soil Mech. and Found. Eng., Moscow.

Karube, D., Namura, K., Morita, N., And Iwasaki, T, (1978) "Stress-Strain Behavior of Unsaturated Soil", Proc. Of JSCE, No. 269, pp. 105-119.

Knight, K, (1961) "The Collapse of Structure of Sandy Subsoils on Wetting", Ph.D. Thesis, University of Witwatersrand, South Africa.

Knight, K, (1963) "The Origin and Occurrence of Collapsible Soils", Proc. Of the 3rd Reg. Conf. for Africa on Soil Mech. & Found. Eng., vol. 1, pp. 127-130.

Kondner, R.L. (1963) "Hyperbolic Stress Strain Response : Cohesive Soils", J. Soil Mech. and Found. Eng. Div., ASCE, 89(1), pp. 115-143.

Leonards, G.A. (1962) "Correspondence", Geotechnique, vol. 12, pp. 345-355.

Lloret, A. And Alonso, E.E. (1980) "Consolidation of Unsaturated Soils Including Swelling and Collapse Behavior", Geotechnique 30, No. 4, pp. 449-477.

Lloret, A. And Alonso, E.E. (1985) "State Surfaces for Partially Saturated Soils", Proc. Of the 11th Int. Conf. Soil Mech. and Found. Eng., Sanfrancisco, pp. 557-562.

Loiselle, A.A. And Hurtubise, J.E. (1976) "Properties and Behavior of Glacial Till as Construction material", Glacial Till, Edited by R.F. Legget, pp. 346-363.

Lutenegger, A.D. and Saber, R.T. (1988) "Determination of Collapse Potential of Soils", Geotech. Testing J., GTJODJ, vol. 11, no. 3, pp. 173-178.

Matyas, E.L. And Radhakrishna, H.S. (1968) "Volume Change Characteristics of Partially Saturated soils", Geotechnique 18, No. 4, pp. 432-448.

Mesri, G. And Ali, S. (1988) "Discussion", J. Geotech. Eng., ASCE, vol. 114, no. 6, pp. 742-746.

M.I.T. Report (1963) "Engineering Behavior of Partially saturated soils", M.I.T. Phase Report No. 1,Soil Stabilization.

Nagaraj, T.S., And Murthy, B.R.S. (1985) "Compressibility of Partially Saturated Soils", ASCE, J. Of Geot. Eng. vol. 111, No. 7, pp. 937-942.

Naylor , D.J., Maranha Das Neves, E., Matter JR., D., And Pinto, A.A. (1986) "Prediction of Construction Performance of Beliche Dam", Geotechnique, 36, No. 3, pp. 359-376.

Newland, P.L. (1965) "Behavior of Soils in Terms of Two Kinds of Effective Stress", Proc. Of a Conf. on Eng. effects of moisture changes in soils, Texas, A. & M. Press, pp. 78-92.

Nwabuokei, S.O. And Lovell, C.W. (1986) "Compressibility and Settlement of Compacted Fills", Consolidation of soils, ASTM, Edited by R.N. Yong and F.C. Townsend, pp. 184-202.

Paré, J.J., Verma, N.S., Keira, H.M.S., And McConnell, A.D. (1984) "Stress Deformation Prediction for LG4 Main Dam", Can. Geotech. J., 21, pp. 213-222.

Pelletier, D. (1988) Documents of a course offered on finite element programing entitled "CONCEPTION DE LOGICIEL D'ELEMENT FINIS", Dept. of Applied Math., Ecole Polytechnique de Montreal.

Penman, A.D.M. (1970) "Cracking of Clay Cores of Dams", Brit. Geot. Society, pp. 115-117.

Radhakrishna, H.S. (1967) "Compressibility of Partially Saturated Soils", Ph.D. Thesis, University of Waterloo.

Schober, W. (1967) "Behavior of Gepatsch Rockfill Dam", Trans. 9th Congress on Large Dams, vol. 3, Istanbul, pp. 677-699.

Seed, H.B., Duncan, J.M., And Idriss, I.M. (1975) "Criteria and Methods For Static and Dynamic Analysis of Earth Dams", Proc. of an Int. Symp. held at Swansea on criteria and assumptions for numerical analysis of dams, pp. 564-589.

Selig, E.T. (1988) "Soil Parameters for Design of Buried Pipelines", Proc. Pipeline Infrastructure Conf., ASCE, 99-116.

Terzaghi, K. (1936) "The Shearing Resistance of Saturated Soils and the Angle Between The Planes of Shear", Proc. Of the 1st Int. Conf. Soil Mech. and Found. Eng., vol. 1.

Terzaghi, K. (1943) "Theoretical Soil Mechanics", John Wiley & Sons, N.Y., p. 510.

Zienkiewicz, O.C. And Taylor, R.L. (1989) "The Finite Element Method", Mc Graw Hill Book Company.

Zur, A. And Wiseman, G. (1973) "A Study of Collapse Phenomena of an unsaturated Loess", Paper submitted to specialty session No. 4, 8Int. Conf. Soil Mech. and Found. Eng., Moscow.

APPENDIX

Subroutines in "INPUT" Block :

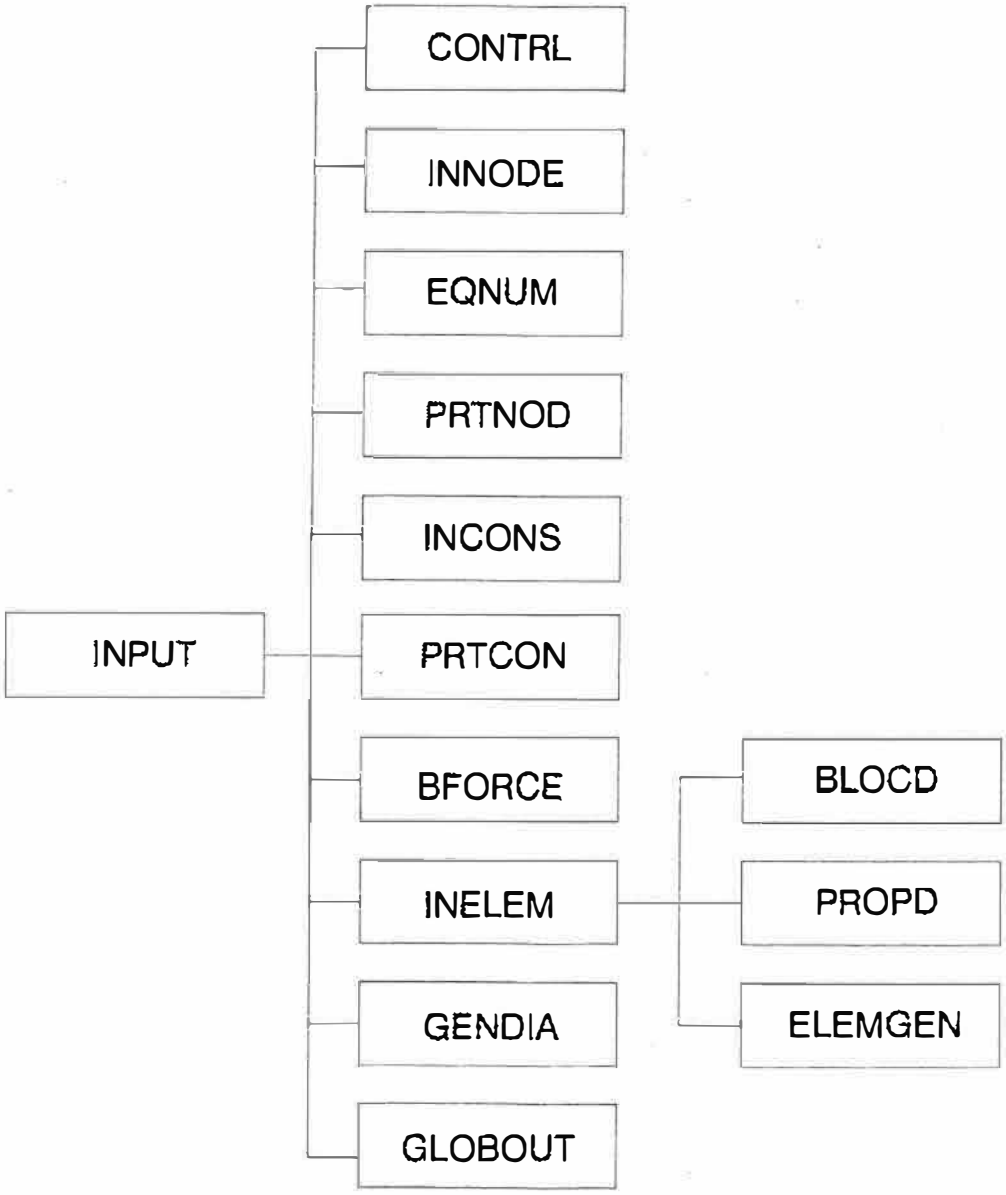

CONTRL : Reads in and echos all control variables.

INNODE : Reads in all node data and forms the array specifying degree of freedom for each node.

EQNUM : Calculates the no. of equations.

PRTNOD : Prints all nodal informations.

INCONS : Reads in and stores boundary conditions (constraints).

BFORCE : Reads in and stores the boundary applied force.

INELEM : Reads in elements' information and generates the global connectivity matrix.

BLOCD : Reads in description block for each group of element.

PROPD : Reads in the properties corresponding to each group of elements.

ELEMGEN : Generates assembly vectors for each element.

GENDIA : Calculates the vector containing diagonal address.

GLOBOUT : Prints out the global connectivity matrix and diagonal address of skyline.

Subroutines in "MODSOL" Block :

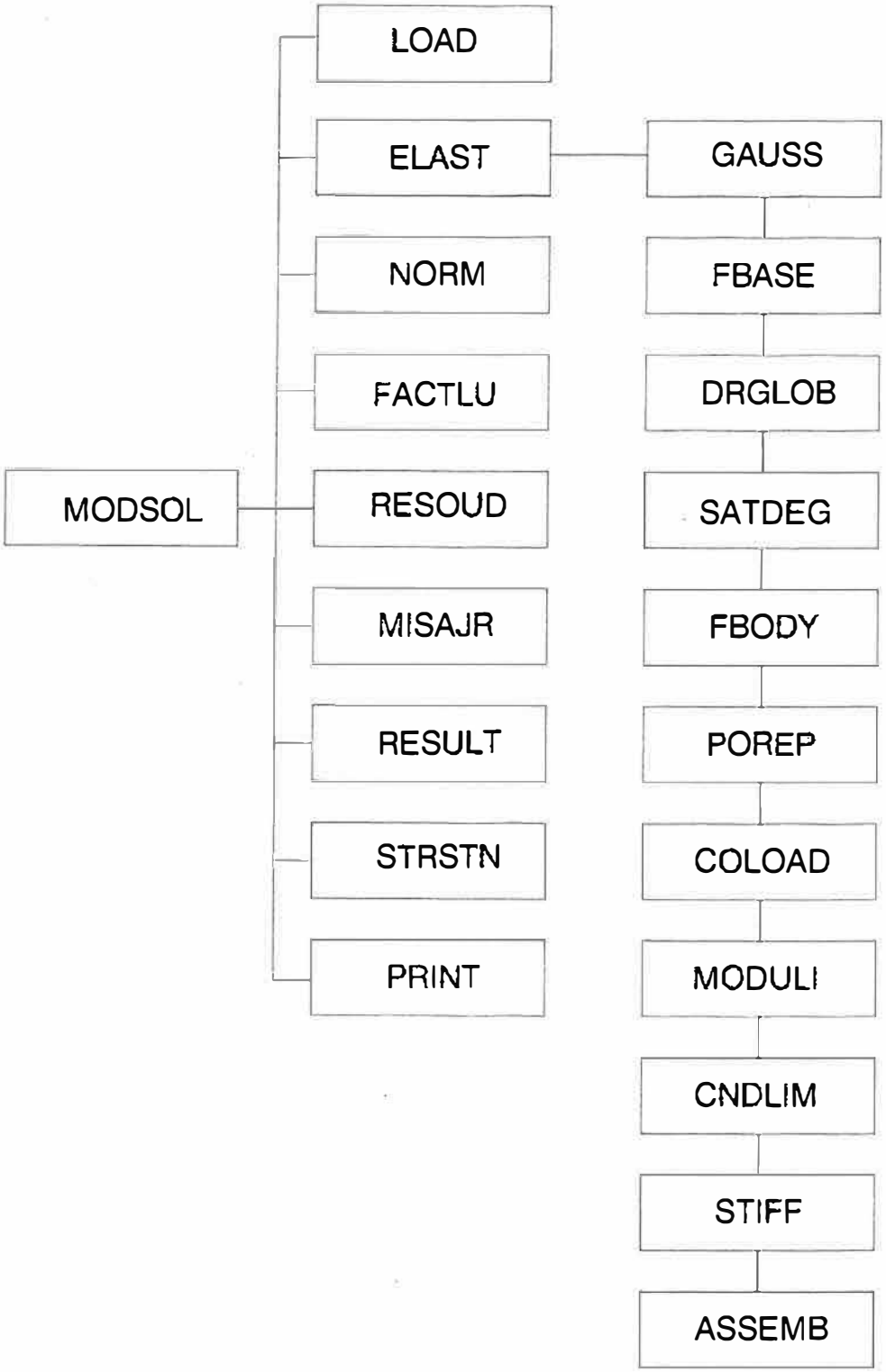

LOAD : Applies specified load increment at the beginning of each iteration.

ELAST : Forms global stiffness matrix.

GAUSS : Calculates the Gauss points and their weight factors.

FBASE : Calculates the shape functions and their local derivatives.

DRGLOB : Calculates global derivatives og shape functions.

SATDEG : Calculates the change in saturation degree and updates its value.

FBODY : Calculates the change in bogy force and updates its value.

POREP : Calculates the change in pore pressure as a result of change in degree of saturation.

COLOAD : Calculates nodal collapse load.

MODULI : Calcultes tangent elastic moduli.

CNDLIM : Imposes the limit condition and element's nodal force (from boundary conditions).

STIFF : Calculates the element stiffness matrix.

ASSEMB : Assembly to form global stiffness matrix.

NORM : Calculates Eucledian and maximum norms of residual.

FACTLU : LU factorization of the global stiffness matrix.

RESOUD : Resolution of the system of equations.

MISAJR : Updates the value of displacements.

RESULT : Express displacements in appropriate form for output.

STRSTN : Calculates stresses and strains in each element.

PRINT : Prints out the results.

For the sake of brevity, only the block "MODSOL" of the computer program is included in this Appendix. The complete computer program is available in a separate document at the Civil Engineering Department, Ecole Polytechnique de Montreal.

```
       SUBROUTINE MODSOL(X,DX,MATGLB,NQ,NESP)
*****************************************************************
*     THIS ROUTINE CALLS THE FOLLOWING ROUTINES TO RESOLVE A PLANE  *
*        ELASTICITY PROBLEM (LINEAR OR NON-LINEAR) :                *
*       -ELAST :TO FORM GLOBAL STIFFNESS MATRIX MATGLOB(ESPMAT) AND *
*               THE RESIDUAL (R)=(B)-(A)(X)  NOTE : (R)=BGLOB(NEQ) *
*       -FACTLU :FOR LU FACTORIZATION OF GLOBAL STIFFNESS MATRIX    *
*       -RESOUD :FOR RESOLVING THE SYSTEM OF EQUATIONS (A)(DX)=(R)  *
*       -MISAJR :FOR UPDATING THE VALUE OF X=X+DX                   *
*       -NORML2 :IT THE CALCULATES THE EUCLUDEAN NORMS OF X,DX,AND R*
*       -NORMAX :IT CALCULATES THE MAXIMUM NORM OF X,DX, AND R      *
*       -RESULT :TO ALLOCATE THE VALUES OF X AND BOUNDARY VALUES    *
*                IN A SUITABLE ARRAY FOR PRESENTATION OF RESULTS    *
*       -PRINT  :IT WILL PRINT OUT THE RESULTS                      *
*     IT THEN ITERATES TO REACH CONVERGENCE                         *
*****************************************************************
      INTEGER MBLANK
      PARAMETER ( MBLANK = 20000 )
*     GLOBAL VARIABLES
*     ---------------
      LOGICAL   DEBUG
      INTEGER   DBGLVL
      COMMON  / BUGS   /   DBGLVL, DEBUG
      INTEGER   ITWO
      COMMON  / DPR   / ITWO
      INTEGER IPRINT
      COMMON / DISKS  / IPRINT
      INTEGER   MTOT
      COMMON  / MEMORY / MTOT
      INTEGER   IA
      COMMON  / BLANK / IA(MBLANK)
      COMMON  /INOUT/ IIN,IOUT
      INTEGER ADDTBL, LOCTBL , SIZEOF , STOROF
      INTEGER NITER,ESPMAT,NESP,NQ,LL,ISTR,ISTN,ISRP,ISNP,NLOAD,ISAT,
     &        NCLOAD
      REAL*8 X(NQ),MATGLB(NESP),DX(NQ),C(3)
      REAL*8 XNORM,DNORM,RNORM,ENORMX,ENORMD,ENORMR,S(4)
      COMMON /CONT/IDIM,ITEMP,NUMNP,NELEM,NGROUP,NNPE,NFIXU,NFIXV,
     &             ISAT,NLOAD
      COMMON /COND/NDEP,NCOORD,NEQ,ESPMAT
      COMMON /ADD/NPROP,NBLOC,NCIEL,ICONEC,ILMG,ICON,ICOORD,NID,IB
      COMMON /COLLPSE/NCLOAD,ILOAD
*
      LL=NFIXU+NFIXV
C-----ALLOCATION OF ARRAYS AND INITIALIZATION-----------------
            IBG=ADDTBL('BGLOB',NEQ,'REAL','MODSOL')
            ISTR=ADDTBL('STRESS',NELEM*4*3,'REAL','MODSOL')
            ISTN=ADDTBL('STRAIN',NELEM*4*3,'REAL','MODSOL')
            ISTT=ADDTBL('STREST',NELEM*4*3,'REAL','MODSOL')
            IUV=ADDTBL('UV',NUMNP*NDEP,'REAL','MODSOL')
            IUY=ADDTBL('UY',NUMNP*NDEP,'REAL','MODSOL')
      CALL INIT3(IA(ISTR),NELEM,4,3)
      CALL INIT3(IA(ISTN),NELEM,4,3)
```

```
      CALL INIT3(IA(ISTT),NELEM,4,3)
      CALL INIT(IA(IUV),NUMNP,NDEP)
      CALL INIT(IA(IUY),NUMNP,NDEP)
*
C----------------NOTE THAT THE NO. OF COLLAPSE LOAD INCREMENTS SHOULD
C-----------------BE CHOSEN LARGE ENOUGH TO AVOID INSTABILITY ------
      NCLOAD=10
      IF(ISAT.GT.0)NLOAD=NLOAD+NCLOAD
      DO 30 ILOAD=1,NLOAD
      CALL INITV(X,NEQ)
      CALL INITV(DX,NEQ)
      CALL LOAD(IA(IB),IA(IBG),NEQ)
      IF(ISAT.GT.0.AND.ILOAD.GT.ISAT.AND.ILOAD.LT.(ISAT+NCLOAD))
     &         CALL INITV(IA(IBG),NEQ)
      NITER=3
      DO 20 II=1,NITER
C-----------INITIALIZING THE MATRICES----
            CALL INITV(MATGLB,NESP)
*
            DO 10 NG=1,NGROUP
               CALL ELAST(IA(NBLOC),IA(NPROP),IA(IBG),MATGLB,NEQ,NESP,
     &              NGROUP,NG,DX,IA(ISTR),IA(ISTN),C,S,II)
  10        CONTINUE
*
            IDIAG=NCIEL
            CALL NORML2(IA(IBG),NEQ,ENORMR)
            CALL NORMAX(IA(IBG),NEQ,RNORM)
            CALL FACTLU(NEQ,ESPMAT,IA(IDIAG),MATGLB)
            CALL RESOUD(NEQ,ESPMAT,IA(IDIAG),MATGLB,IA(IBG),DX)
            CALL MISAJR(X,DX,NEQ)
            CALL RESULT(IA(IUV),IA(NID),IA(ICON),DX,NUMNP,NDEP,NEQ,LL)
            CALL STRSTN(IA(NBLOC),IA(ICOORD),IA(IUV),IA(ICONEC),C,S,
     &              IA(ISTR),IA(ISTN),NGROUP,NUMNP,NELEM,NNPE,NCOORD,
     &              IA(ISTT),ILOAD,ISAT,IA(NPROP))
            CALL NORML2(X,NEQ,ENORMX)
            CALL NORML2(DX,NEQ,ENORMD)
            CALL NORMAX(X,NEQ,XNORM)
            CALL NORMAX(DX,NEQ,DNORM)
            CALL PRINT(IA(IUV),NDEP,NUMNP,ENORMX,ENORMD,ENORMR,ILOAD,
     &                 XNORM,DNORM,RNORM,II,IA(ISTR),IA(ISTN),NELEM,
     &                 IA(IUY))
  20  CONTINUE
  30  CONTINUE
            CALL RMVTBL('UY')
            CALL RMVTBL('UV')
            CALL RMVTBL('STREST')
            CALL RMVTBL('STRAIN')
            CALL RMVTBL('STRESS')
            CALL LISTBL('MODSOL')
      RETURN
      END
```

```
      SUBROUTINE ELAST(BLOC,PROP,BGLOB,MATGLB,NQ,NESP,NG,N,DX,STRESS,
     &                 STRAIN,C,S,II)
*****************************************************************
*     THIS ROUTINE DOES THE FOLLOWINGS :                        *
*      -EXTRACTS DESCRIPTION BLOCK : BLOCK(N,8), PROP(N,16)     *
*      -ALLOCATES NECESSARY SPACE FOR DIFFERENT VECTORS AND ARRAYS BY*
*       USING LIBRARY OF DYNAMIC MEMORY ALLOCATION.             *
*      -CALLS NECESSRY ROUTINES TO PRODUCE :                    *
*            -SHAPE FUNCTIONS (FOR VELOCITY AND PRESSURE FIELD) *
*            -LOCAL DERIVATIVES OF SHAPE FUNCTIONS              *
*            -GLOBAL DERIVATIVES OF SHAPE FUNCTIONS             *
*            -ELEMENT DIFFUSION MATRIX                          *
*            -ELEMENT PENALTY MATRIX                            *
*            -GLOBAL RESIDUAL VECTOR , (R)=BGLOB(NEQ)=(B)-(A)(X)*
*            -ASSEMBLING ELEMENT MATRICES TO FORM GLOBAL MATRIX,*
*             MATGLOB(ESPMAT)                                   *
*      -OUTPUT :                                                *
*              MATGLOB(ESPMAT), AND BGLOB(NEQ)                  *
*****************************************************************
      INTEGER MBLANK
      PARAMETER ( MBLANK = 20000 )
*     GLOBAL VARIABLES
*     ---------------
      LOGICAL   DEBUG
      INTEGER   DBGLVL
      COMMON  / BUGS   /   DBGLVL, DEBUG
      INTEGER   ITWO
      COMMON  / DPR    / ITWO
      INTEGER IPRINT
      COMMON / DISKS  / IPRINT
      INTEGER   MTOT
      COMMON  / MEMORY / MTOT
      INTEGER   IA
      COMMON  / BLANK / IA(MBLANK)
      COMMON  /INOUT/ IIN,IOUT
      INTEGER ADDTBL, LOCTBL , SIZEOF , STOROF
      INTEGER TYPE,NELGRP,INTGV,INTGP,NDP,LL,NEL,ISAT,ILOAD,
     &        NQ,ESPMAT,NESP,NG,MELDOF,MVISC,MCP,MCON
      INTEGER BLOC(NG,8),KK
      REAL*8 PROP(NG,16),MATGLB(NESP),BGLOB(NQ),DX(NQ),C2(3),TETA,C(3)
      REAL*8 GAMA,VDR,DS(4),FP,STRESS(NELEM,4,3),STRAIN(NELEM,4,3),EV,
     &       S(4),A
      COMMON /CONT/IDIM,ITEMP,NUMNP,NELEM,NGROUP,NNPE,NFIXU,NFIXV,
     &             ISAT,NLOAD
      COMMON /COND/NDEP,NCOORD,NEQ,ESPMAT
      COMMON /ADD/NPROP,NBLOC,NCIEL,ICONEC,ILMG,ICON,ICOORD,NID,IB
      COMMON /COLLPSE/NCLOAD,ILOAD
*
      TYPE=BLOC(N,1)
      NELGRP=BLOC(N,2)
      NDP=BLOC(N,3)
      INTGV=BLOC(N,4)
      INTGP=BLOC(N,5)
```

```
*
      GAMA=PROP(N,1)
      VDR=PROP(N,4)
      SI=PROP(N,5)
      G=PROP(N,6)
      A=PROP(N,13)
      LL=NFIXU+NFIXV
      MELDOF=NDEP*NDP
*
      NINTGP=INTGP**NCOORD
      NINTGU=INTGV**NCOORD
*
      ICOR=ADDTBL('CORDE',NDP*NCOORD,'REAL','ELAST')
      ILM=ADDTBL('LM',MELDOF,'INTEGER','ELAST')
      IMAT=ADDTBL('MATELM',MELDOF*MELDOF,'REAL','ELAST')
      IELM=ADDTBL('BELM',MELDOF,'REAL','ELAST')
      IGU=ADDTBL('XGAUSU',NINTGU*NCOORD,'REAL','ELAST')
      IWU=ADDTBL('WU',NINTGU,'REAL','ELAST')
      ISHU=ADDTBL('SHAPEU',NINTGU*NDP,'REAL','ELAST')
      IDSU=ADDTBL('DSLOCU',NINTGU*NDP*NCOORD,'REAL','ELAST')
      IDGU=ADDTBL('DSGLBU',NINTGU*NDP*NCOORD,'REAL','ELAST')
      IJACU=ADDTBL('DJACU',NINTGU,'REAL','ELAST')
      IGP=ADDTBL('XGAUSP',NINTGP*NCOORD,'REAL','ELAST')
      IWP=ADDTBL('WP',NINTGP,'REAL','ELAST')
      ISHP=ADDTBL('SHAPEP',NINTGP*NDP,'REAL','ELAST')
      IDSP=ADDTBL('DSLOCP',NINTGP*NDP*NCOORD,'REAL','ELAST')
      IDGP=ADDTBL('DSGLBP',NINTGP*NDP*NCOORD,'REAL','ELAST')
      IJACP=ADDTBL('DJACP',NINTGP,'REAL','ELAST')
*
      CALL GAUSS(INTGV,NCOORD,NINTGU,IA(IGU),IA(IWU))
      CALL FBASE(NINTGU,NDP,NCOORD,IA(IGU),IA(ISHU),IA(IDSU),TYPE)
      CALL GAUSS(INTGP,NCOORD,NINTGP,IA(IGP),IA(IWP))
      CALL FBASE(NINTGP,NDP,NCOORD,IA(IGP),IA(ISHP),IA(IDSP),TYPE)
*
      DO 20 NEL=1,NELGRP
         CALL INIT(IA(IMAT),MELDOF,MELDOF)
         CALL INITV(IA(IELM),MELDOF)
         CALL TRANS(IA(ICOORD),IA(ILMG),IA(ICONEC),IA(ILM),IA(ICOR),
     &              BLOC,N,NG,NCOORD,NEL,NUMNP,NDP,NELEM,MELDOF)
         CALL DRGLOB(NINTGU,NDP,NCOORD,IA(ICOR),IA(IDSU),IA(IDGU),
     &               IA(IJACU))
         CALL DRGLOB(NINTGP,NDP,NCOORD,IA(ICOR),IA(IDSP),IA(IDGP),
     &               IA(IJACP))
         IF (II.EQ.1) THEN
             CALL SATDEG(NINTGP,STRAIN,NELEM,NEL,BLOC,N,NG,SI,
     &                   S,VDR,EV,DS,ISAT,ILOAD)
            IF(ILOAD.EQ.1.OR.ISAT.EQ.(ILOAD-1))THEN
            CALL FBODY(IA(ISHP),IA(IJACP),NDP,MELDOF,GAMA,
     &                 IA(IWP),NINTGP,EV,DS,IA(IELM),ILOAD)
            CALL POREP(IA(IJACP),IA(IDGP),NDP,MELDOF,IA(IWP),A,
     &                 NINTGP,STRAIN,IA(IELM),NELEM,S,DS,ILOAD)
         ENDIF
         IF(ISAT.GT.0.AND.ILOAD.LT.(ISAT+NCLOAD))
```

```
     &          THEN
                CALL COLOAD(STRESS,STRAIN,BLOC,N,NG,NEL,IA(IELM),S,
     &               MELDOF,IA(IWP),NINTGP,NDP,IA(IJACP),IA(IDGP),PROP)
            ENDIF
         ENDIF
         KK=0
         CALL MODULI(C2,STRESS,STRAIN,NELEM,BLOC,N,NG,NEL,S,PROP,KK,
     &               ISAT,ILOAD)
         TETA=.60
         C(1)=(1-TETA)*C(1)+TETA*C2(1)
         C(2)=(1-TETA)*C(2)+TETA*C2(2)
         C(3)=(1-TETA)*C(3)+TETA*C2(3)
         CALL STIFF(IA(ISHU),IA(IDGU),IA(IJACU),NDP,MELDOF,C,
     &              IA(IWU),IA(IGU),IA(IMAT),NINTGU)
         CALL CNDLIM(NEQ,LL,MELDOF,DX,IA(ICON),IA(ILM),IA(IMAT),
     &               IA(IELM),BGLOB)
         IDIAG=NCIEL
         C(1)=C2(1)
         C(2)=C2(2)
         C(3)=C2(3)
         CALL STIFF(IA(ISHU),IA(IDGU),IA(IJACU),NDP,MELDOF,C,
     &              IA(IWU),IA(IGU),IA(IMAT),NINTGU)
         CALL ASSEMB(NESP,NEQ,IA(IDIAG),MATGLB,IA(ILM),MELDOF,IA(IMAT))
20    CONTINUE
      CALL RMVTBL('DJACP')
      CALL RMVTBL('DSGLBP')
      CALL RMVTBL('DSLOCP')
      CALL RMVTBL('SHAPEP')
      CALL RMVTBL('WP')
      CALL RMVTBL('XGAUSP')
      CALL RMVTBL('DJACU')
      CALL RMVTBL('DSGLBU')
      CALL RMVTBL('DSLOCU')
      CALL RMVTBL('SHAPEU')
      CALL RMVTBL('WU')
      CALL RMVTBL('XGAUSU')
      CALL RMVTBL('BELM')
      CALL RMVTBL('MATELM')
      CALL RMVTBL('LM')
      CALL RMVTBL('CORDE')
      RETURN
      END
```

```
      SUBROUTINE FBASE(NPGAUS,NDP,NCOORD,XGAUS,SHAPE,DSLOC,TYPE)
*****************************************************************
*     THIS ROUTINE CALCULATES THE SHAPE FUNCTIONS FOR THE FOLLOWING  *
*     ELEMENTS:                                                      *
*               TYPE=1 :  QUAD4                                      *
*               TYPE=2 :  QUAD9                                      *
*     INPUT :                                                        *
*               XGAUS(NPGAUS,NCOORD) :GAUSS POINTS                   *
*     OUTPUT:                                                        *
*               SHAPE(N,I) : ITH SHAPE FUNCTION CALCULATED AT GAUSS  *
*                            POINT N                                 *
*               DSLOC(N,I,J) :LOCAL DERIVATIVE OF THE ITH SHAPE      *
*                             FUNCTION W.R.T. JTH LOCAL COORDINATE   *
*                             CALCULATED AT GAUSS POINT N            *
*****************************************************************
      INTEGER NPGAUS,NDP,NCOORD,TYPE,NP(9)
      REAL*8 XGAUS(NPGAUS,NCOORD),ETA,XI,XIT,ETAT,SHAPE(NPGAUS,NDP),
     &       X(9,2),S,DSLOC(NPGAUS,NDP,NCOORD)
      DATA S/1.0D0/
      DATA NP/1,2,3,4,5,7,6,8,9/
      DATA X/-1.0D0,2*1.0D0,-1.0D0,0.0D0,1.0D0,0.0D0,-1.0D0,0.0D0,
     &        2*-1.0D0,2*1.0D0,-1.0D0,0.0D0,1.0D0,2*0.0D0/
*
      DO 10 N=1,NPGAUS
         XI= XGAUS(N,1)
         ETA=XGAUS(N,2)
      DO 20 I=1,NDP
         IF(TYPE.EQ.1)THEN
           XIT= S+XI*X(I,1)
           ETAT=S+ETA*X(I,2)
           SHAPE(N,I)=.25D0*XIT*ETAT
           DSLOC(N,I,1)=.25D0*X(I,1)*ETAT
           DSLOC(N,I,2)=.25D0*X(I,2)*XIT
         ELSEIF(TYPE.EQ.2)THEN
            J=NP(I)
            XIT= S+XI*X(J,1)
            ETAT=S+ETA*X(J,2)
            IF(I.GT.4)GO TO 30
            SHAPE(N,J)=.25D0*XIT*ETAT*X(J,1)*XI*X(J,2)*ETA
          DSLOC(N,J,1)=.25D0*X(J,1)*X(J,2)*ETA*ETAT*(S+2.D0*X(J,1)*XI)
          DSLOC(N,J,2)=.25D0*X(J,2)*X(J,1)*XI*XIT*(S+2.D0*X(J,2)*ETA)
            GO TO 20
   30       IF(I.GT.6)GO TO 40
            SHAPE(N,J)=.5D0*(S-XI*XI)*ETAT*X(J,2)*ETA
            DSLOC(N,J,1)=-XI*X(J,2)*ETA*ETAT
            DSLOC(N,J,2)=.5D0*(S-XI*XI)*X(J,2)*(S+2.D0*X(J,2)*ETA)
            GO TO 20
   40       IF(I.GT.8)GO TO 60
            SHAPE(N,J)=.5D0*(S-ETA*ETA)*XIT*X(J,1)*XI
            DSLOC(N,J,2)=-ETA*X(J,1)*XI*XIT
            DSLOC(N,J,1)=.5D0*(S-ETA*ETA)*X(J,1)*(S+2.D0*X(J,1)*XI)
            GO TO 20
   60       SHAPE(N,J)=(S-XI*XI)*(S-ETA*ETA)
```

```
            DSLOC(N,J,1)=-2.D0*XI*(S-ETA*ETA)
            DSLOC(N,J,2)=-2.D0*ETA*(S-XI*XI)
         ELSE
            WRITE(IOUT,*)'ERROR IN TYPE=',TYPE
         ENDIF
20    CONTINUE
10    CONTINUE
      RETURN
      END
```

```
      SUBROUTINE DRGLOB(NPGAUS,NDP,NCOORD,CORDE,DSLOC,DSGLOB,DETJ)
*********************************************************************
*     THIS ROUTINE TRANSFERS LOCAL DERIVATIVES OF SHAPE FUNCTIONS    *
*     INTO GLOBAL COORDINTES USING JACOBIAN MATRIX :                 *
*                  (GLOBAL DERIV.) = (INV. OF JAC.)(LOCAL DERIV.)    *
*     DJAC(NCOORD,NCOORD) :JACOBIAN MATRIX                           *
*     DJINV(NCOORD,NCOORD):INVERSE OF JACOBIAN MATRIX                *
*                                                                    *
*     INPUT : NPGAUS :NO. OF GAUSS POINTS                            *
*             DSLOC(NPGAUS,NDP,NCOORD):LOCAL DEIVATIVES              *
*             CORDE(NDP,NCOORD) :ELEMENT'S NODAL COORDINTES          *
*     OUTPUT :                                                       *
*             DET(NPGAUS):JACOBIAN DETERMINANT                       *
*             DSGLOB(NPGAUS,NDP,NCOORD): GLOBAL DERIVATIVES          *
*********************************************************************
      INTEGER NPGAUS,NDP,NCOORD
      REAL*8 DSLOC(NPGAUS,NDP,NCOORD),DETJ(NPGAUS),
     &       DSGLOB(NPGAUS,NDP,NCOORD),CORDE(NDP,NCOORD)
      REAL*8 DJINV(2,2),DJAC(2,2)
*
      DO 30 N=1,NPGAUS
      DO 15 I=1,NCOORD
      DO 15 J=1,NCOORD
         DJAC(I,J)=0.0D0
         DO 10 K=1,NDP
  10     DJAC(I,J)=DJAC(I,J)+DSLOC(N,K,I)*CORDE(K,J)
  15     CONTINUE
         DETJ(N)=DJAC(1,1)*DJAC(2,2)-DJAC(1,2)*DJAC(2,1)
         DJINV(1,1)=DJAC(2,2)/DETJ(N)
         DJINV(2,2)=DJAC(1,1)/DETJ(N)
         DJINV(1,2)=-DJAC(1,2)/DETJ(N)
         DJINV(2,1)=-DJAC(2,1)/DETJ(N)
      DO 25 I=1,NCOORD
      DO 25 J=1,NDP
         DSGLOB(N,J,I)=0.0D0
      DO 20 K=1,NCOORD
 20      DSGLOB(N,J,I)=DSGLOB(N,J,I)+DJINV(I,K)*DSLOC(N,J,K)
 25   CONTINUE
 30   CONTINUE
      RETURN
      END
```

```
      SUBROUTINE STIFF(SHAPE,DSGLOB,DJAC,NDP,MELDOF,C,WU,XGAUS,
     &                 MATELM,NPGAUS)
*********************************************************************
*        THIS ROUTINE CALCULATES THE ELEMENT'S STIFFNESS MATRIX .    *
*     INPUT:                                                        *
*             SHAPE(NPGAUS,NDP) :SHAPE FUNCTIONS                    *
*             DSGLOB(NPGAUS,NDP,NCOORD) :GLOBAL SHAPE FUNCTION DERIV.*
*             DJAC(NPGAUS) :JACOBIAN DETERMINANT                    *
*             XGAUS(NPGAUS,NCOORD) :GAUSS POINTS                    *
*             WU(NPGAUS) :WEIGHT FACTORS FOR GAUSS POINTS           *
*             MELDOF :ELEMENT'S MAXIMUM DEGREE OF FREEDOM           *
*     OUTPUT :                                                      *
*             MATELM(MELDOF,MELDOF) :ELEMENT STIFFNESS MATRIX       *
*********************************************************************
      INTEGER NPGAUS,NDP,MELDOF,NDF
      REAL*8 SHAPE(NPGAUS,NDP),DSGLOB(NPGAUS,NDP,2),DJAC(NPGAUS),
     &       MATELM(MELDOF,MELDOF),WU(NPGAUS),SX(9,9)
      REAL*8 SY(9,9),SXY(9,9),XGAUS(NPGAUS,2),CONST,C(3)
*
      CALL INIT(SX,NDP,NDP)
      CALL INIT(SY,NDP,NDP)
      CALL INIT(SXY,NDP,NDP)
*
      DO 10 N=1,NPGAUS
      CONST=DJAC(N)*WU(N)
      DO 20 I=1,NDP
      DO 30 J=1,NDP
            SX(I,J)=SX(I,J)+CONST*DSGLOB(N,I,1)*DSGLOB(N,J,1)
            SY(I,J)=SY(I,J)+CONST*DSGLOB(N,I,2)*DSGLOB(N,J,2)
            SXY(I,J)=SXY(I,J)+CONST*DSGLOB(N,I,1)*DSGLOB(N,J,2)
 30   CONTINUE
 20   CONTINUE
 10   CONTINUE
      KK=MELDOF/2
      DO 100 I=1,NDP
      DO 120 J=1,NDP
             MATELM(I,J)=C(1)*SX(I,J)+C(3)*SY(I,J)
             MATELM(I+KK,J)=C(2)*SXY(J,I)+C(3)*SXY(I,J)
             MATELM(I,J+KK)=C(2)*SXY(I,J)+C(3)*SXY(J,I)
             MATELM(I+KK,J+KK)=C(3)*SX(I,J)+C(1)*SY(I,J)
 120  CONTINUE
 100  CONTINUE
      RETURN
      END
```

```
      SUBROUTINE MODULI(C,STRESS,STRAIN,NELEM,BLOC,N,NG,NEL,SS,PROP,LL,
     &                  ISAT,ILOAD)
*****************************************************************
*     THIS ROUTINE UPDATES THE TANGENTIAL ELASTIC MODULI BASED ON THE*
*           CURRENT STRESS AND STRAIN LENELS                        *
*     INPUT:                                                        *
*           STRESS(NELEM,NPGAUS,3) : CURRENT STATE OF STRESS        *
*           STRAIN(NELEM,NPGAUS,3) : CURRENT STATE OF STRAIN        *
*           BLOC(NG,8) : DESCRIPTION BLOCK                          *
*           PROP(NG,16) : PROPERTIES AND PARAMETER BLOCK            *
*           SS(NPGAUS) : DEGREE OF SATURATION AT GAUSS POINTS       *
*           SIG(NDEP) : PRINCIPLE STRESSES                          *
*           STR(NDEP) : PRINCIPAL STRAINS                           *
*           TETA : PRINCIPLE DIRECTION W.R.T. Y-DIRECTION           *
*           ANU : TANGENTIAL POISSON'S RATIO                        *
*           BM  : TANGENTIAL BULK MODULUS                           *
*           SM  : TANGENTIAL SHEAR MODULUS                          *
*           ET  : TANGENTIAL YOUNG MODULUS                          *
*           KS  : TANGENTIAL BULK MODULUS FROM PARTIAL SATURATION   *
*           PHI : FRICTION ANGLE                                    *
*           CO  : COHESION                                          *
*           PA  : ATMOSPHERIC PRESSURE                              *
*     OUTPUT :                                                      *
*           C(3) : UPDATED ELASTICITY COEFFICIENTS                  *
*****************************************************************
      INTEGER NELEM,BLOC(NG,8),N,NEL,LL
      REAL*8 STRESS(NELEM,4,3),STRAIN(NELEM,4,3),C(3),SS(4),Z,Z1,Z2,
     &       Z3,Z4,Z5
      REAL*8 E,ANU,BM,SM,DD,STV,SIGV,KS,KSIG,A,B,X2,X3,X4,S,K,PA,EI
     &       ET,RF,PHI,CO,NN,SIG3,SIGD,SIG(2),STR(2),TETA,PROP(NG,16)
      COMMON /EPOREP/EPORE
*
      S=SS(1)
      II=NEL
      IF(N.NE.1)II=II+BLOC(N-1,2)
      Z1=0.0
      Z2=0.0
      Z3=0.0
      Z4=0.0
      Z5=0.0
      IF(LL.NE.0)GO TO 20
      DO 10 NP=1,4
          CALL PDIRCT(STRESS,STRAIN,NELEM,II,NP,SIG,STR,TETA)
          Z1=Z1+SIG(1)
          Z2=Z2+SIG(2)
          Z3=Z3+STR(1)
          Z4=Z4+STR(2)
          Z5=Z5+TETA
  10  CONTINUE
      SIG(1)=Z1/4.0
      SIG(2)=Z2/4.0
      STR(1)=Z3/4.0
      STR(2)=Z4/4.0
```

```
      TETA=Z5/4.0
      GO TO 15
   20     CALL PDIRCT(STRESS,STRAIN,NELEM,II,LL,SIG,STR,TETA)
   15  IF(BM.GT.0.0)ANU=(3.*BM-ET)/(6.*BM)
      IF(ANU.LT.0.0)ANU=0.1
      STV=STR(1)+STR(2)
      SIGV=(SIG(1)+SIG(2))*(1+ANU)/3.
      CO=PROP(N,2)
      PHI=PROP(N,3)
      PA=PROP(N,7)
      A=PROP(N,8)
      B=PROP(N,9)
      K=PROP(N,10)
      NN=PROP(N,11)
      RF=PROP(N,12)
      X2=PROP(N,14)
      X3=PROP(N,15)
      X4=PROP(N,16)
      PHI=PHI*3.1415/180.
      DPHI=8.0*3.1415/180.
*
*----------------PARAMETER VALIDATION------------------
----------------
         IF(ANU.LE.(0.0).OR.ANU.GT.(0.5))WRITE(6,*)'ERROR IN ANU=',ANU
         IF(ET.LT.(0.0).OR.BM.LT.(0.0))WRITE(6,*)'ERROR E,K=',ET,BM
*
      KSIG=A*PA/((1-B*STV)*(1-B*STV))
      KS=PA*(1./2.**(S**X4))*(X2/((1-X3*STV)*(1-X3*STV)))**(1-S**X4)
      BM=(KSIG+KS)
      SIGD=DABS(SIG(1)-SIG(2))
      SIG3=SIG(2)
      IF(SIG3.LT.(0.50*PA))SIG3=0.50*PA
      EI=K*PA*(SIG3/PA)**NN
      ET=RF*(1.-DSIN(PHI))*SIGD/(2.*CO*DCOS(PHI)+2.*SIG3*DSIN(PHI))
      ET=EI*(1.-ET)*(1.-ET)
      ANU=.5-ET/(6.*BM)
      IF(ANU.GT.0.5)WRITE(6,*)'  ERROR-2 IN ANU-- ANU=',ANU
      IF(ANU.GT.0.49D0)ANU=0.49D0
      IF(ANU.LT.0.1D0)ANU=0.10D0
       SM=1.5*BM*(1-2.*ANU)/(1+ANU)
      IF((3.0*BM).LT.ET)SM=1.50*BM
      C(1)=BM+(4./3.)*SM
      C(2)=BM-(2./3.)*SM
      C(3)=SM
      RETURN
      END
```

```
      SUBROUTINE SATDEG(NPGAUS,STRAIN,NELEM,NEL,BLOC,N,NG,SI,S,VDR,
     &                  EV,DS,ISAT,ILOAD)
*********************************************************************
*      THIS ROUTINE CALCULATES THE CHANGE IN SATURATION DEGREE AND   *
*            UPDATES THE DEGREE OF SATURATION                        *
*      INPUT :                                                       *
*         STRAIN(NELEM,NPGAUS,3) : STRAIN LEVEL AT THE GAUSS POINTS  *
*         BLOC(NGROUP,8) : DESCRIPTION BLOCK                         *
*         SI : INITIAL DEGREE OF SATURATION                          *
*         VDR : INITIAL VOID RATIO                                   *
*         ILOAD :LOAD INCREMENT NUMBER                               *
*      OUTPUT :                                                      *
*         DS(4): CHANGE IN DEGREE OF SATURATION                      *
*         S(4) : UPDATED DEGREE OF SATURATION                        *
*********************************************************************
      INTEGER NELEM,NEL,NPGAUS,N,ILOAD,BLOC(NG,8)
      REAL*8 STRAIN(NELEM,4,3),S(4),DS(4),EV,VDR,SI,E2,S1(20,4)
*
      II=NEL
      IF(N.NE.1)II=II+BLOC(N-1,2)
      IF(ILOAD.EQ.1)THEN
         DO 10 I=1,NPGAUS
 10         S1(II,I)=SI
      ENDIF
      DO 20 I=1,NPGAUS
            EV=STRAIN(II,I,1)+STRAIN(II,I,2)
            S(I)=SI*VDR/(VDR-EV*(1+VDR))
            IF(ISAT.GT.0.AND.(ILOAD-1).GE.ISAT)S(I)=1.0
            DS(I)=S(I)-S1(II,I)
            S1(II,I)=S(I)
 20   CONTINUE
       RETURN
       END
```

```
      SUBROUTINE FBODY(SHAPE,DJAC,NDP,MELDOF,GAMA,WP,NPGAUS,
     &                 EV,DS,BELM,ILOAD)
*********************************************************************
*    THIS ROUTINE CALCULATES THE BODY FORCE AT NODES DUE TO GRAVITY  *
*              AND UPDATING THE CHANGE IN UNIT WEIGHT               *
*       INPUT :                                                     *
*             SHAPE(NPGAUS,NDP) :SHAPE FUNCTIONS                    *
*             DJAC(NPGAUS) :JACOBIAN DETERMINANT                    *
*             WU(NPGAUS) :WEIGHT FACTORS FOR GAUSS POINTS           *
*             MELDOF :ELEMENT'S MAXIMUM DEGREE OF FREEDOM           *
*             GAMA : UNIT WEIGHT                                    *
*             SI : INITIAL DEGREE OF SATURATION                     *
*             VDR : INITIAL VOID RATIO                              *
*             ILOAD :LOAD INCREMENT NUMBER                          *
*             S(4) : UPDATED DEGREE OF SATURATION                   *
*     OUTPUT :                                                      *
*             BELM(MELDOF) : ELEMENT'S NODAL FORCES                 *
*********************************************************************
      INTEGER NPGAUS,MELDOF,NDP,ILOAD
      REAL*8 SHAPE(NPGAUS,NDP),DJAC(NPGAUS),WP(NPGAUS),BELM(MELDOF),
     &       CONST,EV,SS(9),DS(4),GAMA,DGAMA(4)
*
      CALL INITV(SS,9)
      DO 50 I=1,NPGAUS
            DGAMA(I)=(EV/(1+EV))*9.81*DS(I)
            IF(ILOAD.EQ.1)DGAMA(I)=GAMA
  50  CONTINUE
      DO 10 N=1,NPGAUS
         CONST=DJAC(N)*WP(N)*DGAMA(N)
         DO 20 I=1,NDP
  20        SS(I)=SS(I)+CONST*SHAPE(N,I)
  10  CONTINUE
      KK=MELDOF/2
C-------THE GRAVITY IS IN NEGATIVE Y DIRECTION ------
      DO 40 I=1,NDP
         BELM(I+KK)=-SS(I)
  40  CONTINUE
 120  RETURN
      END
```

```
      SUBROUTINE POREP(DJAC,DSGLOB,NDP,MELDOF,WP,A,NPGAUS,STRAIN,
     &                 BELM,NELEM,S,DS,ILOAD)
*****************************************************************
*        THIS ROUTINE CALCULATES THE ELEMENT'S PRESSURE TERM AND ADDS*
*             IT TO THE BODY FORCE. ( PORE PRESSURE IS UPDATED )     *
*     INPUT:                                                        *
*           DSGLOB(NPGAUS,NDP,NCOORD) :GLOBAL SHAPE FUNCTION DERIV.*
*             DJAC(NPGAUS) :JACOBIAN DETERMINANT                   *
*             WP(NPGAUS) :WEIGHT FACTORS FOR GAUSS POINTS          *
*             MELDOF :ELEMENT'S MAXIMUM DEGREE OF FREEDOM          *
*     OUTPUT :                                                      *
*             BELM(MELDOF) :ELEMENT RIGHT HAND SIDE VECTOR         *
*****************************************************************
      INTEGER NPGAUS,NDP,MELDOF,NDF
      REAL*8 DSGLOB(NPGAUS,NDP,2),DJAC(NPGAUS),STRAIN(NELEM,4,3),
     &       BELM(MELDOF),WP(NPGAUS),SX(9),P(4),S(4),DS(4)
      REAL*8 SY(9),CONST,A,B,U,DU,FS,DFS
      COMMON /EPOREP/EPORE
*
      CALL INITV(SX,NDP)
      CALL INITV(SY,NDP)
*
C--------- COMPRESSION IS POSITIVE-------------
      DO 15 I=1,NPGAUS
         IF(S(I).GE.0.48.AND.S(I).LT.0.53)THEN
            U=387.0*S(I)-256.87
            DU=387.0*DS(I)
         ELSEIF(S(I).GE.0.53.AND.S(I).LT.0.62)THEN
            U=194.0*S(I)-154.50
            DU=194.0*DS(I)
         ELSEIF(S(I).GE.0.62.AND.S(I).LT.0.72)THEN
            U=170.0*S(I)-139.40
            DU=170.0*DS(I)
         ELSEIF(S(I).GE.0.72.AND.S(I).LT.0.84)THEN
            U=142.0*S(I)-119.00
            DU=142.0*DS(I)
         ELSEIF(S(I).GE.0.84.AND.S(I).LE.1.0)THEN
            U=0.0
            DU=140.0*DS(I)
         ELSE
             WRITE(6,*)'ERROR IN SATURATION DEGREE  S=',S(I)
         ENDIF
         B=-2.4*S(I)**A
         FS=1.1*(1-DEXP(B))
         DFS=1.1*DEXP(B)*2.4*A*DS(I)*S(I)**(A-1)
         P(I)=FS*DU+U*DFS
         IF(ILOAD.EQ.1)P(I)=FS*U
         EPORE=DU
  15  CONTINUE
      DO 10 N=1,NPGAUS
      CONST=DJAC(N)*WP(N)*P(N)
      DO 20 I=1,NDP
            SX(I)=SX(I)+CONST*DSGLOB(N,I,1)
```

```
            SY(I)=SY(I)+CONST*DSGLOB(N,I,2)
20    CONTINUE
10    CONTINUE
      KK=MELDOF/2
      DO 100 I=1,NDP
             BELM(I)=BELM(I)+SX(I)
             BELM(I+KK)=BELM(I+KK)+SY(I)
100   CONTINUE
120   RETURN
      END
```

```
      SUBROUTINE COLOAD(STRESS,STRAIN,BLOC,N,NG,NEL,BELM,SS,
     &                  MELDOF,WP,NPGAUS,NDP,DJAC,DSGLOB,PROP)
*********************************************************************
*     THIS ROUTINE CALCULATES THE ELEMENT NODAL COLLAPSE LOAD AS A    *
*           RESULT OF INCREASE IN DEGREE OF SATURATION                *
*     INPUT:                                                          *
*          STRESS(NELEM,NPGAUS,3) : CURRENT STATE OF STRESS           *
*          STRAIN(NELEM,NPGAUS,3) : CURRENT STATE OF STRAIN           *
*          BLOC(NG,8) : DESCRIPTION BLOCK                             *
*          PROP(NG,16) : PROPERTIES AND PARAMETER BLOCK               *
*          DSGLOB(NPGAUS,NDP,2) : GLOBAL DERIVATIVE OF SHAPE FUNCTIONS*
*          DJAC(NPGAUS) : JACOBIAN DETERMINENT                        *
*          WP(NPGAUS) : WEIGHT FACTORS AT GAUSS POINTS                *
*          MELDOF : ELEMENT'S MAX. DEGREE OF FREEDOM                  *
*          BELM(MELDOF) : ELEMENT'S RIGHT HAND SIDE FORCE VECTOR      *
*      OUTPUT :                                                       *
*          BELM(MELDOF) : REVISEDELEMENT'S FORCE VECTOR TAKING INTO   *
*                         ACCOUNT THE COLLAPSE LOAD                   *
*********************************************************************
      COMMON /CONT/IDIM,ITEMP,NUMNP,NELEM,NGROUP,NNPE,NFIXU,NFIXV,
     &             ISAT,NLOAD
      COMMON /EPOREP/EPORE
      INTEGER NELEM,BLOC(NG,8),N,NEL,NSTEP,MELDOF,NDP,NPGAUS,KK,NCLOAD,
     &        NC
      REAL*8 STRESS(NELEM,4,3),STRAIN(NELEM,4,3),BELM(MELDOF),SS(4),
     *       WP(NPGAUS),DJAC(NPGAUS),DSGLOB(NPGAUS,NDP,2),SIG(2),STR(2)
      REAL*8
ANU,DD,STV,SIGV,KS,KSIG,A,B,X2,X3,X4,S,K,PA,EI,PROP(NG,16),
     &       ET,RF,PHI,CO,NN,SIG3,SIGD,BM,CSIGV,CSIGD,E1,B1,B2,TETA,
     &       DSIGD,DSTV,CSIG1,CSIG3,P(4,3),CONST,SX(9),SY(9),SIGV3D,Z
      COMMON /COLLPSE/NCLOAD,ILOAD
*
      NC=1
      IF(ILOAD.GT.ISAT)NC=NCLOAD
      IF((ILOAD-1).GT.ISAT)GO TO 80
      CALL INITV(SX,NDP)
      CALL INITV(SY,NDP)
      S=0.00
      DO 5 I=1,NPGAUS
  5      S=S+SS(I)
      S=S/NPGAUS
           WRITE(6,*)'   S  NC=',S,NC
      II=NEL
      IF(N.NE.1)II=II+BLOC(N-1,2)
      CO=PROP(N,2)
      PHI=PROP(N,3)
      PA=PROP(N,7)
      A=PROP(N,8)
      B=PROP(N,9)
      K=PROP(N,10)
      NN=PROP(N,11)
      RF=PROP(N,12)
      X2=PROP(N,14)
```

```
      X3=PROP(N,15)
      X4=PROP(N,16)
      PHI=PHI*3.1415/180.
      DO 20 NP=1,NPGAUS
      CALL PDIRCT(STRESS,STRAIN,NELEM,II,NP,SIG,STR,TETA)
      SIGD=DABS(SIG(1)-SIG(2))
        STV=STR(1)+STR(2)
        STD=STR(1)-STR(2)
        IF(STV.LT.0.0.OR.STD.LT.0.0)WRITE(6,*)' ERROR STV STD=',STV,STD
        NSTEP=50
        DSTV=STV/NSTEP
        DSTD=STD/NSTEP
         STV=0.0
         STD=0.0
         SIGD=0.0
         SIGV=0.0
         BM=0.0
         ET=0.0
         ANU=0.0
      DO 10 I=1,NSTEP+1
         STV=STV+DSTV
         STD=STD+DSTD
      SIG3=DSIGV-DSIGD
      IF(SIG3.LT.(0.5*PA))SIG3=0.5*PA
      EI=K*PA*(SIG3/PA)**NN
         ET=RF*(1.-DSIN(PHI))*DABS(SIGD)/(CO*DCOS(PHI)+SIG3*DSIN(PHI))
         ET=EI*(1.-ET)*(1.-ET)
         SIGV3D=SIGV*(1+ANU)*2./3.
         KSIG=A*PA/((1-B*STV)*(1-B*STV))
         KS=PA*(1./2.**(S**X4))*(X2/((1-X3*STV)*(1-X3*STV)))**(1-S**X4)
         BM=(KSIG+KS)
         ANU=(3.*BM-ET)/(6.*BM)
         IF((3.*BM).LT.ET)ANU=0.0
         G=1.5*BM*(1-2.*ANU)/(1+ANU)
         DSIGV=(BM+G/3.)*DSTV
         DSIGD=G*DSTD
         SIGV=SIGV+DSIGV
         SIGD=SIGD+DSIGD
10    CONTINUE
         CSIGV=(SIG(1)+SIG(2))/2.0
         CSIGD=(SIG(1)-SIG(2))/2.0
         CSIGV=CSIGV-SIGV
         CSIGD=CSIGD-SIGD
      P(NP,1)=CSIGV-CSIGD*DCOS(TETA)
      P(NP,2)=CSIGV+CSIGD*DCOS(TETA)
      P(NP,3)=CSIGD*DSIN(TETA)
      STRESS(II,NP,1)=STRESS(II,NP,1)-P(NP,1)
      STRESS(II,NP,2)=STRESS(II,NP,2)-P(NP,2)
      STRESS(II,NP,3)=STRESS(II,NP,3)-P(NP,3)
      CONST=DJAC(NP)*WP(NP)
      DO 30 I=1,NDP
            SX(I)=SX(I)+CONST*(DSGLOB(NP,I,1)*P(NP,1)+DSGLOB(NP,I,2)*
     &            P(NP,3))/NC
```

```
            SY(I)=SY(I)+CONST*(DSGLOB(NP,I,2)*P(NP,2)+DSGLOB(NP,I,1)*
     &            P(NP,3))/NC
30    CONTINUE
20    CONTINUE
80    KK=MELDOF/2
      DO 100 I=1,NDP
             BELM(I)=BELM(I)-SX(I)
             BELM(I+KK)=BELM(I+KK)-SY(I)
100   CONTINUE
      RETURN
      END
```

```
      SUBROUTINE PDIRCT(STRESS,STRAIN,NELEM,II,NP,SIG,STR,TETA)
*********************************************************************
*      THIS ROUTINE CALCULATES THE PRINCIPAL STRESSES AND STRAINS AND *
*           THEIR ORIENTATION W.R.T. THE X-Y COORDINATE               *
*      INPUT :                                                       *
*           STRESS(NELEM,NPGAUS,3) : CURRENT STATE OF STRESS         *
*           STRAIN(NELEM,NPGAUS,3) : CURRENT STATE OF STRAIN         *
*           II :  ELEMENT NUMBER                                     *
*           NP :  GAUSS POINT NUMBER                                 *
*      OUTPUT :                                                      *
*           SIG(2) : PRINCIPAL STRESSES AT THE GAUSS POINT           *
*           STR(2) : PRINCIPAL STRAINS AT THE GAUSS POINT            *
*           TETA   : DIRECTION OF MAJOR PRINCIPAL STRESS OR STRAIN   *
*                    W.R.T. THE Y- DIRECTION                         *
*********************************************************************
      INTEGER NELEM,II,NP
      REAL*8 STRESS(NELEM,4,3),STRAIN(NELEM,4,3),SIG(2),STR(2),TETA,
     &       A,B,C
      A=(STRESS(II,NP,1)+STRESS(II,NP,2))/2.0
      B=-(STRESS(II,NP,1)-STRESS(II,NP,2))/2.0
      C=DSQRT(B*B+STRESS(II,NP,3)*STRESS(II,NP,3))
      SIG(1)=A+C
      SIG(2)=A-C
      IF(B.EQ.0.0)B=.1E-20
      TETA=DATAN(STRESS(II,NP,3)/B)
      A=(STRAIN(II,NP,1)+STRAIN(II,NP,2))/2.0
      B=(STRAIN(II,NP,1)-STRAIN(II,NP,2))/2.0
      C=DSQRT(B*B+STRAIN(II,NP,3)*STRAIN(II,NP,3))
      STR(1)=A+C
      STR(2)=A-C
      RETURN
      END
```

```
      SUBROUTINE MISAJR(X,DX,NEQ)
*************************************************************************
*     THIS ROUTINE UPDATES THE VALUE OF X(NEQ) FOR NEXT ITERATION       *
*     INPUT :                                                           *
*            X(NEQ)                                                     *
*            DX(NEQ)                                                    *
*     OUTPUT :                                                          *
*            X(NEQ) UPDATED                                             *
*************************************************************************
      INTEGER NEQ
      REAL*8 X(NEQ),DX(NEQ)
*
      DO 20 I=1,NEQ
  20  X(I)=X(I)+DX(I)
      RETURN
      END
```

```
      SUBROUTINE TRANS(COORD,LMGLOB,CONNEC,LM,CORDE,BLOC,N,NG,NCOORD,
     &                 NEL,NUMNP,NDP,NELEM,MELDOF)
*********************************************************************
*     THIS ROUTINE EXTRACTS ELEMENTS' INFORMATION FROM CORRESPONDING  *
*     GLOBAL TABLES.                                                  *
*     INPUT :                                                         *
*            CONNEC(NELEM,NDP) :GLOBAL CONNECTIVITY MATRIX            *
*            COORD(NUMNP,NCOORD) :GLOBAL COORDINATE TABLE             *
*            LMGLOB(NELEM,MELDOF) :GLOBAL ASSEMBLING MATRIX           *
*            BLOC(NGROUP,8) :DESCRIPTION BLOCK                        *
*     OUTPUT :                                                        *
*            CORDE(NDP,NCOORD) :ELEMENT'S NODAL COORDINATE            *
*            LM(MELDOF) :ELEMENT'S ASSEMBLING VECTOR                  *
*********************************************************************
      INTEGER N,NEL,NG,NCOORD,NUMNP,NDP,NELEM,MELDOF
      REAL*8 COORD(NUMNP,NCOORD),CORDE(NDP,NCOORD)
      INTEGER LMGLOB(NELEM,MELDOF),CONNEC(NELEM,NDP),LM(MELDOF),
     &        BLOC(NG,8),NODE
*
         II=NEL
         IF(N.NE.1)II=II+BLOC(N-1,2)
         DO 30 JJ=1,NDP
            NODE=CONNEC(II,JJ)
            DO 40 KK=1,NCOORD
 40            CORDE(JJ,KK)=COORD(NODE,KK)
 30      CONTINUE
         DO 50 LL=1,MELDOF
 50         LM(LL)=LMGLOB(II,LL)
      RETURN
      END
```

```
      SUBROUTINE RESULT(UV,ID,CONSTR,DX,NUMNP,NDEP,NEQ,LL)
*****************************************************************
*     THIS ROUTINE TRANSFERS THE RESULTS INTO MATRIX UV(NUMNP,NDEP) IN*
*     ORDER OF NODE NUMBERS AND CORRESPONDING DEGREES OF FREEDOM FOR  *
*     THE PRESENTATION OF RESULTS.                                    *
*     INPUT :                                                         *
*            CONSTR(LL) :VECTOR OF BOUNDARY CONDITIONS                *
*            X(NEQ) :VALUS OBTAINED FOR ACTIVE DEGREES OF FREEDOM     *
*            ID(NUMNP,NDEP) :TABLE GIVING STUTUS OF EACH D.O.F.       *
*     OUTPUT :                                                        *
*          UV(NUMNP,NDEP) :TABLE OF RESULTS FOR EACH NODE AND CORRES-*
*                           -PONDING DEGREES OF FREEDOM               *
*****************************************************************
      INTEGER NUMNP,NDEP,NEQ,LL
      INTEGER ID(NUMNP,NDEP)
      REAL*8 DX(NEQ),UV(NUMNP,NDEP),CONSTR(LL)
      COMMON /DOF/ KDOF(4),LDOF(4)
*
      CALL INIT(UV,NUMNP,NDEP)
      K=0
      NC=0
      DO 10 N=1,NUMNP
         DO 20 I=1,NDEP
            IE=ID(N,I)
            IF(IE.EQ.1)GO TO 20
            IF(IE.EQ.2)THEN
               NC=NC+1
               UV(N,KDOF(I))=CONSTR(NC)
               GO TO 20
            ENDIF
            IF(IE.EQ.0)THEN
               K=K+1
               UV(N,KDOF(I))=DX(K)
            ENDIF
 20      CONTINUE
 10   CONTINUE
      RETURN
      END
```

```
      SUBROUTINE STRSTN(BLOC,COORD,UV,CONNEC,C,S,STRESS,STRAIN,NGROUP,
     &          NUMNP,NELEM,NNPE,NCOORD,STREST,ILOAD,ISAT,PROP)
*****************************************************************
*     THIS ROUTINE CALCULATES THE STRESSES AND STRAINS AT THE CENTER  *
*     OF ELEMENTS.                                                    *
*     INPUT :                                                         *
*            CONNEC(NELEM,NDP) :GLOBAL CONNECTIVITY MATRIX            *
*            UV(NUMNP,NCOORD) :GLOBAL DISPLACEMENT TABLE              *
*            C(3) : COEFFICIENTS OF PLANE STRAIN ELASTICITY MATRIX    *
*            BLOC(NGROUP,8) :DESCRIPTION BLOCK                        *
*     OUTPUT :                                                        *
*            STRESS(NELEM,3) :STRESSES IN EACH ELEMENT                *
*            STRAIN(NELEM,3) :STRAINS IN EACH ELEMENT                 *
*****************************************************************
      INTEGER MBLANK
      PARAMETER ( MBLANK = 20000 )
*     GLOBAL VARIABLES
*     ----------------
      LOGICAL   DEBUG
      INTEGER   DBGLVL
      COMMON  / BUGS   /   DBGLVL, DEBUG
      INTEGER   ITWO
      COMMON  / DPR    / ITWO
      INTEGER IPRINT
      COMMON / DISKS  / IPRINT
      INTEGER   MTOT
      COMMON  / MEMORY / MTOT
      INTEGER   IA
      COMMON  / BLANK / IA(MBLANK)
      COMMON  /INOUT/ IIN,IOUT
      INTEGER ADDTBL, LOCTBL , SIZEOF , STOROF
*
      INTEGER NGROUP,NUMNP,NELEM,NNPE,NODE,TYPE,NDP,NCOORD,NINTGP
      INTEGER BLOC(NGROUP,8),CONNEC(NELEM,NNPE),FLAG,ILOAD,ISAT
      REAL*8 UV(NUMNP,2),C(3),STRESS(NELEM,4,3),STRAIN(NELEM,4,3),TETA,
     &       DSGLBP(4,9,2),CORDE(9,2),COORD(NUMNP,NCOORD),C2(3),S(4)
      REAL*8 W(9,2),UX,UY,VX,VY,STREST(NELEM,4,3),ST1,ST2,ST3,
     &       PROP(NGROUP,16)
      DO 10 NG=1,NGROUP
         TYPE=BLOC(NG,1)
         NELGRP=BLOC(NG,2)
         NDP=BLOC(NG,3)
         INTGP=BLOC(NG,5)
         NINTGP=INTGP**NCOORD
      IGP=ADDTBL('XGAUSP',NINTGP*NCOORD,'REAL','STRSTN')
      IWP=ADDTBL('WP',NINTGP,'REAL','STRSTN')
      ISHP=ADDTBL('SHAPEP',NINTGP*NDP,'REAL','STRSTN')
      IDSP=ADDTBL('DSLOCP',NINTGP*NDP*NCOORD,'REAL','STRSTN')
      IJACP=ADDTBL('DJACP',NINTGP,'REAL','STRSTN')
*
      CALL GAUSS(INTGP,NCOORD,NINTGP,IA(IGP),IA(IWP))
      CALL FBASE(NINTGP,NDP,NCOORD,IA(IGP),IA(ISHP),IA(IDSP),TYPE)
*
```

```
      DO 20 NEL=1,NELGRP
         II=NEL
         IF(NG.NE.1)II=II+BLOC(NG-1,2)
         DO 30 JJ=1,NDP
            NODE=CONNEC(II,JJ)
            DO 40 KK=1,NCOORD
               CORDE(JJ,KK)=COORD(NODE,KK)
 40            W(JJ,KK)=UV(NODE,KK)
 30      CONTINUE
         CALL DRGLOB(NINTGP,NDP,NCOORD,CORDE,IA(IDSP),DSGLBP,
     &              IA(IJACP))
         DO 200 LL=1,NINTGP
          UX=0.0D0
          UY=0.0D0
          VX=0.0D0
          VY=0.0D0
          DO 100 I=1,NDP
              UX=UX+W(I,1)*DSGLBP(LL,I,1)
              UY=UY+W(I,1)*DSGLBP(LL,I,2)
              VX=VX+W(I,2)*DSGLBP(LL,I,1)
              VY=VY+W(I,2)*DSGLBP(LL,I,2)
 100      CONTINUE
*
C----------- STRAIN CALCULATION -----------------------------
           STRAIN(II,LL,1)=STRAIN(II,LL,1)-(UX)
           STRAIN(II,LL,2)=STRAIN(II,LL,2)-(VY)
           STRAIN(II,LL,3)=STRAIN(II,LL,3)-(UY+VX)
*
         IMAX=25
         TOLR=0.5
         FLAG=0
         DO 50 ITER=1,IMAX
       CALL MODULI(C2,STREST,STRAIN,NELEM,BLOC,NG,NGROUP,NEL,S,PROP,LL,
     &             ISAT,ILOAD)
         TETA=.60
         C2(1)=(1-TETA)*C(1)+TETA*C2(1)
         C2(2)=(1-TETA)*C(2)+TETA*C2(2)
         C2(3)=(1-TETA)*C(3)+TETA*C2(3)
          ST1=STRESS(II,LL,1)-C2(1)*UX-C2(2)*VY
          ST2=STRESS(II,LL,2)-C2(2)*UX-C2(1)*VY
          ST3=STRESS(II,LL,3)-C2(3)*(UY+VX)
          IF(DABS(STREST(II,LL,1)-ST1).LE.TOLR.AND.DABS(STREST(II,LL,2
     &      )-ST2).LE.TOLR.AND.DABS(STREST(II,LL,3)-ST3).LE.TOLR)FLAG=1
           STREST(II,LL,1)=ST1
           STREST(II,LL,2)=ST2
           STREST(II,LL,3)=ST3
           IF(FLAG.EQ.1)GO TO 55
 50      CONTINUE
         WRITE(6,*)'NO OF ITERATIONS PASSED IMAX',ITER
C------------ STRESS CALCULATION -----------------------------
 55       STRESS(II,LL,1)=STRESS(II,LL,1)-C2(1)*UX-C2(2)*VY
          STRESS(II,LL,2)=STRESS(II,LL,2)-C2(2)*UX-C2(1)*VY
          STRESS(II,LL,3)=STRESS(II,LL,3)-C2(3)*(UY+VX)
```

```
200   CONTINUE
 20   CONTINUE
 10   CONTINUE
      CALL RMVTBL('DJACP')
      CALL RMVTBL('DSLOCP')
      CALL RMVTBL('SHAPEP')
      CALL RMVTBL('WP')
      CALL RMVTBL('XGAUSP')
      RETURN
      END
```

```
      SUBROUTINE LOAD(B,BGLOB,NEQ)
      INTEGER NEQ
      REAL*8 B(NEQ),BGLOB(NEQ)
      DO 10 I=1,NEQ
         BGLOB(I)=B(I)
10    CONTINUE
      RETURN
      END
```

```
      SUBROUTINE PRINT(UV,NDEP,NUMNP,EX,ED,ER,ILOAD,XN,DN,RN,NI,
     &                 STRESS,STRAIN,NELEM,UY)
*********************************************************************
*     THIS ROUTINE PRINTS OUT THE RESULTS WITH MAXIMUM AND EUCLIDEAN *
*     NORMS OF X(NEQ),DX(NEQ), AND THE RESIDUE R(NEQ)                *
*                                                                    *
*     UV(NUMNP,NDEP) :TABLE OF RESULTS                               *
*     EX,EDX,ER :EUCLIDEAN NORMS                                     *
*     XN,DN,RN  :MAXIMUM NORMS                                       *
*********************************************************************
      INTEGER NI,NDEP,NUMNP,ILOAD
      REAL*8 UV(NUMNP,NDEP),STRESS(NELEM,4,3),STRAIN(NELEM,4,3),
     &       UY(NUMNP,NDEP),EX,ED,ER,XN,DN,RN,STR(3),SIG(3),EPSV
      COMMON /INOUT/ IIN,IOUT
*
      WRITE(IOUT,10)ILOAD,NI
      DO 18 I=1,NUMNP
         DO 15 J=1,NDEP
  15     UY(I,J)=UY(I,J)+UV(I,J)
  18  CONTINUE
      DO 20 I=1,NUMNP
  20     WRITE(IOUT,50)I,(UY(I,J),J=1,NDEP)
      WRITE(IOUT,55)
      WRITE(IOUT,60)EX,XN
      WRITE(IOUT,62)ED,DN
      WRITE(IOUT,65)ER,RN
      DO 30 I=1,NELEM
        WRITE(IOUT,75)I
        CALL INITV(SIG,3)
        CALL INITV(STR,3)
        DO 25 L=1,4
           SIG(1)=SIG(1)+STRESS(I,L,1)
           SIG(2)=SIG(2)+STRESS(I,L,2)
           SIG(3)=SIG(3)+STRESS(I,L,3)
           STR(1)=STR(1)+STRAIN(I,L,1)
           STR(2)=STR(2)+STRAIN(I,L,2)
           STR(3)=STR(3)+STRAIN(I,L,3)
  25    CONTINUE
        SIG(1)=SIG(1)/4.0
        SIG(2)=SIG(2)/4.0
        SIG(3)=SIG(3)/4.0
        STR(1)=STR(1)/4.0
        STR(2)=STR(2)/4.0
        STR(3)=STR(3)/4.0
C---------TO CONVERT GAMAXY TO EPSXY----------
        STR(3)=STR(3)/2.0
        EPSV=STR(1)+STR(2)
          WRITE(IOUT,80)(SIG(J),J=1,3)
          WRITE(IOUT,85)(STR(J),J=1,3)
          WRITE(IOUT,90)EPSV
  30  CONTINUE
*********************************************************************
*                          FORMATS                                  *
```

```
*****************************************************************
  10  FORMAT('1',2X,'LOAD INCREMENT :',I2,3X,'NO. OF ITERATIONS=',I1,/,
     &       30('-'),/,4X,'NODE',8X,'U',8X,'V',/,30('-'))
  50  FORMAT(2X,I5,2X,4F10.3)
  55  FORMAT(//,2X,'EUCLIDEAN NORM',10X,'MAX. NORM',/,36('-'))
  60  FORMAT(2X,'X',F10.4,10X,F10.4)
  62  FORMAT(1X,'DX',F10.4,10X,F10.4)
  65  FORMAT(2X,'R',E10.4,10X,E10.4)
  75  FORMAT(//,2X,'ELEMENT NO.',I2)
  80  FORMAT(2X,'AVERAGED STRESS :',/,5X,'(SIGX, SIGY, SIGXY)=',3F10.3)
  85  FORMAT(2X,'AVERAGED STRAIN :',/,5X,'(EPSX, EPSY, EPSXY)=',3F10.5)
  90  FORMAT(6X,'VOLUMETRIC STRAIN =',F10.5)
      RETURN
      END
```